ZooKeys 873: 1–7 (2019)
doi: 10.3897/zookeys.873.36458
http://zookeys.pensoft.net

SHORT COMMUNICATION

A peer-reviewed open-access journal
ZooKeys
Launched to accelerate biodiversity research

First record of the New Guinea flatworm *Platydemus manokwari* (Platyhelminthes, Geoplanidae) as an alien species in Hong Kong Island, China

Junjie Hu[1,2], Muhua Yang[3,5], Elysia Ruoyan Ye[4,5], Yulong Ye[1], Yao Niu[6]

1 *School of Biological Sciences, Yunnan University, Kunming, 650091, China* **2** *Southeast Asia Biodiversity Research Institute, Chinese Academy of Science, Yezin, Nay Pyi Taw 05282, Myanmar* **3** *St Joseph's College, Hong Kong 999077, China* **4** *Chinese International School, Hong Kong 999077, China* **5** *Hong Kong Youth Science Academy, Hong Kong 999077, China* **6** *School of Life Science, Henan Normal University, Xinxiang 453007, China*

Corresponding author: *Junjie Hu* (jjhu@ynu.edu.cn)

Academic editor: *David Gibson* | Received 23 May 2019 | Accepted 9 August 2019 | Published 29 August 2019

http://zoobank.org/2DDFE810-A2A7-4F33-9F54-DD8E1D9F7828

Citation: Hu J, Yang M, Ye ER, Ye Y, Niu Y (2019) First record of the New Guinea flatworm *Platydemus manokwari* (Platyhelminthes, Geoplanidae) as an alien species in Hong Kong Island, China. ZooKeys 873: 1–7. https://doi.org/10.3897/zookeys.873.36458

Abstract

The New Guinea flatworm (*Platydemus manokwari*) caused extinction of the native land snails on several Pacific island in past decades, and therefore it has been listed among the top 100 of the world's worst invasive alien species. Using morphological and molecular methods, New Guinea flatworms were discovered and identified for the first time in Hong Kong Island during a field investigation in July and August 2018. The flatworms were 32–60 mm long, 3–5 mm wide, and 1–2 mm thick. The dorsal side of the flatworm was dark brown with a thin yellow central line, and its ventral side appeared pale grey. To further verify this species, both 18S rDNA and mitochondrial cytochrome c oxidase subunit I gene (COX1) obtained from three specimens of *P. manokwari* were sequenced and analysed. While comparing these sequences with those previously deposited in GenBank, these 18S rDNA sequences shared 100% identity with the single available 18S rDNA sequence of *P. manokwari*; and the obtained COX1 sequences were identical to those of *P. manokwari* world genotype. Two native snails, *Criptosoma imperator* and *Bradybaena similaris*, have been found to be the prey of this predator during this investigation. Therefore, the invasive New Guinea flatworm certainly will cause a serious impact on the biodiversity of native snail populations, and an economic and environmental risk assessment for *P. manokwari* need to be completed in the near future in Hong Kong.

Keywords

distribution, morphological characterisation, 18S rDNA, COX1

Introduction

The land planarian *Platydemus manokwari* de Beauchamp, 1963, or New Guinea flatworm, is a highly invasive species, and the only flatworm listed in the top 100 of the world's worst invasive alien species (Lowe et al. 2000). This species was first found on the New Guinea Island, but until now has been reported in 16 territories around the world (Justine et al. 2014, 2015, Chaisiri et al. 2018). The flatworms are carnivores, and feed upon a variety of soil organisms such as earthworms, isopods, insects, and snails, and may cause economic or environmental harm (Sugiura 2010, Justine et al. 2014). Additionally, they can harbour zoonotic pathogens which may possibly adversely affect human health (Chaisiri et al. 2018).

Morphological characteristics have traditionally been used as criteria to identify and distinguish different species of planarians. In the last decades, molecular methods have been used for delineation of marine, freshwater, and land planarians using different genetic markers (Carranza et al. 1998; Álvarez-Presas et al. 2008). To date, there are only one partial 18S rDNA sequence, one partial 28 rDNA sequence, and many partial mitochondrial cytochrome c oxidase subunit I gene (COX1) sequences obtained from limited isolates of *P. manokwari* available in GenBank. Interestingly, based on COX1, *P. manokwari* has been divided into two genetic haplotypes, "world" and "Australian" (Justine et al. 2015).

In the present study, New Guinea flatworms were discovered and identified based on the morphological and molecular characteristics in Hong Kong Island, China. To our knowledge, this is the first report of New Guinea flatworm in Hong Kong, even in China.

Materials and methods

Hong Kong is a special administrative region of China and surrounded by the South China Sea on all sides except the north, which neighbours Shenzhen city along the Sham Chun River. The territory's area consists of Hong Kong Island, the Kowloon Peninsula, the New Territories, Lantau Island, and more than 200 other islands. It has a humid subtropical climate, and approximately 40% of the remaining land area is devoted to country parks and nature reserves (Bernie and Raynor 2007). New Guinea flatworms were surveyed in nine localities (Fig. 1) including seven in Hong Kong Island, one in Lantau Island, and one in Lamma Island in July and August 2018. All these localities are along the coasts and covered by secondary forest. The flatworms were observed by the naked eye (32–60 mm long) and photographed using a Sony RX10 II camera.

For molecular identification, three specimens of *P. manokwari*, collected by hand and fixed in room-temperature ethanol (85%) were shipped to laboratory of zoology, Yunnan University, Kunming City, China. In the laboratory, a small piece of the body (ca. 4 mm^3) was taken from the lateral edge of each ethanol-fixed individual. The remaining specimens were deposited at the Zoological Specimen Museum of Yunnan University (collection numbers Worm 2019011–13).

Figure 1. Localities of surveys for *Platydemus manokwari*. Green: not found; Red: found.

Genomic DNA was extracted using the phenol/chloroform method, after five rounds of freezing and thawing, and 0.01% proteinase K and 0.25% trypsin digestion. The 18S rDNA was amplified with primer pairs, 18SPmF/18SPmR (5'-ACCGCG-GATGGCTCATTATA-3'/5'-ACGGAAACCTTGTTACGACTTTTA-3') designed using Premier 5 (Premier Biosoft International) based on the highly conserve regions of 18S rDNA sequences for members of Family Geoplanidae deposited in GenBank. The mitochondrial COX1 was amplified with primer pairs, BarS/ COI-ASmit2 (5'-GTTATGCCTGTAATGATTG-3'/ 5'-TAAAGAAAGAACATAATGAAAATG-3') designed by Álvarez-Presas et al. (2011) and Littlewood et al. (1997), respectively. Polymerase chain reaction (PCR) was performed in a total volume of 25 µl PCR cocktail that included 1X PCR buffer, 0.15 mmol $MgCl_2$, 0.25 mmol dNTPs, 1 U Taq DNA polymerase (TakaRa, Dalian, China), 50–100 ng of DNA, and 25 pmol of each primer. For 18S rDNA, the amplification protocol was: 5 minutes at 94 °C, followed by 35 cycles of 95 °C for 1 minutes, 58 °C for 1 minutes, 72 °C for 2 minutes, with a final extension at 72 °C for 10 minutes. For mitochondrial *COX1*, PCR amplifications were performed as previously described (Justine et al. 2015). PCR products were gel purified and cloned to PMD-19T vector (TakaRa), and then sequenced on an ABI 3730XL automatic DNA sequencer (Applied Biosystems, Foster City, CA, USA). The sequences were assembled using multiple over lapping regions using the SeqMan II program (DNAStar, Madison, Wisconsin, USA), and then uploaded to GenBank and compared with other deposited sequences using the NCBI BLAST program.

Results and discussion

New Guinea flatworms were only found in two of the nine localities, Seaview Promenade and Kennedy Road, both located in Hong Kong Island, Hong Kong. The habitats of this flatworm were in the deep mass of dead leaves. The flatworms were 32–60 mm long, 3–5 mm wide and 1–2mm thick (n = 12). The bodies were broadest in the middle, tapering at the both ends. Two small eyes were situated back from the tip of the elongate snout-like head (Fig. 2a). In cross section the flatworm was convex dorsally and flat ventrally. The dorsum was a dark olive brown colour, which under a lens showed a fine pale brownish graininess. A pale cream median dorsal longitudinal stripe, some 0.1 mm wide, began just behind the eyes and continued to the posterior tip (Fig. 2a). A thin sub-marginal cream stripe with fine lower greyish margin ran laterally from the anterior end along the length of the body (Fig. 2b). The ventral surface appeared off-white (Fig.2b).

Genomic DNA was extracted from the three individual specimens of *P. manokwari*, respectively, and the 18S rDNA and mitochondrial COX1 were amplified successfully using their DNA as templates. The three 18S rDNA nucleotide sequences (MK959224–MK959226), each from an individual specimen of *P. manokwari* were 1697 bp in length, and completely identical. The most similar sequence in GenBank was that of *P. manokwari* (AF048766, 100% identity), followed by *Caenoplana* sp. (AJ270156, 94.7% identity). The three mitochondrial COX1 nucleotide sequences (MK959221–MK959223), also obtained from the three individuals were 948 bp in length and shared 100% identity. The most similar sequences in GenBank were those of *P. manokwari* world haplotype (100% identity) from Singapore (KR349579 and KR349580), the Solomon Islands (KR349586, KR349588-92), New Caledonia (KR349600-01, KT004666–KT004671), France (KR349594, KF887958), French Polynesia (KR349595), and USA (KR349610 and KR349611), followed by *P. manokwari* Australian haplotype (95.1–96.3% identity, on average 95.4 identity) from Australia (KR349581–KR349585, KF178320) and the Solomon Islands (KR349593, KR349602).

The external morphological characteristics of the specimens found in Hong Kong are similar to *P. manokwari* previously described from USA, Singapore, New Caledonia, French Polynesia, France, and Thailand (Justine et al. 2014, 2015; Chaisiri et al. 2018). Currently, *P. manokwari* has been recorded from 16 different territories, distributed in Australia, Asia, Europe, and central and South America, but mostly in the Indo-Pacific region where it originates (Justine et al. 2014, Chaisiri et al. 2018). As far as we are aware, this is the first report of New Guinea flatworms in Hong Kong, and therefore in China. This flatworm was introduced into Hong Kong probably through the international commercial trade of materials, particularly pottery and commercially and imported plants (either the soil or the plants themselves), which could be contaminated and easily transport the flatworm to new places (Sugiura 2009; Justine et al. 2014).

In our analysis, the new 18S rDNA sequences showed 100% identity among three specimens and completely identical to that of *P. manokwari* previously deposited in

Figure 2. External morphological characteristics of *Platydemus manokwari*. Specimen collected in a dry ditch covered by dead leaves, Seavie Promenade, Hong Kong **A** dorsal view: note dorsal (D) with a median longitudinal line (arrow) and small eye situated back from the tip of the elongate snout-like head (arrowhead); **B** partial ventral view, showing the cream and faint grey marginal stripe (arrow) between dorsal (D) and ventral (V). Ruler in cm and mm.

GenBank; the new mitochondrial COX1 sequences were also identical among different specimens, with 100% identity with those of *P. manokwari* world haplotype from different areas in GenBank. At mitochondrial COX1, *P. manokwari* has been divided into two haplotypes, "world" recorded from France, French Polynesia, Wallis and Futuna, New Caledonia, Singapore, Solomon Islands, USA, and Thailand; however, "Australian" only recorded those from the Solomon Islands and Australia (Justine et al. 2015; Chaisiri et al. 2018). The two haplotypes couldn't be separated according to their external morphological characteristics (Justine et al. 2015), but the new obtained mitochondrial COX1 sequences of the world type only shared 95.4% identity with those of *P. manokwari* Australian type, and both invariably differed in 45 transitions/substitutions of a 948-bp-long portion of the gene. Therefore, the "world type" and the "Australian type" represented a same or separate species within the genus *Platydemus* need more morphological and multi-genetic markers data to clarify their taxonomic positions in the future.

Platydemus manokwari has been recorded to feed mainly on land gastropod molluscs, but also on earthworms, insects, and nemerteans (Justine et al. 2014). During the present investigation, the native terrestrial molluscs, the arboreal snail (*Megaustenia imperator* Gould, 1859) and the Asian tramp snail (*Bradybaena similaris* Férussac, 1821) have been observed to be eaten by *P. manokwari* in the field. Therefore, the invasive New Guinea flatworm certainly will cause a serious impact on the biodiversity of native snail populations, and an economic and environmental risk assessment for *P. manokwari* need to be considered in the very near future.

Acknowledgements

We would like to thank Dr. Dongmei Jiang from Hong Kong Youth Science Academy for valuable comments. This work was supported by the Southeast Asia Biodiversity Research Institute, Chinese Academy of Science (grant Y4zk111B01).

References

Álvarez-Presas M, Baguñà J, Riutort M (2008) Molecular phylogeny of land and freshwater planarians (Tricladida, Platyhelminthes): from freshwater to land and back. Molecular Phylogenetics and Evolution 47: 555–568. https://doi.org/10.1016/j.ympev.2008.01.032

Álvarez-Presas M, Carbayo F, Rozas J, Riutort M (2011) Land planarians (Platyhelminthes) as a model organism for fine-scale phylogeographic studies: understanding patterns of biodiversity in the Brazilian Atlantic Forest hotspot. Journal of Evolutionary Biology 24: 887–896. https://doi.org/10.1111/j.1420-9101.2010.02220.x

Bernie O, Raynor S (2007) Hong Kong Landscapes: Shaping the Barren Rock. Hong Kong University Press, Hong Kong, 264 pp.

Carranza S, Littlewood DT, Clough KA, Ruiz-Trillo I, Baguñà J, Riutort M (1998) A robust molecular phylogeny of the Tricladida (Platyhelminthes: Seriata) with a discussion on morphological synapomorphies. Proceedings of the Royal Society B 265: 631–640. https://doi.org/10.1098/rspb.1998.0341

Chaisiri K, Dusitsittipon S, Panitvong N, Ketboonlue T, Nuamtanong S, Thaenkham U, Morand S, Dekumyoy P (2018) Distribution of the newly invasive New Guinea flatworm *Platydemus manokwari* (Platyhelminthes: Geoplanidae) in Thailand and its potential role as a paratenic host carrying *Angiostrongylus malaysiensis* larvae. Journal of Helminthology 20: 1–9. https://doi.org/10.1017/S0022149X18000834

Justine JL, Winsor L, Barrière P, Fanai C, Gey D, Han AW, La Quay-Velázquez G, Lee BP, Lefevre JM, Meyer JY, Philippart D, Robinson DG, Thévenot J, Tsatsia F (2015) The invasive land planarian *Platydemus manokwari* (Platyhelminthes, Geoplanidae): records from six new localities, including the first in the USA. PeerJ 3: e1037. https://doi.org/10.7717/peerj.1037

Justine JL, Winsor L, Gey D, Gros P, Thévenot J (2014) The invasive New Guinea flatworm *Platydemus manokwari* in France, the first record for Europe: time for action is now. PeerJ 2: e297. https://doi.org/10.7717/peerj.297

Littlewood DT, Rohde K, Clough KA (1997) Parasite speciation within or between host species? Phylogenetic evidence from site-specific polystome monogeneans. International Journal for Parasitology 27: 1289–1297. https://doi.org/10.1016/S0020-7519(97)00086-6

Lowe S, Browne M, Boudjelas S, De Poorter M (2000) 100 of the World's Worst Invasive Alien Species. A selection from the Global Invasive Species Database. The Invasive Species Specialist Group (ISSG), a specialist group of the Species Survival Commission (SSC) of the World Conservation Union (IUCN), Auckland, 12 pp.

Sugiura S (2009) Seasonal fluctuation of invasive flatworm predation pressure on land snails: Implications for the range expansion and impacts of invasive species. Biological Conservation 142: 3013–3019. https://doi.org/10.1016/j.biocon.2009.07.032

Sugiura S (2010) Prey preference and gregarious attacks by the invasive flatworm *Platydemus manokwari*. Biological Invasions 12: 1499–1507. https://doi.org/10.1007/s10530-009-9562-9

ZooKeys 873: 9–23 (2019)
doi: 10.3897/zookeys.873.36702
http://zookeys.pensoft.net

RESEARCH ARTICLE

A peer-reviewed open-access journal
ZooKeys
Launched to accelerate biodiversity research

A new species of freshwater crab of the genus *Mediapotamon* Türkay & Dai, 1997 (Crustacea, Decapoda, Brachyura, Potamidae) from Guizhou, China

Song-bo Wang[1], Xian-min Zhou[1,2], Jie-xin Zou[1]

1 *Research Laboratory of Freshwater Crustacean Decapoda & Paragonimus, School of Basic Medical Sciences, Nanchang University, 461 Bayi Avenue, Nanchang City, Jiangxi Province 330006, China* **2** *Key Laboratory of Poyang Lake Environment and Resource Utilization, Ministry of Education, Nanchang University, 1299 Xuefu Avenue, Nanchang City, Jiangxi Province 330031, China*

Corresponding author: *Jie-xin Zou* (jxzou@ncu.edu.cn)

Academic editor: *S. De Grave* | Received 2 June 2019 | Accepted 5 August 2019 | Published 29 August 2019

http://zoobank.org/3E20828E-F1D7-41E9-BA12-0D5F2BD93ED9

Citation: Wang S-b, Zhou X-m, Zou J-x (2019) A new species of freshwater crab of the genus *Mediapotamon* Türkay & Dai, 1997 (Crustacea, Decapoda, Brachyura, Potamidae) from Guizhou, China.. ZooKeys 873: 9–23. https://doi.org/10.3897/zookeys.873.36702

Abstract

A new species of *Mediapotamon* Türkay & Dai, 1997 from a karst system in southwest China is described. The new species can be separated from congeners by the combination of a sharp and distinct epibranchial tooth, the anterolateral region lined with few scattered granules, the terminal segment of the male first gonopod distinctly bent with a constant diameter, and the position of the female vulvae. Mitochondrial 16S rDNA genetic data was used to investigate the systematic position of the new species, which is supported as a new taxon.

Keywords

freshwater crab, *Mediapotamon liboense*, systematics, taxonomy, 16S rDNA

Introduction

China has the highest number of freshwater crab species in the world, with more than 300 species (Dai 1999, Cumberlidge et al. 2011). There are unique karst landforms in Guizhou, China where numerous caves are distributed (Han et al. 2010), and researchers have discovered a number of new freshwater crab species in these caves (Ng and Trontelj 1996, Ng 2017, Huang et al. 2017). To investigate the species diversity of freshwater crabs in this area, the authors conducted scientific investigations twice in 2010 and 2017 to collect specimens of *Chinapotamon* Dai & Naiyanetr, 1994, *Mediapotamon* Türkay & Dai, 1997, *Daipotamon* Ng & Trontelj, 1996, and *Longpotamon* Shih, Huang & Ng, 2016, some of which have already been published (Shih et al. 2016). After morphological comparison of the collected specimens, the specimen from Yaozhai village, Dongtang town, Libo County, Qiannan Buyei and Miao Autonomous Prefecture, was found to be a new species of *Mediapotamon*. This new species is described in this paper, and although also distributed in the karst landforms, is found not in caves but in a hill stream between densely populated mountains. Individuals of this species do not have the characteristics of cave crabs, which determined it as not a karst species but also living in a surrounding karst system. We sequenced the mitochondrial 16S rDNA gene of a specimen and combined the sequence with related reference sequences in GenBank to establish a phylogenetic tree based on Bayesian Inference (BI) and Maximum Likelihood (ML) methods. The molecular data analysis was consistent with the morphological identification results, confirming that it is a new species.

Materials and methods

Specimens were collected from Banzhai Hill, Yaozhai village (25.2128°N, 108.0041°E), Dongtang town, Lino County, Qiannan Buyei and Miao Autonomous Prefecture, Guizhou Province; preserved in 95% ethanol; and deposited at the Department of Parasitology of the Medical College of Nanchang University, Jiangxi, China (**NCU MCP**). Comparative materials were deposited at the Sun Yat-sen Museum of Biology, Sun Yat-sen University, Guangzhou, China (**SYSBM**) and the Institute of Zoology, Chinese Academy of Sciences, Beijing, China (**IZCAS CB**). Carapace width and length were measured in millimetres. The abbreviations **G1** and **G2** refer to the first and second gonopods, respectively. The terminology used herein primarily follows that of Dai (1999) and Davie et al. (2015).

Pereiopod muscle tissue was extracted from specimens of the new species with a DP1902 Tissue Kit (BioTeke Inc., Beijing). The mitochondrial 16S rDNA gene was obtained by PCR amplification with the primers 1471 (5'-CCTGTTTANCAAAAACAT-3') and 1472 (5'-AGATAGAAACCAACCTGG-3') (Shih et al. 2004). The PCR extension procedure is as follows: denaturation for 50 s at 94 °C, 33 cycles of annealing for 40 s at 52 °C and extension for 1 min at 72 °C and a final extension for 10 min at 72 °C. The PCR products were sequenced on an ABI 3730 automatic sequencer.

For molecular data analysis, the mitochondrial 16S rDNA from 52 species in 41 genera was used to construct a phylogenetic tree (Table 1). Sequences were aligned using MAFFT ver. 7.215 (Katoh and Standley 2013) based on the G-INS-I method. The best model for BI analysis was GTR+ I + G, which was determined by ModelGenerator ver. 8.5.1 (Katoh and Standley 2013) and the Bayesian information criterion (BIC). The BI tree was constructed by MrBayes ver. 3.2.6 (Ronquist et al. 2012). Four Markov chain Monte Carlo (MCMC) chains were run for 2000000 generations, with samples stored every 1000 generations, and the first 25% were discarded as burn-in. The effective sample size (ESS) values were checked by TRACER ver. 1.6 (Rambaut and Drummond 2013) (all ESSs were greater than 200). The best evolutionary model for ML analysis was HKY+I+G, as determined by MEGA 7.0 (Kumar et al. 2016) and ModelTest ver. 3.7 (David 2003) based on the Akaike information criterion (AIC) standard. A ML tree was built based on 1000 bootstrap replicates in MEGA 7.0 (Kumar et al. 2016).

Taxonomy

Family Potamidae Ortmann, 1896
Mediapotamon Türkay & Dai, 1997

Mediapotamon liboense sp. nov.

http://zoobank.org/69B0792B-F233-403A-ADC2-6666B007F093

Figs 1–5

Type locality. China, Guizhou Province: Qiannan Bouyei and Miao Autonomous Prefecture, Lino County, Dongtang Town, Yaozhai Village, Banzhai Hill, 25.2128°N, 108.0041°E, under rock in small hill stream.

Type specimen. Holotype male, with gonopods in a separate microvial. Original label: "China, Guizhou Province: Qiannan Bouyei and Miao Autonomous Prefecture, Lino County, Dongtang Town, Yaozhai Village, Banzhai Hill, 25.2128°N, 108.0041°E, 10 Oct. 2010, Xian-min Zhou", "NCU MCP 343001". Paratypes, male, same collection data as for holotype, "NCU MCP 343002"; female, same collection data as for holotype, "NCU MCP 343003".

Material examined. Holotype. CHINA • ♂, NCU MCP 343001, 24.2 × 19.6 mm, Guizhou Province, Qiannan Bouyei and Miao Autonomous Prefecture, Lino County, Dongtang Town, Yaozhai Village, Banzhai Hill, under rock in small hill stream, catch by hand, 10 Oct 2010, Xian-min Zhou leg.

Paratypes. ♂, NCU MCP 343002,19.4 × 15.6 mm • ♀, NCU MCP 343003, 23.4 × 19.0 mm, same collection data as for holotype.

Other material. ♂, NCU MCP 343004, 30.9 × 24.7 mm • 4 ♀♀; NCU MCP 343005, 21.5 × 16.8mm; NCU MCP 343006, 19.2 × 14.6 mm; NCU MCP 343007, 25.0 × 20.0 mm; NCU MCP 343008, 20.0 × 15.8 mm; same collection data as for holotype.

Comparative material. *Mediapotamon angustipedum* (Dai & Song, 1982): 2 ♂♂; IZCAS CB 00995, 15.3 × 13.1 mm; IZCAS CB 00988, 18.4 × 16.0 mm; Guangxi Zhuang Autonomous Region, Baise City, Jingxi County, Hurun Town, Xinxing Village, 7 Oct 1978. *Mediapotamon leishanense* (Dai, 1995): 1♂, IZCAS CB 05181, 14.8 × 11.5 mm, Guizhou Province, Qiandongnan Miao and Dong

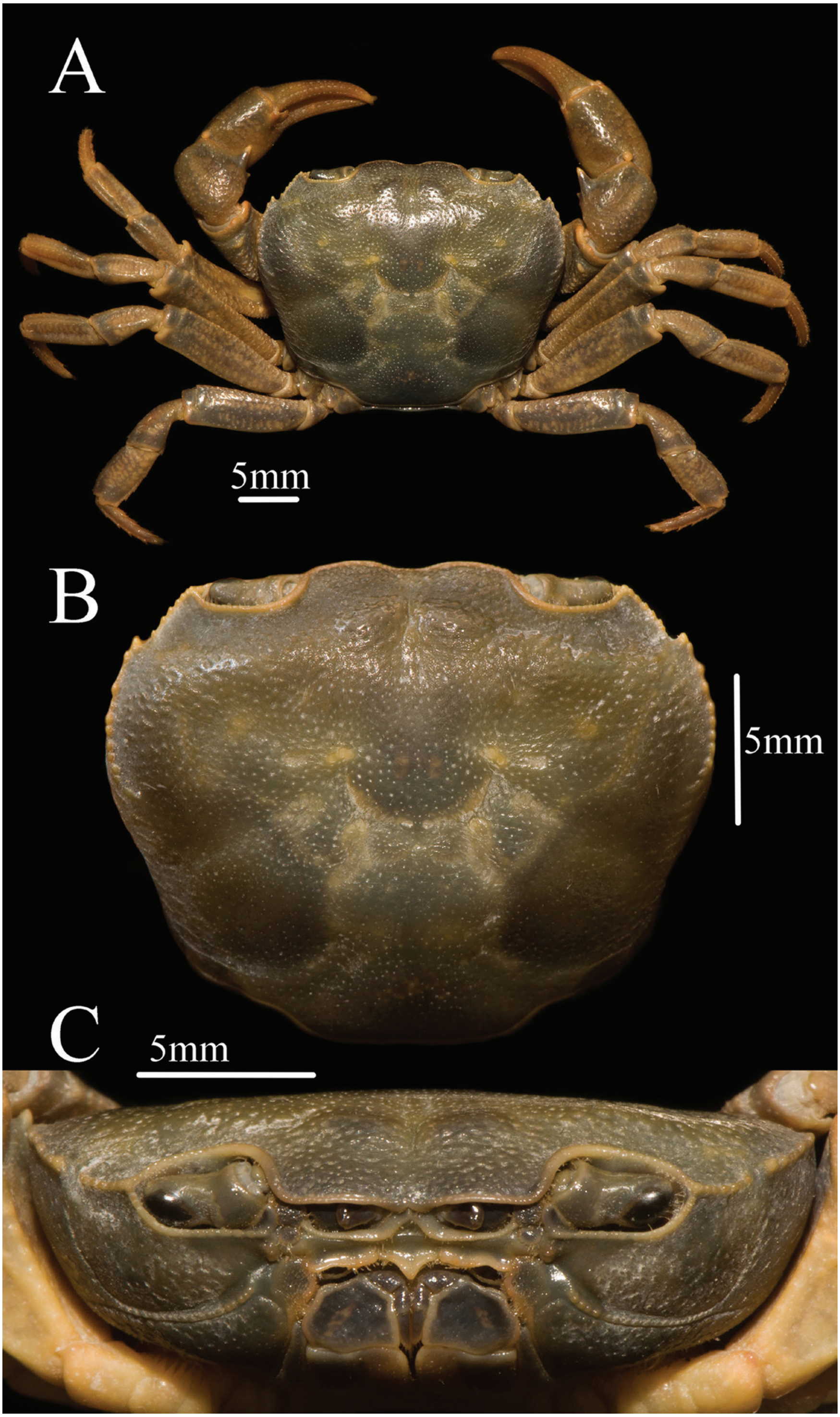

Figure 1. *Mediapotamon liboense* sp. nov. Holotype male (24.2 × 19.6 mm) (NCU MCP 343001). **A** overall habitus **B** dorsal view of carapace **C** frontal view of cephalothorax.

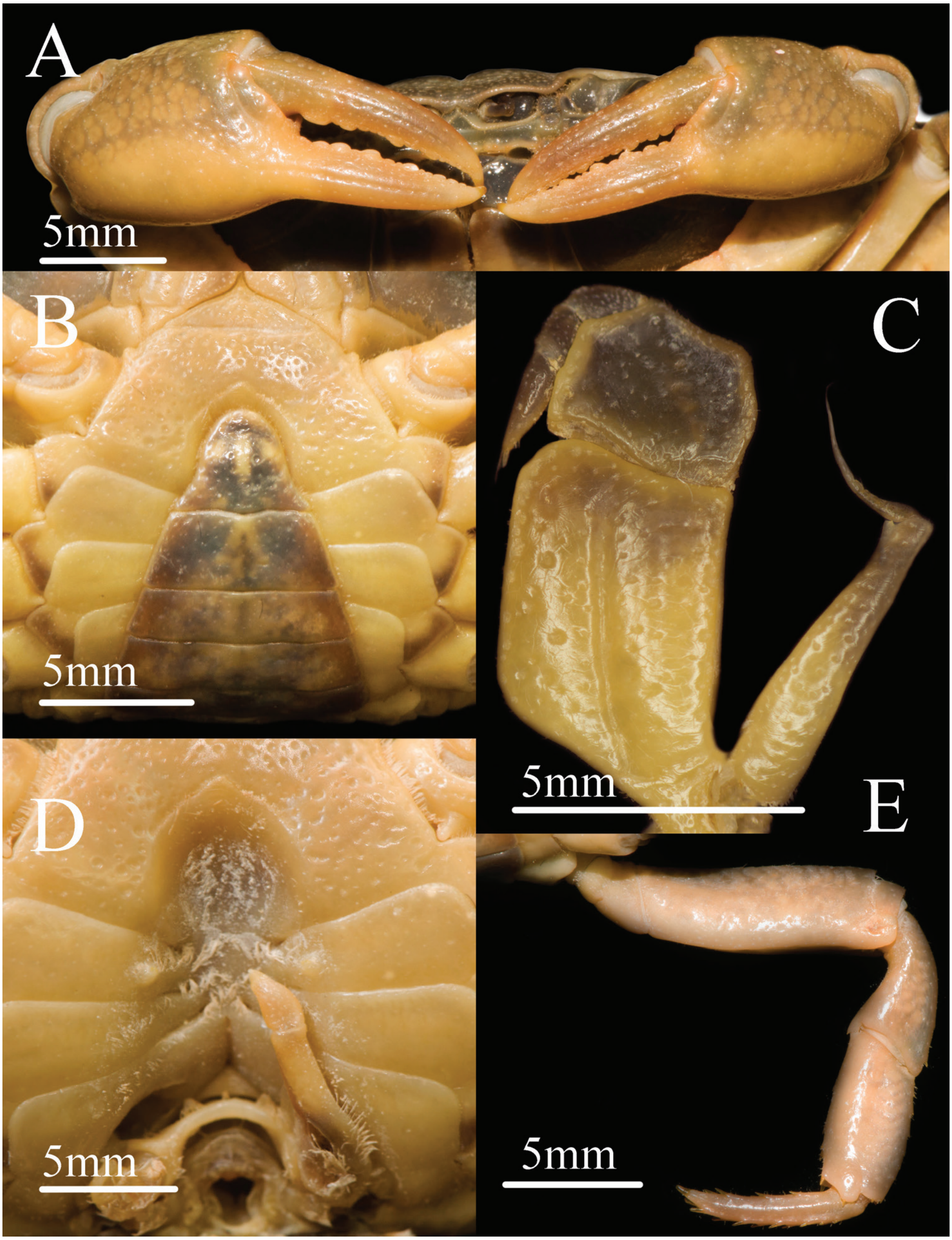

Figure 2. *Mediapotamon liboense* sp. nov. Holotype male (24.2 × 19.6 mm) (NCU MCP 343001). **A** outer view of chelipeds **B** ventral view of anterior thoracic sternum and pleon **C** left third maxilliped **D** ventral view of sterno-pleonal cavity with left G1 in situ **E** right fourth ambulatory leg, low view.

Autonomous Prefecture, Leishan County, Leigong Mountain, 23 Apr. 1988; 1♂, SYSBM 001094, 15.5 × 12.4 mm, Guizhou Province, Qiannan Bouyei and Miao Autonomous Prefecture, Lino County, coll. C. Huang, Jul 2013. *Mediapotamon* sp. nov. (sequence number LC155165 in Fig. 8): 1♂, SYSBM 001255, 26.7 ×

21.4 mm, 1 ♀, SYSBM 001259, 17.5 × 13.6 mm, Guizhou Province, Qiannan Bouyei and Miao Autonomous Prefecture, Lino County, coll. C. Huang, Jul 2013. *Daipotamon minos* (Ng & Trontelj, 1996): 1♂, NCU MCP 195501, 20.1 × 16.3 mm, 1 ♀, NCU MCP 195502, 18.8 × 15.1 mm, Guizhou Province, Qiannan Bouyei and Miao Autonomous Prefecture, Lino County, Chaoyang Town, Buyong Village, coll. L. J. Yang, 17 Jul 2010.

Diagnosis. Carapace trapezoidal, regions indistinct, dorsal surface flat, epigastric cristae indistinct, postorbital cristae convex, cervical groove indistinct, H-shaped groove inconspicuous (Figs 1A, B, 3A). External orbital angle triangular, epibranchial tooth sharp, anterolateral margin lined with scattered granules, posterolateral surface smooth (Figs 1A, B, 3A). Third maxilliped exopod with slender flagellum, extending equal to width of merus (Fig. 1C). Male pleon narrow triangular, telson with arc-shaped apex in male (Fig. 2B). G1 slender, terminal segment bend inwards obviously in sub-proximal portion with constant diameter, G1 terminal segment oblique toward dorsal in mesial view in the demarcation between G1/G2 (Figs 4A, F, 7A). Proximal part of G2 sub-ovate (Fig. 4C). Female vulva large-sized, not reaching suture sternites 5/6, vulval membrane extending outward (Fig. 3B).

Description. Carapace: outline trapezoidal, width 1.2–1.3 × length (n = 8); dorsal surface flat with numerous pits, anterolateral region wrinkled (Figs 1A, B, 3A). Epigastric cristae indistinct; cervical groove shallow, indistinct; H shaped groove between gastric and cardiac regions inconspicuous (Figs 1A, B, 3A). Postorbital cristae slightly convex, not fused with epigastric cristae, separate with epibranchial tooth (Figs 1A, B, 3A). External orbital angle bluntly triangular, separate with anterolateral margin by conspicuous gap (Figs 1A, C, 3A). Epibranchial tooth sharp, distinct; anterolateral margin convex laterally, cristae, lined with approximately 9 or10 scattered granules (Figs 1A, B, 3A). Posterolateral surface smooth, with inconspicuous oblique striae, posterolateral margins converging posteriorly (Figs 1A, B, 3A). Orbits medium-size; supraorbital margin cristate and lateral portion, infraorbital margins lined with scattered inconspicuous granules (Fig. 1C). Sub-orbital, sub-hepatic and pterygostomial regions covered with low round granules (Fig. 1C). Epistome posterior margin slightly oblique laterally, with broadly triangular median lobe (Fig. 1C).

Third maxilliped: exopod reaching proximal 1/3 of merus length, with slender flagellum extending equal to width of merus (Figs 1C, 2C). Merus subquadrate, 1.3 times as broad as long, generally flat (Figs 1C, 2C). Ischium trapezoidal, 1.4 times as long as broad, with distinct median sulcus (Fig. 2C).

Chelipeds (pereiopod 1): slightly unequal (Fig. 2A). Merus surface smooth; carpus surface with pits and a sharp spine at inner-distal angle (Figs 1A, 3A). Palm of larger chela length 1.4 × height in males (n = 3), 1.5–1.6 × in females (n = 5); dactylus 1 × palm length in males (n = 3), 0.9–1 × in females (n = 5); dactylus as long as pollex (Figs 1A, 2A, 3A). Inner margin of fingers with few round blunt teeth, with little gap when fingers closed (Fig. 2A).

Ambulatory legs (pereiopods 2–5): slender; pereiopod 3 merus 0.5 × carapace length in males (n = 3), 0.4 × carapace length in females (n = 5) (Figs 1A, 3A). Pereio-

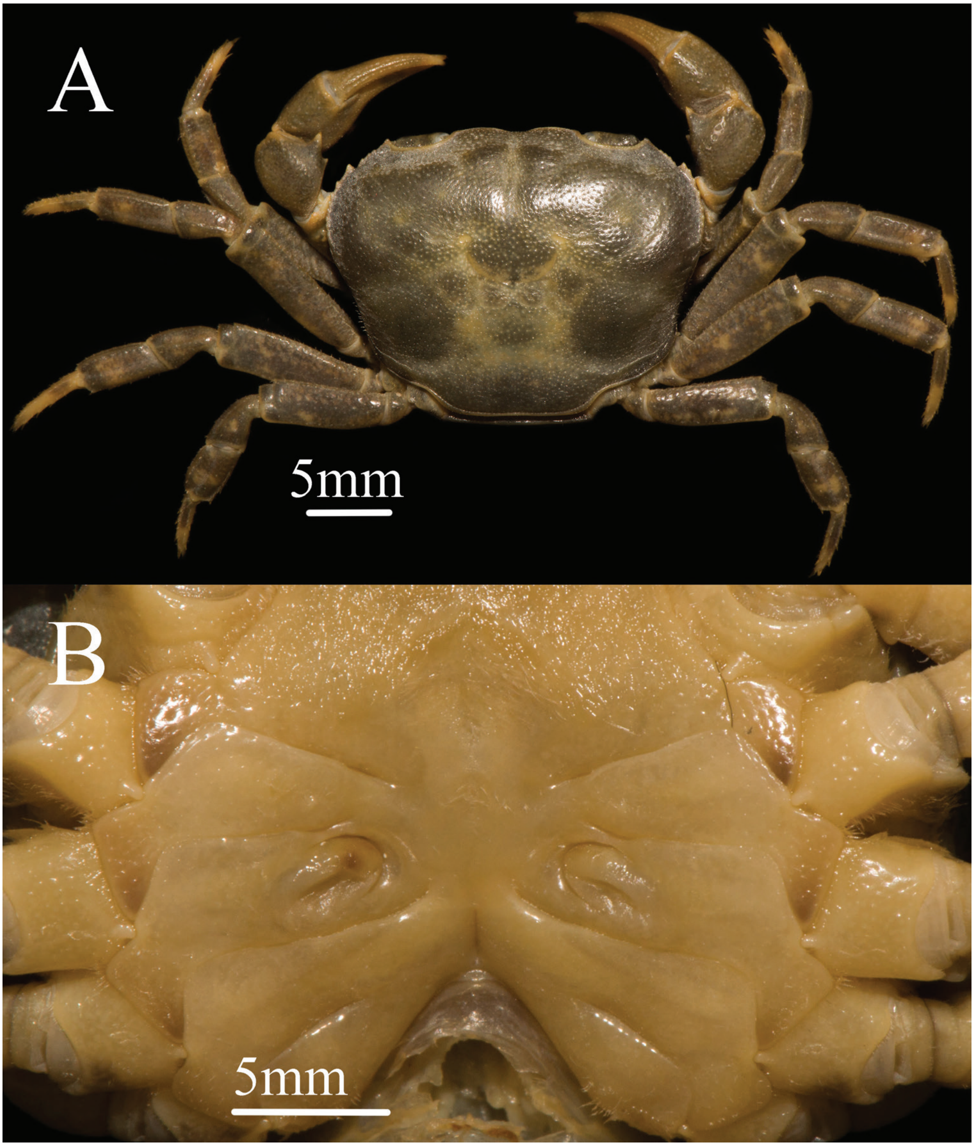

Figure 3. *Mediapotamon liboense* sp. nov. Paratype female (23.4 × 19.0 mm) (NCU MCP 343003). **A** overall habitus **B** ventral view of thoracic sternum and vulvae.

pods 5 propodus 1.9 × as long as broad in males (n = 3), 1.9–2.1 × as long as broad in females (n = 5) (Fig. 2E); shorter than dactylus (n = 8) (Figs 1A, 2E, 3A).

Male thoracic sternum: flat and covered with pits; sternites 2-4 broad, width ca. 2 × length; sternites 2 very broad triangular with sharp apex; suture between sternites 2/3 transverse, clear; sternites 3/4 fused but with slight oblique demarcation superficially (Fig. 2B). Male sterno-pleonal cavity deep and narrow, barely reaching anteriorly to level of mid-length of cheliped coxae base; median longitudinal groove present be-

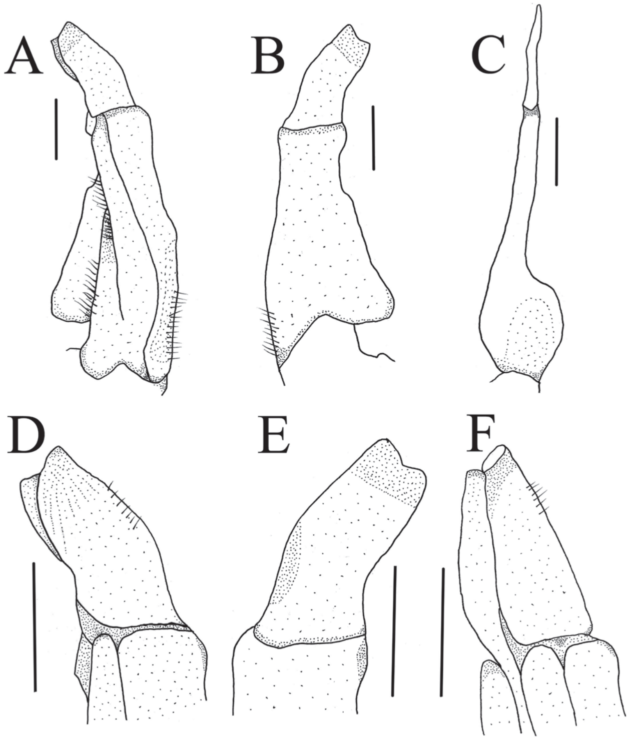

Figure 4. *Mediapotamon liboense* sp. nov. Holotype male (24.2 × 19.6 mm) (NCU MCP 343001). **A** ventral view of the left G1 **B** dorsal view of the left G1 **C** ventral view of the left G2 **D** ventral view of the terminal segment of left G1 **E** dorsal view of the terminal segment of left G1 **F** mesial view of the terminal segment of left G1. Scale bars: 1 mm (**A–F**).

tween sternites 7 and 8 medium in length; male pleonal locking tubercle position at middle of sternite 5 (Fig. 2D).

Male pleon: narrow triangular (Fig. 2B); somites 4-6 progressively narrowed distally, lateral margins oblique; telson width 1.3 × length with arc-shaped apex in males (n = 3); somite 6 width 2.4 × length in males (n = 3) (Fig. 2B).

G1: slender (Figs 4A, 7A); terminal segment bend inwards obviously in the subproximal portion with constant diameter, distal end reaching but not beyond pleonal locking tubercle *in situ* (Fig. 2D); subterminal segment length 2.9 × length of terminal segment (Figs 4A, 7A). The mesial view of G1 terminal segment not straight but oblique toward dorsal in the demarcation between G1/G2 (Fig. 4F). Basal segment of G2 sub-ovate, subterminal segment length 1.8 × length of distal segment, the distal segment is slender and sharp (Fig. 4C).

Female vulva: large, not reaching sternites 5/6 in situ, with the opening outward and the outer membrane extending outward (Fig. 3B). Reaching approximate three-fifths width of sternite 6 and the position generally distantly each other (Fig. 3B).

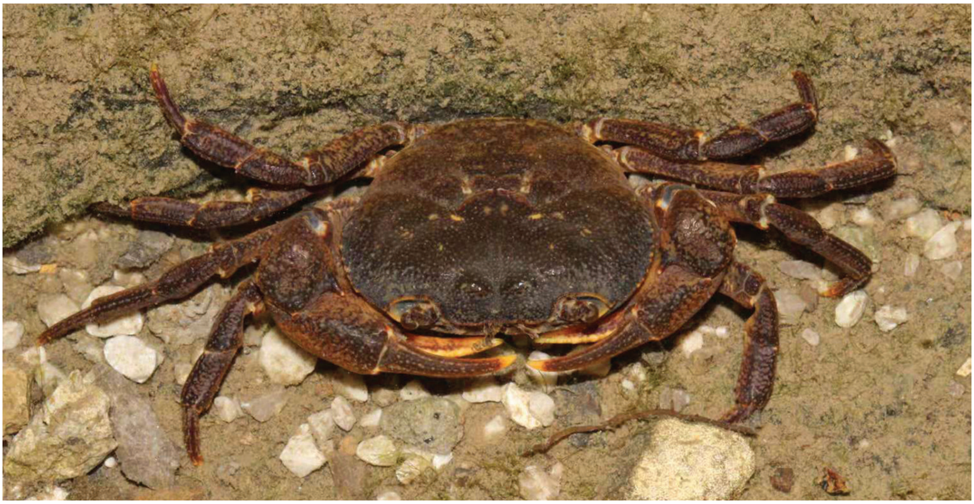

Figure 5. *Mediapotamon liboense* sp. nov. Colour in life, not collected (photograph by Chao Huang).

Etymology. The species is named after the type locality, Libo County, Qiannan Bouyei and Miao Autonomous Prefecture, Guizhou Province.

Colour in life. The overall colour is brownish black, which is similar to the colour of the surrounding environment (Fig. 5).

Distribution. The new species is presently known only from the type locality: Libo County, Qiannan Bouyei and Miao Autonomous Prefecture, Guizhou Province.

Ecology. This species lives in karst mountain locations surrounded by low crests and covered with diverse vegetation (Figs 6A, B). The species lives along the stream flowing down the mountain and remains hidden under rocks during the day.

Remarks. The new species fits the characteristics of *Mediapotamon* Türkay & Dai, 1997, viz., carapace intermediate or small in size (15–20 mm), surface smooth without a conspicuous bulge or depression, anterolateral margin lined with granules, male telson triangular, and G1 slender without any projection and reaching the pleonal locking tubercle *in situ* (Türkay and Dai 1997). *Mediapotamon liboense* sp. nov. is similar to *M. angustipedum* (Dai & Song, 1982), *M. leishanense* Dai, 1995, and *Daipotamon minos*, Ng & Trontelj, 1996, but the new species can be differentiated from its congeners by some distinct characters: epibranchial tooth sharp and distinct, anterolateral margin lined with a few scattered granules [versus sharp and distinct in *M. angustipedum* but blunt and indistinct in *M. leishanense*, both lined with numerous inseparable granules (cf. Table 2)]; shape of the male telson narrow triangular [versus broad triangular in congeners (cf. Table 2, Fig. 7)]; and shape of G1 slender, terminal segment distinctly bent with a constant diameter [versus very slender, terminal segment straight and thinner gradually in *M. angustipedum* and very slender, terminal segment bent obviously and thinner gradually in *M. leishanense* (cf. Table 2, Fig. 7)]. Its differences compared to *D. minos* can be found in Table 2 and Figure 7.

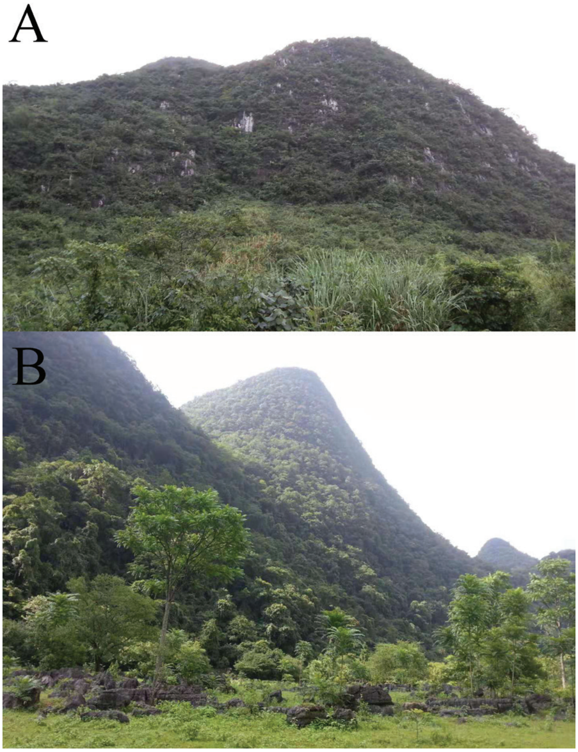

Figure 6. Karst terrain of Libo County (photographs by Chao Huang).

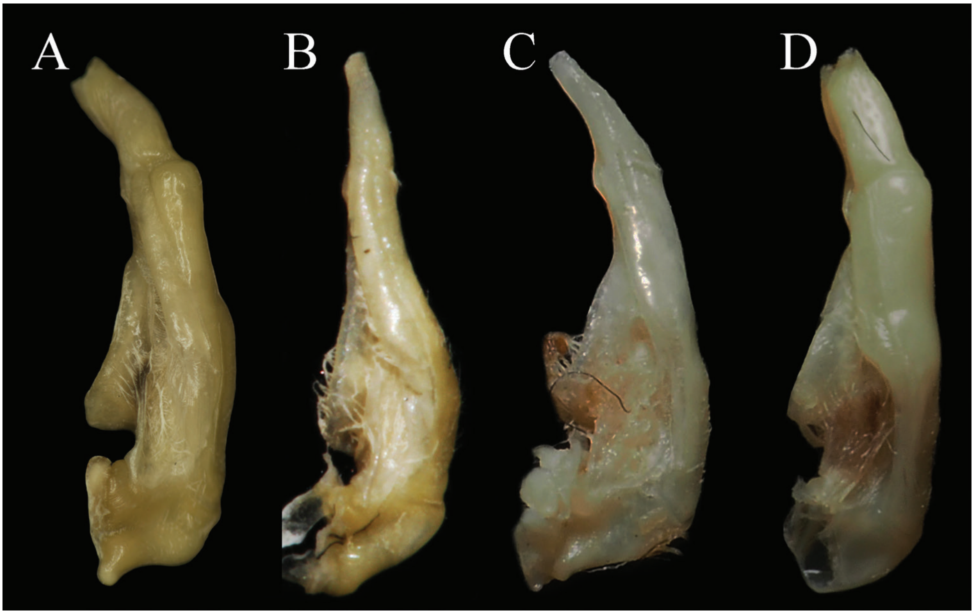

Figure 7. Left G1s. **A** *Mediapotamon liboense* sp. nov. NCU MCP, 24.2 × 19.6 mm **B** *M. angustipedum* (Dai & Song, 1982), IZCAS CB 00995, 15.3 × 13.1 mm **C** *M. leishanense* Dai, 1995, IZCAS CB 05181,14.8 × 11.5 mm **D** *Daipotamon minos*, Ng & Trontelj, 1996, NCU MCP 195501, 20.1 × 16.3 mm.

DNA analyses and discussion

We used the mitochondrial 16S rDNA gene sequence for phylogenetic analyses, and 52 species from 41 potamid genera were included (Table 1), using BI and ML analyses to construct phylogenetic trees with support values. The results are shown in Figure 8, and both analysis methods support most of the clades (Shih et al. 2009). The new species clusters with the same species as *M. liboense* and *M. leishanense* (specimen collected by Chao Huang in the Maolan Nature Reserve of Libo County in July 2013). After discussion with Huang, we think that the other new species of *Mediapotamon* with sequence number is LC155165 and *M. liboense* sp. nov. are the same species, although

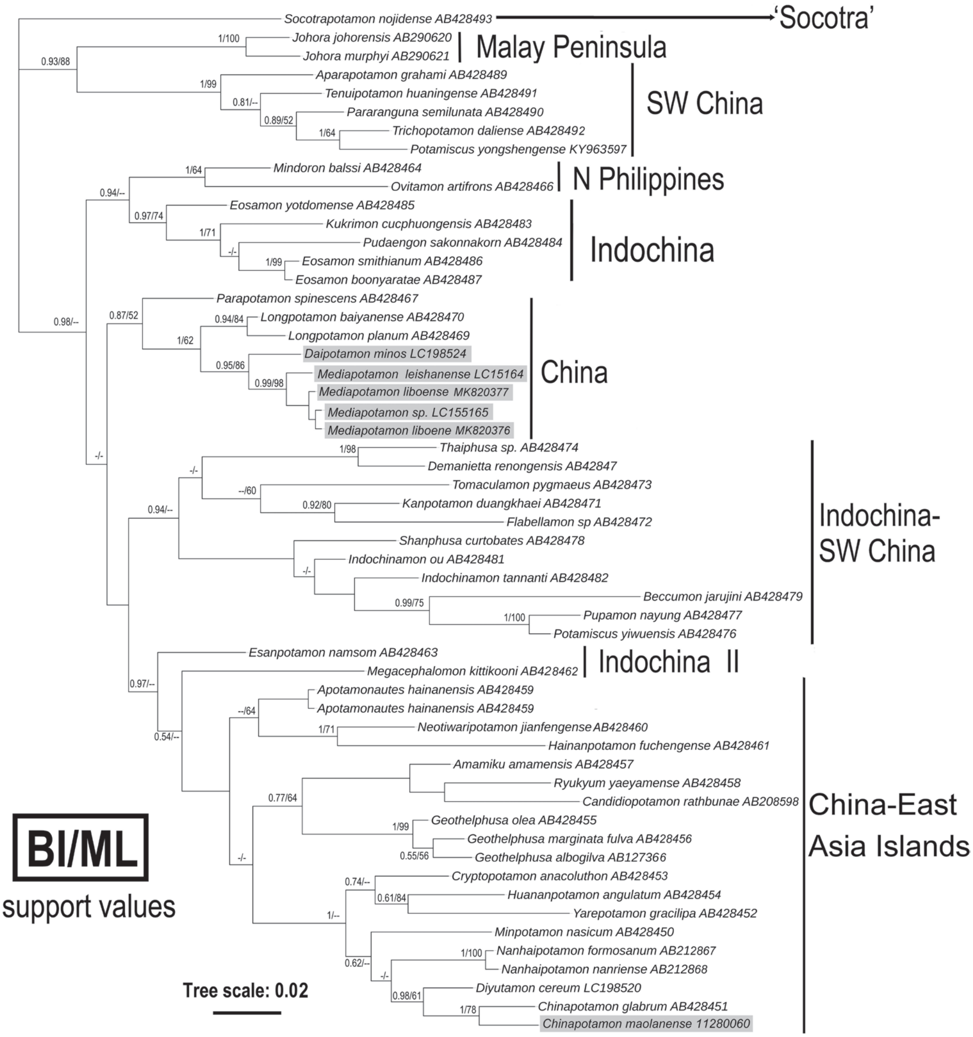

Figure 8. A Bayesian inference (BI) tree based on 16S rDNA with the sequences and accession numbers from Shih et al. (2009) with some additional species from Guizhou. The species collected from the type locality and its surroundings are highlighted in grey. The probability values at the nodes represent support values for BI and maximum likelihood (ML). Only values > 50% are displayed.

Table 1. The 16S rDNA of 52 species from 41 genera of the family Potamidae from Asia. All sequences retrieved from GenBank except for the new species described herein.

Species	Museum catalogue number	Locality	GenBank number
Amamiku amamense (Minei, 1973)	NCHUZOOL 13125	Amami, the Ryukyus	AB428457
Aparapotamon grahami (Rathbun, 1929)	ZRC YCM 0334(II)	Yunnan, China	AB428489
Apotamonautes hainanensis (Parisi, 1916)	ZRC	Hainan, China	AB428459
Beccumon jarujini (Ng & Naiyanetr, 1993)	ZRC 1991.1865 (paratype)	Chiangma, Thailand	AB428479
Candidiopotamon rathbunae (De Man, 1914)	NCHUZOOL	Nantou, Taiwan	AB208598
Chinapotamon glabrum (Dai, Song, Li & Liang, 1980)	CAS	Guangxi, China	AB428451
Chinapotamon maolanense Zou, Bai & Zhou, 2018	NCU MCP 196101	Guizhou, China	11280060
Cryptopotamon anacoluthon (Kemp, 1918)	NCHUZOOL 13122	Hong Kong	AB428453
Daipotamon minos Ng & Trontelj, 1996	ZRC	Guizhou, China	LC198524
Demanietta renongensis (Rathbun, 1905)	ZRC 1998.146	Ranong, Thailand	AB428475
Diyutamon cereum Huang, Shih & Ng, 2017	SYSBM	Guizhou, China	LC198520
Eosamon boonyaratae (Naiyanetr, 1987)	ZRC 1991.1861	Trat, Thailand	AB428487
Eosamon smithianum (Kemp, 1923)	ZRC	Chantaburi, Thailand	AB428486
Eosamon yotdomense (Naiyanetr, 1984)	ZRC 1991.1851	Ubon Ratchathani, Thailand	AB428485
Esanpotamon namsom Naiyanetr & Ng, 1997	ZRC 1997.776 (paratype)	Udon Thani, Thailand	AB428463
Flabellamon sp.	ZRC	Mae Sot, Thailand	AB428472
Geothelphusa albogilva Shy, Ng & Yu, 1994	NCHUZOOL	Pingtung, Taiwan	AB127366
Geothelphusa marginata fulva Naruse, Shokita & Shy, 2004	NCHUZOOL 13124	Iriomote, the Ryukyus	AB428456
Geothelphusa olea Shy, Ng & Yu, 1994	NCHUZOOL 13123	Taichung, Taiwan	AB428455
Hainanpotamon fuchengense Dai, 1995	NCHUZOOL 13128	Hainan, China	AB428461
Huananpotamon angulatum (Dai & Lin, 1979)	ZRC	Fujian, China	AB428454
Indochinamon ou (Yeo & Ng, 1998)	ZRC	Phongsali, Laos	AB428481
Indochinamon tannanti (Rathbun, 1904)	ZRC 1998.264	Yunnan, China	AB428482
Johora johorensis (Roux, 1936)	ZRC 1990.576	Gunung Pulai, Johor, Malaysia	AB290620
Johora murphyi Ng, 1986	ZRC 2001.2267	Kota Tinggi, Johor, Malaysia	AB290621
Kanpotamon duangkhaei Ng & Naiyanetr, 1993	ZRC	Kanchanaburi, Thailand	AB428471
Kukrimon cucphuongense (Dang, 1975)	ZRC NHH9729 160997	Ninh Binh, Vietnam	AB428483
Longpotamon baiyanense Ng & Dai, 1997	ZRC	Hunan, China	AB428470
Longpotamon planum Dai, 1992	ZRC 1998.1178	Anhui, China	AB428469
Mediapotamon leishanense Dai, 1995	SYSBM001094	Guizhou, China	LC155164
Mediapotamon liboense sp. nov.	NCU MCP 343004	Guizhou, China	MK820377
Mediapotamon liboense sp. nov.	NCU MCP 343008	Guizhou, China	MK820376
Mediapotamon sp. nov., leg. Chao Huang	SYSBM001259	Guizhou, China	LC155165
Megacephalomon kittikooni (Yeo & Naiyanetr, 1999)	ZRC 1998.22 (holotype)	Xieng Khuang, Laos	AB428462
Mindoron balssi (Bott, 1968)	ZRC	Mindoro, the Philippines	AB428464
Minpotamon nasicum (Dai & Chen, 1979)	NCHUZOOL 13121	Fujian, China	AB428450
Nanhaipotamon formosensis (Parisi, 1916)	NCHUZOOL 13144	Tainan, Taiwan	AB212867
Nanhaipotamon nanriense Dai, 1997	CAS CB05103	Fujian, China	AB212868
Neotiwaripotamon jianfengense Dai & Naiyanetr, 1994	NCHUZOOL 13127	Hainan, China	AB428460

Ovitamon artifrons (Bürger, 1894)	ZRC	Luzon, the Philippines	AB428466
Parapotamon spinescens (Calman, 1905)	NCUDP	Yunnan, China	AB428467
Pararanguna semilunatum Dai & Chen, 1985	ZRC	Yunnan, China	AB428490
Potamiscus yiwuensis Dai & Cai, 1998	ZRC	Yunnan, China	AB428476
Potamiscus yongshengense Dai & Chen, 1985	NNU150951	Yunnan, China	KY963597
Pudaengon sakonnakorn Ng & Naiyanetr, 1995	ZRC	Thailand	AB428484
Pupamon nayung (Naiyanetr, 1993)	ZRC 1995.558 (paratype)	Udon Thani, Thailand	AB428477
Ryukyum yaeyamense (Minei, 1973)	NCHUZOOL 13126	Iriomote, the Ryukyus	AB428458
Shanphusa curtobates (Kemp, 1918)	NRM 13920	Taunggyi, Shan State, Myanmar	AB428478
Socotrapotamon nojidensis Apel & Brandis, 2000	ZRC 2000.2232	Socotra, Yemen	AB428493
Tenuipotamon huaningense Dai & Bo, 1994	CAS CB05175	Yunnan, China	AB428491
Thaiphusa sp.	ZRC 1997.656	Thailand	AB428474
Tomaculamon pygmaeus Yeo & Ng, 1997	ZRC 1997.326-330 (paratype)	Phitsanulok, Thailand	AB428473
Trichopotamon daliense Dai & Chen, 1985	NCHUZOOL 13130	Yunnan, China	AB428492
Yarepotamon gracilipa (Dai, Song, Li & Liang, 1980)	ZRC	Guangxi, China	AB428452

Key to institutional abbreviations: CAS, The Chinese Academy of Sciences, Beijing, China; NCHUZOOL, Zoological Collections of the Department of Life Science, National Chung Hsing University, Taichung, Taiwan; NCUDP, Department of Parasitology, Nanchang University, Jiangxi, China; NRM, Swedish Museum of Natural History, Stockholm, Sweden; ZRC, Zoological Reference Collection of the Raffles Museum of Biodiversity Research, National University of Singapore, Singapore.

the two specimens were collected separately. In the phylogenetic tree, *Daipotamon* is clustered with *Mediapotamon* in two separate branches, and the phylogenetic relationships between the new species and *Chinapotamon maolanense*, which was also collected in Libo County, are distant (Fig. 8)

Despite the new species clustering with congeners and *Daipotamon* in the larger clade, the genetic distance suggests that the congeners are closer, while *Daipotamon* is farther away. For the habitat, *Daipotamon* lives in limestone formations and collected from one of karst caves and was determined as a karst species (Ng and Trontelj 1996), while the new species lives in hill streams, which is consistent with congeners, so the new species can be separated from *Daipotamon* in morphology, phylogenetic analyses, and ecology (Table 2, Fig. 8). *Mediapotamon* contains *M. leishanense* and *M. angustipedum* (Dai 1999), but we were unable to obtain molecular data for the latter, so its phylogenetic relationship with the new species is unclear. From molecular and morphological data, it is distinct from *M. leishanense.* Although there is no molecular data for *M. angustipedum*, the distinct morphological differences and more than 400 kilometres geographical distance separate the new species from *M. angustipedum* clearly. Morphological differences among the three *Mediapotamon* species, including the new species described in this study, are described in detail (Table 2).

Before our study, only three new species, namely *Diyutamon cereum*, *Qianguimon elongatum*, and *Chinapotamon maolanense*, collected in Guizhou had been published in the past 20 years (Huang et al. 2017, Huang 2018, Zou et al. 2018), implying that the freshwater crabs in this area still have high taxonomic research value. With the new species presently described, there are now 31 species of 13 potamid genera in Guizhou (Shih and Ng 2011).

Table 2. Differences between *Mediapotamon liboense* sp. nov., *M. angustipedum* (Dai & Song, 1982), *M. leishanense* Dai, 1995 and *Daipotamon minos*, Ng & Trontelj, 1996.

Character/ Species	*M. liboense* sp. nov.	*M. angustipedum*	*M. leishanense*	*Daipotamon minos*
Carapace	Flat, cervical groove indistinct	Swollen, cervical groove indistinct	Flat, cervical groove distinct	Slightly swollen, cervical groove distinct
Epibranchial tooth	Sharp, distinct	Sharp, distinct	Blunt, indistinct	Blunt, indistinct
Anterolateral margin	Lined with scattered granules	Lined with numerous inseparable granules	Lined with numerous inseparable granules	Lined with numerous inseparable granules
Shape of male telson	Narrow triangular	Broad triangular	Broad triangular	Tongue-shape
G1 *in situ*	Reaching pleonal locking tubercle	Reaching pleonal locking tubercle	Reaching pleonal locking tubercle	Not reaching pleonal locking tubercle
Shape of G1	Slender, terminal segment obviously bent with constant diameter	Very slender, terminal segment straight and gradually narrowing	Very slender, terminal segment obviously bent and gradually narrowing	Stout, terminal segment slightly bent with constant diameter
Female vulvae	Large-sized, not reaching sternites 5/6 in situ	Medium-sized, reaching sternites 5/6 in situ	Large-sized, reaching sternites 5/6 in situ	Medium-sized, not reaching sternites 5/6 in situ

Acknowledgements

The present study is supported by the National Sharing Service Platform for Parasite Resources (TDRC-22), the National Natural Science Foundation of China (No. 31560179, 31460156), the Natural Science Foundation of Jiangxi Province (No. 20171BAB205108), Nanchang University College Students' Innovation and Entrepreneurship Training Program (No. 2018388). Thanks are due to Chao Huang, who also collected a specimen, for providing several original materials for the images and for appraising the new species when we identified it. We also thank Ya-Nan Zhang and Meng-Jun Zhao for their help in the molecular work and Xin-Nan Jia and Shu-Xin Xu for their help in constructing the phylogenetic tree.

References

Cumberlidge N, Ng PKL, Yeo DCJ, Naruse T, Meyer KS, Esser LJ (2011) Diversity, endemism and conservation of the freshwater crabs of China (Brachyura: Potamidae and Gecarcinucidae). Integrative Zoology 6(1): 45–55. https://doi.org/10.1111/j.1749-4877.2010.00228.x

Dai AY (1999) Fauna Sinica: Arthropoda Crustacea Malacostraca Decapoda Parathelphusidae Potamidae. Science Press, Beijing. [in Chinese with English summary]

David P (2003) Using MODELTEST and PAUP* to select a model of nucleotide substitution. Current protocols in bioinformatics, 6: Unit 6.5. https://doi.org/10.1002/0471250953.bi0605s00

Davie PJF, Guinot D, Ng PKL (2015) Anatomy and functional morphology of Brachyura. In: Castro P, Davie PJF, Guinot D, Schram FR, von Vaupel Klein JC (Eds) Treatise on Zoology – Anatomy, Taxonomy, Biology. The Crustacea. Volume 9C–I. Decapoda: Brachyura, 1049–1130. https://doi.org/10.1163/9789004190832

Han G, Tang Y, Wu Q (2010) Hydrogeochemistry and dissolved inorganic carbon isotopic composition on karst groundwater in Maolan, southwest China. Environmental Earth Sciences 60: 893–899. https://doi.org/10.1007/s12665-009-0226-y

Huang C (2018) Revision of *Yarepotamon* Dai & Türkay, 1997 (Brachyura: Potamidae), freshwater crabs endemic to southern China, with descriptions of two new genera and four new species. Journal of Crustacean Biology 38: 173–189. https://doi.org/10.1093/jcbiol/rux120

Huang C, Shih HT, Ng PKL (2017) A new genus and new species of Potamidea (Crustacea: Decapoda: Brachyura: Potamoidae), the first stygomorphic cave crab known from china and east Asia. Zootaxa 4232: 71–84. https://doi.org/10.11646/zootaxa.4232.1.5

Katoh K, Standley DM (2013) MAFFT multiple sequence alignment software version 7: Improvements in performance and usability. Molecular Biology and Evolution 30: 772–780. https://doi.org/10.1093/molbev/mst010

Kumar S, Stecher G, Tamura K (2016) MEGA7: Molecular evolutionary genetics analysis version 7.0 for bigger datasets. Molecular Biology and Evolution 33: 1870–1874. https://doi.org/10.1093/molbev/msw054

Ng PKL (2017) Descriptions of two new cavernicolous species of *Chinapotamon* Dai & Naiyanetr, 1994 (Crustacea: Brachyura: Potamidae) from China. Crustacean Research 46: 1–16. https://doi.org/10.18353/crustacea.46.01

Ng PKL, Trontelj P (1996) *Daipotamon minos*, a new genus and species of potamid crab (Crustacea: Decapoda: Brachyura) from a cave in China. Proceedings of the Biological Society of Washington 109(3): 476–481.

Rambaut A, Drummond AJ (2013) Tracer v1.6. http://beast.bio.ed.ac.uk/Tracer

Ronquist F, Teslenko M, van der Mark P, Ayres DL, Darling A, Hohna S (2012) MrBayes 3.2: Efficient Bayesian phylogenetic inference and model choice across a large model space. Systematic Biology 61: 539–542. https://doi.org/10.1093/sysbio/sys029

Shih HT (2004) Systematics of the Genus *Geothelphusa* (Crustacea, Decapoda, Brachyura, Potamidae) from Southern Taiwan: A Molecular Appraisal. Zoological Studies 43: 561–570.

Shih HT, Darren CJY, Ng PKL (2009) The collision of the Indian plate with Asia: molecular evidence for its impact on the phylogeny of freshwater crabs (Brachyura: Potamidae). Journal of Biogeography 36: 703–719. https://doi.org/10.1111/j.1365-2699.2008.02024.x

Shih HT, Huang C, Ng PKL (2016) A re-appraisal of the widely-distributed freshwater crab genus *Sinopotamon* Bott, 1967, from China, with establishment of a new genus (Crustacea: Decapoda: Potamidae). Zootaxa 4138: 309. https://doi.org/10.11646/zootaxa.4138.2.5

Shih HT, Ng PKL (2011) Diversity and biogeography of freshwater crabs (Crustacea: Brachyura: Potamidae, Gecarcinucidae) from East Asia. Systematics and Biodiversity 9: 1–16. https://doi.org/10.1080/14772000.2011.554457

Türkay M, Dai AY (1997) Review of the Chinese freshwater crabs previously placed in the genus *Malayopotamon* Bott, 1968 (Crustacea: Decapoda: Brachyura: Potamidae). Raffles Bulletin of Zoology 45(2): 189–207.

Zou JX, Bai J, Zhou XM (2018) A new species of karst-dwelling freshwater crab of the genus *Chinapotamon* Dai & Naiyanetr, 1994 (Crustacea: Decapoda: Brachyura: Potamidae), from Guizhou, southwest China. Peer J 6: e5947. https://doi.org/10.7717/peerj.5947

ZooKeys 873: 25–42 (2019)
doi: 10.3897/zookeys.873.35421
http://zookeys.pensoft.net

RESEARCH ARTICLE

A peer-reviewed open-access journal
ZooKeys
Launched to accelerate biodiversity research

Description of a new species of *Membranobalanus* (Crustacea, Cirripedia) from southern Australia

Andrew M. Hosie[1,2], Jane Fromont[1], Kylie Munyard[2], Diana S. Jones[1]

1 *Aquatic Zoology, Western Australian Museum, 49 Kew St, Welshpool 6106 WA, Australia* **2** *School of Pharmacy & Biomedical Sciences, Curtin Health Innovation Research Institute, Curtin University, Bentley, 6102 WA, Australia*

Corresponding author: *Andrew M. Hosie* (andrew.hosie@museum.wa.gov.au)

Academic editor: *Kai Horst George* | Received 16 April 2019 | Accepted 9 August2019 | Published 29 August 2019

http://zoobank.org/6149E423-3C28-47BB-89FC-927209B5D2DE

Citation: Hosie AM, Fromont J, Munyard K, Jones DS (2019) Description of a new species of *Membranobalanus* (Crustacea, Cirripedia) from southern Australia. ZooKeys 873: 25–42. https://doi.org/10.3897/zookeys.873.35421

Abstract

A new species of sponge-inhabiting barnacle, *Membranobalanus porphyrophilus* **sp. nov.**, is described herein. This species can be distinguished from all other congeners by a combination of characters, in particular by the shapes of the tergum and scutum and the armament of the cirri. COI sequence data from the type specimens have been lodged with GenBank and a morphological key to the species of *Membranobalanus* is provided to aid future research. The host of the new species is the southern Australian endemic demosponge *Spheciospongia purpurea*. The new species of barnacle is thought to be host species specific.

Keywords

Archaeobalanidae, bioeroder, commensal, Clionaidae, computed tomography, Demospongiae, specificity, *Spheciospongia purpurea*, symbiosis, temperate reef.

Introduction

Barnacles of the genus *Membranobalanus* Hoek, 1913 are obligate symbionts of sponges. While the identity of sponge hosts for most sponge-dwelling barnacles have been poorly documented, this is not the case for *Membranobalanus*. All species have been found embedded only in the genera *Cliona* Grant, 1826 and *Spheciospongia* Marshall, 1892 in the family Clionaidae D'Orbigny, 1851 (van Syoc 1988; van Syoc et al. 2015), with the exception of *M. longirostrum* (Hoek, 1913), which has been additionally reported from the genus *Suberites* Nardo, 1833 in the family Suberitidae Schmidt 1870 (Ilan et al. 1999; Wibowo et al. 2011; Sulistiono et al. 2014) and *M. orcuttiformis* (Kolosváry, 1941) where no host has been reported.

The Clionaidae (Demospongiae, Clionaida) is a group of sponges well known for bioeroding calcareous structures such as mollusc shells and scleractinian coral skeletons (Rutzler 1975). Sponges in the genus *Spheciospongia* excavate limestone substrates in early life history stages and can become massive sponges with age (Vicente et al. 1991). The barnacles are found embedded within the host, the tissues of which are in direct contact with the calcareous parietes of the barnacles, seemingly undeterred by the potential bioeroding effects of the sponge.

This study describes a new species *Membranobalanus* collected as part of a broader study on sponge-inhabiting barnacles in Australian waters. The host species, *Spheciospongia purpurea* (Lamarck, 1815), is endemic to southern Australia and easily recognised due to its vibrant purple colouration, which it retains even in ethanol or a dry state. The dense royal purple pigment reported in this species and other species of *Cliona* and *Spheciospongia* is a porphyrin, specifically spongioporphyrin (Bergquist 1978).

Methods

Prior to dissection, the designated holotype was scanned via µCT using a Zeiss Versa XRM-520 X-ray microscope at the Centre for Microscopy, Characterisation and Analysis at the University of Western Australia. Processing of the resulting data followed the methods described in Semple et al. (2019) using the software packages Drishti 2.6.4 (Limaye 2012), Meshlab 2016 (Cignoni et al. 2008), and Adobe Acrobat Pro X.

For direct morphological examination of barnacle shell plates and arthropodal characters, the body and associated soft tissues were removed from the shell. The remnants of the barnacle tissue and host sponge on the surfaces of the parietes, scutum and tergum were removed using forceps. The shell was then immersed in 2% bleach for ~2 h to completely digest the organic tissue and subsequently rinsed in purified water. Any remaining debris or contaminants were then removed by cleaning in an ultrasonic cleaner for less than 20 s for shell plates and 5 s for arthropodal parts. The specimens were examined under a Leica M205 C (Leica, Germany) stereomicroscope and digital photographs produced with a Leica DMC4500. For scanning electron microscopy, specimens were first dehydrated in an ethanol series (70%, 80%, 90%, 100%, 5 minutes each) then transferred to hexamethyldisilazane for 10 min. Excess liquid was then removed with an eye-dropper and specimens were left to dry in a fume hood for 30 min. The dissected specimens were mounted on stubs, sputter coated with gold, and observed using a Hitachi TM3030 tabletop SEM. All images were processed using Adobe Photoshop CS3.

Adductor or depressor muscle tissues were subsampled from specimens, and genomic DNA was extracted using either a Bioline Isolate II or Qiagen DNeasy extraction kit following the manufacturers' instructions. Partial fragments of the cytochrome c oxidase I gene were amplified using the primers dgLCO1490 5'-GGTCAACAAATCATAAAGAYATYGG-3' and dgHCO2198 5'-GGTCAACAAATCATAAAGAYATYGG-3' (Meyer et al. 2003) in a 25 µL reaction volume consisting of 1 unit MyTaq DNA polymerase, 1× MyTaq PCR buffer, 0.5 µL of each primer, and 2 µL template. The following polymerase chain reaction conditions were used: 2 min at 95 °C for initial denaturing, then 35 cycles of 30 s at 95 °C, 30 s at 46 °C, 45 s at 72 °C, and a final extension for 7 min at 72 °C. The resulting amplicons were sequenced by the Australian Genome Research Facility, Perth, using the same primers. The sequences were assembled and trimmed using Geneious Prime and submitted to GenBank (Table 1; https://www.ncbi.nlm.nih.gov/genbank/).

Specimens of both barnacles and sponges are housed at the Western Australian Museum, Perth (WAM) and South Australian Museum, Adelaide (SAMA).

Systematics

Suborder Balanomorpha Pilsbry, 1916
Superfamily Balanoidea Leach, 1817
Family Archaeobalanidae Newman & Ross, 1976

Genus *Membranobalanus* Hoek, 1913

Type species. *Balanus declivis* Darwin, 1854: 275, pl. 7 fig. 4a–d; by subsequent designation (Pilsbry 1916: 229).

Species composition. *M. brachialis* (Rosell, 1972); *M. costatus* Zullo & Standing, 1983; *M. cuneiformis* (Hiro, 1936); *M. declivis* (Darwin, 1854); *M. koreanus* Kim & Kim, 1983; *M. longirostrum* (Hoek, 1913); *M. nebrias* (Zullo & Beach, 1973); *M. orcutti* (Pilsbry, 1907); *M. porphyrophilus* sp. nov.; *M. robinae* Van Syoc, 1988.

Nomen dubium. *M. orcuttiformis* (Kolosváry, 1941).

Diagnosis. Parietes solid, unornamented, weakly articulated, basis membranous. Rostrum scoop or boat-shaped, often elongate relative to other parietes. Tergum with spur furrow open. Cirrus IV with erect spines, with or without recurved teeth on anterior ramus.

Remarks. With the addition of the below described species, there are now 10 species included within *Membranobalanus.* Utinomi (1968) synonymised the taxa *Balanus* (*Membranobalanus*) *longirostrum* var. *krusadaiensis* Daniel, 1955, *B.* (*M.*) *basicupula* Suhaimi, 1966, and *B.* (*M.*) *roonwali* Prem-Kumar & Daniel, 1968 under *M. longiro-*

Table 1. Accession details for COI sequences of *Membranobalanus porphyrophilus* sp. nov. deposited with GenBank.

Specimen catalogue	GenBank #
WAM C66803	MK900684
WAM C71853	MK789771
WAM C71881	MK789772

strum, proposing that the differences observed are within the bounds of intraspecific variability. Recently, van Syoc et al. (2015) transferred *Acasta acuta* (Kolbasov, 1993) out of *Membranobalanus* based primarily on the presence of calcareous spines on the parietal wall, a character no other *Membranobalanus* possess and in reference to a cladistic analysis in an unpublished thesis. The fact that *A. acuta* is found in sponges of the family Petrosiidae (order Haplosclerida), not the Clionaidae as reported for the remaining members of the genus, separates this species ecologically from *Membranobalanus*, was used as further justification. The general appearance, membranous basis and elongated rostrum of *A. acuta* are typical features of *Membranobalanus*, however. While we treat this reassignment with caution, we have no evidence with which to dispute it.

Kolosváry (1941) described *Balanus* (*M.*) *orcuttiformis* based on the parietes of a single empty specimen. The locality details of the specimen are vague, only given as "India Orient.", but presumably meaning eastern India. No detail regarding a host was given. The description is very brief, giving very few clues to the identification of this species, and the only illustration of the specimen, in lateral view, could belong to a number of genera, but not *Membranobalanus* as currently defined. Most notable is the absence of any elongation of the rostrum and the largely horizontal basal rim of the parietal wall gives the appearance that it was attached to, rather than embedded within, a substrate. Additionally, the exceptionally broad alae and absent radii are reminiscent of the Pachylasmatoidea, which possess solid parietes and often have a membranous base (see Jones 2000). *Membranobalanus orcuttiformis* has not been recorded since its description and unfortunately the specimens are missing from the Museo di Storia Naturale dell'Università di Firenze, Italy and thus cannot be reexamined (Innocenti 2006). For these reasons, this species is considered herein a *nomen dubium* and has been excluded from the key below.

The remaining *Membranobalanus* species can be separated into two morphological lineages, approximating an American centred group and an Indo-West Pacific group. The former have recurved teeth, similar to those present in some members of the Acastinae, as well as erect spines on cirrus IV, smooth growth lines on the scutum and the articular ridge and groove of the scutum is prominent, extending well beyond the articular margin, with a correspondingly wide articular groove on the tergum. The latter group bears only the erect spines on cirrus IV, finely striated growth lines, and has relatively weak articular structures on the opercular plates. From a biogeographic perspective one species disrupts this pattern: *Membranobalanus koreanus* from the waters around the Korean Peninsula. As described and figured by Kim and Kim (1983), *M. koreanus* has recurved teeth and a large articular ridge on the scutum. The records of *M. orcutti* by Barnard (1924) and Rosell (1973, 1975) from South Africa and the Sulu Archipelago, respectively, were considered suspect by Zullo and Beach (1973) and Van Syoc and Winther (1999). The Sulu Archipelago specimens lack the recurved teeth on cirrus IV of the specimens described from Catalina Island by Zullo and Beach (1973), and while Barnard's description specifically mentions recurved teeth on cirrus IV, most of his description is deferred back to either Pilsbry's (1907, 1916) descriptions of *M. orcutti* or Hoek's (1913) description of *M. longirostrum*. Of particular note in Barnard's description is that the scutum has an external, setose membrane, a character seen in some species of the Acastinae, but not *Membranobalanus*. Both reports should be considered *species inquirenda*, but potentially represent previously undescribed species.

Membranobalanus porphyrophilus **Hosie & Jones sp. nov.**

http://zoobank.org/170E814F-E3ED-4120-8622-EC4230353C65
Figures 1–6

Material examined. Holotype. AUSTRALIA • WAM C66803, 1 hermaphrodite; 9 mm rostro-carinal diameter; Western Australia SE of Rottnest Island, Wallace Island, The Count; 32°0.89'S, 115°33.53'E; 12 m; coll. A.M. Hosie; 23 Feb 2017; host: WAM Z86929, *Spheciospongia purpurea*.

Paratypes. AUSTRALIA • WAM C71852, 1 hermaphrodite; 8 mm rostro-carinal diameter; empty shell; same as data as for holotype. • WAM C71853, 1 hermaphrodite; same as data as for holotype. • WAM C71881, 1 hermaphrodite; same as data as for holotype. • SAMA C12706, 1 hermaphrodite; South Australia, Kangaroo Island, off Second Gully between Western River Cove and Snug Cove; 32 m; coll. J. Thiselton; 19 Nov 2002; host: SAMA S2910, *S. purpurea*. • SAMA C12707, 1 hermaphrodite; same data as for previous. • SAMA C12708, 1 hermaphrodite; 14 mm rostro-carinal diameter; same data as for previous.

Diagnosis. Shell wall robust, cylindrical, growth ridges weak; orifice toothed, large; rostrum basal margin broadly rounded, extending below basal plane of remaining parietes. Tergum narrow, beaked, spur narrow, separated from basiscutal angle by half its own width; scutum with faint, external longitudinal striations; basitergal angle broadly rounded. Cirri III and IV with row of strong, erect spines on anterodistal margin of anterior ramus; cirrus IV pedicel without erect spines; cirri IV and V with row of stout spines on posterior margin of anterior ramus basal segment.

Description. All shell plates, prosoma, and internal organs stained purple *in vivo*, otherwise white. Shell walls (Figs 1, 2) parallel, except bowed rostrum; parietes externally with horizontal growth lines raised, ridge-like, giving shell a roughened appearance; radii prominent, summits oblique, sutural edges roughened, alae wide, summits oblique. Internally parietes smooth, sheath occupying approximately half of shell height, with horizontal growth lines, basal margin adpressed. Carina approximately as wide as lateral plate, carinolateral narrowest plate, approximately one-third width of lateral plate. Rostrum elongate, extending below basal margin of other parietes, almost twice length and twice width of lateral plate, basal margin broadly rounded below basal margin of latera. Basal margins of carina and carinolatera more or less perpendicular to shell vertical axis, latera basal margins curving basally to form contiguous rim connecting latera with rostrum. Basis membranous, follows contour of basal rim, not depending below parietes.

Scutum (Fig. 3A–D, I, J) triangular, height 1.3–1.8 times width, growth lines prominent with faint longitudinal striations; basal and tergal margins separated by broadly rounded basitergal angle. Internal surface, slightly ridged apically near tergal

Figure 1. Interactive 3D, μCT derived volume reconstruction of *Membranobalanus porphyrophilus* sp. nov. holotype (WAM C66803). Only the well-calcified plates are illustrated as scanning limitations prevented the softer prosoma from being differentiated. Note: To enable the interactive function of this figure, open the PDF in Adobe Reader program or web plug-in.

margin, otherwise smooth; adductor muscle pit distinct; lateral depressor muscle pit distinct, without depressor muscle crests, extending one-third distance to beginning of articular ridge bounded by low, rounded adductor muscle ridge. Articular groove deep, narrow; articular ridge barely projecting beyond articular margin, basal margin curved.

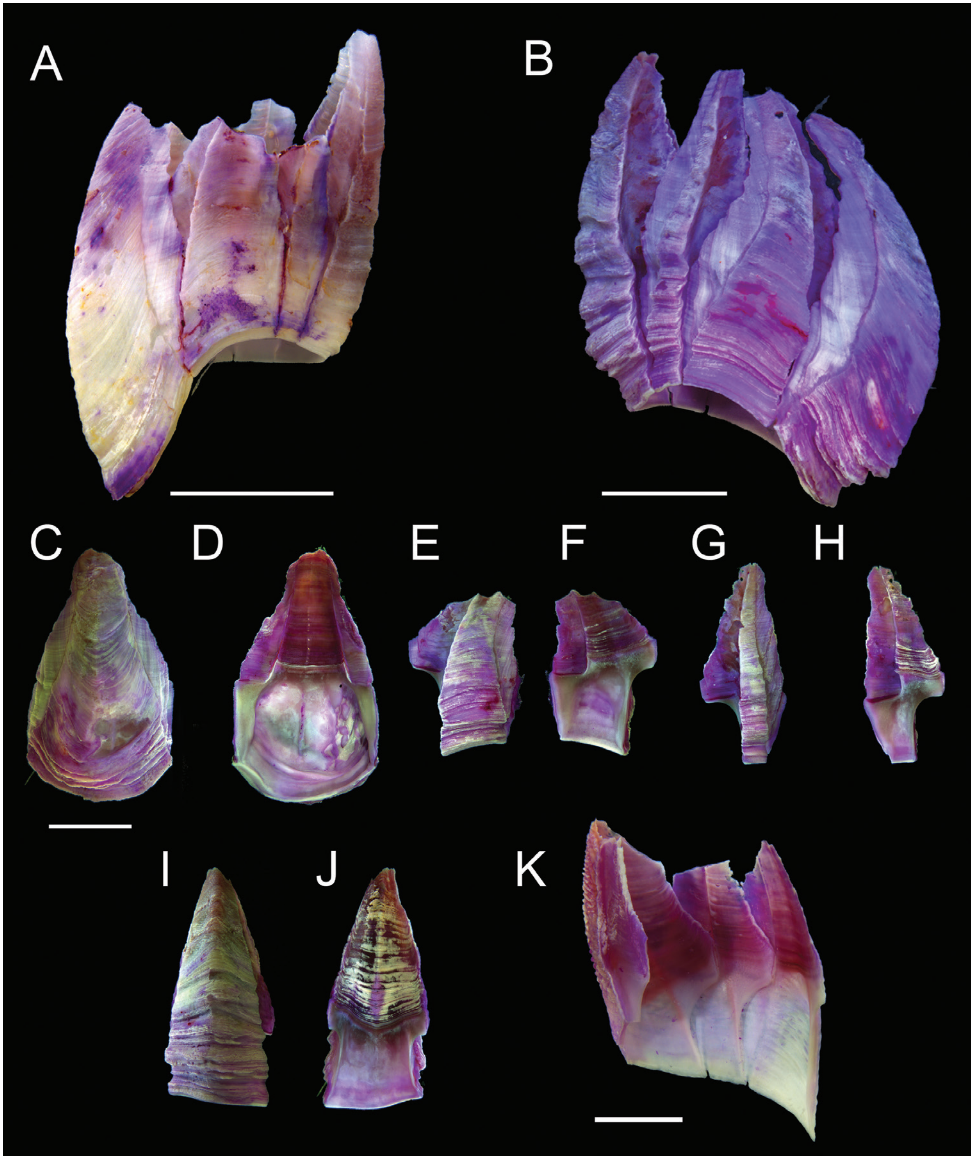

Figure 2. *Membranobalanus porphyrophilus* sp. nov. parietes **A** holotype (WAM C66803) **B–J** paratype (SAMA C12708) **K** paratype (SAMA C12706). **A** Whole shell lateral view **B** whole shell lateral view **C, D** rostrum, external and internal view **E, F** left lateral plate, external, and internal view **G, H** left carinolateral, external and internal view **I, J** carina external and internal view **K** internal view of articulated right carina, carinolateral and lateral plates. Scale bars: 5 mm (**A–J**); 2 mm (**K**).

Tergum (Fig. 3E–H, K, L) narrow, height more than twice width, articular and carinal margins arcuate with beaked apex; external growth lines conspicuous, but less raised than those of scutum; spur furrow indicated by shift in growth lines and slight depression; basiscutal angle sloping into spur; spur narrow, separated from basiscutal

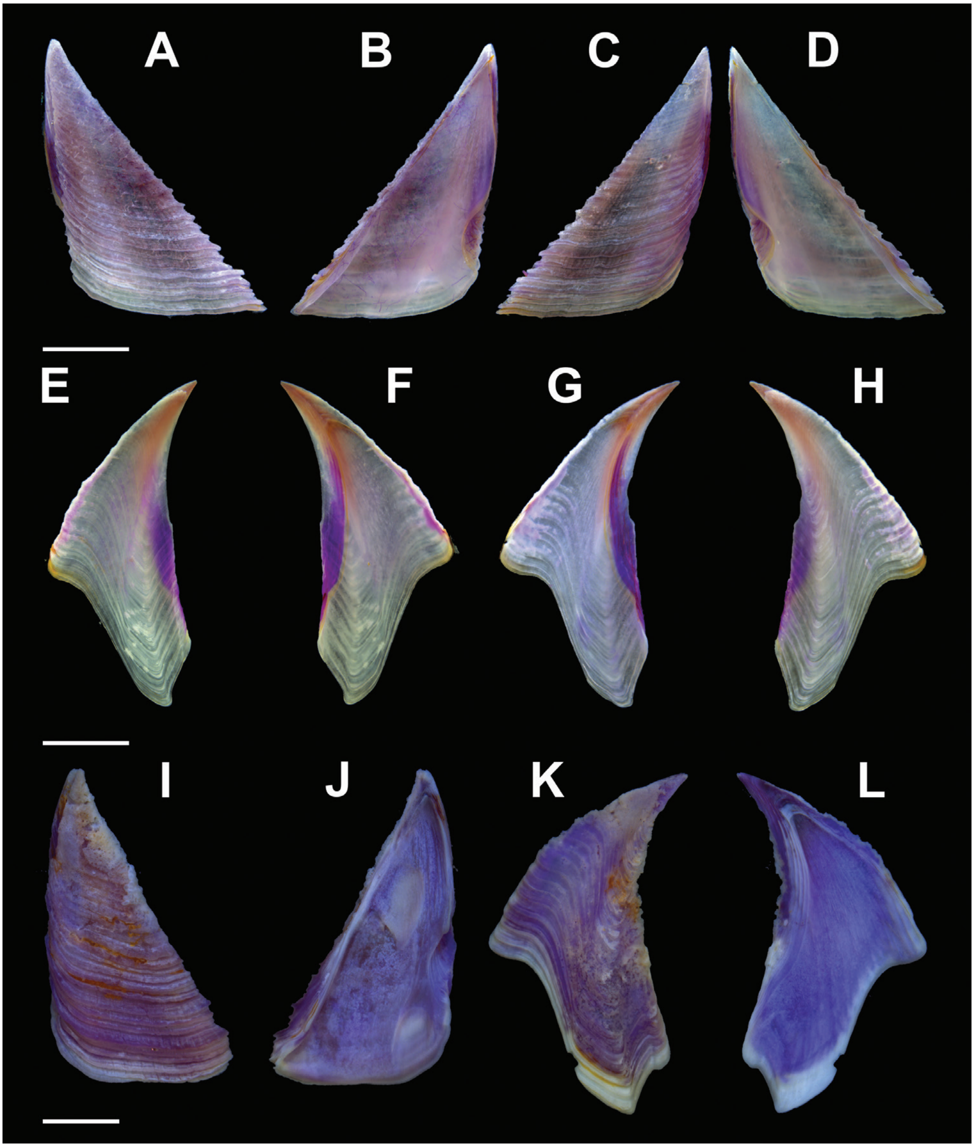

Figure 3. *Membranobalanus porphyrophilus* sp. nov. opercular plates **A–H** holotype (WAM C66803) **I–L** paratype (SAMA C12708). **A** Left scutum, external view **B** left scutum, internal view **C** right scutum, external view **D** right scutum, internal view **E** left tergum, external view **F** left tergum, internal view **G** right tergum, external view **H** right tergum, internal view **I** left scutum, external view **J** left scutum, internal view **K** left tergum, external view **L** left tergum, internal view. Scale bars: 2 mm.

angle by half its width, basally truncate. Internally smooth, depressor muscle crests weak (may be absent in small specimens), articular groove wide, open, shallow; articular ridge low, becoming confluent with scutal margin basally.

Labrum (Fig. 4A–F) bilobed, with deep medial notch bounded by rounded crests, each with two or three marginal teeth and numerous fine setae.

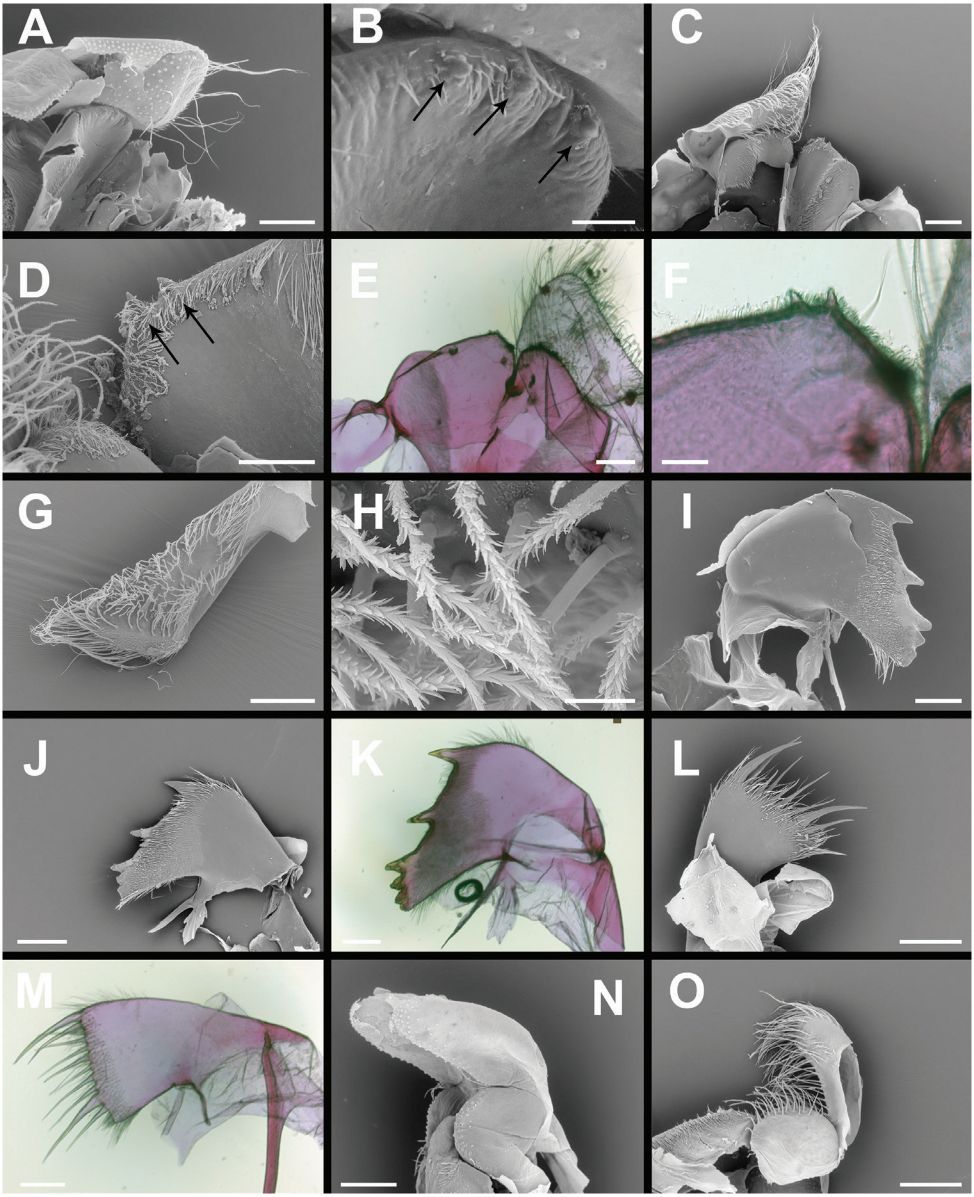

Figure 4. *Membranobalanus porphyrophilus* sp. nov. mouthparts **A, B, G, H, I, L, N** holotype (WAM C66803) **C, D, J, O** paratype (SAMA C12708) **E, F, K, M** paratype (SAMA C12706). **A, C** Labrum and right mandiblular palp (left removed, damaged) **B, D** close up of A and D, arrows indicate teeth on labrum **E** left mandibular palp **F** detail of serrulate setae on mandibular palp ventral face **G–I** mandibles **J** maxillule **K, L** maxilla. Note: G, H, L damaged, setae lost during sonication in A & K. Scale bars: 200 μm (**A, C, E, G, I–O**); 40 μm (**B, F**); 100 μm (**D**); 50 μm (**H**).

Mandibular palp (Fig. 4A, C, E, G, H) rhomboid, apex obliquely truncate, anterior margin concave, posterior margin straight; setae (Fig. 4F) heavily serrulate, becoming longer and denser distally.

Mandible (Fig. 4I–K) with four distinct teeth, 2nd and 3rd tooth bifid, 4th tooth much smaller than preceding three, 5th tooth obsolescent, confluent with molariform inferior angle; short setae covering inner and outer faces, longer fine setae on inferior and superior margins.

Maxillule (Fig. 4l, M) with 10 robust setae on cutting margin, first, second, and ninth longer and more robust than remaining setae, inferior angle with several short robust setae. Cutting margin straight, with very slight notch below second seta. Dense, short setae regularly spaced on inner and outer faces, longer fine setae on inferior and superior margin

Maxilla (Fig. 4N, O) bilobed, basal lobe ovate, serrulate setae arranged on anterior margin; distal lobe elongate, serrulate setae on anterior margin becoming more dense at apex, longer than those on basal lobe.

Cirrus I (Fig. 5A) with unequal rami, anterior ramus twice length of posterior ramus, both rami bearing serrulate and simple setae. Posterior ramus segments with protuberant anterior margins, more densely setose than anterior ramus, arranged in tufts on anterior margins.

Cirrus II (Fig. 5B) shorter than other cirri, rami subequal; anterior margins of both rami slightly protuberant with serrulate and simple setae.

Cirrus III (Fig 5C, D) pedicel with plumose setae on anterior and posterior margins of both segments; rami equal; anterior ramus with erect spines and ctenoid scales on anterodistal portion of medial segments, tuft of long serrulate setae on rounded anterior margin up to approximately three times as long as segment, tuft of serrulate setae as long as segment at posterodistal angle.

Cirrus IV (Fig. 5E–L) pedicel without erect teeth on anterodistal margins, pedicel with numerous small denticles on posterior and anterior margins of mesial face, tuft of short setae at posterodistal angle, small ctenoid scale-like denticles at anterodistal margin. Rami subequal in length; basal-most segment with up to 13 stout spines along posterior margin (holotype with six), basal segments with one or two stout spines at posterodistal angle. Anterior ramus intermediate segments with row of erect spines on anterodistal portion of all but most distal segments, much reduced in posterior ramus, without recurved teeth on anterior faces, posterodistal angles with tuft of setae.

Cirrus V (Fig. 6A–C) characters intermediate between cirri IV and VI; pedicel with numerous small denticles on posterior and anterior margins of mesial face, tuft of short setae at posterodistal angle, small ctenoid scale-like denticles on anterodistal margin. Rami equal, segments becoming elongate distally from half as long as wide to three times longer than wide, both rami with four pairs of serrulate setae on anterior margin, distal most pair longest, approximately 3 times length of segment; tuft of simple setae at anterodistal angle, setae up to half length of segment; erect teeth on anterior margins of intermediate segments less pronounced than those on cirrus IV; stout spines on posterior margins of rami similar to cirrus IV.

Cirrus VI (Fig. 6D–G) rami equal, pedicel with numerous small denticles on posteromesial face, tuft of simple setae at posterodistal angle; intermediate segments of both rami becoming elongate distally from 1.5 times wider than long to three times

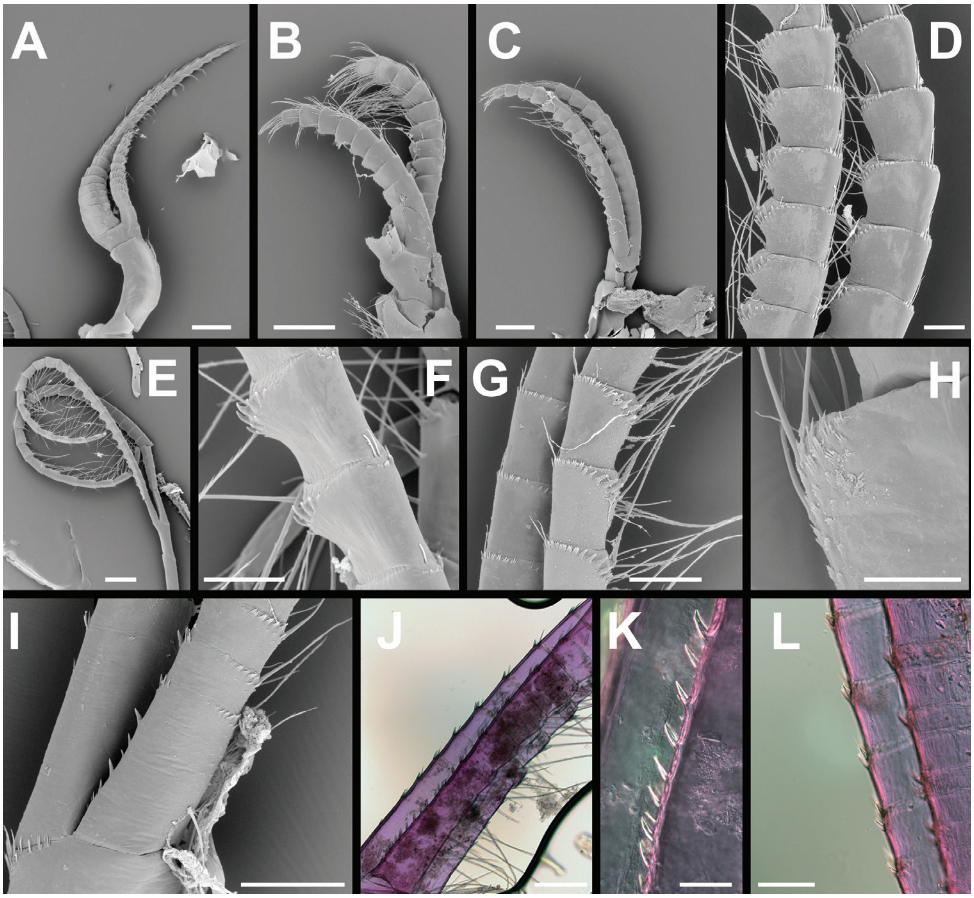

Figure 5. *Membranobalanus porphyrophilus* sp. nov. cirri **A–F** holotype (WAM C66803) **G–I** paratype (SAMA C12706) **J–L** paratype (SAMA C12708). **A–C** Right cirrus I–III lateral view **D** right cirrus III intermediate segments **E** right cirrus IV lateral view **F** same, anterior ramus intermediate segments **G** left cirrus IV anterior ramus intermediate segments **H** right cirrus IV anterodistal angle of distal segment of pedical showing ctenoid scales **I, J** left cirrus IV basal segments of rami showing posterior spines **K** close up of spines on posterior margin of J **L** close up of spines and posterodistal spines basal segments of J. Note: B, C, E damaged. Scale bars: 400 µm (**A–C, E**); 100 µm (**D, F, L**); 150 µm (**G, I**); 50 µm (**H, K**); 200 µm (**J**).

longer than wide, both rami with four pairs of serrulate setae on anterior margin, distal most pair longest, approximately three times the length of segment, basal pair 0.3 times length of segment; tuft of simple setae at anterodistal angle, setae up to 0.5 length of segment; anterior margins of all segments without erect teeth, posterior margins without stout spines.

Cirral segment counts as follows (anterior ramus, posterior ramus):

	Cirrus	I	II	III	IV	V	VI
WAM C66803	L	21, 9	9, 11	17, 13	27, 30	34, 32	33, 33
	R	20, 9	11, 9	17, 14	30, 30	32, 34	36, 34

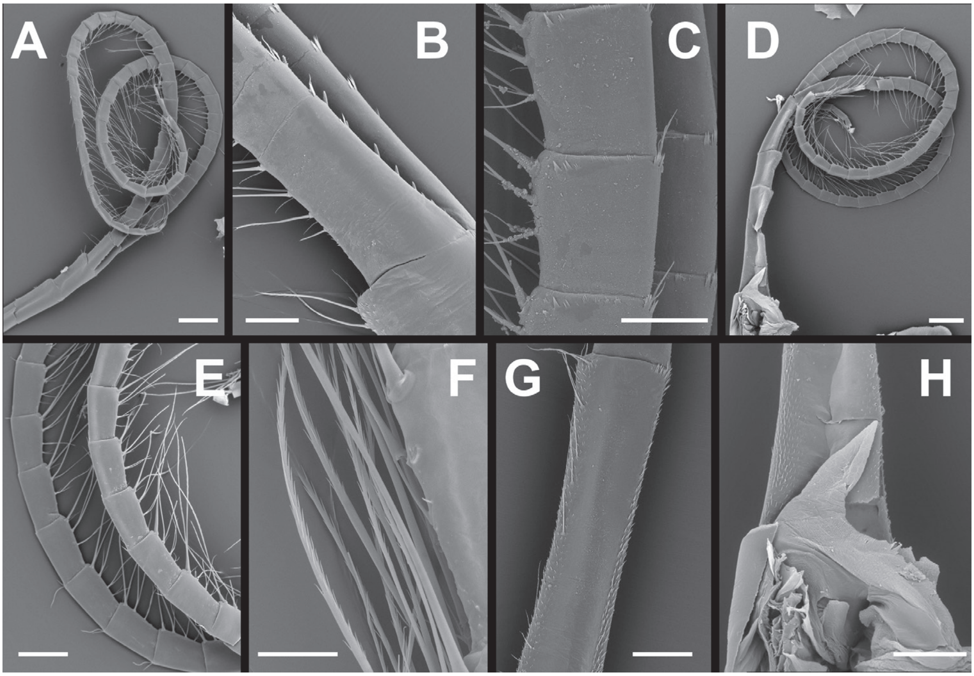

Figure 6. *Membranobalanus porphyrophilus* sp. nov. cirri **A, B, D, E, H** holotype (WAM C66803) **C, F, G** paratype (SAMA C12706). **A** Right cirrus V lateral view **B** basal segments of cirrus V rami **C** intermediate segments of cirrus V anterior ramus **D** right cirrus VI mesial view (damaged) **E** same, intermediate segments **F** example of long serrulate setae on cirrus VI **G** basal segment of pedicel of right cirrus VI, mesial view showing denticles on anterior and posterior margin **H** basidorsal point of penis. Scale bars: 400 µm (**A, D**); 100 µm (**B, C)**; 50 µm (**F**); 150 µm (**G, H**); 80 µm (**E**).

Penis longer than CVI, annulated, sparsely setose along length; basidorsal point (Fig. 6H) prominent, triangular, height twice width.

Distribution. Southern Australia, from Perth to Adelaide.

Etymology. From Greek *porphyra*, purple and *philos*, indicating a love of; gender masculine. In reference to the vibrant purple colour of the only known host.

Remarks. *Membranobalanus porphyrophilus* sp. nov. is most readily distinguished from its congeners by the narrow, beaked tergum. The absence of recurved teeth on cirrus IV, the finely striated scutal growth lines, and the weak articular structure of the opercular plates further separates the newly described species from the predominantly American group of species, viz. *M. costatus*, *M. declivis*, *M. koreanus*, *M. nebrias*, *M. orcutti*, and *M. robinae*. The remaining species in the genus, *M. brachialis*, *M. cuneiformis*, and *M. longirostrum* all bear prominent, erect spines on the pedicel of cirrus IV and lack the stout spines on the posterior margins of the rami of cirri IV–VI. This is only the second member of the genus reported from Australian waters. The other, *M. cuneiformis*, is known from near Darwin and was reported by Hiro (1936) as commensal with an unidentified species of *Cliona* that was bioeroding the shell of *Pinctada maxima* (Jameson, 1901). Externally, *M. cuneiformis* can be separated from *M. porphyrophilus* by the conical shape of the shell, resulting in a small orifice and absent radii.

Discussion

Only a single sequence, identified as *M. longirostrum* (GenBank accession #KC138493; Chen et al. 2013), represents the genus *Membranobalanus* on GenBank, and the sequences generated herein are less than 85% similar, indicating a rather distant relationship with *M. porphyrophilus* sp. nov.

The degree of elongation and curvature of the rostrum is variable in *M. porphyrophilus* sp. nov. and does not appear to be directly related to increasing size, as the rostrum of both the larger and smaller specimens can be relatively short. The development of the rostrum will be in large part an adaptation to prevent being overgrown by the host, and it is likely that the aspects of the rostral form will be determined by the placement of the barnacle relative to the direction of growth of the host.

While *Spheciospongia* are bioeroders generally only in early life history stages, the bioeroding capacity does appear to have impacted on the barnacle shells. The older parts of the shell plates are often pitted and scarred, indicative of the potential bioeroding effects of the sponge. The shell plates, exoskeleton, and tissues are brightly stained by the purple pigments of the host sponge (persistent even in ethanol), and are the most obvious impact of the sponge on the barnacle.

Spheciospongia purpurea has had a complex taxonomic history and at one stage many species were listed in synonymy and thus the species was considered to be widely distributed (see Vosmaer 1911: 6 for list of synonyms). Topsent (1918) brought many of these species back out of synonymy and *S. purpurea* is now considered to be endemic to southern Australia (Atlas of Living Australia 2019). In Hoek's (1913) report on the cirripedes collected during the *Siboga* Expedition he listed *S. purpurea* as the host sponge in his description of *M. longirostrum* collected from the seas around Indonesia, far outside the known range of *S. purpurea*. Hoek's record is, thus, considered to be a misidentification, most likely based on the identifications in Vosmaer's (1911) account of the sponges from the same expedition. It is unclear if the records of *S. purpurea* as the host by Rosell (1972) from the Philippines and by Utinomi (1968) from Japan are based on their material or simply repeated from Hoek's report, but here they are considered to be errors for the same reason.

No other barnacle species were found inhabiting any of the 15 *S. purpurea* specimens examined during the course of this study. Over 200 morphospecies of sponge have been found to host barnacles in Australian waters (Hosie and Fromont unpublished data), including five other species of *Spheciospongia*, and *Membranobalanus porphyrophilus* sp. nov. has been found inhabiting only *S. purpurea*, making it likely to be restricted to this species and therefore also an Australian endemic.

Host specificity of *Membranobalanus* was first discussed by van Syoc (1988), and the newly described species supports the hypothesis that they are restricted to inhabiting species of the Clionaidae. The exception to this is *M. longirostrum*, which has also been reported inhabiting species of the Suberitidae in the Red Sea (Ilan et al. 1999) and Indonesia (Wibowo et al. 2011; Sulistiono et al. 2014). The potential for the misidentification of host species by Ilan et al. (1999) was raised by van Syoc (2015), as the genus *Suberites* is morphologically similar to *Spheciospongia.* This similarity has led to species of both genera being confounded; as an example, *Suberites wilsoni* Carter, 1885 is considered a subjective synonym of *S. purpurea*. The existing records of *Membranobalanus* embedded in *Suberites*, as well as any future collections, need to be examined by sponge specialists to determine if they have been correctly assigned.

Key to the genus *Membranobalanus*

1	Cirrus IV anterior ramus bearing recurved teeth and erect spines	**2**
–	Cirrus IV anterior ramus bearing only erect spines	**7**
2	Rostrum much longer than other parietes	**3**
–	Rostrum approximately as long as other parietes	**5**
3	Radii absent	***M. orcutti***
–	Radii present	**4**
4	Scutum with radius-like ledge on occludent margin	***M. koreanus***
–	Scutum occludent margin normal, lacking ledge	***M. declivis***
5	Parietes costate	***M. costatus***
–	Parietes not costate	**6**
6	Basal margin of all parietes rounded; tergal articular ridge low, articular groove open	***M. robinae***
–	Basal margin of laterals more or less straight; tergal articular ridge overhanging articular groove	***M. nebrias***
7	Radii broad, conspicuous; tergal spur narrow, longer than wide, cirrus IV pedicel without erect spines on anterodistal margins	***M. porphyrophilus* sp. nov.**
–	Radii absent or very narrow, tergal spur wider than long, cirrus IV pedicel with erect spines on anterodistal margins	**8**
8	Rostrum with median furrow, elongated basal portion tapering, very narrow	**10**
–	Rostrum without median furrow, basal portion wedge-shaped	***M. cuneiformis***
9	Basal membrane with spine-like processes	***M. brachialis***
–	Basal membrane without spine-like processes	***M. longirostrum***

Acknowledgments

This study was funded in part by the Australian Biological Resources Study Grant #RF213-25, Gorgon Barrow Island Net Conservation Benefits Fund, and the Australian Government Research Training Program. Nikolai Tatarnic (WAM) carried out the CT scans at Australian Microscopy & Microanalysis Research Facility at the Centre for Microscopy, Characterisation & Analysis, The University of Western Australia, a facility funded by the University, State, and Commonwealth Governments. We thank Andrea Crowther (SAM) for hosting visits to the collections by AMH and for making specimens from South Australia available for study, Ana Hara and Oliver Gomez (both WAM) for assistance with specimen handling and processing in the lab and field, and Michelle Condy, Linette Umbrello, and Kara Layton for their work undertaking extractions and PCRs in the WAM Molecular Systematics Unit. The comments and suggestions on the manuscript by Meng-Chen Yu, as reviewer, were also greatly appreciated.

References

Atlas of Living Australia (2019) *Spheciospongia purpurea* (Lamarck, 1815) records. https://bie.ala.org.au/species/urn:lsid:biodiversity.org.au:afd.taxon:2a815069-da70-4531-9822-74e3ca64816d [Accessed on: 2019-7-22]

Barnard KH (1924) Contributions to the crustacean fauna of South Africa. No. 7, Cirripedia. Annals of the South African Museum 20: 1–103. https://biodiversitylibrary.org/page/11101069

Bergquist PR (1978) Sponges. Hutchinson & Co. Ltd, London, 267 pp.

Carter HJ (1885) Descriptions of sponges from the neighbourhood of Port Phillip Heads, South Australia. Annals and Magazine of Natural History (Series 5) 15(86): 107–117. https://doi.org/10.1080/00222938509459306

Chen H-N, Høeg JT, Chan BKK (2013) Morphometric and molecular identification of individual barnacle cyprids from wild plankton: an approach to detecting fouling and invasive barnacle species, Biofouling 29(2): 133–145. https://doi.org/10.1080/08927014.2012.753061

Cignoni P, Callieri M, Corsini M, Dellepiane M, Ganovell F, Ranzuglia G (2008) Meshlab: an open-source mesh processing tool. In: Scarano V, De Chiara R, Erra U (Eds) Eurographics Italian Chapter Conference, Salerno (Italy), 2008, The Eurographics Association, 129–136. https://doi.org/10.2312/LocalChapterEvents/ItalChap/ItalianChapConf2008/129-136

Daniel A (1955) The Cirripedia of the Madras coast. Bulletin of the Madras Government Museum (New Series) Natural History Section 6: 1–40. http://www.e-books-chennaimuseum.tn.gov.in/chennaimuseum/images/248/book.html#p=2

Darwin C (1854) A monograph on the subclass Cirripedia with figures for all species. The Balanidae, the Verrucidae etc. The Ray Society, London, 681 pp. http://darwin-online.org.uk/content/frameset?itemID=F339.2&viewtype=side&pageseq=1

D'Orbigny AD (1851) Cours élémentaire de paléontologie et de géologie stratigraphiques. Vol. 1(1), Masson, Paris, 382 pp. https://gallica.bnf.fr/ark:/12148/bpt6k6260677z.texteImage

Grant, RE (1826) Notice of a new zoophyte (*Cliona celata* Gr.) from the Firth of Forth. Edinburgh New Philosophical Journal 1: 78–81. https://www.biodiversitylibrary.org/page/2471191

Hiro F (1936) Report on the Cirripedia collected in Malayan waters by the Ship "Zuihomaru." Japan Journal of Zoology 3: 621–636.

Hoek PPC (1913) The Cirripedia of the Siboga Expedition. B. Cirripedia Sessilia. Siboga Expeditie Monographe XXXIb E.J. Brill, Leiden, 129–275. https://doi.org/10.5962/bhl.title.12959

Ilan M, Loya Y, Brickner I, Kolbasov GA (1999) Sponge-inhabiting barnacles on Red Sea coral reefs. Marine Biology 133: 709–716. https://doi.org/10.1007/s002270050512

Innocenti G (2006) Collections of the Natural History Museum, Zoological Section "La Specola" of the University of Florence. XXIII. Crustacea, Class Maxillopoda, Subclass Thecostraca, Infraclass Cirripedia. Atti della Società Toscana di Scienze Naturali, Memorie serie B 113: 1–11. http://www.stsn.it/images/pdf/serB113/01.pdf

Jameson HL (1901) On the identity and distribution of the mother of pearl oysters with a revision of the subgenus *Margaritifera*. Proceedings of the Zoological Society of London 1901(1): 372–394. https://doi.org/10.1111/j.1469-7998.1901.tb08552.x

Jones DS (2000) Crustacea Cirripedia Thoracica: Chionelasmatoidea and Pachylasmatoidea (Balanomorpha) of New Caledonia, Vanuatu and Wallis and Futuna islands, with a review of all currently assigned taxa. Mémoires du Muséum National d'Histoire Naturelle 184: 141–283.

Kim HS, Kim IH (1983) A new species of *Membranobalanus* Crustacea Cirripedia from Korean waters. Korean Journal of Zoology 26: 41–47.

Kolbasov GA (1993) Revision of the genus *Acasta* Leach (Cirripedia: Balanoidea). Zoological Journal of the Linnean Society 109: 395–427. https://doi.org/10.1111/j.1096-3642.1993.tb00307.x

Kolosváry G (1941) Revisione della collezione de Balanidi del Museo Zoologico della R. Universita de Firenze. Monitore Zoologico Italiano 52: 183–195.

Lamarck JBPA de Monet, Comte de (1815) Suites des polypiers empâtés. Mémoires du Muséum National d'Histoire Naturelle, Paris 1: 69–80, 162–168, 331–340.

Leach WE (1817) The Zoological Miscellany; Being Descriptions of New, or Interesting Animals. Vol. 3. E. Nodder and Son, Covent Garden and London, 151 pp. [ps 121–149]

Limaye A (2012) Drishti: a Volume Exploration and Presentation Tool. Proceedings of the Society of Photo-Optical Instrumental Engineers 8506, Developments in X-Ray Tomography VIII, 85060X. https://doi.org/10.1117/12.935640

Marshall W (1892) Spongiologische Beiträge. In: Festschrift zur siebzigsten Wiederkehr des Geburtstages von Rudolf Leuckart. C.F. Winter, Leipzig, 36 pp. https://doi.org/10.5962/bhl.title.61018

Meyer C, Geller J, Paulay G (2005) Fine scale endemism on coral reefs: Archipelagic differentiation in turbinid gastropods. Evolution 59: 113–125. https://doi.org/10.1111/j.0014-3820.2005.tb00899.x

Nardo GD (1833) Auszug aus einem neuen system der spongiarien, wonach bereits die aufstellung in der Universitäts-Sammlung zu Padua gemacht ist. Isis, oder Encyclopädische Zeitung. Oken, Jena, 519–523.

Newman WA, Ross A (1976) Revision of the balanomorph barnacles; including a catalogue of the species. San Diego Natural History Society Memoirs 9: 1–108. https://www.biodiversitylibrary.org/page/4328558

Pilsbry HA (1907) Notes on some Pacific cirripedes. Proceedings of the Academy of Natural Sciences of Philadelphia 59: 360–362. https://www.jstor.org/stable/4063151

Pilsbry HA (1916) The sessile barnacles (Cirripedia) contained in the collections of the U.S. National Museum; including a monograph of the American species. Bulletin of the United States National Museum, Washington: 93: 1–366. https://doi.org/10.5479/si.03629236.93.1

Prem-Kumar VK, Daniel A (1968) A new species of operculate barnacle of the sub-genus *Membranobalanus* (Cirripedia, Thoracica) from sponges in the Indian seas. Crustaceana 14: 147–150. https://doi.org/10.1163/156854068X00520

Rosell NC (1972) Some barnacles (Cirripedia Thoracica) of Puerto Galera found in the vicinity of the U. P. Marine Biological Laboratory. Philippines University Natural and Applied Science Bulletin 24: 143–285.

Rosell NC (1973) On two less well-known balanids (Cirripedia, Thoracica) from the Sulu Archipelago, Philippines. University of the Phillippines Natural Science Research Center Technical Report 4: 1–12.

Rosell NC (1975) On two noteworthy balanids (Cirripedia Thoracica) from the Sulu Archipelago, Philippines. Crustaceana 29(2): 206–214. https://doi.org/10.1163/156854075X00216

Rützler K (1975) The role of burrowing sponges in bioerosion. Oecologia 19: 203–216. https://doi.org/10.1007/BF00345306

Schmidt O (1870) Grundzüge einer Spongien-Fauna des atlantischen Gebietes. Wilhelm Engelmann, Leipzig, 88 pp.

Semple TL, Peakall R, Tatarnic NJ (2019) A comprehensive and user-friendly framework for 3D data visualisation in invertebrates and other organisms. Journal of Morphology 280(2): 223–231. https://doi.org/10.1002/jmor.20938

Sulistiono S, Kawaroe M, Madduppa H, Prabowo RE (2014) Karakteristik morfologi teritip spons Indonesia. Depik 3(2): 178–186. https://doi.org/10.13170/depik.3.2.1553

Suhaimi A (1966) A new species of *Balanus* (Crustacea: Cirripedia) from Singapore. Bulletin of the National Museum Singapore 33: 65–69.

Topsent E (1918) Éponges de San Thomé. Essai sur les genres *Spirastrella*, *Donatia* et *Chondrilla*. Archives de Zoologie Expérimentale et Générale 57: 535–618

Utinomi H (1968) Pelagic, shelf and shallow water cirripedia from the Indo West Pacific. Videnskabelige Meddelelser fra Dansk Naturhistorisk Forening 131: 161–186.

Van Syoc RJ (1988) Description of *Membranobalanus robinae*, a new species of sponge barnacle (Cirripedia, Archaeobalanidae) from Baja California, with a key to the genus. Proceedings of the Biological Society of Washington 101: 832–837. https://www.jstor.org/stable/20106147

Van Syoc RJ, Van Soest RW, Xavier JR, Hooper JN (2015) A phylogenetic overview of sponge-inhabiting barnacles and their host specificity (Crustacea, Cirripedia). Proceedings of the California Academy of Sciences (Series 4) (62): 331–357.

Van Syoc RJ, Winther R (1999) Sponge-inhabiting barnacles of the Americas: a new species of *Acasta* (Cirripedia, Archaeobalanidae), first record from the Eastern Pacific, including discussion of the evolution of cirral morphology. Crustaceana 72: 467–486. https://doi.org/10.1163/156854099503528

Vicente VP, Rützler K, Carballeira NM (1991) Comparative morphology, ecology, and fatty acid composition of West Indian *Spheciospongia* (Demospongea). Marine Ecology 12(3): 211–226. https://doi.org/10.1111/j.1439-0485.1991.tb00254.x

Vosmaer, GCJ (1911). The Porifera of the *Siboga* Expedition: 2. The genus *Spirastrella*. Siboga Expeditie Monographe. E.J. Brill, Leiden, 1–69. https://biodiversitylibrary.org/page/2034921

Wibowo RA, Prabowo RE, Nuryanto A (2011) Biodiversitas teritip yang hidup pada spons di Perairan Pantai Kepulauan Karimunjawa. In: Prosiding Kongres dan Seminar Masyarakat Taksonomi Kelautan Indonesia, Jakarta 20–22 September 2011, 219–235.

Zullo VA, Beach DB (1973) New species of *Membranobalanus* Hoek and *Hexacreusia* Zullo (Cirripedia, Balanidae) from the Galapagos Archipelago. Los Angeles County Natural History Museum Contributions in Science 249: 1–16. https://biodiversitylibrary.org/page/52110555

Zullo VA, Standing JD (1983) Sponge-inhabiting barnacles (Cirripedia: Archaeobalanidae) of the Carolinian Province, southeastern United States, with the description of a new species of *Membranobalanus* Pilsbry. Proceedings of the Biological Society of Washington 96: 468–477. https://www.jstor.org/stable/20106147

ZooKeys 873: 43–53 (2019)
doi: 10.3897/zookeys.873.36863
http://zookeys.pensoft.net

RESEARCH ARTICLE

A peer-reviewed open-access journal
ZooKeys
Launched to accelerate biodiversity research

Frankliniella species from China, with nomenclatural changes and illustrated key (Thysanoptera, Thripidae)

Zhaohong Wang[1,2], Laurence Mound[2], Xiaoli Tong[1]

1 *Department of Entomology, College of Agriculture, South China Agricultural University, Guangzhou 510642, China* **2** *Australian National Insect Collection, CSIRO, Canberra, Australia*

Corresponding author: *Xiaoli Tong* (xtong@scau.edu.cn)

Academic editor: *Yasen Mutafchiev* | Received 6 June 2019 | Accepted 15 July 2019 | Published 29 August 2019

http://zoobank.org/9C441696-B998-444E-AE3A-AA5026B76A93

Citation: Wang Z, Mound L, Tong X (2019) *Frankliniella species* from China, with nomenclatural changes and illustrated key (Thysanoptera, Thripidae). ZooKeys 873: 43–53. https://doi.org/10.3897/zookeys.873.36863

Abstract

Species of the genus *Frankliniella* are almost all originally from the New World. Although eleven species in this genus have been listed from China before, only seven species here are recognised. The records of *F. pallida* and *F. tritici* from China are rejected as inadequately supported, *F. hainanensis* is a new synonym of *F. schultzei*, and *F. zizaniophila* is now considered a member of the genus *Iridothrips*. An identification key for the seven species is provided here, two of them are widespread across the Palearctic (*F. intonsa* and *F. tenuicornis*), one is presumably Oriental (*F. lilivora*), and four are introduced from the Americas (*F. occidentalis*, *F. schultzei*, *F. cephalica* and *F. williamsi*).

Keywords

distribution, identification, new synonyms

Introduction

The genus *Frankliniella* is one of the most species-rich genera of Thysanoptera, with 238 species listed currently (ThripsWiki 2019). Most of these are from Central and South America (Mound and Marullo 1996), with only six from the Old World. Although some species in the genus appear to be host specific on particular plants, a surprisingly large number of *Frankliniella* are polyphagous, breeding in the flowers and leaves of a range of different plants. Species with this type of biology are effectively pre-adapted to become crop pests.

In China, the Western Flower Thrips, *Frankliniella occidentalis*, is currently one of the most important insect pests of agriculture and horticulture (Cao et al. 2019), both for its direct feeding damage and for its ability to transmit tospoviruses to plants (Reitz et al. 2011). Originally from western USA, this pest is now established widely around the world, presumably distributed by the horticultural trade (Kirk and Terry 2003). A recent list of Thysanoptera species recorded from China included 12 species of *Frankliniella* (Mirab-balou et al. 2011), but this was reduced recently to 11 with some further records considered doubtful (Zhang et al. 2018). Several of the records are here recognised as incorrect, and the number of species in this genus that are validly recorded from China is now considered to be no more than seven. Two of these seven are clearly native to Palearctic, *F. intonsa* and *F. tenuicornis*, and these are often abundant with a natural distribution across China. One rare species, *F. lilivora*, was described on specimens taken in quarantine in Japan and apparently imported from China (Kurosawa 1937), but it is not known from any specimens collected in China. The remaining four species are all clearly introduced to China from other parts of the world, *F. occidentalis* from western north America, *F. cephalica* and *F. williamsi* from Meso-America, and *F. schultzei* from South America (or possibly from Africa).

Unverified species records from China

As discussed below under *F. schultzei*, one species described from Hainan as *F. hainanensis* is here recognised as a synonym of that widespread tropical pest species. A further difference from the checklist provided by Mirab-balou et al. (2011) is that the species described from China as *F. zizaniophila* is now considered a species of *Iridothrips* (Wang et al. 2019). Two further problems with the published checklist are as follows. *F. pallida* (Uzel) was recorded from China (Feng 1992) based on two males collected from flowers of *Paeonia* in Yangling, Shaanxi Province. The author provided no indication as to how these specimens were identified. Moreover, the two specimens were not distinguished from the very similar males of the two common species, *intonsa* and *occidentalis*. In view of the lack of information, the record of *pallida* from China is considered unsubstantiated. *F. tritici* is listed from China based on a single female taken in Taiwan. This female was originally described by Moulton (1948) as *F. salicis* but was subsequently recognised by Nakahara (1997: 377) as a female of *tritici*. No other specimens of *tritici* have ever been reported from Taiwan (Wang 2002), nor from mainland China, nor yet from anywhere outside of the Americas (Cavalleri and Mound 2012). In the absence of any further records, it is here assumed that the female of *salicis* came from somewhere in North America and was mislabeled during slide mounting. A similar situation was reported (Marullo and Mound 1994) concerning the record of a Californian species from India by Moulton (1927).

Materials and methods

Nomenclatural details for all taxa mentioned in this paper are available in ThripsWiki (2019). Examined specimens were slide-mounted in Canada balsam using the method of Zhang et al. (2006), and specimens are deposited in **SCAU** (Insect Collection, South China Agricultural University, Guangzhou) and **ANIC** (Australian National Insect Collection, CSIRO, Canberra). Observations were made with a Nikon Eclipse 80i phase contrast microscope, and the illustrations taken through a Leica DM 2500 microscope with DIC illumination using Automontage software, although Figure 18 was provided by Masami Masumoto.

Key to *Frankliniella* species in China

1 Abdominal tergite VIII with complete posteromarginal comb of long slender microtrichia, sometimes arising from broad triangular bases (Figs 12, 14, 16) **2**

– Abdominal tergite VIII posteromarginal comb absent at least medially, some with irregular weak teeth laterally (Figs 13, 15, 17) **4**

2 Postocular setae pair IV short, much shorter than distance between hind ocelli (Fig. 4); pronotum anterior margin generally with 1 pair of small setae between the major anteromarginal pair (Fig. 7) .... ***intonsa***

– Postocular setae pair IV as long as or longer than distance between hind ocelli (Fig. 5); pronotum anterior margin generally with 2 pairs of small setae between major anteromarginal pair (Fig. 3) **3**

3 Head and body pale yellow, tergites uniformly pale; sternite II usually with 1 or 2 long discal setae medially (Fig. 8) .... ***williamsi***

– Body colour variable brown to yellow, if tergites pale then with dark area medially (Fig. 11); sternite II without discal setae medially .... ***occidentalis***

4 Antennal segment II with pair of stout dark setae arising from apical projection; segment III pedicel with sharp-edged ring, base of segment cup-shaped (Fig.10) .... ***cephalica***

– Antennal segment II without a pair of stout dorsal apical setae; segment III pedicel without prominent ring (Fig. 9) **5**

5 Ocellar setae pair III arising within ocellar triangle, between hind ocelli (Fig. 6) .... ***schultzei***

– Ocellar setae pair III arising further apart, near margins of ocellar triangle (Fig. 2) **6**

6 Mesonotum with median pair of setae near posterior margin; metanotum with median pair of setae at anterior margin, campaniform sensilla absent (Fig. 19) .... ***tenuicornis***

– Mesonotum with median pair of setae far from posterior margin (Fig. 18); metanotum with median pair of setae behind anterior margin, campaniform sensilla present .... ***lilivora***[*]

---

[*] from description

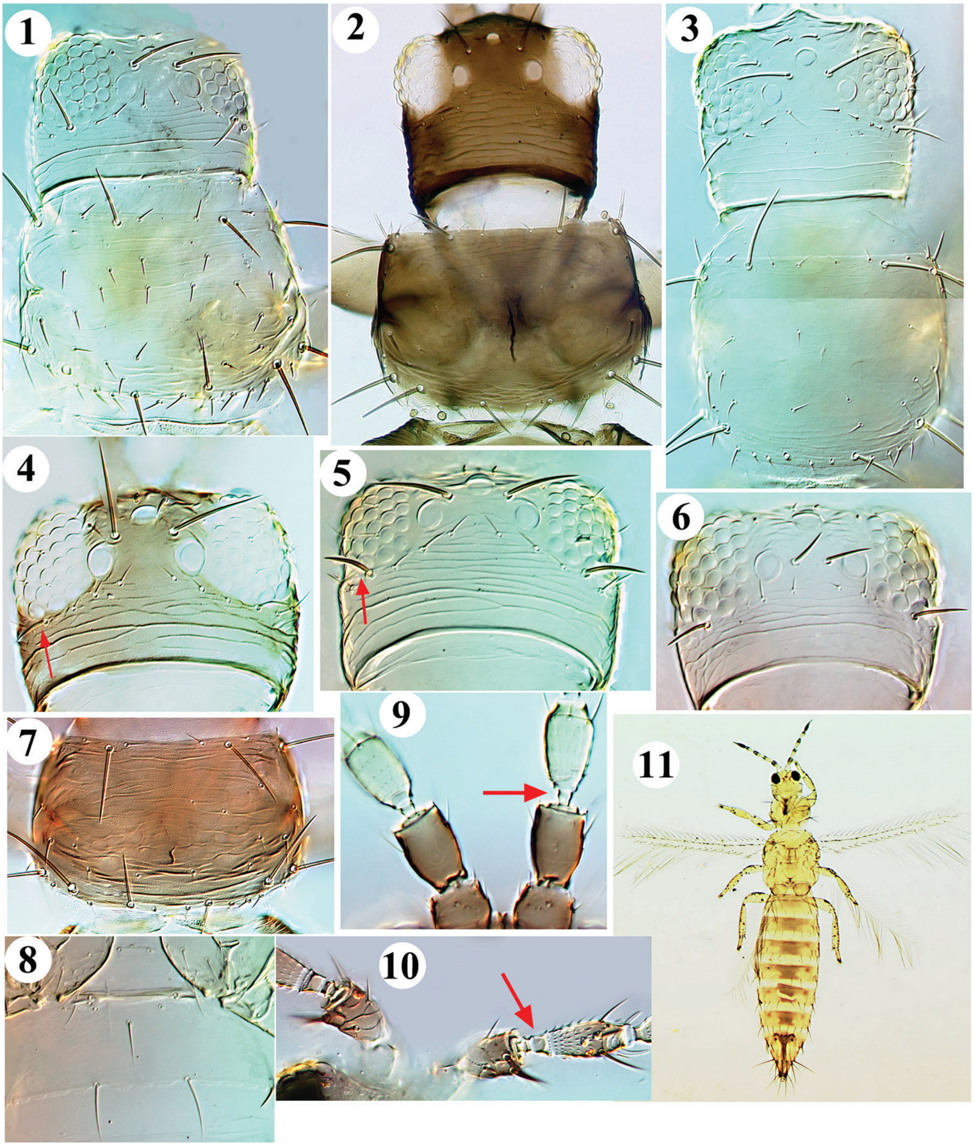

Figures 1–11. *Frankliniella* from China. Head & Pronotum: **1** *cephalica* **2** *tenuicornis* **3** *williamsi*. Head: **4** *intonsa* **5** *occidentalis* **6** *schultzei*. **7** *intonsa* pronotum. **8** *williamsi* sternite II. Antennal segments II–III: **9** *intonsa* **10** *cephalica* **11** *occidentalis* female.

Frankliniella cephalica (Crawford)

Remarks. Native to Central America and the Caribbean where it is one of the most common flower-thrips, this species has been studied in tropical areas in China from Guangdong, Guangxi, Hainan as well as Taiwan (Wang et al. 2010; Tong and Lv 2013). It has also been seen from Okinawa, Japan (Masumoto and Okajima 2004).

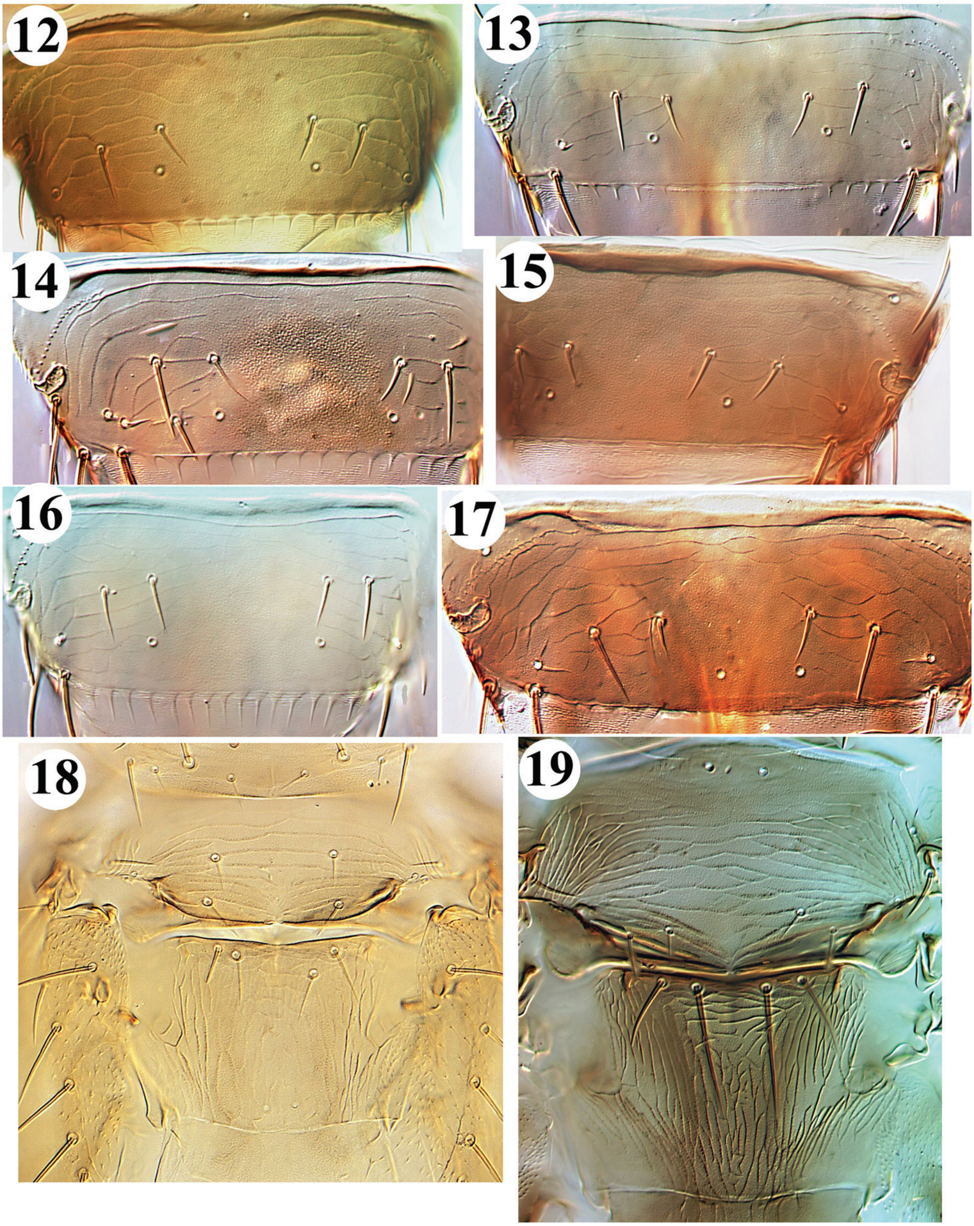

Figures 12–19. *Frankliniella* from China. Tergite VIII: **12** *intonsa* **13** *cephalica* **14** *occidentalis* **15** *schultzei* **16** *williamsi* **17** *tenuicornis*. Meso- & metanotum: **18** *lilivora* **19** *tenuicornis*.

Structurally it is unusual in that the base of the third antennal segment is strongly expanded into a sharp-edged ring (Fig. 10). In Central America this species is common in white flowers (Mound and Marullo 1996), but in China and Japan it seems to be particularly associated with the flowers of *Bidens pilosa* [Asteraceae] (Masumoto and

Okajima 2004; Tong and Lv 2013). *F. cephalica* was reported as a tospovirus vector (Ohnishi et al. 2006), and the plant *B. pilosa* has been reported as a host of Tomato spotted wilt virus in China (Huang et al. 2016). Because of its vector ability, there is a high possibility of *F. cephalica* becoming a crop pest in China.

Frankliniella intonsa (Trybom)

Remarks. This polyphagous flower thrips is widespread in the Old World and is also reported from northwestern America (Mound et al. 2019). It is one of the most common species in China, being widespread from Xinjiang to Taiwan, feeding and breeding in many different flowers. This species has been recorded as a tospovirus vector (Wijkamp et al. 1995), but its transmission efficiency was relatively low compared to *F. occidentalis* (Sakurai et al. 2004). It has been considered an important pest in China, Japan and Korea, involving hundreds of experiments but with limited evidence of yield reduction on crops. In Taiwan, this species was considered important in the international flower trade due to quarantine problems (Wang 2002). From our collection experience in the field, this species is possibly a significant pollinator.

Frankliniella lilivora Kurosawa

Remarks. Described from Japan on specimens taken in quarantine on lily bulbs imported from China (Dalian and Shanghai) and Korea (Kurosawa 1937). There are no records of the species from China, including Taiwan, and only a few specimens are known from Japan. According to the original description, it is different in having short antennae and no posteromarginal comb but a few weak and irregular teeth laterally on tergite VIII. However, it is readily distinguished from other *Frankliniella* species by the anterior position of the mesonotal median setae, and the position of the metanotal median setae behind the anterior margin (Fig. 18).

Frankliniella occidentalis (Pergande)

Remarks. Originally from the western parts of North America, it is now widespread across temperate parts of the world (Kirk and Terry 2003). It causes extensive damage to many horticultural crops, both through direct feeding damage particularly in young buds, and also through vectoring tospoviruses, it has been referred to as the most studied thrips species (Reitz 2009). Although normally phytophagous, *occidentalis* is also known to function as a predator of spider mites on leaves (Trichilo and Leigh 1986). In China, it was first recorded as a major thrips pest of horticulture and ornamental plant production in glasshouses in Beijing (Zhang et al. 2003). The species has now been found in many provinces in China (Yang et al. 2012), mainly in provinces involved in the extensive flower trade (Lv et al. 2011), and a wide potential distribution across China was reported (Cheng et al. 2006). It is not usually found in lowland tropical areas with a high humidity, but it can live on plants grown in tropical montane areas. This species exhibits variation in body colour, with dark, light, and intermediate colour morphs reported (Bryan and Smith 1956). The dark forms can be particularly common in cooler montane areas and in winter in Yunnan (Shen et al. 2015), while populations associated with crops usually involve just the intermediate form (Fig. 11). A further problem with this species is that cryptic species have been found using molecular data, but these species lack supporting biological or morphological evidence (Rugman-Jones et al. 2010).

***Frankliniella schultzei* (Trybom)**

Remarks. Commonly known as the Tomato Thrips, this species has probably been transported by human trade in plants for many years. As a result, its country of origin remains unclear, and could have been either South America or Africa. A species from China, *F. hainanensis* (Zheng et al. 2009) might be a synonym of *schultzei* according to its original descriptions and illustrations, which was also indicated by Zhang et al. (2018). Recently, Shimeng Zhang helped examine the type specimens of *hainanensis* and confirmed that it is a new synonym of *schultzei*. A further species described from Taiwan, *F. gossypii* (Shiraki 1912), was recognised as a synonym of *schultzei* by Nakahara (1997). This tropical species is exceptional within the genus in having ocellar setae pair III arising close together within the ocellar triangle (Fig. 6) and tergite VIII with almost no posteromarginal comb (Fig. 15). As an important crop pest and vector of several tospovirus diseases (Riley et al. 2011), *schultzei* shares with *occidentalis* the remarkable ability to act as a predator of leaf mites (Wilson et al. 1996). The species is widespread in tropical and subtropical countries around the world, and has been found in southern China in Guangxi, Guangdong, Hainan, Fujian and Taiwan (Zheng et al. 2009; Wang et al. 2010; Xie et al. 2011), but molecular studies in Australia have suggested that a series of sibling species may be involved (Hereward et al. 2017).

***Frankliniella tenuicornis* (Uzel)**

Remarks. This is one of the few species of *Frankliniella* that breeds on grasses, including cereal crops, and is one of the main pests that feed on young leaves of *Zea mays* in northern China (Han et al. 1979; Zhang et al. 2014a, b). It occurs widely across the Holarctic (Mound et al. 2018), and in China is found mainly in the Palaearctic areas, based on our collecting experiences (and communication with Hongrui Zhang). Records from southern provinces of China (Han 1997) require further confirmation. As a large, dark brown species, it is distinctive in the genus for the projection of the head in front of the compound eyes (Fig. 2). Moreover, postocular setae pair IV are small, and the pronotal posteromarginal setae IV are longer than pairs III and V.

Frankliniella williamsi Hood

Remarks. This yellow species is closely associated with crops of *Zea mays*, on which it is reported to be a virus vector in addition to causing feeding damage to young leaves (O'Donnell and Mound 2016). It presumably originated in Central or South America in association with maize, although it has also been taken from other species of Poaceae. It is widespread in tropical areas around the world, and in China is reported from Hainan and Taiwan. In most parts of the world it is easy to recognise from other pale coloured *Frankliniella* species by the presence of one or two discal setae on the second abdominal sternite (Fig. 8).

Acknowledgements

This study was supported by the National Natural Science Foundation of China (31372236) and South China Agricultural University Doctoral Students Overseas Joint Education Programs (No.2018LHPY022). We are grateful to Masami Masumoto for kindly supplying Figure 18 together with comments on *Frankliniella lilivora*, and to Shimeng Zhang for help checking type specimens of *hainanensis*. Thanks are also due to the referees for their advice and comments.

References

Bryan DE, Smith RF (1956) The *Frankliniella occidentalis* (Pergande) complex in California. University of California Publications in Entomology 10: 359–410.

Cao Y, Li C, Yang H, Li J, Li S, Wang Y, Gao Y (2019) Laboratory and field investigation on the orientation of *Frankliniella occidentalis* (Thysanoptera: Thripidae) to more suitable host plants driven by volatiles and component analysis of volatiles. Pest Management Science 75(3): 598–606. https://doi.org/10.1002/ps.5223

Cavalleri A, Mound LA (2012) Toward the identification of *Frankliniella* species in Brazil (Thysanoptera, Thripidae). Zootaxa 3270: 1–30. https://doi.org/10.11646/zootaxa.3270.1.1

Cheng J, Wan F, Guo J (2006) Analysis of potential distribution of the invaded insect *Frankliniella occidentalis* (Pergande) (Thysanoptera: Thripidae) in China. Acta Entomologica Sinica 49(3): 438–446. https://europepmc.org/abstract/cba/619342

Feng JN (1992) Seven new records of Thripidae from China. Entomotaxonomnia 14(3): 235–236.

Han YF (1997) Economic Insect Fauna of China. 55 Thysanoptera. Editorial Committee of Fauna Sinica, Science Press, Beijing, 266 pp.

Han YF, Pan YC, Wang DQ (1979) Studies on the thrips on corns in Peking suburbs. Acta Entomologica Sinica 22(2): 133–140.

Hereward J, Hutchinson JA, McCulloch GA, Silva R, Walter GH (2017) Divergence among generalist herbivores: the *Frankliniella schultzei* species complex in Australia (Thysanoptera: Thripidae). Arthropod-Plant Interactions 11(6): 875–887. https://doi.org/10.1007/s11829-017-9543-3

Huang CJ, Liu Y, Yu HQ, Liu BZ, Qing L (2016) *Bidens pilosa* is a natural host of Tomato spotted wilt virus in Yunnan Province, China. Plant Disease 100(9): 1957. https://doi.org/10.1094/PDIS-03-16-0344-PDN

Kirk WDJ, Terry LI (2003) The spread of the western flower thrips *Frankliniella occidentalis* (Pergande). Agricultural and Forest Entomology 5: 301–310. https://doi.org/10.1046/j.1461-9563.2003.00192.x

Kurosawa (1937) Descriptions of four new thrips in Japan. Kontyu 11: 266–275.

Lv YB, Zhang ZJ, Wu QJ, Du YZ, Zhang HR, Wang ED, Wang MH, Wang MQ, Tong XL, Lv LH, Tan XQ, Fu WD (2011) Research progress of the monitoring, forecast and sustainable management of invasive alien pest *Frankliniella occidentalis* in China. Chinese Journal of Applied Entomology 48: 488–496. http://www.ent-bull.com.cn/viewmulu.aspx?qi_id=624&mid=15652&xuhao=3

Marullo R, Mound LA (1994) Discontinuous distribution and systematic relationships of the genus *Orothrips* (Aeolothripidae; Thysanoptera) and related taxa in Mediterranean climates. Journal of the New York Entomological Society 101: 561–566. https://www.jstor.org/stable/25010041

Masumoto M, Okajima S (2004) A new record of *Frankliniella cephalica* (Thysanoptera, Thripidae) from Japan. Japanese Journal of Applied Entomology and Zoology 48(3): 225–226. https://doi.org/10.1303/jjaez.2004.225

Mirab-balou M, Tong XL, Feng JN, Chen XX (2011) Thrips (Insecta: Thysanoptera) of China. Check List (Journal of Species Lists and Distribution) 7(6): 720–744. https://doi.org/10.15560/11009

Moulton D (1927) Thysanoptera – New species and notes. Bulletin of the Brooklyn Entomological Society 22: 181–202.

Moulton D (1948) The genus *Frankliniella* Karny, with keys for the determination of species (Thysanoptera). Revista de Entomologia 19: 55–114. https://www.cabdirect.org/cabdirect/abstract/20057006768

Mound LA, Marullo R (1996) The Thrips of Central and South America: An Introduction. Memoirs on Entomology, International 6: 1–488.

Mound LA, Collins DW, Hastings A (2018) Thysanoptera Britannica et Hibernica – Thrips of the British Isles. https://keys.lucidcentral.org/keys/v3/british_thrips/index.html [30 May 2019]

Mound LA, Hoddle MS, Hastings A (2019) Thysanoptera Californica – Thrips of California. https://keys.lucidcentral.org/keys/v3/thrips_of_california_2019/ [2 Jul. 2019]

Nakahara S (1997) Annotated list of the *Frankliniella* species of the world (Thysanoptera: Thripidae). Contributions on Entomology, International 2(4): 355–389. https://www.cabdirect.org/cabdirect/abstract/19981105670

O'Donnell CA, Mound LA (2016) The confused identity of *Frankliniella williamsi* Hood (Thysanoptera, Thripidae). Florida Entomologist 99(4): 683–685. https://doi.org/10.1653/024.099.0416

Ohnishi J, Katsuzaki H, Tsuda S, Sakurai T, Akutsu K, Murai T (2006) *Frankliniella cephalica*, a new vector for Tomato spotted wilt virus. Plant Disease 90(5): 685–685. https://doi.org/10.1094/PD-90-0685B

Reitz SR (2009) Biology and ecology of the western flower thrips (Thysanoptera: Thripidae): The making of a pest. Florida Entomologist 92: 7–13. https://doi.org/10.1653/024.092.0102

Reitz SR, Gao Y, Lei Z (2011) Thrips: pests of concern to China and the United States. Agricultural Sciences in China 10(6): 867–892. https://doi.org/10.1016/S1671-2927(11)60073-4

Riley DG, Joseph SV, Srinivasan R, Diffie S (2011) Thrips vectors of tospoviruses. Journal of Integrated Pest Management 2(1): 11–110. https://doi.org/10.1603/IPM10020

Rugman-Jones PF, Hoddle MS, Stouthamer R (2010) Nuclear-mitochondrial barcoding exposes the global pest Western flower thrips, *Frankliniella occidentalis* (Thysanoptera: Thripidae) as two sympatric cryptic species in its native California. Journal of Economic Entomology 103: 877–886. https://doi.org/10.1603/EC09300

Sakurai T, Inoue T, Tsuda S (2004) Distinct efficiencies of Impatiens necrotic spot virus transmission by five thrips vector species (Thysanoptera: Thripidae) of tospoviruses in Japan. Applied Entomology and Zoology 39: 71–78. https://doi.org/10.1303/aez.2004.71

Shen DR, He C, Liu J, Yuan SY, He SY, Zhang HR (2015) The damage and morphological variations of *Frankliniella occidentalis* in Yunnan. Jiangsu Agricultural Science 43(7): 121–123. http://www.cqvip.com/main/confirm.aspx?id=665622773

Shiraki (1912) Insect pests of Cotton. Special Report No. 5, Agricultural Experiment Station Government of Formosa 5: 65–67.

ThripsWiki (2019) ThripsWiki – providing information on the World's thrips. http://thrips.info/wiki/Main_Page [13 Jun 2019]

Tong XL, Lv YB (2013) *Frankliniella cephalica* (Crawford) (Thysanoptera, Thripidae), a newly recorded exotic invasive species in Mainland China. Chinese Journal of Applied Entomology 50(2): 496–499. https://www.cabi.org/ISC/abstract/20133242219

Trichilo PJ, Leigh TF (1986) Predation on spider mite eggs by the western flower thrips, *Frankliniella occidentalis* (Thysanoptera: Thripidae), an opportunist in a cotton agroecosystem. Environmental Entomology 15: 821–825. https://doi.org/10.1093/ee/15.4.821

Wang CL (2002) Thrips of Taiwan: Biology and Taxonomy. Special publication 99. Taiwan Agricultural Research Institute, Taichung, 193pp.

Wang CL, Lin FC, Chiu YC, Shih HT (2010) Species of *Frankliniella* Trybom (Thysanoptera: Thripidae) from the Asian-Pacific Area. Zoological Studies 49(6): 824–838.

Wang ZH, Mound LA, Tong XL (2019) Relationships of the Frankliniella genus-group based on morphological analysis, with a revision of Iridothrips (Thysanoptera, Thripidae). Zootaxa 4651 (1): 141–154. https://doi.org/10.11646/zootaxa.4651.1.9

Wijkamp I, Almarza N, Goldbach R, Peters D (1995) Distinct levels of specificity in thrips transmission of tospoviruses. Phytopathology 85: 1069–1074. https://doi.org/10.1094/Phyto-85-1069

Wilson LJ, Bauer LR, Walter GH (1996) Phytophagous thrips are predators of twospotted spider mites (Acari: Tetranychidae) on cotton in Australia. Bulletin of Entomological Research 86: 297–305. https://doi.org/10.1017/S0007485300052597

Xie YH, Li ZY, Zhang HR (2011) Phytophagous thrips species in Guangxi province and one newly recorded species of the genus *Frankliniella* from China. Chinese Journal of Applied Entomology 48(3): 757–763. http://www.cqvip.com/qk/94734a/201103/38241222.html

Yang XM, Sun JT, Xue XF, Li JB, Hong XY (2012) Invasion Genetics of the Western Flower Thrips in China: Evidence for Genetic Bottleneck, Hybridization and Bridgehead Effect. PLoS ONE 7(4): e34567. https://doi.org/10.1371/journal.pone.0034567

Zhang HR, Okajima S, Mound LA (2006) Collecting and slide preparation methods for thrips. Chinese Bulletin of Entomology 43(5): 725–728. http://www.ent-bull.com.cn/asp/qikan/manage/ wenzhang /06050725.pdf

Zhang SM, Mound LA, Hastings A (2018) Thysanoptera Chinensis. Thripidae Genera from China. https://keys.lucidcentral.org/keys/v3/thysanoptera_chinensis/index.html [5 May 2019]

Zhang SQ, Han JL, Zhang LJ, Han XQ, Duan HM (2014a) Effects of different sowing dates on yield of corn and amount of thrips in corn field of Eastern Hebei Area. Journal of Hebei Agricultural Sciences 18(5): 51–53.

Zhang SQ, Han JL, Zhang LJ, Han XQ, Duan HM (2014b) Control efficiency of seven insecticides against *Frankliniella tenuicornis* (Uzel). Journal of Anhui Agricultural Sciences 42(19): 6248–6249. http://ahny.cbpt.cnki.net/WKB/WebPublication/paperDigest.aspx?paperID=474d1236-ce20-4a1a-a276-812de82b442f

Zhang YJ, Wu QJ, Xu BY, Zhu GR (2003) The occurrence and damage of *Frankliniella occidentalis* (Thysanoptera: Thripidae): a dangerous alien invasive pest in Beijing. Plant Protection 4: 58–59. http://www.cqvip.com/qk/90218x/200304/8185568.html

Zheng JW, Zhang XC, Feng JN (2009) A new species of the genus *Frankliniella* (Thysanoptera: Thripidae) from China. Entomotaxonomia 31(3): 173–175. https://www.cabdirect.org/cabdirect/abstract/20093334193

ZooKeys 873: 55–63 (2019)
doi: 10.3897/zookeys.873.36661
http://zookeys.pensoft.net

RESEARCH ARTICLE

A peer-reviewed open-access journal
ZooKeys
Launched to accelerate biodiversity research

The genus *Saissetia* (Hemiptera, Coccomorpha, Coccidae) in China, with description of a new species

Tong Cao[1], Na Zhang[1], Jinian Feng[1]

[1] *Key Laboratory of Plant Protection Resources and Pest Management, Ministry of Education, Entomological Museum, College of Plant Protection, Northwest A&F University, Yangling, Shaanxi Province, 712100, China*

Corresponding author: *Jinian Feng* (jinianf@nwafu.edu.cn)

Academic editor: *Roger Blackman* | Received 31 May 2019 | Accepted 9 August 2019 | Published 29 August 2019

http://zoobank.org/FC5DAFDC-9790-44B7-94BB-36B87368D81C

Citation: Cao T, Zhang N, Feng J (2019) The genus *Saissetia* (Hemiptera, Coccomorpha, Coccidae) in China, with description of a new species. ZooKeys 873: 55–63. https://doi.org/10.3897/zookeys.873.36661

Abstract

Saissetia kunmingensis Cao & Feng, **sp. nov.**, a member of the genus *Saissetia* Kanda, 1960, is a new species in China that is described and illustrated in this study, based on adult females. This species was found on *Osmanthus fragrans* (Oleaceae) plants from Kunming, Yunnan Province (China). An updated key to females of the eight species of *Saissetia* which occur in China was developed.

Keywords

Coccoidea, plant pest, soft scales, taxonomy

Introduction

Soft scale insects (Hemiptera, Coccomorpha, Coccidae) are the third largest family in the Coccomorpha, followed by the Diaspididae (armored scales) and the Pseudococcidae (mealybugs) (García Morales et al. 2016). Many species of soft scales are distributed in many countries throughout the world and considered to be important pests on agricultural and horticultural crops as well as ornamental plants (Henderson and Hodgson 2005). In China, they are also important pests on all of these types of plants (Yang 1982).

Prior to this study, the genus *Saissetia* Deplanche consisted of 45 known species in the world of which seven species had been reported from China (García Morales et al. 2016). In this study, we describe and illustrate a new species *Saissetia kunmingensis* sp. nov. from China. This new species shares certain characteristics with *S. coffeae* (Walker) and *S. oleae* (Olivier). An updated key to adult females of the eight species in the genus *Saissetia* known to occur in China is provided.

Materials and methods

Scale insect samples were collected from leaves and twigs of *Osmanthus fragrans* (Thunb.) Lour. (Oleaceae) in Yunnan Province in China and then stored in envelopes. Specimens were immersed in chloroform to remove wax secretions before the preparation of slides. Slides were mounted using methods described by Henderson and Hodgson (2000). Insect morphology was observed under an EVOS digital inverted microscope. The illustration of the adult female (Fig. 1) was drawn with an Olympus BH-2 stereoscopic microscope. In the illustration, the dorsum is depicted on the left side and the venter on the right side and important characters are shown around the main illustration. Photographs of ventral tubular ducts of young adult females (Fig. 2) were taken by an EVOS digital inverted microscope and a Nikon ECLIPSE Ti-U microscope. Photographs were enhanced with Adobe Photoshop CS6. All measurements were made using NIT-Elements D software and are presented in micrometers (μm) or millimeters (mm).

All specimens were deposited in the Northwest A&F University, Yangling, Shaanxi, China (**NWAFU**).

Taxonomy

Genus *Saissetia* Deplanche, 1859

Type-species. *Saissetia coffeae* (Walker, 1852).

Saissetia Deplanche, 1859: 6; Newstead 1917: 361; Hall 1935: 73; De Lotto 1956: 239; De Lotto 1957: 170; De Lotto 1963: 191; De Lotto 1965: 219; Tang 1991: 215; Henderson and Hodgson 2000: 208; Choi and Lee 2017: 101; Zhang et al. 2018: 97.

Generic diagnosis. Adult female. Body dorsum convex, H-shaped ridge present medially on dorsum. Derm with sclerotized reticulations and dermal areolations becoming well developed in older females; dorsal setae conical, thick and sturdy; submarginal tubercles present or absent on submarginal area; dorsal tubular ducts absent; anal plates triangular, together quadrate, each with a distinct discal seta; some discal setae with a sharp and pointed apex, or with a fimbriate and frayed apex. Marginal setae slender or curved, spinose with pointed apexes, bifid, frayed, or fimbriate and branched, all with well-developed basal sockets. Legs well developed, each with or without a well-developed tibio-tarsal articulatory sclerosis; claw without a denticle; multilocular disc-pores with 10–12 loculi, usually 10, present in vulvar area and on anterior abdominal segments, some sparsely present on thorax; ventral tubular ducts (VTDs) present in a broad submarginal band; 1 to 4 types of VTDs, including type I: ducts with a long outer ductule and a narrow inner ductule, width

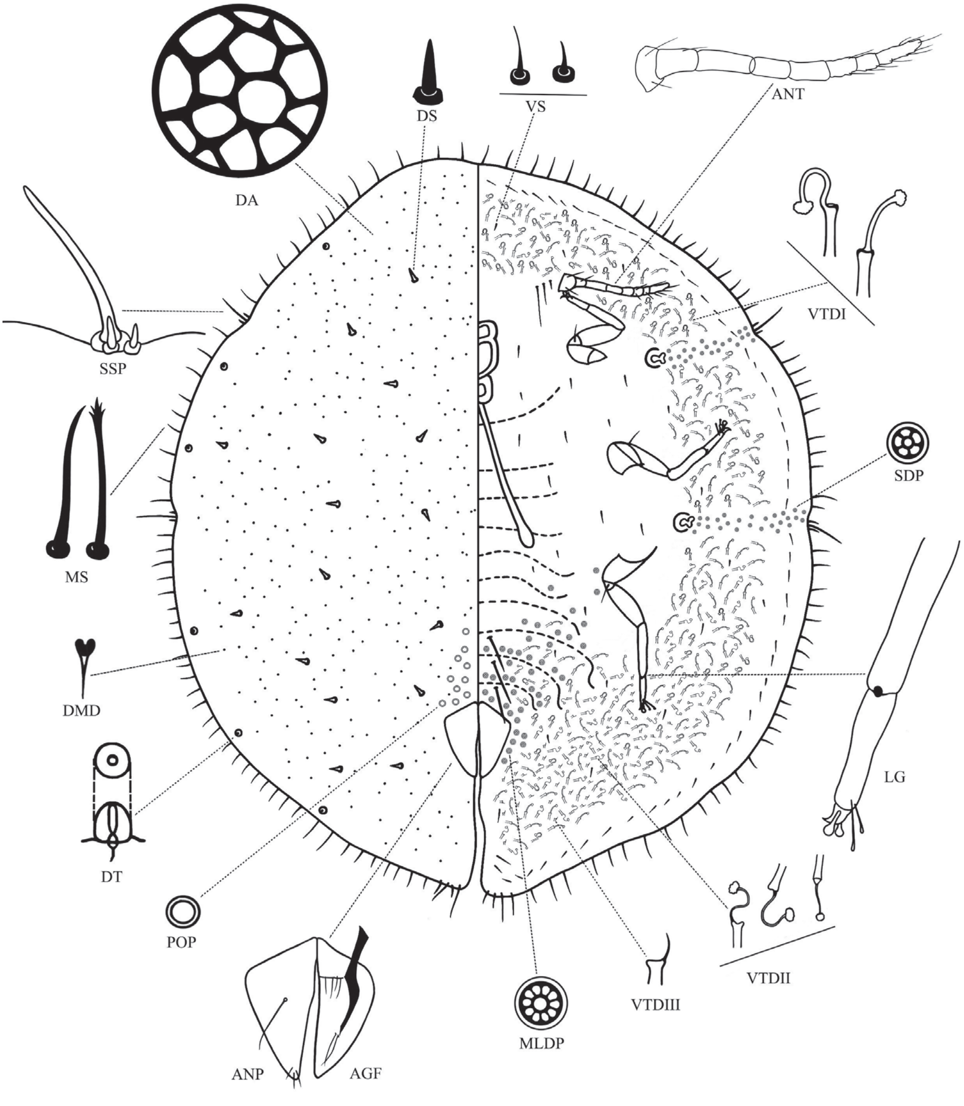

Figure 1. *Saissetia kunmingensis* Cao & Feng, sp. nov., adult female. The dorsal surface is depicted on the left side and the ventral surface on the right side, with some important characters shown enlarged around the main illustration. Abbreviations: **AGF** ano-genital fold **ANP** anal plates **ANT** antenna **DMD** dorsal microduct **DS** dorsal seta **DT** dorsal tubercles **LG** tibio-tarsus of hind leg **MS** marginal setae **MLDP** multilocular disc-pore **POP** preopercular pores **SDP** spiracle disc-pore **SSP** stigmatic spines **VTD** ventral tubular ducts of type I–III **VS** ventral setae.

of inner ductule half or less than half width of outer ductule, with a flower-shaped terminal gland; type II: ducts with a moderately long outer ductule and a long, extremely narrow inner ductule with a well-developed terminal gland; type III: a short, small duct with a filament-like inner ductule without a glandular end; type IV: a duct with a broad inner ductule of similar width and length as the outer ductule, with a well-developed terminal gland.

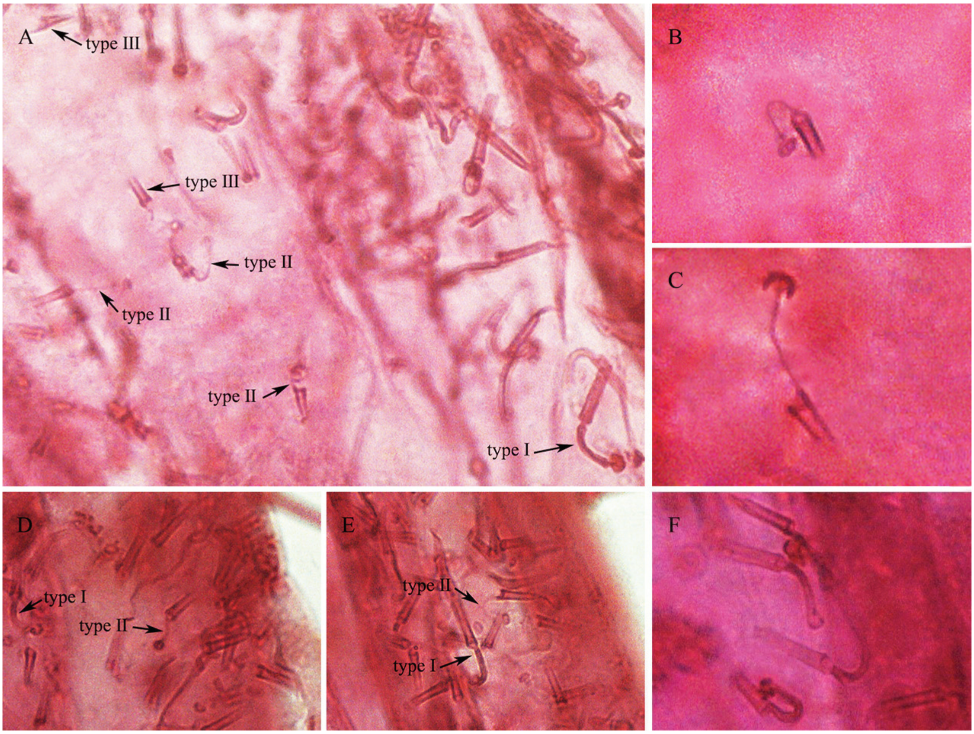

Figure 2. Ventral tubular ducts of *Saissetia kunmingensis* Cao & Feng, sp. nov. **A** type I, type II and type III VTDs present submarginally on posterior abdominal segments **B** type II VTD present submarginally on posterior abdominal segments **C** type II VTD present mediolaterally on posterior abdominal segments **D** type I and type II VTDs present submarginally around body **E** type I and type II VTDs present submarginally around body **F** type I VTDs present mediolaterally on posterior abdominal segments.

Saissetia kunmingensis Cao & Feng, sp. nov.

http://zoobank.org/8EDE0261-9C80-4CA2-86CF-E8B24EB1FDB8

Material examined. Holotype: adult female. Kunming, Yunnan Province, China. 25°04'N, 102°42'E. 1.vii.2018, on *Osmanthus fragrans* (Oleaceae), Cao Tong, Zhang Na (NWAFU). **Paratypes:** one adult female on the same slide with holotype, in the lower left corner, 4 adult females on another 2 slides, each slide with 2 specimens, data same as holotype.

Diagnosis. The adult females of *S. kunmingensis* sp. nov. can be diagnosed by a combination of the following features: (1) body almost circular to broad oval; (2) derm with sclerotized reticulations well developed; (3) dorsal submarginal tubercles convex, one or two between anterior stigmatic clefts, one or two between anterior and posterior stigmatic clefts, and three or four between each posterior stigmatic cleft and anal cleft; (4) dorsal tubular ducts absent; (5) dorsal setae conical, thick and spinose; (6) anal plates each with a distinct long discal setae with a sharp and pointed apex; (7) marginal setae slender, straight, mostly with a toothed apex, occasionally with a simple pointed apex; (8) antennae with 8 segments; (9) spiracles normal, with a distinct sclerotic plate, rarely indistinct; (10) legs with tibio-tarsal articulation and a small tibio-tarsal articulatory sclerosis; (11) multilocular disc-pores usually have 10 loculi, occasionally 11, present around vulva, across mediolateral of all abdominal segments, a few present laterad to metacoxa, sometimes present on thorax; (12) three types of VTDs (for descriptions and distributions of these see species description).

Description. Appearance of live insects. Insects yellow brown, mature adult females dark brown and reddish brown. Body broadly oval, almost circular. Dorsum of mature adults strongly sclerotized, distinctly convex with H-shaped ridge present.

Slide-mounted adult female. (Fig. 1) Body broadly oval, almost circular, broadest in anterior abdomen and thorax; body length 2.0–3.0 mm, width 1.5–2.0 mm. Anal cleft approximately 1/7–1/6 of the body length.

Dorsum. Derm with cell-like and polygonous clear areas (areolations), sclerotized reticulations on mature insects. Dorsal setae conical and sturdy, each with a pointed apex and a well-developed basal socket, scattered on dorsum, total length about 20.1–28.9 μm long (or 14.2–21.0 μm long excluding a basal socket). Submarginal tubercles numbering 1 or 2 between anterior stigmatic clefts on head, 1 or 2 between anterior and posterior stigmatic clefts, and 3 or 4 between each posterior stigmatic cleft and anal cleft. Dorsal microducts distinctly present in cell-like clear areas. Dorsal tubular ducts absent. Preopercular pores distinct, slightly convex and circular, present in front of anal plates, numbering 16–20. Anal plates each triangular, together quadrate, 240.8–267.2 μm long, 211.9–229.6 μm wide, anterolateral margin slightly convex, 118.9–140.3 μm long, posterolateral margin slightly convex, 208.3–215.6 μm long, posterior margin longer than anterior margin, outer angle slightly obtuse; plates with a well-developed supporting bar, a distinct long discal seta with a sharp and pointed apex, and 3 apical setae. Ano-genital fold with 4 pairs of anterior margin setae, 42.1–47.2 μm long and 2 lateral marginal setae, 70.9–74.6 μm long. Anal ring subcircular, with 8 anal ring setae.

Margin. Marginal setae 66.9–80.6 μm long, with well-developed basal sockets, mostly slender and straight, with a frayed, fimbriate and branched apex, but a few marginal setae with sharp and rather bluntly pointed apices; with 38–44 setae between anterior stigmatic clefts, 9–10 setae between anterior and posterior stigmatic clefts on each side, and 27–31 setae between the posterior stigmatic cleft and anal cleft. Stigmatic clefts not deep but distinct, each cleft containing three slender, tapered and bluntly spinose stigmatic spines, with well-developed basal sockets; median spine longest, 129.8–133.9 μm long, about 5 to 6 times as long as the lateral spines, each 26.2–29.0 μm long.

Venter. Derm membranous. Antennae with 8 segments, rarely 7 segments, total antennal length 453.8–463.4 μm; segment III longest. Usually 3 pairs of setae present between antennae near their base, 1 pair of short inner setae and 2 pairs of long outer setae. Three pairs of long pregenital setae present, 160.8–183.5 μm long. Other ventral setae setose, short and fine, quite sparsely distributed, 8.4–17.1 µm long. Submarginal setae 22.7–37.5 µm long, present in a single row around body. Legs well developed, each with tibio-tarsal articulation and a tibio-tarsal articulatory sclerosis which are rarely absent, tibia 154.8–176.4 µm long, longer than tarsus, which is 119.6–128.9 µm long. Claw without a denticle; claw digitules broad and expanded at apex, about 32.0–32.4 µm long. Tarsal digitules longer than claw digitules, slender, knobbed, expanded at apex, about 48.6–54.9 µm long. Spiracles normal, with a distinct sclerotic plate (rarely indistinct). Spiracular disc-pores mostly with five loculi in the outer ring; spiracular pore bands narrow, each 3–4 rows wide. Anterior spiracular pore band with 11–19 pores, posterior spiracular pore band with 12–20 pores. Multilocular disc-pores each primarily with 10 loculi, occasionally 11, present around vulva, becoming progressively less frequent anteriorly, but present across mediolateral areas of all abdominal segments, a few present laterad to metacoxa, sometimes present on thorax. Ventral tubular ducts (VTDs) present, of three types; I, II and III (Fig. 2). Type I ducts have a rather long, broad outer ductule, 23.9–28.5 µm long, and a narrow inner ductule of similar length, 24.9–29.8 µm long, width of inner ductule being half or less than half of width of outer ductule, with a well-developed flower-shaped terminal gland; type I ducts are present submarginally in a broad band around the body, and mediolaterally on posterior abdominal segments. Type II ducts have a slightly short, broad outer ductule, 13.2–20.8 µm long, and an extremely narrow filament-like inner ductule longer than the outer ductule, 17.1–31.6 µm long, with a well-developed terminal gland; type II ducts are located submarginally and mediolaterally on posterior abdominal segments, becoming sparse, few and discrete between 2 spiracular pore bands and on the anterior of the head. Type III ducts have a short outer ductule, 7.4–11.1 µm long, and a fine inner filament-like ductule without any terminal gland; these are distributed submarginally on posterior abdominal segments, and rarely on the outer submarginal area of the head.

Etymology. The species epithet *kunmingensis* refers to the place where this new species was collected, i.e., the city of Kunming.

Host plant. *Osmanthus fragrans* (Thunb.) Lour.

Distribution. Yunnan Province (China).

Key to adult females of Saissetia species occurring in China

1	Each stigmatic cleft containing 3 stigmatic spines	**2**
–	Each stigmatic cleft containing 4–7 stigmatic spines	***Saissetia vivipara* Williams & Watson, 1990**
2	One type of ventral tubular duct (VTD) present	**3**
–	More than one type of VTD present	**5**
3	Legs with tibio-tarsal articulation and articulatory sclerosis	**4**
–	Legs with tibio-tarsal articulation but without articulatory sclerosis	***Saissetia neglecta* De Lotto, 1969**

4 Mature adults red; spiracle with a sclerotic plate; VTDs with enlarged inner ductules; marginal setae mostly sharp, setose and pointed............................ .... ***Saissetia bobuae* Takahashi, 1935**

– Mature adults dark brown to black; spiracle without a sclerotic plate; VTDs with narrow inner ductules; marginal setae mostly strongly frayed, fimbriate and branched.....***Saissetia miranda* (Cockerell and Parrott in Cockerell 1899)**

5 VTDs of three or four types present; legs with tibio-tarsal articulation and articulatory sclerosis; discal setae sharp and pointed...................................**6**

– VTDs of two types present (types I and III); legs with tibio-tarsal articulation but without articulatory sclerosis; discal setae frayed and fimbriate .... ***Saissetia oleae* (Olivier, 1791)**

6 VTDs present with enlarged inner ductules; VTDs with a filament-like inner ductule (type III) present in submarginal band; multilocular disc-pores present laterad to each metacoxa and mesocoxa **7**

– No VTDs with enlarged inner ductules; VTDs with a filament-like inner ductule (type III) present at posterior end near vulvar area; multilocular disc-pores absent from near each mesocoxa ....***Saissetia kunmingensis* Cao & Feng, sp. nov.**

7 VTDs of three types present (types II, III and IV); 3 pairs of setae on ano-genital fold.. ***Saissetia coffeae* (Walker, 1852)**

– VTDs of four types present (types I to IV); 4 or 5 pairs of setae on ano-genital fold.................... ***Saissetia puerensis* Zhang & Feng in Zhang et al., 2018**

Morphological separation of *S. kunmingensis* sp. nov. from *S. coffeae* and *S. oleae*

Saissetia kunmingensis sp. nov. is morphologically similar to *S. coffeae*, which also has three types of VTDs, but these can be separated by the features shown in Table 1. (For descriptions of the types of VTDs see the generic diagnosis).

Saissetia kunmingensis sp. nov. also has similar morphology to *S. oleae*. The morphological features that can be used to separate these two species are shown in Table 2.

Discussion

The new species is at present only known from Kunming, Yunnan Province. Further studies should be conducted to explore the distribution of this new species and other *Saissetia* species, especially in the north-east region of China. The only host plant found in this study was *Osmanthus fragrans*, so the host range also needs to be further studied. *Saissetia kunmingensis* sp. nov. is potentially an important pest in China. The adult females infest branches, twigs and leaves, and glassy wax and honeydew secreted by this species can make the leaves adhere to each other, which can lead to decay or even death of the host plants.

Table 1. Morphological features that can be used to separate *S. kunmingensis* sp. nov. and *S. coffeae*. VTDs = ventral tubular ducts.

Morphological features	*S. kunmingensis* sp. nov.	*S. coffeae*
Type I VTDs	Present submarginally in a broad band around body, mediolaterally on posterior abdominal segments	Absent
Type II VTDs	Present submarginally and mediolaterally on posterior abdominal segments, sparse, few and discrete between 2 spiracular pore bands and head	Present on inner submarginal area around body and medial thorax (Tang 1991; Choi and Lee 2017)
Type III VTDs	Present submarginally and inner submarginally on posterior abdominal segments, rarely present on submarginal area of head	Present on outer submarginal area around body (Tang 1991; Choi and Lee 2017)
Type IV VTDs	Absent	Present on medial submarginal area around body (Tang 1991; Choi and Lee 2017)
Distribution of VTDs	Distributed irregularly, type I and type II ventral tubular ducts mixed mediolaterally on posterior abdominal segments, and in a broad band around body, type III ducts mixed with them submarginally on posterior abdominal segments	Distributed regularly (Tang 1991; Choi and Lee 2017)
Dorsal setae	Thick and long, 20.1–28.9 µm long including basal socket, 14.2–21.0 µm long without a basal socket	Rather short, 6.0–9.0 µm long (Choi and Lee 2017)

Table 2. Morphological features that can be used to separate *S. kunmingensis* sp. nov. from *S. oleae*. VTDs = ventral tubular ducts.

Morphological features	*S. kunmingensis* sp. nov.	*S. oleae*
Type I VTDs	Present submarginally in a broad band around body, mediolaterally on posterior abdominal segments	Only present on submarginal area (Tang 1991; Hodgson and Henderson 2000)
Type II VTDs	Present submarginally and mediolaterally on posterior abdominal segments, sparse and discrete between two spiracular pore bands and on the top of anterior head	Absent
Type III VTDs	Present on submarginal posterior abdominal segments, rarely present on outer submarginal area of head	Only present mediolaterally on posterior abdominal segments (Hodgson and Henderson 2000)
Anal plates	Posterior margin much longer than anterior margin	Length of posterior margin almost equal to or slightly longer than anterior margin (Tang 1991; Hodgson 1994)
Marginal setae	38–44 setae between anterior stigmatic clefts on head; mostly fimbriate	15–30 setae between anterior stigmatic clefts on head; mostly sharp (Hodgson and Henderson 2000)

Acknowledgements

We are grateful to Prof. William H. Reissig from Cornell University (New York, USA) for helpful suggestions and comments on the manuscript and proof-reading it before submission. We also thank him for language support of the manuscript. This study is supported by the National Science Foundation of China (Grant No. 31772502).

References

Choi J, Lee S (2017) Taxonomic review of the tribe Saissetiini (Hemiptera: Coccidae) in Korea. Journal of Asia-Pacific Entomology 20: 101–111. https://doi.org/10.1016/j.aspen.2016.11.012

Cockerell TDA (1899) Rhynchota, Hemiptera-Homoptera [Aleurodidae and Coccidae]. Biologia Centrali-Americana 2: 1–37.

De Lotto G (1956) The identity of some East African species of *Saissetia* (Homoptera, Coccidae). Bulletin of Entomological Research 47(2): 239–249. https://doi.org/10.1017/S0007485300046691

De Lotto G (1957) Notes on some African species of *Saissetia* (Homoptera: Coccoidea: Coccidae). Journal of the Entomological Society of southern Africa 20(1): 170–182. https://hdl.handle.net/10520/AJA00128789_3049

De Lotto G (1963) New species and a new genus of hard scales from East Africa (Homoptera: Coccidae). Proceedings of the Royal Entomological Society of London 32: 191–200. https://doi.org/10.1111/j.1365-3113.1963.tb01590.x

De Lotto G (1965) On some Coccidae (Homoptera), chiefly from Africa. Bulletin of the British Museum (Natural History) Entomology 16: 175–239. https://doi.org/10.5962/bhl.part.21865

De Lotto G (1969) On a few old and new soft scales and mealybugs (Homoptera: Coccoidea). Journal of the Entomological Society of southern Africa 32(2): 413–422. https://hdl.handle.net/10520/AJA00128789_3584

Déplanche E (1859) Analysis of a memoir on a disease of coffee by M.E. Déplanche, presented by M. Etudes-Deslongchamps. Bulletin de la Société Linnéenne de Normandie 4: 203–207.

García Morales M, Denno BD, Miller DR, Miller GL, Ben-Dov Y, Hardy NB (2016) ScaleNet: a literature-based model of scale insect biology and systematics. https://doi.org/10.1093/database/bav118; http://scalenet.info.

Hall WJ (1935) Observations on the Coccidae of Southern Rhodesia-VI. Stylops 4(4): 73–84. https://doi.org/10.1111/j.1365-3113.1935.tb00561.x

Henderson RC, Hodgson CJ (2000) Coccidae (Insecta: Hemiptera: Coccoidea). Fauna of New Zealand 41: 1–264. https://doi.org/10.11646/zootaxa.854.1.1

Henderson RC, Hodgson CJ (2005) Two new species of Umbonichiton (Hemiptera: Sternorrhyncha: Coccoidea: Coccidae) from New Zealand. Zootaxa 854: 1–11. https://doi.org/10.11646/zootaxa.854.1.1

Hodgson CJ (1994) The scale insect family Coccidae: an identification manual to genera. CAB International Wallingford, Oxon, 639 pp.

Newstead R (1917) Observations on scale-insects (Coccidae)-III. Bulletin of Entomological Research 7(4): 343–380. https://doi.org/10.1017/S000748530001806X

Olivier GA (1791) Cochenille. *Coccus*. Genre d'insectes de la première section de l'ordre des Hemiptères. Encyclopedie methodique, Paris.

Takahashi R (1935) Observations on the Coccidae of Formosa. V. Report Department of Agriculture Government Research Institute, Formosa 66: 1–37.

Tang FD (1991) The Coccidae of China. Shanxi United Universities Press, Taiyuan, 377pp.

Walker F (1852) List of the specimens of homopterous insects in the collection of the British Museum, Part IV. British Museum (Natural History), London, 1188 pp.

Williams DJ, Watson GW (1990) The scale insects of the Tropical South Pacific Region. Pt. 3: The Soft Scales (Coccidae) and Other Families. CAB International Wallingford, Oxon, 267 pp.

Yang PL (1982) General Classification of Scale Insects in China. Shanghai Science & Technology Press, Shanghai, 425 pp.

Zhang N, Cao T, Feng JN (2018) Description of a new species of *Saissetia* from China (Hemiptera, Coccomorpha, Coccidae). ZooKeys 791: 97–105. https://doi.org/10.3897/zookeys.791.27186

ZooKeys 873: 65–83 (2019)
doi: 10.3897/zookeys.873.35922
http://zookeys.pensoft.net

RESEARCH ARTICLE

A peer-reviewed open-access journal
ZooKeys
Launched to accelerate biodiversity research

Descriptions of the mature larva and pupa of the Scaly strawberry weevil, *Sciaphilus asperatus* (Bonsdorff, 1785) (Coleoptera, Curculionidae, Entiminae) and observations of its biology

Rafał Gosik[1], Peter Sprick[2], Tetiana Tiahunova[3]

[1] Department of Zoology, Maria Curie–Skłodowska University, Akademicka 19, 20–033 Lublin, Poland **2** *Curculio–Institute e.V. (CURCI), Weckenstraße 15, 30451 Hannover, Germany* **3** *Olzhycha 8/51, 04086 Kiev, Ukraine*

Corresponding author: *Rafał Gosik* (cossonus@gmail.com)

Academic editor: *M. Alonso-Zarazaga* | Received 4 May 2019 | Accepted 2 August 2019 | Published 29 August 2019

http://zoobank.org/676946DD-F771-412F-84E7-6453C12D6AE9

Citation: Gosik R, Sprick P, Tiahunova T (2019) Descriptions of the mature larva and pupa of the Scaly strawberry weevil, *Sciaphilus asperatus* (Bonsdorff, 1785) (Coleoptera, Curculionidae, Entiminae) and observations of its biology. ZooKeys 873: 65–83. https://doi.org/10.3897/zookeys.873.35922

Abstract

The mature larva of *Sciaphilus asperatus* is redescribed and illustrated, and the pupa is described for the first time. Supplements to the identification keys for larvae and pupae of selected Palaearctic Entiminae genera and species are given. Data on the life history, especially oviposition capacity and voltinism, of *S. asperatus* are provided and discussed, and the number of the six larval instars was confirmed. The economic importance of *S. asperatus* is briefly highlighted.

Keywords

Biology, chaetotaxy, determination, host plants, larval instar, life history, morphology, plant protection, weevils

Introduction

The weevil genus *Sciaphilus* Schönherr, 1823 contains five valid species: *S. humeralis* Desbrochers des Loges, 1902 occurs in North Africa, *S. helenae* Schilsky, 1912 in the Middle East, *S. costulatus* Kiesenwetter, 1852 and *S. ebeninus* Chevrolat, 1873 are known from isolated localities in Europe, while *S. asperatus* (Bonsdorff, 1785), the species treated in this paper, is widespread in the Western Palaearctic, Central Asia (Kazakhstan), and western Siberia (Tomsk region) (Morris 1997; Legalov 2010; Borovec 2013; Alonso-Zarazaga et al. 2017). It was recently accidentally introduced to North America (Bright and Bouchard 2008).

Species of *Sciaphilus* form a rather uniform group characterized in the adult stage by: (1) small body size (< 6 mm); (2) short rostrum with acute carina close to apex; (3) flat eyes; (4) long, slender antennae; (5) rounded elytra densely covered with oblong, erect and spherical adherent scales, the latter forming a more or less contrasting pattern; (6) femora with a conspicuous tooth (Hoffmann 1950; Smreczyński 1966; Freude et al. 1981). *Sciaphilus asperatus* (Figs 1–3) is a wingless, parthenogenetic, triploid species (Suomalainen 1969; Morris 1997). The adult is a polyphagous feeder on leaves of many herbs, shrubs and trees, mainly in the herb or even in the lower shrub layer, producing more or less characteristic notches on the leaf edge (Fig. 4). In the larval stage it feeds on the roots of plants like strawberry (*Fragaria* L.), cinquefoil (*Potentilla* L.), raspberry, blackberry (both *Rubus* L.), hawthorn (*Crataegus* L., all Rosaceae), and primrose (*Primula* L., Primulaceae). In the Berggarten area of Hannover-Herrenhausen it was regularly found in beds of *Astilbe* Buch.-Ham. ex D. Don, *Tiarella* L. (both Saxifragaceae), *Epimedium* L. (Berberidaceae) and small *Rhododendron* L. species (Ericaceae) (Sprick and Stüben 2012). In Lublin adults of *S. asperatus* were observed feeding also on *Weigela florida* (Bunge) DC. (Caprifoliaceae). In the laboratory, adults readily fed on a great number of plant species from more than 15 families (Willis 1964; Dieckmann 1980; Burakowski et al. 1993; Sprick and Stüben 2012), many of which may also be host plants. It is a eurytopic species reported from a large variety of biotopes, preferring rather moist and shady places. It occurs mostly in forests, bushes, fallow grassland and on river banks, but also in cultivations, like tree nurseries, parks and gardens (Koch 1992; Burakowski et al. 1993; Morris 1997; Gosik 2007; Sprick and Stüben 2012).

Biology and life-cycle of *Sciaphilus asperatus* have been described by Willis (1964), Krause (1978), Dieckmann (1980), and Burakowski et al. (1993). Adults are observed on host plants from mid-April to the beginning of October (Dieckmann 1980). The oviposition period in the field extends from late April to the end of July. Eggs are laid in batches between adjoining surfaces which was stated by Marvaldi (1999a) to be a common oviposition type in many Entiminae genera. Willis (1964) reported egg masses of 6 to 157 eggs, while Dieckmann (1980) recorded ca. 80 eggs (several observations). In the laboratory, we observed masses of 21 and 95 eggs (Fig. 23), deposited in two or three rows and glued with a secretion between layers of filter paper, or between the paper or a leaf placed in the box as food supply and the substrate. In the field, eggs are glued between overlapping leaves, to leaf folds, leaf petioles and stems, usually close to the ground (Willis 1964). Dieckmann (1980) and Willis (1964) reported that per year a single specimen can produce up to 880 or to 1000 eggs, respectively.

The larva develops in spring and summer, and this species usually overwinters in the adult stage (Krause 1978). According to Willis (1964), a small number of newly emerged weevils lay eggs – after a rather long pre-oviposition period of 24–31 days (only 12 days in spring) – also between mid-August and the beginning of September,

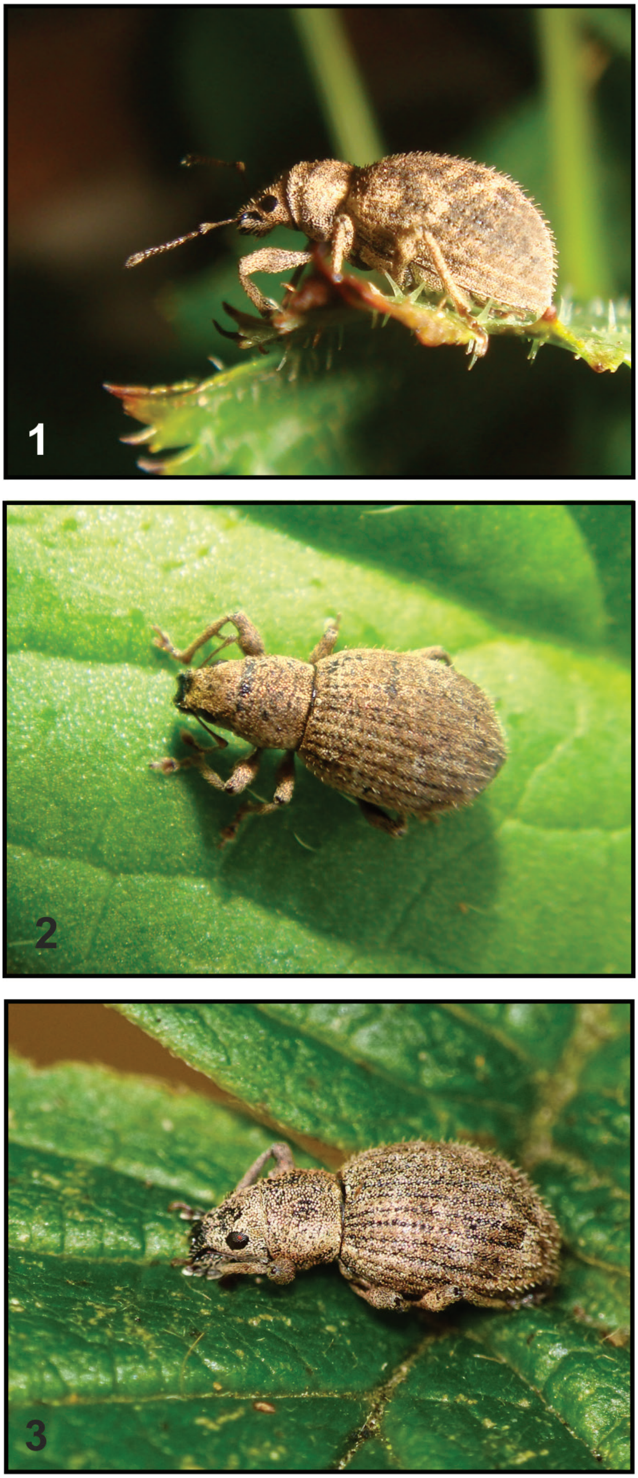

Figures 1–3. *Sciaphilus asperatus* adult, field photographs (photograph P. Sprick).

Figure 4. Leaves of *Weigela florida* with traces of feeding by adults of *Sciaphilus asperatus* (photograph R. Gosik).

which approximates the life-cycle of *S. asperatus* to that of many other soil-dwelling weevils by the presence of overwintering adults and larvae (see Gosik et al. 2016, Gosik et al. 2019). *S. asperatus* pupates between June and August; pupation in the field lasts between 14 and 21 days (Willis 1964).

The economic importance of *Sciaphilus asperatus* is usually low, compared to that of several *Otiorhynchus* species. Willis (1964) reported only two cases of severe damage in commercial strawberry cultivations in Northern Ireland and concluded: "From the limited data available it appears probable that severe damage to strawberry plants by larvae of *S. asperatus* occurs infrequently in Northern Ireland and tends to be associated with areas of light, well-drained soil." Alford (1999) also restricted the potential economic importance to strawberries: "Weevils from related genera [other than *Otiorhynchus*] (e.g. *Exomias* Bedel, 1883 and *Sciaphilus*) are also of pest status, e.g. on strawberry." Sprick and Stüben (2012), who studied the soil-dwelling weevil fauna of many tree nurseries, garden centres and parks in Germany, also ranked this species in the category of minor economic importance: "Species that usually rarely cause damage". In a study from North America, *S. asperatus* comprised nearly 10% of the total larvae in forest soils (ten sites) from the Great Lakes region in Michigan and Wisconsin (Pinski et al. 2005). *S. asperatus* sometimes forms rather large populations, which is possible, given its parthenogenesis and oviposition capacity, but Morris (1997) stated that this species rarely occurs in large numbers in Great Britain. In a small number of cultivations, mainly of Rosaceae herbs and preferably strawberries, it achieved large numbers and therefore pest status, too.

The morphology of immatures of *Sciaphilus asperatus* is still incompletely known. A piece of information on this topic is given by Emden (1950, 1952): his paper contains descriptions of spiracles and the body shape of first larval instars, as well as diagnostic characters at genus and species level. Moreover, differences between first instar larva and the mature larva are provided. But only diagrams of labrum and epipharynx of the first instar larva are presented. On the other hand, the pupa remained still unknown. On the basis of head measurements, Willis (1964) reported the presence of six larval instars in *S. asperatus*.

Materials and methods

Specimens examined

Eleven mature larvae; eight pupae, 11.07.2013, Hannover-Herrenhausen, Berggarten, botanical garden, collected from a bed of *Waldsteinia geoides* Willd. (Rosaceae).

All the larvae and pupae were collected in the field at a site where the life cycle had previously been studied using pitfall traps (see Sprick and Stüben 2012). The field work in the consecutive season was concentrated on obtaining materials for morphological study. The mature larva and pupa were described, whereas the first instar larva was used only for measurement purposes in order to ascertain the number of developmental stages (see for example Sprick and Gosik 2014 or Gosik et al. 2019). Immature stages were preserved in 75% ethanol and used for measurements and morphological descriptions.

Slide preparation basically followed May (1994). The larvae selected for study under the microscope were cleared in 10% potassium hydroxide (KOH), then rinsed in distilled water and dissected. After clearing, head, mouthparts and body (thoracic and abdominal segments) were separated and mounted on permanent microscope slides in Faure-Berlese fluid (50 g Gum Arabic and 45 g chloral hydrate dissolved in 80 g of distilled water and 60 cm^3 of glycerol) (Hille Ris Lambers 1950). The specimens and slides are deposited in the collections of the Department of Zoology, Maria Curie-Skłodowska University (Lublin, Poland).

The study was conducted using a light compound microscope (Ampliwal) with calibrated oculars and a drawing tube (MNR–1). Drawings and outlines were processed by computer software (Corel Photo-Paint X6, Corel Draw X6). The photographs were taken with an Olympus BX63 microscope and processed by Olympus cellSens Dimension software. We follow the chaetotaxy nomenclature proposed by Anderson (1947), Scherf (1964), May (1994), Marvaldi (1997, 1998, 1999b, 2003) and Skuhrovec et al. (2015), with the antennae terminology following Zacharuk (1985).

Morphological abbreviations

Larva

Abd. 1–10	abdominal segments 1–10,	**Se**	sensorium,
at	antenna,	**sa**	sensillum ampullaceum,
clss	clypeal sensorium,	**sb**	sensillum basiconicum,
st	stemmata,	**sc**	sensilla cluster,

lr	labral rods,
als	anterolateral seta,
ams	anteromedial seta,
as	alar seta,
cls	clypeal seta,
des	dorsal seta,
dms	dorsal malar seta,
ds	dorsal seta,
eps	epipleural seta,
eus	eusternal seta,
fs	frontal seta,
les	lateral epicranial seta,
ligs	ligular seta,
lrs	labral seta,
ls	lateral seta,
lsts	laterosternal seta,
mbs	malar basiventral seta,
mds	mandibular seta,
mes	median seta,
mps	maxillary palp seta,
pda	pedal seta,
pds	postdorsal seta,
pes	postepicranial seta,
pfs	palpiferal seta,
pms	postlabial seta,
prms	prelabial seta,
prns	pronotal seta,
prs	prodorsal seta,
ps	pleural seta,
ss	spiracular seta,
stps	stipal seta,
sts	sternal seta,
ts	terminal seta,
Th. 1–3	thoracic segments 1–3,
vms	ventral malar seta.

Pupa

as	apical seta,
d	dorsal seta,
ds	discal seta,
es	epistomal seta,
fes	femoral seta,
os	orbital seta,
pas	postantennal seta,
rs	rostral seta,
sls	superlateral seta,
sos	superorbital seta,
ss	spiracular seta,
ur	urogomphi,
v	ventral seta,
vs	vertical seta.

Results

Description of the mature larva

All data in [mm], (^{n}: number of exemplars).

First instar larvae: Head width 0.224^1, 0.230^1.

Mature larvae: Head width 1.05^1, 1.10^5, 1.15^3, 1.17^2; body length: 3.50^1, 4.00^2; 4.50^1, 5.00^2, 5.50^2, 6.00^3; body width: 1.50^5, 1.75^2, 2.00^4.

Body (Figs 5–9) slender, slightly curved, rounded in cross section. Prothorax slightly bigger than mesothorax; metathorax as wide as mesothorax. Abdominal segments 1–6 of almost equal length; segments 7–9 tapering gradually to the terminal parts of the body; segment 10 reduced to four anal lobes of unequal size: the biggest dorsal, the smallest ventral, both lateral equal in size. Spiracle of thorax bicameral, and of abdominal segments 1–8 annular. Chaetotaxy well developed, setae capilliform, variable in length, light yellow. Each side of prothorax with nine *prns* of unequal lengths: one long, three moderately long, five short or minute (seven of them placed on pronotal sclerite, next two close to spiracle); two *ps* (one long, one medium); and one very short *eus*. Meso- and metathorax (Fig. 5) on each side with one short *prs*, four *pds*, variable in length (*pds*$_1$, *pds*$_3$ and *pds*$_4$ medium, *pds*$_2$ relatively short), one medium *as*, one medium and one minute *ss*, one medium *eps*, one medium *ps,* and one short *eus*. Each pedal area of thoracic segments with six *pda*, variable in length (seta "*z*" invisible). Abd. 1–7 (Figs 7–9) on each side with one short *prs*, five *pds*, variable in length (*pds*$_1$, *pds*$_3$, and *pds*$_5$ very long, *pds*$_2$ and *pds*$_4$ very short) and arranged along the posterior margin of each segment, one minute and one long *ss*, one minute and one long *eps*, one minute and one medium *ps*, one short *lsts* and two short *eus*. Abd. 8 (Figs 7–9) on each side with one short *prs*, three *pds*, variable in length (*pds*$_1$ and *pds*$_3$ very long, *pds*$_2$ very short) and arranged along the posterior margin of the segment, one minute *ss*, one minute and one long *eps*, one minute and one medium *ps*, one short *lsts* and two short *eus*. Abd. 9 (Figs 7–9) on each side with three *ds* (*ds*$_1$ and *ds*$_3$ very short, *ds*$_2$ long), all located close to the posterior margin of the segment, one short and one long *ps* and two short *sts*. Each lateral anal lobe (Abd. 10) with a pair of minute *ts*.

Head (Fig. 10) light to dark yellow with some dark, vertical stripes, suboval, slightly narrowed bilaterally; frontal suture distinct, Y-shaped, endocarina absent. Setae on head capilliform. *Des*$_{1, 2, 3, 5}$ equal in length; *des*$_1$ and *des*$_2$ located in centre of epicranium, *des*$_3$ placed on frontal suture, *des*$_4$ absent, *des*$_5$ located anterolaterally. *Fs*$_{4, 5}$ equal in length, *fs*$_4$ located anteromedially, *fs*$_5$ anterolaterally, close to epistoma. *Les*$_1$ and *les*$_2$ equal in length, as long as *des*$_1$. Postepicranial area with four very short *pes*. A pair of small stemmata (st$_{1, 2}$) located anterolaterally on each side of head, variable in size. Antennae (Fig. 11) inserted at end of frontal suture; antennal segment membranous with cushion–like, relatively short Se, located medially and with seven sensilla of different types: two sa and five sb. Labrum (Fig. 12) semicircular, anterior margin smooth; three pairs of *lrs* equal in length; *lrs*$_1$ and *lrs*$_2$ placed medially, *lrs*$_3$ laterally. Clypeus (Fig. 12) trapezoid, anterior margin of clypeus gently arcuate inwards; two pairs of *cls* strongly reduced, vestigial, located posteromedially; clss clearly visible, placed medially between *cls*. Epipharynx (Figs 13, 14) with three pairs of rod-shaped *als* of almost equal length; two pairs of *ams* rod-shaped, variable in size, both distinctly shorter than *als*; 2 pairs of rod-shaped *mes* of almost equal length: the first pair placed medially, the second pair anteriorly, very close to *ams*. There is a pair of sensilla clusters (sc) close to *mes*$_2$. Labral rods elongate, curved outwards (both form a shape close to "Y"). Anterior margin of epipharynx smooth, medial part serrate due to presence of thorn-like asperities placed between labral rods. Labral rods rather short, slightly converging posteriorly. Mandibles (Figs 15–17) distinctly curved, narrow, with divided apex (teeth variable in length). A protruding additional tooth on the cutting edge between apex and middle of mandible; single *mds* capilliform, medium long. Maxilla (Figs 18, 19) with one long *stps* and two *pfs* of equal length; mala with seven finger-like *dms*, variable in size, and four *vms* (Figs 15, 16); *vms* rod-like, variable in length, always shorter than *dms*; *mbs* very short. Maxillary palpi with two

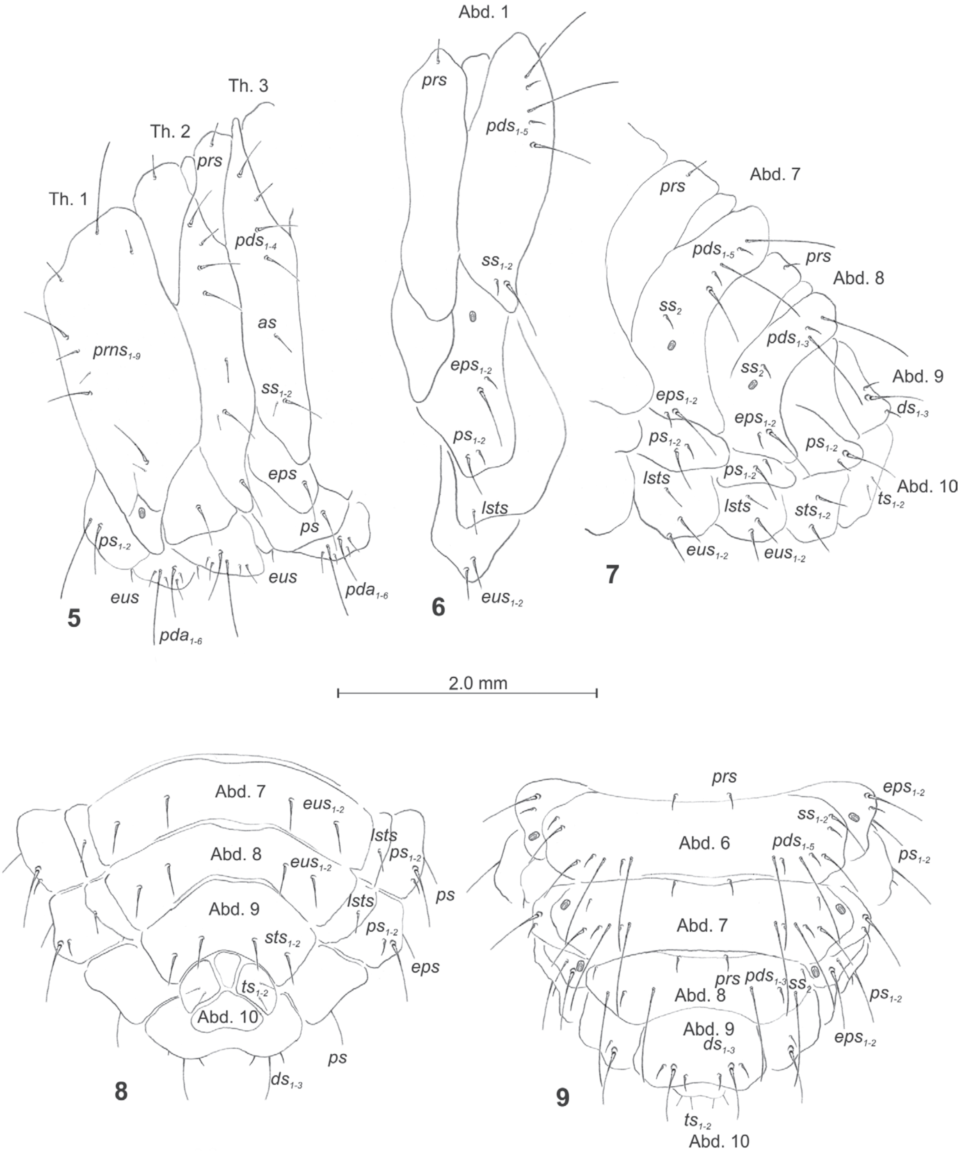

Figures 5–9. *Sciaphilus asperatus* mature larva, habitus and chaetotaxy. **5** Thoracic segments, lateral view **6** First abdominal segment, lateral view **7** Abdominal segments 7–10, lateral view **8** Abdominal segments 7–10, ventral view **9** Abdominal segments 6–10, dorsal view. Abbreviations: Th. 1–3 – thoracic segments 1–3, Abd. 1–10 – abdominal segments 1–10, setae: *as* – alar, *ps* – pleural, *eps* – epipleural, *ds* – dorsal, *lsts* – laterosternal, *eus* – eusternal, *pda* – pedal, *pds* – postdorsal, *prns* – pronotal, *prs* – prodorsal, *ss* – spiracular, *sts* – sternal, *ts* – terminal.

palpomeres, basal with short *mps*; distal palpomere apically with a group of sensilla, each palpomere with a pore. Basal palpomere distinctly wider and longer than distal, basal to distal length ratio: 1.5:1. Prelabium (Fig. 18) almost rounded with one

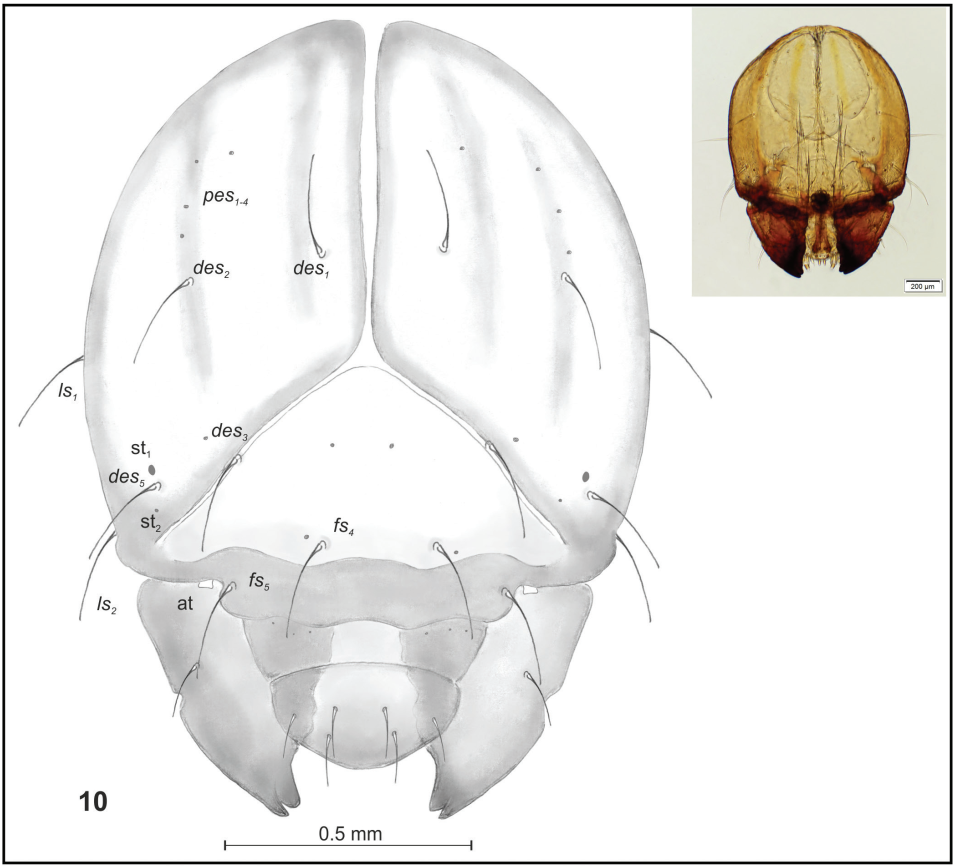

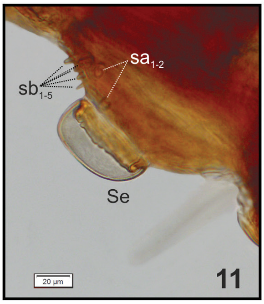

Figure 10, 11. 10 *Sciaphilus asperatus* mature larva, head, frontal view. Abbreviations: at – antenna, st – stemmata, setae: *des* – dorsal epicranial, *fs* – frontal, *les* – lateral epicranial, *pes* – postepicranial, *ves* – ventral **11** *Sciaphilus asperatus* mature larva, right antenna. Abbreviations: se – sensorium, sa – sensillum ampullaceum, sb – sensillum basiconicum.

very long *prms*, located medially. Ligula with two pairs of capilliform *ligs* of variable length. Premental sclerite clearly visible, trident-shaped, its posterior extension truncated, expanded at apex. Labial palpi two-segmented; apex of distal palpomere with some sensilla; each palpomere with a pore. Basal palpomere wider and distinctly

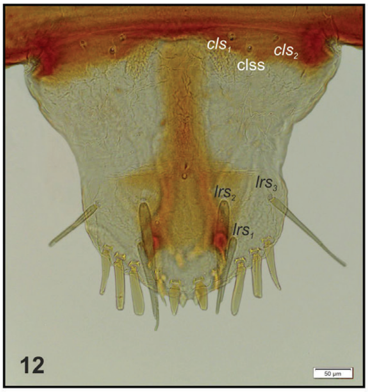

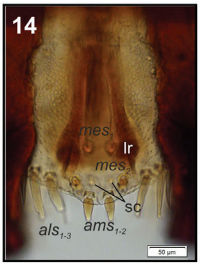

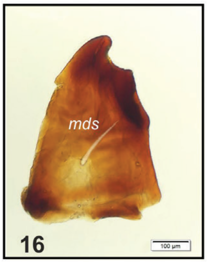

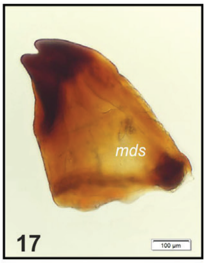

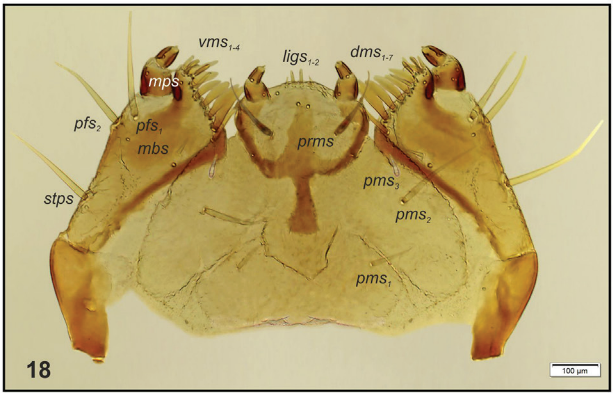

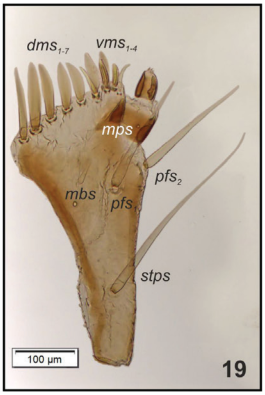

Figures 12–19. 12 *Sciaphilus asperatus* mature larva, clypeus and labrum. Abbreviations: clss – clypeal sensorium, setae: *cls* – clypeal, *lrs* – labral **13** *Sciaphilus asperatus* mature larva, epipharynx. Abbreviations: lr – labral rods, setae: *als* – anterolateral, *ams* – anteromedial, *mes* – median **14** *Sciaphilus asperatus* mature larva, epipharynx (magnification 200×). Abbreviations: lr – labral rods, sc– sensilla cluster, setae: *als* – anterolateral, *ams* – anteromedial, *mes* – median **15–17** *Sciaphilus asperatus* mature larva, right mandible **15** Lateral view **16** Dorsal view **17** Ventral view. Abbreviations: *mds* – mandibular seta **18, 19** *Sciaphilus asperatus* mature larva, body parts **18** Maxillolabial complex, ventral aspect **19** Right maxilla, ventral aspect. Abbreviations: dms – dorsal malar, ligs – ligular, mbs – malar basiventral, mps – maxillary palp, pfs – palpiferal, prms – prelabial, pms – postlabial, stps – stipal, vms – ventral malar.

longer than distal, basal to distal length ratio: 2:1. Postlabium (Fig. 18) with three capilliform *pms*, the first pair located proximally, the second medially, and the third laterodistally; pms_1 short, pms_2 and pms_3 very long.

Description of the pupa

All data in [mm].

Body length: 4.00^2, 4.75^1, 5.25^1, 5.50^4; body width: 3.00^3, 3.25^2, 3.50^3.

Head width: 1.20^4, 1.24^2.

Body moderately slender, straight, whitish. Cuticle densely covered with asperites. Rostrum short, 1.3 times as long as wide, extended beyond procoxae. Antennae relatively long and slender. Pronotum almost 2.0 times as wide as long. Abdominal segments 1–3 of almost equal length, segments 4–6 tapering gradually, 7 semicircular, 8 smaller than previous segments, 9 strongly reduced. Urogomphi short, conical, slightly sclerotized at apex (Figs 20–22).

Chaetotaxy well developed, setae of various lengths and shapes: on head (except *vs*), rostrum and mandibular thecae, capilliform, straight; on dorsal parts of thoracic (except *ls*) and abdominal segments, thorn-like. Setae yellowish to brownish, usually located on visible protuberances. Head capsule and rostrum with one pair of *vs*, two pairs of *sos*, *os*, *pas*, three pairs of *rs*, and two pairs of *es*. *Vs* thorn-like, medium-sized; all *sos*, *os*, *pas* and *rs* medium long, straight, equal in length; *es* and *mts* straight, very short (Fig. 20). Pronotum with two pairs of *as*, *ls*, *ds*, *pls*, and three pairs of *sls*. Only *ls* and sls_3 thin, capilliform, remaining setae thorn-like, placed on distinct protuberances. Sls_2 and sls_3 growing together on a single protuberance (Fig. 22).

Meso- and metathorax each with five pairs of rather small setae forming a line medially. Abdominal segments 1–7 each with 4 pairs of thorn-like *ds* (placed along posterior margin), and 2 minute, capilliform *ls*. Dorsal setae on abdominal segments 1 and 2 small, equal in length, on next segments increasing gradually in size; segment 8 with two pairs of minute, capilliform *ls*, two minute, capilliform *vs*, and three pairs of *ds*: first and second thorn-like, third capilliform, ds_2 and ds_3 growing together on a single protuberance; segment 9 with two pairs of minute, capilliform *vs*, next two with minute setae on each urogomphus (Fig. 22). Apex of femora with 2 *fes*; fes_1 long, straight, fes_2 short, thorn-like, both placed on protuberances (Figs 20–22).

Discussion

Sciaphilus asperatus is a common species. Biology and life cycle are in general well known. However, some special aspects of development, such as number of larval instars, voltinism and oviposition capacity have to be discussed herein. Some differences in chaetotaxy between *S. asperatus* and selected genera from Entiminae are also discussed. Finally, larva and pupa are integrated in current determination keys.

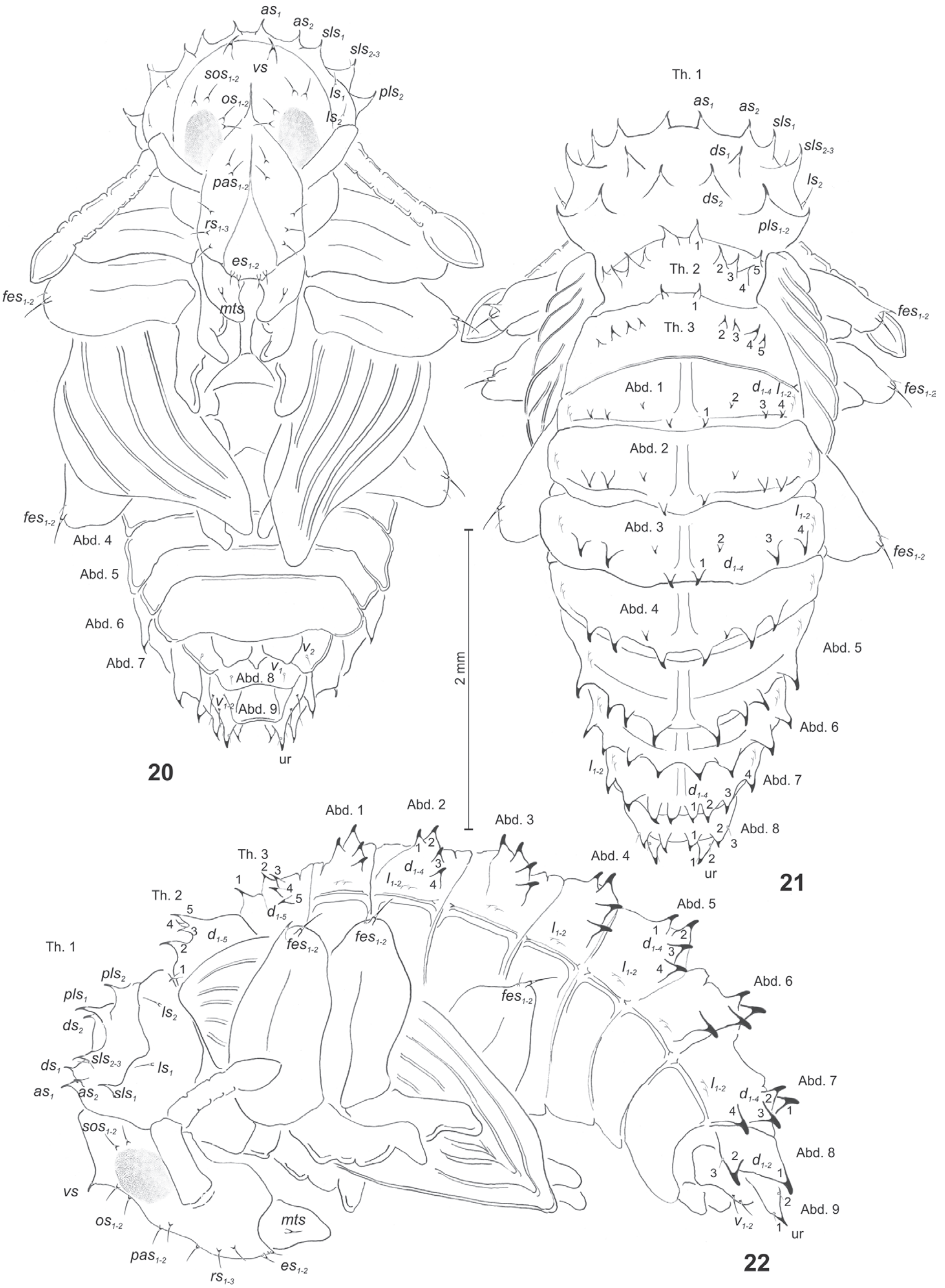

Figures 20–22. *Sciaphilus asperatus* pupa. **20** Ventral view **21** Dorsal view **22** Lateral view. Abbreviations: Th. 1–3 – pro-, meso- and metathorax, Abd. 1–9 – abdominal segments 1–9, ur – urogomphus, setae: as – apical, d – dorsal, ds – discal, es – epistomal, fes – femoral, l, ls – lateral, mts – mandibular theca, os – orbital, pas – postantennal, pls – posterolateral, rs – rostral, sls – superlateral, sos – superorbital, v – ventral, vs – vertical.

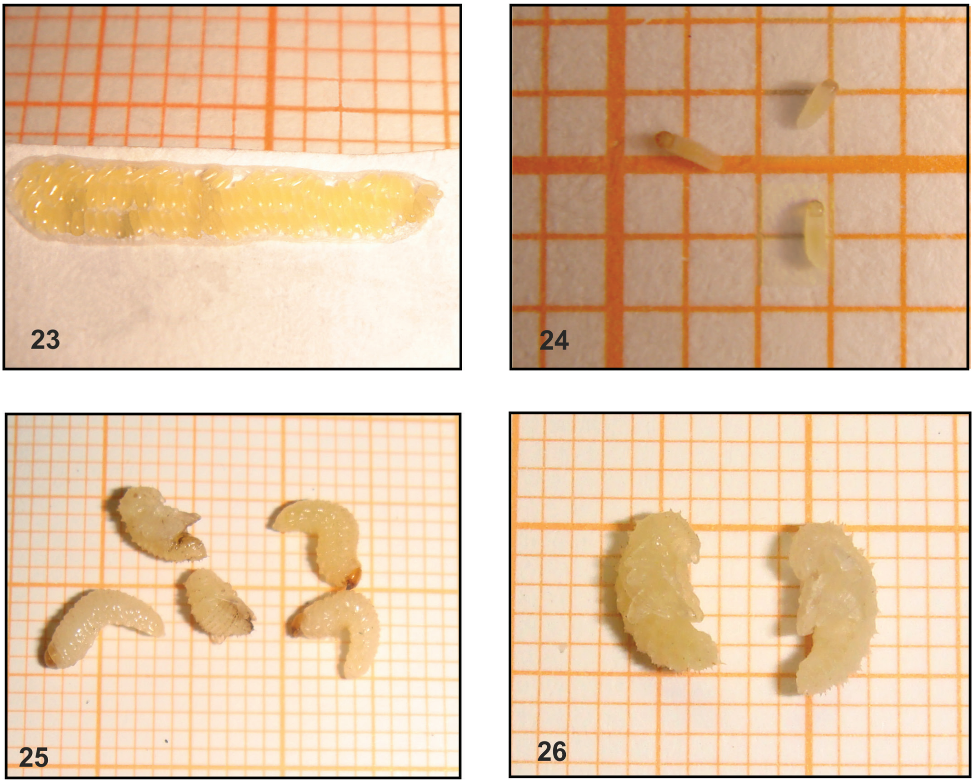

Figures 23–26. *Sciaphilus asperatus* immature stages from the laboratory (eggs, L_1 larvae) and from the field (mature larvae, pupae). **23** Eggs **24** First instar larvae **25** Mature larvae and pupae **26** Pupae (photograph P. Sprick).

Larval instar determination

Willis (1964) reported six larval instars, but the diagram on which the results of his measurements are based shows only five. He provides measurement data for 377 larvae. We checked this using the method of Sprick and Gosik (2014) or Gosik et al. (2019): see Tables 1, 2.

The data listed in Table 1 show that the mean values are very close for L_1 larvae: 0.277 mm (our data) and 0.233 mm according to Emden (1952). In mature larvae the range is a little larger but also quite close: 1.117 mm (our data) and 1.215 mm (Emden 1952). The HW of six measured pupae lies within this range. These are the best pre-conditions for larval instar determination (Table 2). The tested Growth Factor (GF) values are around 1.40, as in some other species (see for example Sprick and Gosik 2014 or Gosik et al. 2019).

From Table 2 it can be inferred that larval growth is rather slow: the best approximation in both cases is achieved with GF values < 1.4: 1.37 – 1.38 (1.375) from our own data and 1.39 – 1.40 (1.391) from the data of Emden (1952). These values are

Table 1. Head width data in *Sciaphilus asperatus* immatures.

Instar	Data [mm]	Mean value ($\bar{x}$) [mm]	Source
L_1	0.22, 0.23, 0.25	0.233	Emden (1952)
L_1	0.224, 0.23	0.227	own data
Indefinite instar	0.6, 0.67	0.635	Emden (1952)
Mature larvae	1.17, 1.26, 1.38*, 1.41*	1.215	Emden (1952)
Mature larvae	1.05, 5× 1.10, 3× 1.15, 1.17	1.117	own data
Pupa	4× 1.20, 2× 1.24	1.213	own data

*: The head widths (HW) of 1.41 and 1.38 mm are beyond the range of Willis' data for > 280 mature larvae (Willis 1964). Hence, these two larvae are not considered typical of this species and will be excluded from the instar determination. Willis' data for mature larvae range between ca. 0.88 mm and 1.35 mm with a maximum at 1.12 mm (71 larvae) according to his figure 45 and between 1.06 mm and 1.30 mm according to the text (page 97).

Table 2. Larval instar and Growth Factor determination in *Sciaphilus asperatus*.

Larval instar	GF values to be tested: 1.37/1.38/1.39/1.40/1.43	GF values to be tested: 1.37/1.38/1.39/1.40/1.43
L_1 (measured)	**0.227**[1)]	**0.233**[2)]
L_2 (calculated)	*0.311/0.313/0.316/0.318/0.325*	*0.319/0.322/0.324/0.326/0.333*
L_3 (calculated)	*0.426/0.432/0.439/0.445/0.464*	*0.437/0.444/0.450/0.457/0.476*
L_4 (calculated)	*0.584/0.597/0.610/0.623/0.664*	*0.599/0.612/0.626/0.639/0.681*
L_5 (calculated)	*0.800/0.823/0.847/0.872/0.949*	*0.821/0.845/0.870/0.895/0.974*
L_6 (calculated)	*1.096/1.136/1.178/1.221/1.357*	*1.124/1.166/1.209/1.253/1.393*
Mature larvae (measured)	**1.117**	**1.215**

Italics: calculated values; bold: measurements (except head line). – 1): own data; 2) data of Emden (1952)

much smaller than in *Tanymecus* (Gosik et al. 2019), where GF values ranged between 1.44 and 1.45. Furthermore, it is immediately obvious that *Sciaphilus asperatus* has six larval instars and that the indefinite larvae of Emden (1952) (Table 1) belong to the 4th larval instar.

Oviposition capacity

Some data are available regarding the egg-laying capacities of *Sciaphilus asperatus*. According to Emden (1952), the volume of a female's abdomen is 277 times that of a single egg. In actual fact, however, the available space must be less because of the space requirements of the digestive system, the ovipositor, viscose fluids, bordering structures and others. The highest recorded egg mass was 157 eggs per oviposition event (Willis 1964).

Willis (1964) and Dieckmann (1980) respectively reported ca. 880 and 1000 eggs laid by a single female during one season. But these data are from (or probably from) weevils maintained in the laboratory. The data relating to weevils maintained under outdoor conditions by Willis (1964) resulted in lower values of 450 to 700 eggs per female. If the pre-oviposition period lasts around 10 days (see Willis 1964), there could be 12 egg deposition events between mid-April and the end of July. If this is right, 38 to 60 eggs could be laid per oviposition event under outdoor conditions.

Generations and voltinism

According to the data presented by Krause (1978) and Dieckmann (1980), *Sciaphilus asperatus* should be a univoltine species: overwintered adults produce eggs, larvae hatch in spring and summer, pupation takes place in summer, and adult weevils of the new generation emerge also in summer. But Burakowski et al. (1993) reported that a small part of the new generation lays eggs in August, producing larvae that overwinter. Moreover Willis (1964) presumed that usually all larvae overwinter. This hypothesis has still to be checked. It appears equally possible that larvae from eggs laid early in the season develop in the same year as is true for many other soil-dwelling weevils (see for example Gosik et al. 2016, Gosik and Sprick 2017).

A species that develops within one season is univoltine, whereas a species that needs longer than one year for its development is semivoltine. Neither definition fits *S. asperatus* or many other soil-dwelling weevils. Apparently, there is a mix of univoltine summer development, and univoltine or semivoltine (if development of the overwintering larvae should last longer than one year) autumn/spring development; in winter there is not usually any development. It seems these definitions are hard to apply to soil-dwelling weevils, as they do not fit the facts very well.

Remarks on chaetotaxy

There are only several small discrepancies between the description of the mature larva given by Emden (1952) and those presently described: e.g. Emden reported two mandibular setae (one prominent and next very small), whereas we observed only a single seta. It is possible that the second (very small) *mds* visible on the first instar larva was torn off during intensive feeding of the mature larva. Emden (1952) reported on the presence of seven setae on the pedal area of the prothorax, the seventh a minute seta (“*z*”), and three further minute setae of each lateral anal lobe. We noticed only six setae on each pedal lobe and only two pairs of minute terminal setae on the lateral lobes of the tenth segment.

It is worth stressing that the presently described mature larva of *S. asperatus* possesses exactly all essential characters listed by Marvaldi (1998) for Entiminae larvae, Type “A”, namely: single *as*; setae mes_1 close together whereas setae mes_2 placed far one another; mes_2 placed close to *ams*; sensilla cluster placed between mes_2; labral rods curved outwards; premental sclerite trident-shaped, with posterior extension truncate, expanded at apex.

Supplement to the key to selected genera and tribes of Palaearctic Entiminae larvae

Based on Gosik et al. (2016), Gosik and Sprick (2017), Gosik et al. (2017), and Gosik et al. (2019): in *Graptus, Peritelus,* and *Sciaphilus* the key is based on one species each (*G. triguttatus triguttatus*, *P. sphaeroides,* and *S. asperatus*).

(Previous step as in Gosik et al. 2019)

2 Abdominal segment 10 reduced to three lobes; clypeus always with well-developed median furrow; meso- and metathorax each with single *ss (sps)*......... .... **Sitonini (*Andrion*, *Charagmus*, *Coelositona*, *Sitona*)**

(next steps as in Gosik and Sprick 2017)

– Abdominal segment 10 reduced to four lobes; clypeus smooth; meso- and metathorax each with 2–3 *ss* (*sps*) **2a**

2a All spiracles (thoracic and abdominal) bicameral.. ....***Otiorhynchus* (Otiorhynchini)**

(next steps as in Gosik et al. 2016)

– At least abdominal spiracles annular..**2b**

2b Meso- and metathorax with 3 *ss* each, Se conical...... ***Graptus* (Byrsopagini)**

– Meso- and metathorax with 2 *ss* each, Se cushion-like............................... **2c**

2c Head unicolour. All spiracles annular. Each pedal area with 4 *pda*, abdominal segment 8 with 4 *prs*; abdominal segment 9 with 4 *ds*....................................... ....***Peritelus* (Peritelini)**

– Head with faint stripes. Thoracic spiracles bicameral, abdominal annular. Each pedal area with 6 *pda*, abdominal segment 8 with 3 *prs*; abdominal segment 9 with 3 *ds*..***Sciaphilus* (Sciaphilini)**

3 All spiracles (thoracic and abdominal) bicameral; head oval .... ***Strophosoma* (Brachyderini)**

(next steps as in Gosik et al. 2017)

– All spiracles (thoracic and abdominal) annular; head narrowed bilaterally..... ....***Philopedon* (Cneorhinini), *Tanymecus* (Tanymecini)**

(next steps as in Gosik et al. 2019)

Upgrade to the key to pupae of selected Palaearctic Entiminae genera and tribes by Gosik and Sprick (2013)

(Previous steps as in the original key)

9 Pronotal and abdominal setae thorn-like, inserted on elongate protuberances .... **Sciaphilini Sharp, 1891**

9a Body length in both sexes < 4.75 mm, head with 1 pair of *os*, rostrum with 4 pairs of *rs*, mandibular thecae without setae; *as*$_1$ distinctly smaller than *as*$_2$, pronotum with 1 pair of *ls* and 2 pairs of *sls*; each abdominal segment 1–7 with 3 pairs of setae, *fes*$_1$ and *fes*$_2$ equal in length .... ***Exomias* Bedel, 1883 (= *Barypeithes* Du Val, 1854, in part)**

9b Body length of females up to 5.50 mm (usually > 4.75 mm), head with 2 pairs of *os*, rostrum with 3 pairs of *rs*, mandibular thecae with 1 pair of *mts*, *as*$_1$ and *as*$_2$ equal in size, pronotum with 2 pairs of *ls* and 3 pairs of *sls*, each abdominal segment 1–7 with 4 pairs of setae, *fes*$_1$ distinctly bigger than *fes*$_2$..................... .... ***Sciaphilus* Schönherr, 1823**

Taking into consideration the shape, number, and distribution of setae, and the general body shape, the pupae of *Sciaphilus asperatus* and of *Exomias pellucidus* (Boheman, 1834) are very similar (see Gosik and Sprick 2013). Especially due to hair-like setae on head and rostrum and to thorn-like setae on pronotum and abdomen, which are observed on both species as well as the presence of paired *sls* growing on single protuberances and the absence of ventral setae on abdominal segments 1–7. This morphological information is coherent with the close systematic position of both species in the tribe Sciaphilini.

Acknowledgements

We would like to express our cordial thanks to Dr Adriana Marvaldi (Buenos Aires) for her very constructive and helpful comments on the manuscript. We express our sincere thanks to Peter Senn (Gdynia) for his linguistic correction of the text. The biology part of this study was supported by the German Federal Agency for Agriculture and Food (BLE, Bonn) and developed from the soil-dwelling weevils project of the Curculio Institute (CURCI).

References

Alford DV (1999) A Textbook of Agricultural Entomology. Wiley-Blackwell, London, 320 pp.

Alonso-Zarazaga MA, Barrios H, Borovec R, Bouchard P, Caldara R, Colonnelli E, Gültekin L, Hlaváč P, Korotyaev B, Lyal CHC, Machado A, Meregalli M, Pierotti H, Ren L, Sánchez-Ruiz M, Sforzi A, Silfverberg H, Skuhrovec J, Trýzna M, Velázquez de Castro AJ, Yunakov NN (2017) Cooperative Catalogue of Palaearctic Coleoptera. Curculionoidea. Sociedad Entomológica Aragonesa, Monografias electrónicas SEA, 8. http://www.sea-entomologia.org [10 November 2017]

Anderson WH (1947) A terminology for the anatomical characters useful in the taxonomy of weevil larvae. Proceedings of the Entomological Society of Washington 49(5): 123–132.

Borovec R (2013) Curculionidae: Entiminae: Sciaphilini In: Löbl I, Smetana A, Catalogue of Palaearctic Coleoptera. Vol. 8. Curculionoidea II. Brill; Leiden, Boston, 377–386.

Bright DE, Bouchard DP (2008) Weevils of Canada and Alaska. Volume 2. Coleoptera, Curculionidae, Entiminae. The Insects and Arachnids of Canada, Part 25. National Research Council of Canada, NRC Research Press, Ottawa, Canada, 327 pp.

Burakowski B, Mroczkowski M, Stefańska J (1993) Chrząszcze (Coleoptera) Ryjkowce – Curculionidae, Catalogus faunae Poloniae 23, 306 pp.

Dieckmann L (1980) Beiträge zur Insektenfauna der DDR: Coleoptera – Curculionidae (Brachycerinae, Otiorhynchinae, Brachyderinae). Beiträge zur Entomologie 30(1): 145–310.

Emden FI Van (1950) Eggs, egg-laying habits and larvae of short-nosed weevils. Eighth International Congress of Entomology, Stockholm 1948: 365–372.

Emden FI Van (1952) On the taxonomy of Rhynchophora larvae: Adelognatha and Alophinae (Insecta: Coleoptera). Proceedings of the Zoological Society of London 122(3): 651–795. https://doi.org/10.1111/j.1096-3642.1952.tb00248.x

Freude H, Harde K, Lohse G (1981) Die Käfer Mitteleuropas. Band 10 (Bruchidae, Anthribidae, Scolytidae, Platypodidae, Curculionidae). Goecke & Evers. Krefeld, 310 pp.

Gosik R (2007) Ryjkowcowate, Col., Curculionoidea zebrane do pułapek lepowych przeciwko szrotówkowi kasztanowcowiaczkowi *Cameraria ohridella* Deschka & Dimić. Chrońmy Przyrodę Ojczystą 63(5): 3–18.

Gosik R, Sprick P (2013) Morphology and identification of the pupae of several species of soil-dwelling broad-nosed weevils from Central Europe (Coleoptera, Curculionidae, Entiminae). Zootaxa 3731(4): 445–472. Incl. Erratum: Zootaxa 3745(2): 299–300. https://doi.org/10.11646/zootaxa.3731.4.2

Gosik R, Sprick P (2017) Description of the larvae and pupae of eight species of the tribe Sitonini Gistel, 1848 (Coleoptera, Curculionidae) from Central Europe. Zootaxa 4324(3): 401–435. https://doi.org/10.11646/zootaxa.4324.3.1

Gosik R, Sprick P, Czerewko K (2017) Morphology of the larvae of three Central European *Strophosoma* Billberg, 1820 (Coleoptera, Curculionidae, Entiminae) species. Deutsche Entomologische Zeitschrift 64: 27–42. https://doi.org/10.3897/dez.64.11446

Gosik R, Sprick P, Morris MG (2019) Descriptions of immature stages of four species of the genera *Graptus*, *Peritelus*, *Philopedon*, and *Tanymecus* and larval instar determination in *Tanymecus* (Coleoptera, Curculionidae, Entiminae). ZooKeys 813: 111–150. https://doi.org/10.3897/zookeys.813.30336

Gosik R, Sprick P, Skuhrovec J, Deruś M, Hommes M (2016) Morphology and identification of the mature larvae of several species of the genus *Otiorhynchus* (Coleoptera, Curculionidae, Entiminae) from Central Europe with an update of the life history traits. Zootaxa 4108(1): 1–67. https://doi.org/10.11646/zootaxa.4108.1.1

Hille Ris Lambers D (1950) On mounting aphids and other soft-skinned insects. Entomologische Berichten 13: 55–58.

Hoffmann A (1950) Coléoptères curculionides (Première partie). Paris: Lechevalier. Faune de France 52: 1–486.

Koch K (1992) Die Käfer Mitteleuropas. Vol. 3 (Ökologie). Goecke & Evers, Krefeld: 380 pp.

Krause R (1978) Untersuchungen zur Biotopbindung bei Rüsselkäfern der Sächsischen Schweiz. Entomologische Abhandlungen 42: 1–210.

Legalov AA (2010) Annotated checklist of species of superfamily Curculionoidea (Coleoptera) from Asian part of the Russia. Amurian Zoological Journal 2: 93–132.

Marvaldi AE (1997) Higher level phylogeny of Curculionidae (Coleoptera: Curculionoidea) based mainly on larval characters, with special reference to broad-nosed weevils. Cladistics 13: 285–312. https://doi.org/10.1111/j.1096-0031.1997.tb00321.x

Marvaldi AE (1998) Larvae of Entiminae (Coleoptera: Curculionidae): tribal diagnoses and phylogenetic key, with a proposal about natural groups within Entimini. Entomologica Scandinavica 29: 89–98. https://doi.org/10.1163/187631298X00212

Marvaldi AE (1999a) Eggs and oviposition habits in Entimini (Coleoptera: Curculionidae). The Coleopterists Bulletin 53(2): 115–126.

Marvaldi AE (1999b) Morfología larval en Curculionidae. Acta zoológica Lilloana 45: 7–24. https://doi.org/10.1163/187631298x00212

Marvaldi AE (2003) Key to larvae of the South American subfamilies of weevils (Coleoptera, Curculionoidea). Revista Chilena de Historia Natural 76: 603–612. https://doi.org/10.4067/S0716-078X2003000400005

May BM (1994) An introduction to the immature stages of Australian Curculionoidea. In: Zimmerman EC (Ed.) Australian weevils. Volume II: Brentidae, Eurhynchidae, Apionidae and a chapter on the immature stages by Brenda May. CSIRO Publications, Melbourne, Victoria, 365–728.

Morris MG (1997) Coleoptera: Curculionidae (Entiminae). Broad-nosed weevils. Royal Entomological Society of London. Handbooks for the identification of British weevils 5, part 17a: 1–106.

Pinski RA, Mattson WJ, Raffa KF (2005): Composition and seasonal phenology of a nonindigenous root-feeding weevil (Coleoptera: Curculionidae) complex in northern hardwood forests in the Great Lakes region. Environmental Entomology 34(2): 298–307. https://doi.org/10.1603/0046-225X-34.2.298

Scherf H (1964) Die Entwicklungsstadien der mitteleuropäischen Curculioniden (Morphologie, Bionomie, Ökologie). Abhandlungen der Senckenbergischen Naturforschenden Gesellschaft 506: 1–335.

Skuhrovec J, Gosik R, Caldara R, Košťál M (2015) Immatures of Palaearctic species of the weevil genus *Sibinia* (Coleoptera, Curculionidae): new descriptions and new bionomic data with suggestions on their potential value in a phylogenetic reconstruction of the genus. Zootaxa 3955(2): 151–187. https://doi.org/10.11646/zootaxa.3955.2.1

Smreczyński S (1966) Ryjkowce (Curculionidae). Podrodziny: Otiorhynchinae, Brachyderinae. Klucze do oznaczania owadów Polski 19: 1–130.

Sprick P, Gosik R (2014) Biology and morphology of the mature larva of *Mitoplinthus caliginosus* (Curculionidae, Molytinae). – SNUDEBILLER: Studies on taxonomy, biology and ecology of Curculionoidea 15, No. 229, CURCULIO-Institute, Mönchengladbach, 10 pp. https://www.curci.de/?beitrag=229

Sprick P, Stüben PE (2012) Rüsselkäfer in anthropogenen Lebensräumen. With 1318 coloured photos, 60 maps und 100 plates, 170 pp. [in German] – SNUDEBILLER*extra* (CD Rom), Curculio-Institute, Mönchengladbach.

Suomalainen E (1969) Evolution in parthenogenetic Curculionidae. Evolutionary Biology 3: 261–296.

Willis RJ (1964) The bionomics and larval morphology of the otiorrhynchid pests of soft fruit crops. – Thesis, The Queen's University of Belfast, Northern Ireland, 250 pp, appendix 60 pp.

Zacharuk RY (1985) Antennae and Sensilla. In: Kerkut GA, Gilbert LI (Eds) Comprehensive Insect Physiology, Chemistry and Pharmacology, 6. Pergamon Press, Oxford, 1–69.

ZooKeys 873: 85–111 (2019)
doi: 10.3897/zookeys.873.36645
http://zookeys.pensoft.net

RESEARCH ARTICLE

A peer-reviewed open-access journal
ZooKeys
Launched to accelerate biodiversity research

Revision of *Claraeola* (Diptera, Pipunculidae) in the Middle East based on morphology and DNA barcodes

Behnam Motamedinia[1,2], Jeffrey H. Skevington[1], Scott Kelso[1]

1 *Canadian National Collection of Insects, Arachnids and Nematodes, Agriculture and Agri-Food Canada, 960 Carling Avenue, Ottawa, ON K1A 0C6, Canada* **2** *Plant Protection Research Department, South Khorasan Agricultural and Natural Resources Research and Education Center, AREEO, Birjand, Iran*

Corresponding author: *Behnam Motamedinia* (Bmoetamedi@yahoo.com)

Academic editor: *Ximo Mengual* | Received 30 May 2019 | Accepted 19 July 2019 | Published 29 August 2019

http://zoobank.org/1D706422-6B99-45E2-AC03-BB350C4676B4

Citation: Motamedinia B, Skevington JH, Kelso S (2019) Revision of *Claraeola* (Diptera, Pipunculidae) in the Middle East based on morphology and DNA barcodes. ZooKeys 873: 85–111. https://doi.org/10.3897/zookeys.873.36645

Abstract

The Middle East species of *Claraeola* Aczél (Diptera, Pipunculidae) are revised based on morphological characteristics and sequence data from the mitochondrial COI barcoding gene, using a novel COI mini-barcode protocol. Four new *Claraeola* species are described: *C. bousynterga* Motamedinia & Skevington, **sp. nov.**, *C. heidiae* Motamedinia & Skevington, **sp. nov.**, *C. khuzestanensis* Motamedinia & Skevington, **sp. nov.,** and *C. mantisphalliga* Motamedinia & Skevington, **sp. nov.** *Eudorylas thekkadiensis* Kapoor, Grewal & Sharma, 1987 is transferred to *Claraeola*, *C. thekkadiensis* (**comb. nov.**). Diagnoses, illustrations, an identification key, and a distributional map are given for the Middle East species.

Keywords

big-headed flies, COI, distribution map, DNA barcoding, identification key, mini barcode protocol

Introduction

Pipunculidae Walker 1834 (Diptera), commonly known as big-headed flies, are important endoparasitoids of Auchenorrhyncha (Hemiptera), particularly the families Cicadellidae, Delphacidae and Cercopidae, and Tipulidae (Diptera) (Koenig and Young 2007; Rafael and Skevington 2010). Females of big-headed flies typically lay only one egg inside each host and rates of parasitism vary from a fraction of a percent to 100% in local populations (Skevington and Marshall 1997). Since many species of Auchenorrhyncha are known to transmit plant diseases (Weintraub and Beanland 2006), Pipunculidae have the potential of becoming biological control agents of economically important pest species such as green rice leafhoppers, *Nephotettix* spp. feeding on rice, or the potato leafhopper, *Empoasca fabae* (Harris, 1841), which severely damages potato and alfalfa crops (Hardy 1964; Jervis 1992). Pipunculidae are characterized by large compound eyes that occupy most of their hemispherical head, distinctive wing venation, the piercer-like shape of the female ovipositor, and the presence of a chitinized postspiracular plate in the last instar larvae of the subfamilies Chalarinae and Pipunculinae (Wada 1991; Rafael and De Meyer 1992). Currently, 1,450 species of pipunculids are recognized worldwide, placed into four subfamilies and 20 genera (Kehlmaier et al. 2014; Kehlmaier et al. 2019; Skevington 2019). The genus *Claraeola* Aczél, 1940 comprises 35 described species, occurring in the Afrotropical (four species; Földvári 2013), Palaearctic (17 species; Kehlmaier 2005a; Kehlmaier 2005b), Oriental (seven species; Kozánek and Kwon 1991; Kozánek et al. 2003, Kehlmaier 2005b), and Australasian (seven species; Skevington 2002) regions. Placed within the diverse tribe Eudorylini, *Claraeola* can best be separated from the other genera by the hind tibia having a mid-anteriorly wrinkled indentation bearing some erect setae and the presence of at least some small but distinct tooth-like projections on the male phallus, which are arranged either on a membranous sheath or on the ejaculatory ducts itself (Kehlmaier 2005a; Motamedinia et al. 2017b). Aczél (1940) erected *Claraeola* from one previously described species, *Dorylas adventitius* Kertész, 1912. This genus has been re-defined by Skevington and Yeates (2001) and found to be senior synonym of *Congomyia* Hardy, 1949 and *Moriparia* Kozánek & Kwon, 1991. Skevington (2002) revised the Australian species of *Claraeola*, whereas Kehlmaier (2005a, 2005b) and Földvári (2013) revised the Palaearctic/Oriental and Afrotropical members of this genus, respectively, but there is no information about its biology or immature stages.

The Middle East [here defined to include Bahrain, Cyprus, Iran, Iraq, Israel, Jordan, Kuwait, Lebanon, Oman, Palestine, Qatar, Saudi Arabia, Syria, Turkey, United Arab Emirates, and Yemen] is located between three zoogeographic realms (Palaearctic, Oriental, and Afrotropical regions). However, only four species of *Claraeola* [*C. halterata* (Meigen, 1838); *C. conjuncta* (Collin, 1949); *C. parnianae* Motamedinia & Kehlmaier, 2017, and *C. khorshidae* Motamedinia & Kehlmaier, 2017] have been previously reported from this region (Kehlmaier 2005a, 2005b; Motamedinia et al. 2017a, 2017b). As recently studied material brought to light additional unnamed species of the genus, the purpose of this work is to revise *Claraeola* species from the Middle East region. The revision includes descriptions of four new species, photo illustrations of important morphological characters, a distribution map and an identification key to the Middle Eastern *Claraeola* species.

Materials and methods

Insect material

The study is based on material deposited in the Canadian National Collection of Insects, Arachnids and Nematodes (**CNC**; Ottawa, Canada), the Hayk Mirzayans Insect Museum (**HMIM**; Insect Taxonomy Research Department, Iranian Research Institute of Plant Protection, Tehran, Iran(, Senckenberg Natural History collections Dresden (**SMTD**; Dresden, Germany); Indian Agriculture Research Institute (**INPC**; New Delhi, Inida), and the Tel Aviv University (**TAU**; Tel Aviv, Israel). The specimens were collected using Malaise traps, sweep nets, and pan traps. Full descriptions are presented for new species only, and a brief diagnosis is provided for known species. Most male genitalia were separated from the abdomen, heated in lactic acid (85%) at 100 °C for 30–240 minutes, and then placed into a drop of glycerin on a microscope slide. Potassium hydroxide was used for terminalia that were very darkly pigmented or that were to be used for photography. For this, terminalia were treated with 10% KOH at 100 °C for 10–30 minutes then immersed in glacial acetic acid for 5 minutes to buffer the reaction and stop the clearing. Following clearing, dissection involved separating syntergosternite 8 and the epandrium from the remainder of the abdomen. For photography, the epandrium was removed to fully expose the hypandrium and phallic structures. The dissected genitalia are stored in plastic microvials with glycerin on the same pin as the source specimen. All specimens are labeled with a unique reference number from the CNC database (e.g., Jeff_Skevington_Specimen12345 and CNC_Diptera12345, abbreviated as JSS12345 and CD12345 respectively) and can be accessed at https://cnc.agr.gc.ca/. Species are described in alphabetical order. SimpleMappr (Shorthouse 2010) was used to create the species distribution map.

External characters were imaged using a Leica DFC450 module fitted on a Leica M205C stereomicroscope using 0.6× lens. Final images were merged using the image-stacking software Zerene Stacker (Littlefield 2018). Images of the genitalia were taken using a Leica DM5500B microscope equipped with a Leica DMC4500 module connected to a personal computer running the Leica Application Suite software (https://www.leica-microsystems.com), which includes an Auto-Montage module that combines multiple layers of photographs into a single fully focused image. All photos were subsequently modified using Adobe Photoshop CS3 imaging software. The morphological terminology follows Skevington (2002) and Kehlmaier (2005a) with the following abbreviations being used throughout the paper:

LF:WF	ratio of length of flagellum to its width.
LW:MWW	ratio of length of wing to maximum width of wing.
LS:LTC	ratio of length of pterostigma to length of third costal segment.
LTC:LFC	ratio of length of third costal segment to length of fourth costal segment.
LT35:WT5	ratio of length of tergites 3–5 to maximum width of tergite 5.
WT5:LT5	ratio of width of tergite 5 to its length.
T5R:T5L	ratio of length of right margin of tergite 5 to length of its left margin.
LT35:WS8	ratio of length of tergites 3–5 to width of syntergosternite 8.
LS8:HS8	ratio of length syntergosternite 8 to its height.
MLE:MWE	ratio of maximum length of epandrium to its maximum width (viewed dorsally).
LP:LB	ratio of length of piercer to length of base (viewed laterally).
LDP:LPP	ratio of length of distal part of piercer to length of its proximal part (viewed laterally).

DNA extraction, PCR amplification, and sequencing

Total genomic DNA was extracted either from two legs or from whole specimens using the DNeasy Blood and Tissue Kit (Qiagen Inc., Santa Clara, CA, USA) following the manufacturer's protocol. Following extraction, specimens were critical-point dried and deposited as vouchers in the CNC.

For DNA barcoding, a 658 bp fragment of the 5' end of the mitochondrial coding gene cytochrome oxidase subunit I (COI) was amplified using the primer pair LCO1490 and COI-Dipt-2183R, as previously described by Gibson et al. (2011). In some cases, initial attempts to amplify the full COI barcode failed, presumably due to the degradation of the DNA. In these cases, a novel COI mini-barcode protocol was employed (Young et al. in prep.) in order to amplify a 214 bp fragment (COI-Fx-C), located at the3'-end of the COI barcode region, for species identification. In the case of putative new species, efforts were made to amplify the5' and middle COI mini-barcode fragments (COI-Fx-A and COI-Fx-B respectively) that, when combined, provide a complete COI barcode sequence. Oligonucleotides (primers) used in this study are listed in Table 1. PCR amplifications were carried out in 25µl volumes, including 15.7µl ddH$_2$O, 2.5µl 10X Ex Taq PCR buffer (containing 20mM MgCl$_2$), 0.65µl 25mM MgCl$_2$, 1µl of each 10µM primer, 2µl 10mM dNTPs, 0.15µl Ex Taq HS DNA polymerase (TaKaRa Bio USA, Madison, WI, USA), and 2µl total DNA. Amplification cycles were performed on an Eppendorf ep Gradient S Mastercycler (Eppendorf AG, Hamburg, Germany). All PCR and sequencing reactions were performed with the following thermal cycler conditions: 94 °C for 3 mins × 1 cycle, 94 °C for 45 secs, 45 °C for 45 secs, 72 °C for 1 min × 45 cycles, 72 °C for 5 minutes × 1 cycle, followed by an unlimited step at 10 °C. Amplification products were visualized on 1% agarose electrophoresis gels and purified prior to sequencing using either Clone-Well 0.8% Egels (Invitrogen™, Carlsbad, CA, USA) for full barcode amplicons, or an ExoSAP-IT protocol (USB Corp., Cleveland, OH, USA) for COI-Fx amplicons. Sequencing reactions were carried out in 10µl volumes, using the ABI BigDye Terminator v3.1 Cycle Sequencing kit (PE Applied Biosystems, Foster City, CA, USA). Bidirectional sequencing reactions were purified using the ABI ethanol/EDTA/sodium acetate precipitation protocol and analyzed on an ABI 3500xl Genetic Analyzer (PE Applied Biosystems, Foster City, CA, USA). Sanger Sequencing was performed at CNC.

Table 1. Cytochrome c oxidase subunit I mitochondrial gene primers.

Gene name/ region	Forward primer name	Forward primer sequence (5'-3')	Primer reference	Reverse primer name	Reverse primer sequence (5'-3')	Primer reference
COI Barcode	LCO1490	GGTCAACAAATCATAAAGATATTGG	Folmer et al. (1994)	COI-Dipt-2183R	CCAAAAAATCARAATARRTGYTG	Gibson et al. (2011)
COI-Fx-A (5' end of barcode)	LCO1490	GGTCAACAAATCATAAAGATATTGG	Folmer et al. (1994)	COI-SYR-1762R	CGDGGRAADGCYATRTCDGG	Young et al. (in prep.)
COI-Fx-B (middle of barcode)	COI-SYR-342F	GGDKCHCCNGAYATRGC	Young et al. (in prep.)	COI-SYR-1976R	GWAATRAARTTWACDGCHCC	Young et al. (in prep.)
COI-Fx-C (3' end of barcode)	COI-SYR-1957F	GGDATWTCHTCHATYYTAGG	Young et al. (in prep.)	COI-Dipt-2183R	CCAAAAAATCARAATARRTGYTG	Gibson et al. (2011)

All sequence chromatograms were edited and contigs formed using Sequencher 5.4.6 (Gene Codes Corp., Ann Arbor, MI, USA). Resulting contigs were hand-aligned using Mesquite 3.6 (Maddison and Maddison 2018). Uncorrected pairwise genetic distances (p-distance) were calculated with Mega7 (Kumar et al. 2016). Sequence accession numbers issued by GenBank (**GB**) and the European Nucleotide Archive (**ENA**) are provided for each specimen.

Results

Key to males of *Claraeola* species in the Middle East

1 Abdominal tergites with narrow but distinct yellow markings (Fig. 9F) **2**
– Abdominal tergites without narrow yellow markings (Fig. 9A–D) **3**
2 Mid and hind tibiae with erect anteromedial setae (Fig. 9E); ejaculatory ducts with small teeth (Fig. 5D) .... ***C. khuzestanensis* sp. nov.**
– Only hind tibia with erect anteromedial setae; ejaculatory ducts without small teeth (Fig. 7D, E) .... ***C. parnianae* Motamedinia & Kehlmaier**
3 Phallus embedded in membranous sheath (Figs 2D, 6D)........................... **4**
– Phallus without distinctly membranous sheath **7**
4 Legs light-brown (Fig. 9B); surstyli with enlarged separation at base (Fig. 6D) .... ***C. mantisphalliga* sp.nov.**
– Legs dark (Fig. 9D); surstyli without enlarged separation at base **5**
5 Abdominal tergite 2 with some long setae laterally (Fig. 9C); surstyli in lateral view with humped base dorsally (Fig. 3D, E); membranous sheath surrounding ejaculatory ducts weak with small teeth (Fig. 3E)... ***C. halterata* (Meigen)**
– Abdominal tergite 2 without some long setae laterally; genitalia not as above ... **6**
6 Syntergosternite 8 large (Fig. 9A); left gonopod longer than right one (Fig. 1B); surstyli as in Fig. 1C–D .... ***C. bousynterga* sp. nov.**
– Syntergosternite 8 small; left gonopod as long as right one (Fig. 2B); surstyli as in Fig. 2D, E... ***C. conjuncta* (Collin)**
7 Surstyli straight in lateral view; ejaculatory ducts with small spines (Fig. 4D, E) .... ***C. heidiae* sp. nov.**
– Surstyli bent in lateral view; ejaculatory ducts with large spines (Fig. 11B, F, G)...................................... ***C. khorshidae* Motamedinia & Kehlmaier**

Claraeola Aczél, 1940

Claraeola Aczél, 1940: 151. Type species: *Dorylas adventitius* Kertész, 1912, by original designation.

Congomyia Hardy, 1949b: 7. Syn. by Skevington and Yeates 2001: 429. Type species: *Congomyia nigripennis* Hardy, 1949, by original designation. Syn. by Skevington and Yeates 2001: 429.

Moriparia Kozánek & Kwon, 1991: 77. Type species: *Moriparia nigripennis* Kozánek & Kwon, 1991, by original designation. Syn.: Skevington and Yeates 2001: 429.

Diagnosis. Medium to large big-headed flies, body length 3.2−7.4 mm, wing length 3.2−8.4 mm, pedicel with 4−10 upper and 3−10 lower bristles, flagellum gray to brownish gray pruinose, frons silver-gray pruinose with a weak median keel, postpronotal lobe with 6−18 setae, scutellum with 8−22 short setae along posterior margin, hind tibia with a wrinkled indentation mid-anteriorly bearing some erect setae, pterostigma present, cross-vein r-m reaches dm at or after one third of the cells length, abdomen ovate or elongate, ground color dark (in some specimens with narrow posterolateral yellow marks), tergite 1 with 3–20 long bristles, situated in one to three rows, tergite 2 with or without lateral bristles, membranous area medium to large, epandrium mostly wider than long (LS8:HS8 < 1), phallus partly clothed in small, but distinct setae or teeth, arranged on membranous sheath or on ejaculatory ducts.

Biology. Unknown

Distribution. Palearctic (Algeria, Austria, Belgium, Canary Islands, China, Cyprus, Czech Republic, Denmark, Egypt, France, Germany, Great Britain, Greece, Hungary, Iran, Israel, Italy, Latvia, Lithuania, Netherlands, North Korea, Russia, Slovakia, South Korea, Sweden, Switzerland, Tunisia), Oriental (Borneo, India, Myanmar, Nepal, Philippines, Taiwan, Thailand, Vietnam), Afrotropical (Burundi, Cameroon, Congo, Madagascar, Malawi, Uganda), and Australian (Australia, Papua New Guinea) (Skevington and Yeates 2001; Skevington 2002; Kehlmaier 2005a, 2005b; Földvári 2013; Motamedinia et al. 2017a, 2017b; Kehlmaier et al. 2019).

Taxonomic treatment of species, in alphabetical order

Claraeola bousynterga Motamedinia & Skevington, sp. nov.

http://zoobank.org/7AB2F6DF-3AFC-4B73-A142-0E0B3537DC68
Figs 1, 8A, 9A

Examined material. *Holotype.* IRAN • ♂; Sistan & Balochestan, Saravan; 27°25'N, 62°17'E; 8 Nov. 2016; F. Hamzavi leg.; pan trap; JSS51920; GB: MN182733; CNC. ***Paratypes.*** IRAN • 1 ♂; same data as holotype; JSS51829; GB: MN182745; CNC • 1 ♀; same data as holotype; 2 Sep. 2015; sweep net; JSS52173; GB: MN182734; CNC.

Diagnosis. Due to the shape of the surstyli, phallus and phallic guide, this species is related to the *clavata* species group: *C. discors* (Hardy, 1966), known from Nepal and partly illustrated by Kehlmaier (2005b), *C. clavata* (Becker, 1897), known from Europe and re-described by Kehlmaier (2005a), *C. conjuncta* (Collin, 1949), *C. khorshidae* Motamedinia & Kehlmaier, 2017 and *C. thekkadiensis* (Kapoor, Grewal & Sharma, 1987) comb. nov. It differs from these species by the shape of surstyli in lateral view being weakly bent, broad syntergosternite 8 and a large membranous area.

Description. Male. Body length (excluding antennae): 4.2–4.3 mm (n = 2). ***Head.*** Scape, pedicel and arista dark brown, pedicel with a pair of short plus long

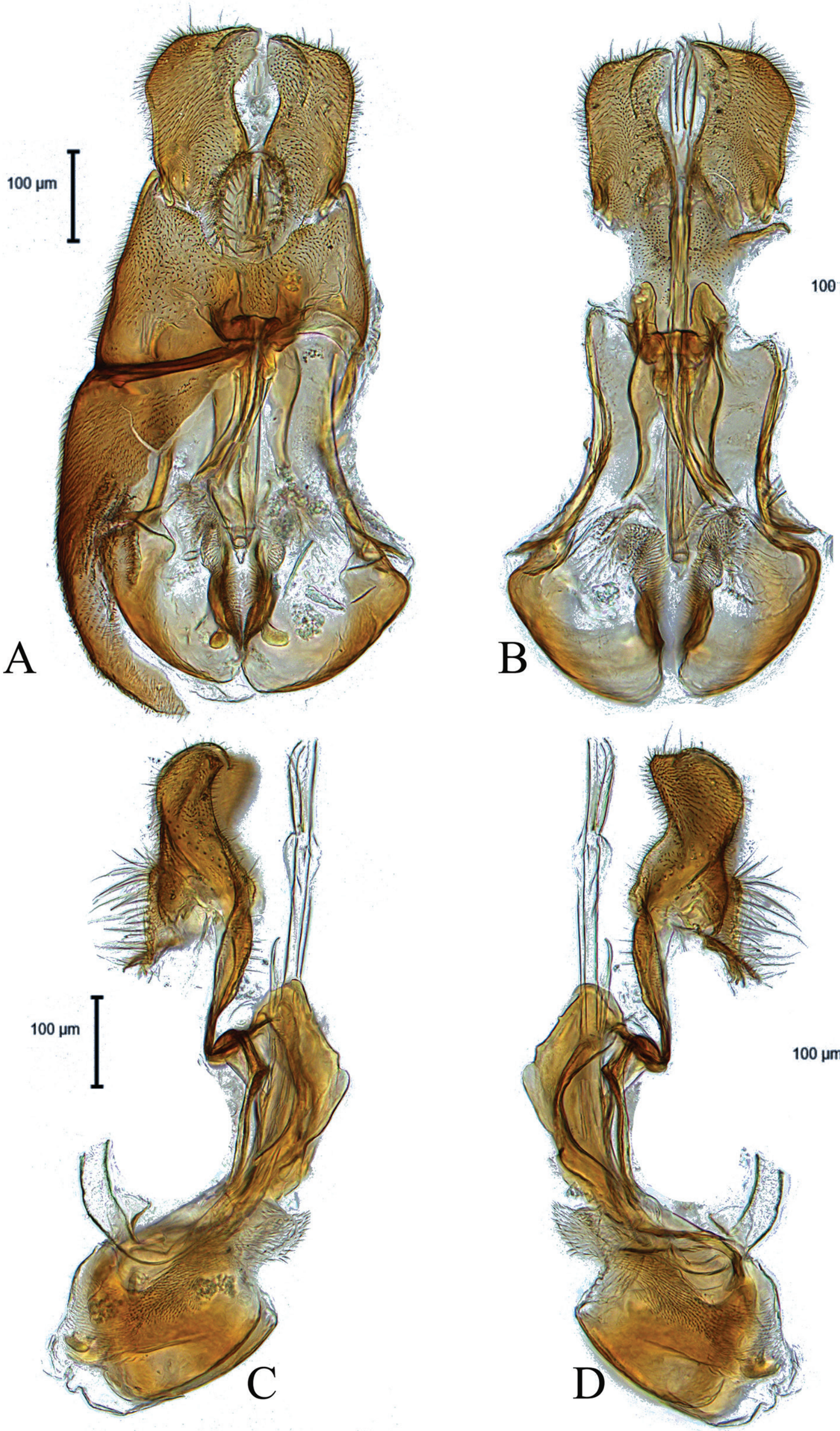

Figure 1. Male genitalia of holotype *Claraeola bousynterga* Motamedinia & Skevington, sp. nov. **A** in dorsal view **B** in ventral view **C, D** in lateral view.

upper and lower bristles, lower bristles longer than upper bristles, flagellum tapering and light brown pruinose (LF:WF = 2.2); arista with thickened base. Eyes meeting for a distance of 16 facets. Frons dark silver-gray pruinose. Vertex black, bearing an elevated slightly ocellar triangle. Occiput dark and gray pruinose with a row of long setae along posterior margin. ***Thorax.*** Postpronotal lobe dark, gray pruinose. Prescutum and scutum black with scattered long setae at anterior supra-alar area. Scutellum black with ca. 12 thin short setae along posterior margin (up to 0.05 mm). Subscutellum black, gray pruinose. Pleura dark brown ***Wing.*** Length: 3.5–3.8 mm. LW:MWW = 3.0. Wing almost entirely covered with microtrichia. Pterostigma dark-brown and complete. LS:LTC = 1.0. LTC:LFC = 1.5. Cross-vein r-m reaches dm shortly after one third of the cell's length. M_1 strongly undulating in middle. Halter length: 0.7 mm, base and knob dark, stem narrowly white or dark. ***Legs.*** Coxae dark, gray pruinose. Mid coxa with two or three black anterior bristles. Trochanters partly gray pruinose, mid trochanter with two or three black anterior bristles, hind trochanter partly yellow with 4–6 brown anterior bristles. Femora dark with pale apices, gray pruinose with two or three wrinkled indentations at base. Mid and hind femora bearing two rows of dark anteroventral small spines in apical half. Tibiae gray pruinose, with two rows of short setae on anterior side and three rows on posterior. Hind tibia with two or three wrinkled indentations in middle without erect anteromedial setae. Tarsi yellowish at posterior margin but darkened with scattered dark setae at anterior margin. Pulvilli yellow. Claws brown with black tips. ***Abdomen.*** Ground color dark, tergite 1 silver-gray pruinose, with three or four dark lateral bristles (up to 0.1 mm). Tergites 2–5 posterolaterally gray pruinose, slightly extending onto dorsal surface along posterior margin, largest on tergite 5 where they extend onto dorsal surface, otherwise brown pruinose. Tergite 5 slightly longer than tergite 4 and almost symmetrical in dorsal view (LT35:WT5 = 1.1, WT5:LT5 = 0.6, T5R:T5L = 1.0). Sternites white-yellow laterally and brown with dark mid-line centrally, gray pruinose. Syntergosternite 8 enlarged, dark brown and gray pruinose without dorsal depression on side of right surstylus. LT35:WS8 = 2.5. Viewed laterally, longer than high (LS8:HS8 = 1.8). Membranous area large and roundish, more than one third of the width of syntergosternite 8. ***Genitalia.*** Genital capsule in dorsal view: epandrium and surstyli dark brown, inner side of both surstyli yellow, gray pruinose. Epandrium wider than long (MLE:MWE = 0.53). Surstyli rather symmetrical. Left surstylus slightly smaller than right one, right surstylus with slightly broadened tip (Fig. 1A). Genital capsule in ventral view: subepandrial sclerite wide with scattered setae, gonopod medium sized with two projections in its middle, inner gonopod slightly higher than outer one (Fig. 1B). Genital capsule in lateral view: phallus straight, strong and long, with three short ejaculatory ducts, two of them bearing small teeth along their sides; both surstyli slightly narrowed in middle, right surstylus slightly larger than left surstylus (Fig. 1C, D). Phallic guide small, reaching base of surstyli. Epandrium without projecting lobe on either side. Genital capsule in dorsal view: surstyli rather rectangular, base and tips broadened (Fig. 1A).

Female. Body length (excluding antennae): 3.6mm (n = 1). Eyes separated. Frons gray pruinose. Occiput gray pruinose. Postpronotal lobe dark, yellow in upper margin, gray pruinose. Scutum black, gray pruinose with scattered setae at anterior supra-alar area. Wing length: 3.7 mm. LW:MWW = 2.4. Pterostigma light-brown and slightly complete (LS:LTC = 0.98, LTC:LFC = 0.9). Mid coxa with 3–5 black anterior bristles. Femora bearing two small ventral rows of dark peg-like spines in the apical third. Hind tibia without distinctly stronger bristly setae. Tergites 1–2 gray pruinose, tergites 3–5 posterolaterally gray pruinose, slightly extending onto dorsal surface along posterior margin, otherwise brown pruinose. ***Ovipositor.*** Viewed laterally: piercer long (LP = 0.7 mm), strongly curved upward and reaching sternite 2 (Fig. 8A). LP:LB=2.3. LDP:LPP = 1.8.

Etymology. From prefix *bou* meaning large in Greek and *synterg* (syntergosternite 8), referring to a large syntergosternite 8.

Distribution. Iran (Fig. 10).

Claraeola conjuncta (Collin, 1949)

Fig. 2

Eudorylas conjunctus Collin 1949: 191.

Examined material. ISRAEL • 2♂♂; Hazeva Field School; 30°43'N, 35°15'E; 21 Jan. 1997, A. Maklakov leg.; Malaise trap; JSS50791; JSS50784; GB: MN182738; TAU • 1♀; 10 Oct. 1997, A. Maklakov leg.; Malaise trap; JSS51646; TAU • 1♀; 12 Dec. 1997; A. Maklakov leg.; Malaise trap; JSS51647; TAU • 1♂; 30°43'N, 35°15'E; 3 Oct. 1997, A. Maklakov leg.; Malaise trap; JSS51705; TAU • 1♂; Qalya; 28 Sep. 1995; A. Freidberg leg.; JSS50783; TAU • 1♂; Zomet Qetura; 29°59'N, 35°4'E; 15 May 2010; A. Freidberg leg.; JSS50804; TAU • 1♀; Ne'ot Semadar; 30°43'N, 35°15'E; 4 Dec. 1995; A. Freidberg leg.; JSS51649; TAU.

Diagnosis. This species can be recognized by large ventral spines on the hind femur, shining on basal half of front and mid femora ventrally; surstyli slightly bow-shaped in dorsal view (Fig. 2A), each gonopod with six to seven strong bristles on inner side (Fig. 2B); phallus with three broad and slightly bent ejaculatory ducts, two of them bearing two to three saw-like teeth along their side; phallic guide short but broad, especially at apex (Fig. 2D, E).

Distribution. Algeria, Egypt, Israel (Fig. 10), Tunisia (Kehlmaier 2005b; Kehlmaier et al. 2019).

Claraeola halterata (Meigen, 1838)

Figs 3, 9C–D

Pipunculus halteratus Meigen 1838: 146.

Examined material. ISRAEL • 1♂; Har Hermon; 31°46'N, 34°37'E; 11 Jun. 2003; A. Freidberg leg.; JSS51645; GB: MN182742; TAU.

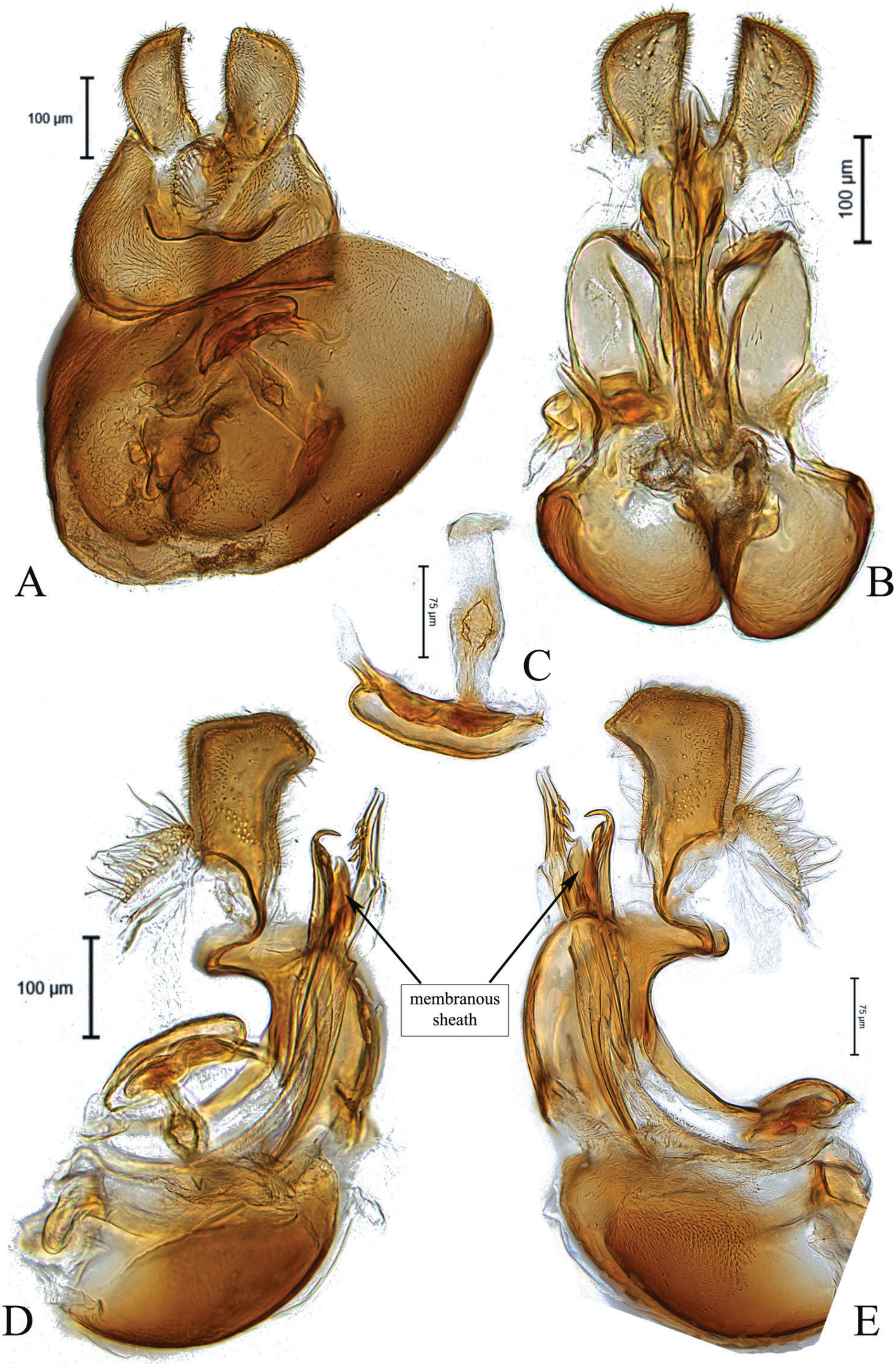

Figure 2. Male genitalia of *Claraeola conjuncta* (Collin) **A** in dorsal view **B** in ventral view **C** ejaculatory apodeme **D, E** in lateral view.

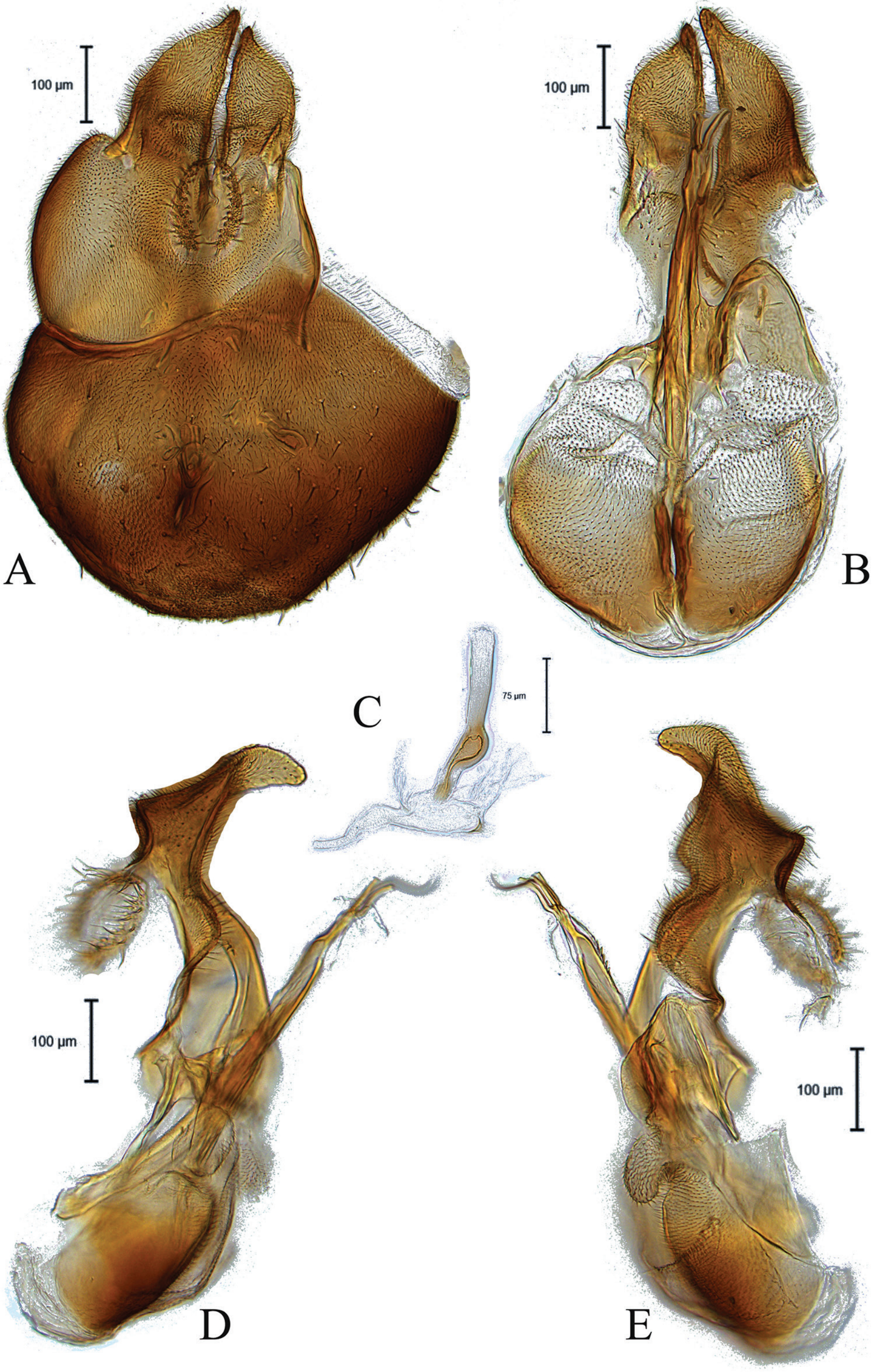

Figure 3. Male genitalia of *Claraeola halterata* (Meigen) **A** in dorsal view **B** in ventral view **C** ejaculatory apodeme **D, E** in lateral view.

Diagnosis. This species can be recognized by dark legs; surstyli in lateral view with dorsally humped base (Fig. 3D, E); large outer gonopod (Fig. 3B).

Distribution. Austria, Belgium, France (mainland), Germany, Great Britain, Hungary, Israel (Fig. 10), Latvia, Netherlands, Slovakia (Kehlmaier 2005a).

Remarks. Meigen (1838) described the species from Belgium. Due to the loss of all type material, Kehlmaier (2005a) designated a neotype and redescribed the species. The neotype is from Vernditch (southern England) and is deposited in The Natural History Museum, London (England). This species was examined by Skevington and Yeates (2001) for their phylogenetic study of Eudorylini.

Claraeola heidiae Motamedinia & Skevington, sp. nov.

http://zoobank.org/F3D2A78C-082F-4EF3-BAAB-752978DDFF1E

Fig. 4

Examined material. ***Holotype.*** YEMEN • ♂; Manakhah; 15°04'N, 43°44'E; 6 Jul.–21 Aug. 2002; Malaise trap; A. van Harten leg.; CD9078; CNC. ***Paratypes.*** YEMEN • 1 ♂; same data as holotype; 24 Jun–4 Aug 2003; CD6823; GB: MN182744; CNC.

Diagnosis. This species can be recognized by dark legs; lack of distinct mid-anterior hind tibial bristles and genitalic characters. Due to the shape of the inner male genitalia, it is closely related to *C. conjuncta*, *C. discors*, and *C. mantisphalliga* (*clavata* species group). It differs from these species by the shape of the surstyli which is straight in lateral view and a chitinized lobe in the right gonopod.

Description. Male. Body length (excluding antennae) 3.1–3.3 mm. ***Head.*** Face dark, silver-gray pruinose. Scape, pedicel, flagellum, and arista dark. Pedicel with three to four dark upper and one long (longer than half of flagellum) and one shorter lower bristle. Flagellum pointed to short tapering (LF:WF = 2.0–2.1) and gray pruinose. Eyes meeting for six or seven times diameter of ocellus. Frons dark, silver-gray pruinose with a weak median keel bearing a shining spot. Vertex dark, lacking pruinosity, bearing an elevated ocellar triangle. Occiput dark, gray pruinose, changing to brown in upper third. ***Thorax.*** Postpronotal lobe brown, gray pruinose and with two to three postpronotal short bristles along upper margin (up to 0.05 mm). Prescutum and scutum dark, predominantly gray-brown pruinose, with two uniseriate dorsocentral rows of dark bristles and longer supra-alar bristles. Scutellum dark, brown pruinose, with a fringe of 10–12 short dark bristles (0.05 mm). Subscutellum large with two gray pruinose patches laterally. ***Wing.*** Length: 3.0–3.2 mm. LW:MWW = 2.4. Wing with microtrichia. Pterostigma light brown and incomplete (LS:LTC = 0.5). LTC:LFC = 1.0. r-m reaches dm between basal third and half of the cell's length. Halter Length: 0.3 mm. Base and knob dark brown, stem light brown. ***Legs.*** Coxae and trochanters brown, gray pruinose. Mid coxa and hind trochanter with two dark strong bristles on inner apical corner. Hind trochanter with six or seven small black bristles on inner apical corner. Femora dark brown, yellow at apex, with two ventral rows of dark, peg-like spines in apical half. Tibiae dark brown, narrowly pale at base and apices.

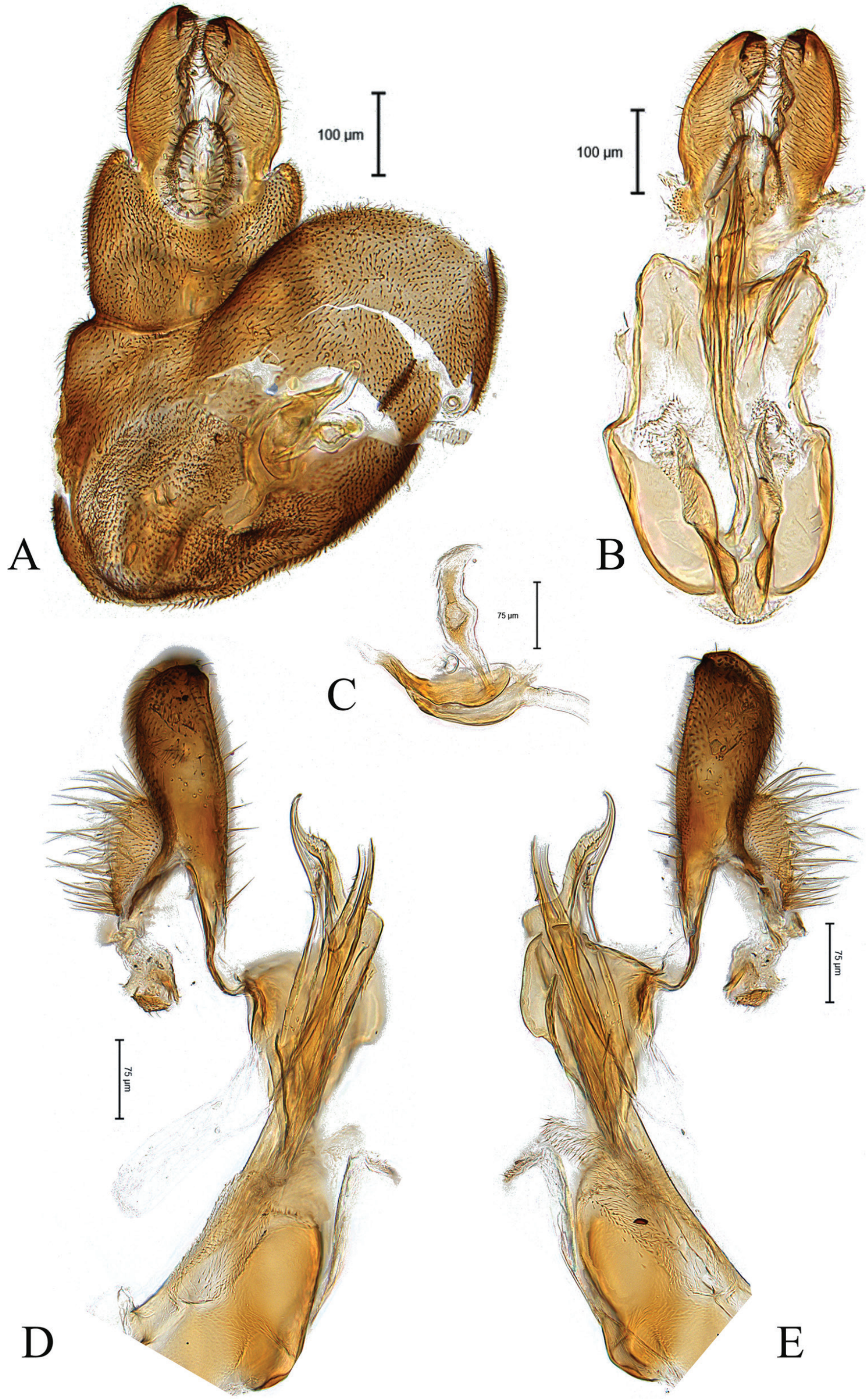

Figure 4. Male genitalia of paratype *Claraeola heidiae* Motamedinia & Skevington, sp. nov. **A** in dorsal view **B** in ventral view **C** ejaculatory apodeme **D, E** in lateral view.

Hind tibia with two or three wrinkled indentations mid-anteriorly without distinct bristles. Distitarsi brown covered with small black bristles and 1–3 long bristles at apex. Pulvilli slightly smaller than distitarsi. ***Abdomen.*** Ground color dark. Tergite 1 gray pruinose with five or six dark lateral bristles. Tergites 2–5 brown pruinose. Tergite 5 slightly longer than other tergites. Sternites 1–7 dark and pale in middle, gray pruinose. LT35:WS8 = 1.6. Syntergosternite 8 dark brown, gray pruinose, viewed laterally as long as high (LS8:HS8 = 1.0). Viewed caudally, membranous area of medium size and ovate. ***Genitalia.*** Genital capsule dorsal view: epandrium dark, gray pruinose and slightly wider than long (MLE:MWE = 0.8–0.9). Surstyli brown, gray pruinose with somewhat longer bristles, symmetrical, ovate shape and elongated (Fig. 4A). Genital capsule ventral view: gonopods, similar in size, right one with small chitinized lobe and rather large (Fig. 4B). Genital capsule lateral view: surstyli slightly broadened apically (Fig. 4D, E). Phallus strong and straight, with three small ejaculatory ducts, two of them bearing one or two saw-like teeth along their sides (Fig. 4D, E). Phallic guide long, reaching middle of surstyli, with hooked tip (Fig. 4D, E). Ejaculatory apodeme nail-shaped with a bulbous middle (Fig. 4C).

Etymology. The name is selected in honor of Scott Kelso's daughter for her interest in entomology.

Distribution. Yemen (Fig. 10).

Claraeola khorshidae Motamedinia & Kehlmaier, 2017

Fig. 11

Examined material. ***Holotype.*** IRAN • ♂; Southern Khorasan province, Mohammadieh; 32°52'N, 59°01'E; 1419 m; 26 Apr. 2015; Malaise trap; B. Motamedinia leg.; ENA: LT626248; HMIM. ***Paratypes.*** IRAN • 2♂♂; same data as holotype; 23 Aug. 2015; HMIM • 1♀; same data as holotype; 15 Apr. 2015; SMTD; ENA: LT626248 • 2♀♀; same data as holotype; 14 Jul. 2016; HMIM.

Diagnosis. This species can be recognized by distinctly large gonopods, strong bent surstyli in lateral view, and long teeth on three ejaculatory ducts (Fig. 11A–G).

Distribution. Iran (Motamedinia et al. 2017b).

Remarks. This species was described by Motamedinia and Kehlmaier (2017) from the east of Iran.

Claraeola khuzestanensis Motamedinia & Skevington, sp. nov.

http://zoobank.org/92df675d-fd91-493a-8a35-bc1390054e84

Figs 5, 8B, 9E, F

Examined material. ***Holotype.*** IRAN • ♂; Khuzestan, Shush; 32°6'N, 48°26'E; 68m; 11 Mar.–10 May 2015; M. Parchami-Araghi leg.; Malaise trap; JSS52300; GB: MN182737; CNC. ***Paratypes.*** IRAN • 1 ♂; 11 Mar.–10 May 2015; E. Gilasian leg.; Malaise trap; JSS52299; GB: 182741; HMIM • 1 ♀; 32°4'N, 48°14'E; same data

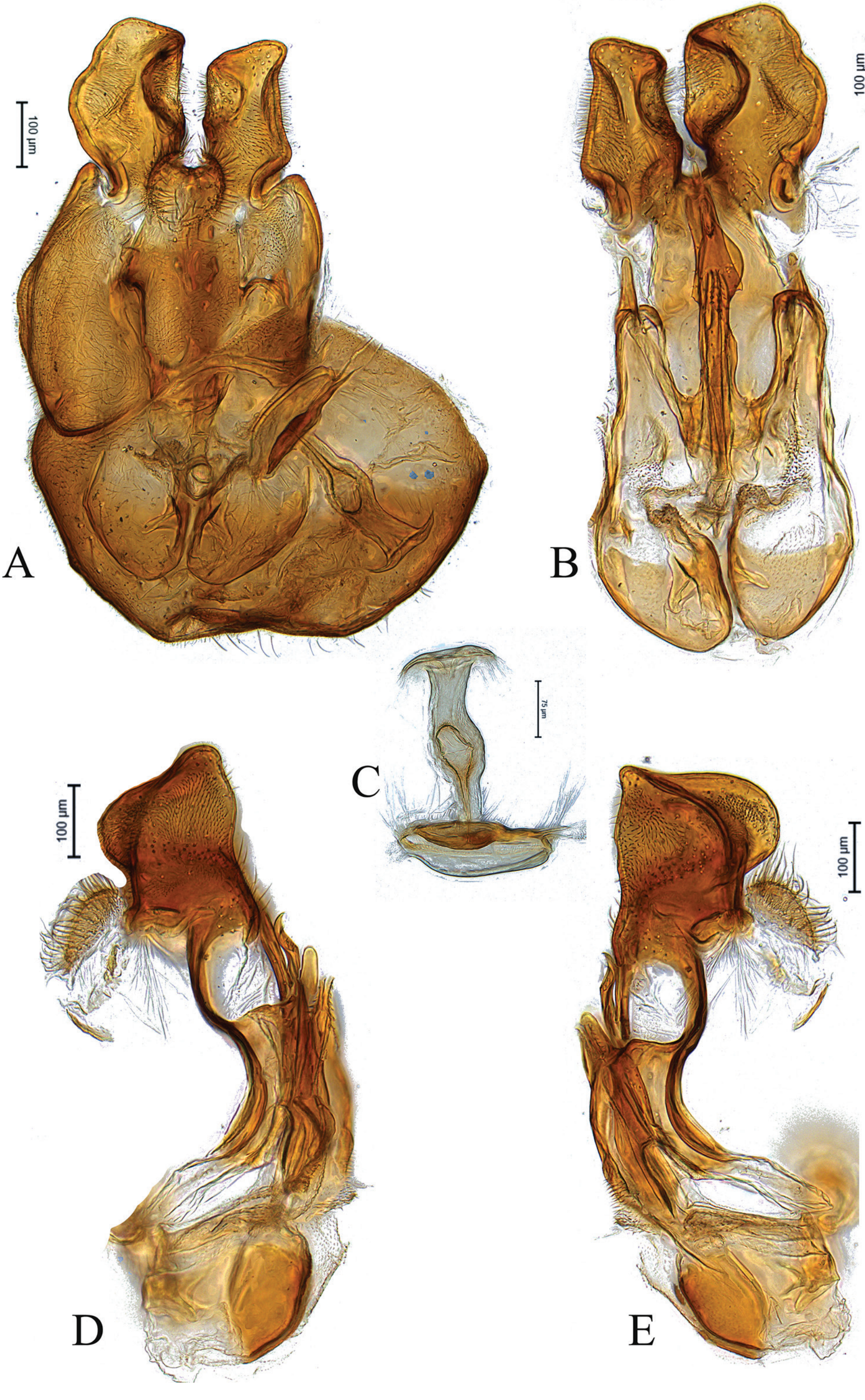

Figure 5. Male genitalia of holotype *Claraeola khuzestanensis* Motamedinia & Skevington, sp. nov. **A** in dorsal view **B** in ventral view **C** ejaculatory apodeme **D, E** in lateral view.

as holotype; JSS52208; GB: MN182740; CNC • 1 ♀; same data as holotype; 29 Mar.–31 Aug. 2013; JSS52188; GB: MN182743; CNC.

Diagnosis. This species is closely related to *C. parnianae* from southeast Iran, described by Motamedinia and Kehlmaier (2017). Both have a long, slender abdomen with narrow but distinct yellow markings on the abdominal tergites, erect anteromedial setae on mid and hind tibiae and a protruding membranous sheath associated with the ejaculatory ducts. It differs by the shape of surstyli in dorsal view and the structure of the membranous sheath, being trilobate at its apex in *C. parnianae* (Fig. 7A, C, D) It is also closely related to *C. oppleta* (Collin, 1941), recorded from Russia and North Korea and re-described by Kehlmaier (2005b), and *C. alata* (Kozánek & Kwon, 1991), described from North Korea by Kozánek and Kwon (1991). It differs by the square shape of the surstyli in lateral view (Fig. 5D, E), the structure of the phallus with short spines and short membranous sheath without spines (Fig. 5E).

Description. Male. Body length (excluding antennae): 4.0–4.3 mm (n = 2). ***Head.*** Face gray pruinose. Scape dark, pedicel partly light brown with four short upper bristles and a long plus a single short lower bristle, flagellum and base of arista completely yellow; flagellum tapering and gray-white pruinose (LF:WF = 3.6). Labellum yellow. Eyes meeting for a distance of 29 facets. Frons silver-gray pruinose. Vertex black, lacking pruinosity. Occiput dark and gray pruinose with scattered small dark bristles. ***Thorax.*** Postpronotal lobe light yellow, gray pruinose. Prescutum black but light brown at lateral margin. Scutum black, gray pruinose with scattered long setae at anterior supra-alar area. Scutellum yellow, with ca. 12 brown setae along posterior margin (up to 0.6 mm). Subscutellum dark, gray pruinose. Pleura dark brown but light brown on anepimeron. ***Wing.*** Length: 3.9–4.1 mm. LW:MWW = 3.1. Wing almost entirely covered with microtrichia. Pterostigma dark-brown and incomplete. LS:LTC = 0.9. LTC:LFC = 1.0. Cross-vein r-m reaches dm shortly after one third of the cell's length. M_1 strongly undulating in middle. Halter length: 0.5 mm. Whitish, narrowly brown at base. ***Legs.*** Yellow but brown-yellow at coxae. Coxae gray pruinose. Mid coxa with two or three black anterior bristles. Trochanters partly gray pruinose. Femora gray pruinose. Mid and hind femora bearing two rows of dark, peg-like anteroventral spines in apical one third. Tibiae gray pruinose, with two rows of short setae on anterior and three rows on posterior side. Mid and hind tibiae bearing two or three wrinkled indentations in middle with erect anteromedial setae. Tarsi yellowish but distitarsi brown, with scattered dark setae at anterior margin. Claws white with black tips. ***Abdomen.*** Long and narrow, ground color dark, tergites 1–3 and partly 4 with two narrow posterolateral yellow spots. Tergite 1 gray pruinose, with three or four dark lateral bristles (up to 0.5 mm) and patch of brown setae. Tergites 1–5 with brown setae; tergite 5 posterolaterally gray pruinose. Tergite 5 slightly longer than tergite 4 and almost symmetrical in dorsal view (LT35:WT5 = 1.6, WT5:LT5 = 1.6, T5R:T5L = 1.0). Sternites white-yellow laterally and brown with dark mid-line centrally, gray pruinose. Syntergosternite 8 dark, gray pruinose without dorsal depression on side of right surstylus. LT35:WS8 = 3.0. Viewed laterally, higher than long (LS8:HS8 = 0.7).

Membranous area ovate in caudal view, small sized. **Genitalia.** Genital capsule in dorsal view: epandrium and surstyli light brown, gray pruinose. Epandrium wider than long (MLE:MWE = 0.6). Surstyli asymmetrical, right larger than left one. Left surstylus rather rectangular. Right surstylus widened in middle (Fig. 5A). Genital capsule in ventral view: gonopods large and equal in height, humped at apices (Fig. 5B). Genital capsule in lateral view: epandrium without projecting lobe on either side. Surstyli with large projecting lobe on dorsal sides (Fig. 5D, E). Phallus straight, strong, with three short ejaculatory ducts covered with strong and small teeth and a protruding membranous sheath, hook-like at apex (Fig. 5D, E). Phallic guide strong, broaden before narrowed at apex. (Fig. 5D, E). Ejaculatory apodeme tube-like, symmetrical, with a bulb in its middle and fungiform at apex (Fig. 5C).

Female. Body length (excluding antennae): 4.1–4.4 mm (n = 2). ***Head.*** Eyes separated, with enlarged frontal facets. Frons gray pruinose in lower half. Occiput gray pruinose. ***Thorax.*** Postpronotal lobe light yellow, gray pruinose with scattered yellow setae. Prescutum and scutum black, gray pruinose with scattered long setae at anterior supra-alar area with two uniseriate dorsocentral rows of hairs. ***Wing.*** Length: 3.8–3.9 mm. LW:MWW = 2.9. Pterostigma light-brown and slightly complete (LS:LTC = 0.8, LTC:LFC = 0.85). ***Legs.*** Yellow, mid coxa and hind trochanter with one or two black anterior bristles. All femora bearing two small ventral rows of dark peg-like spines in the apical third. Hind tibia with two or three wrinkled indentations in middle but without distinctly stronger bristly setae. Basal segment of hind tarsi broad with dense black and yellow bristles. Pulvilli longer than distitarsi. ***Abdomen.*** Tergites with small black bristles. Tergites 1–6 with two narrow posterolateral yellow spots with gray pruinosity. ***Ovipositor.*** Gray pruinose but dorsally with scattered long brown bristles. Viewed laterally: base of piercer curved, piercer slightly angled between proximal and distal part and longer than base (Fig. 8B). LP:LB = 1.9. LDP:LPP = 2.3.

Etymology. Named after Khuzestan, the province from where the holotype originated.

Distribution. Iran (Fig. 10).

Claraeola mantisphalliga Motamedinia & Skevington, sp. nov.

http://zoobank.org/64EB602E-60BF-4FF6-B62B-AF28029234BD

Figs 6, 9B

Examined material. ***Holotype.*** YEMEN • ♂; Seyun; 15°57'N, 48°48'E; 20–22 Aug. 2002; light trap; A. van Harten leg.; CD9071; CNC. ***Paratypes.*** YEMEN • 2 ♂♂; same data as holotype; Oct.–Nov. 2002; CD9090; CD9091; CNC.

Diagnosis. This species can be recognized by yellow legs, hind tibia with a wrinkled indentation mid-anteriorly bearing one distinctly stronger bristle and each gonopod with six to seven strong bristles on inner side. It is closely related to *C. conjuncta* and *C. thekkadiensis* (*clavata* species group). It differs by the shape of surstyli in lateral

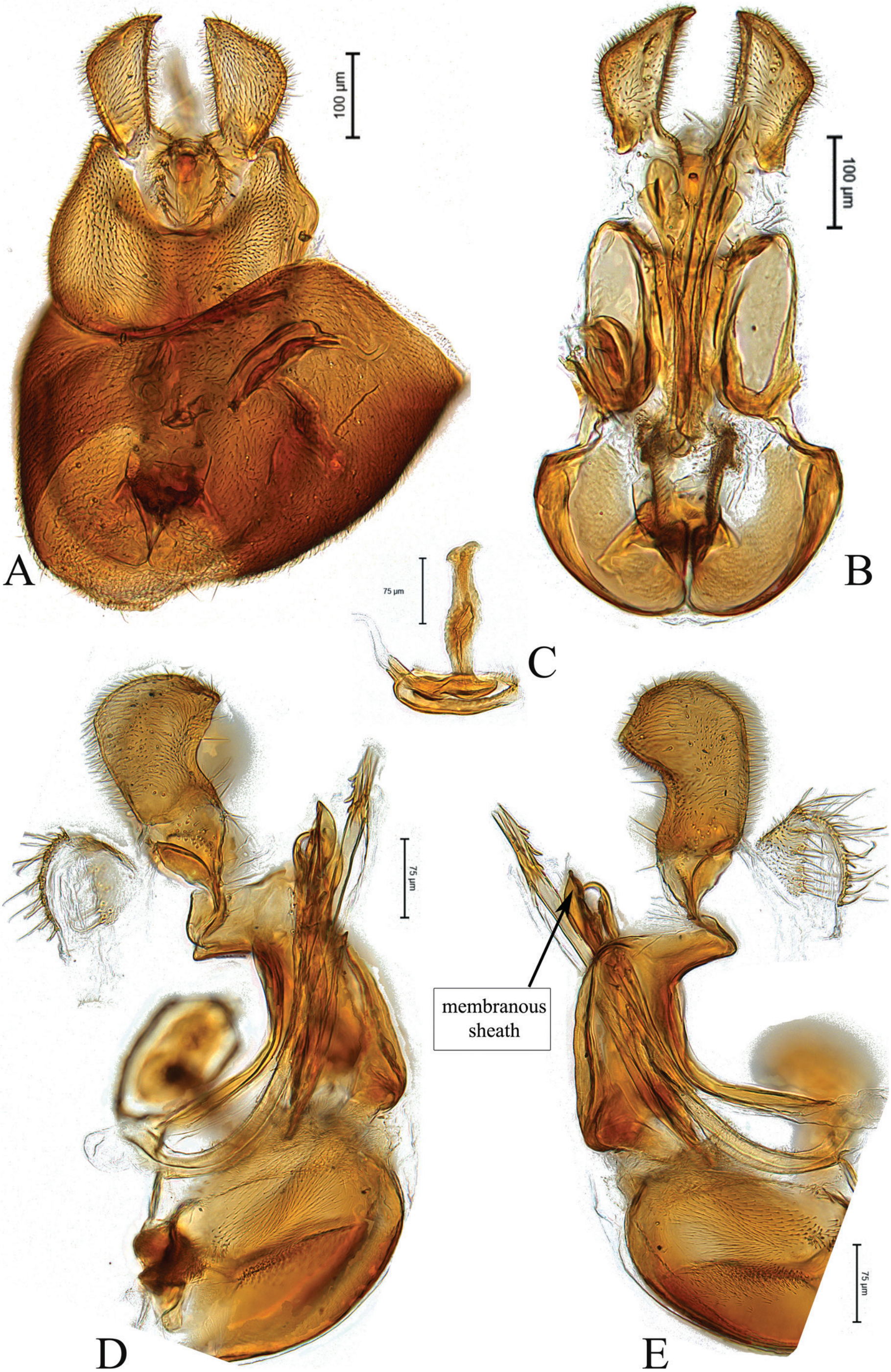

Figure 6. Male genitalia of holotype *Claraeola mantisphalliga* Motamedinia & Skevington, sp. nov. **A** in dorsal view **B** in ventral view **C** ejaculatory apodeme **D, E** in lateral view.

view and the specific shape of the phallic guide with two projecting lobes on either side in ventral view.

Description. Male. Body length (excluding antennae) 3.7–3.8 mm (n = 3). ***Head.*** Face dark, silver-gray pruinose. Scape dark. Pedicel brown, with four dark upper and two lower bristles (the long one is longer than half of flagellum). Flagellum light brown, pointed to tapering (LF:WF = 2.0–2.1) and gray pruinose. Arista dark. Eyes meeting for 11 to 12 times diameter of ocellus. Frons dark, silver-gray pruinose. Vertex dark, lacking pruinosity, bearing an elevated ocellar triangle. Occiput dark, gray pruinose with scattered dark and small bristles. ***Thorax.*** Postpronotal lobe pale, gray pruinose and with three to four postpronotal bristles along upper margin (up to 0.08 mm). Prescutum and scutum dark, predominantly gray pruinose, only dorsocentrally with some brown pruinosity to various extents, with two uniseriate dorsocentral rows of brown bristles and longer supra-alar bristles. Scutellum dark, gray pruinose, with a fringe of 11–13 short dark bristles (up to 0.05 mm). Subscutellum large with two patches of brown-gray pruinose laterally. ***Wing.*** Length: 3.0–3.2 mm. LW:MWW = 2.4. Wing with microtrichia. Pterostigma brown and complete (LS:LTC = 1.0; LTC:LFC = 1). r-m reaches dm between basal third and half of the cell's length. Halter Length: 0.5 mm and yellow. ***Legs.*** Light brown. Coxae and trochanters gray pruinose. Mid coxa and hind trochanter with one or two dark bristles on inner apical corner. All femora with two ventral rows of dark peg-like spines in apical half. Hind tibia with a wrinkled indentation mid-anteriorly bearing one distinctly stronger bristle. Distitarsi brown covered with small black bristles and three long bristles at apex. Pulvilli slightly longer than distitarsi. ***Abdomen.*** Ground color dark. Tergite 1 gray pruinose with four to five dark lateral bristles. Tergite 2 gray pruinose. Tergites 3–5 laterally gray pruinose, extending onto dorsal surface along posterior margin and largely meeting, otherwise brown pruinose. Sternites 1–7 brown and dark in middle, gray pruinose. LT35:WS8 = 2.3. Syntergosternite 8 dark, gray pruinose, viewed laterally as long as high (LS8:HS8 = 1.0). Viewed caudally, membranous area of medium size, somewhat ovate. ***Genitalia.*** Genital capsule dorsal view: epandrium light brown, gray pruinose and slightly wider than long (MLE:MWE = 0.8–0.9). Surstyli somewhat pale, gray pruinose, symmetrical, slightly bow-shaped and enlarged separation at base (Fig. 6A). Genital capsule ventral view: gonopods equal, rather large, each with six or seven strong bristles on inner side (Fig. 6B). Genital capsule lateral view: phallus with a strong and straight base, with three small ejaculatory ducts, two of them bearing two or three saw-like small teeth along their side (Fig. 6D, E). Phallic guide long and broad, especially at apex with two projecting lobes on either side with hooked tip (Fig. 6D, E). Epandrium with small projecting lobe on either side. Surstyli broadened apically (Fig. 6D, E). Ejaculatory apodeme nail-shaped with a bulbous middle (Fig. 6C).

Etymology. From *mantis* (common name of Mantidae family) and *phalliga* (phallic guide), referring to the similarity between the shape of the phallic guide and a mantis in ventral view.

Distribution. Yemen (Fig. 10).

Claraeola parnianae Motamedinia & Kehlmaier, 2017

Figs 7, 8C

Examined material. IRAN • 3♂♂; Sistan & Balochestan, Zabol, Sadesistan; 31°5'N, 61°26'E; 485m; 14 Apr. 2015; H. Derafshan leg.; Malaise trap; JSS51911; GB: MN182735; JSS51912, JSS51913 • 1♀; JSS51910; GB: MN182736; all CNC.

Diagnosis. This species stands closely to *C. oppleta* (Collin) and *C. alata* (Kozánek & Kwon). It can be identified by the narrow but distinct yellow markings on the abdominal tergites; erect anteromedial setae on hind tibia; the lateral shape of the surstyli and the trilobate structure of membranous sheath at its apex (Fig. 7; Motamedinia et al. 2017b: fig. 3B).

Distribution. Iran (Fig. 10) (Motamedinia et al. 2017b).

Remarks. This species was described by Motamedinia and Kehlmaier (2017) from southeast Iran.

Claraeola thekkadiensis (Kapoor, Grewal & Sharma, 1987), comb. nov.

Eudorylas thekkadiensis Kapoor, Grewal & Sharma, 1987:111

Examined materal. ***Holotype.*** • ♂; Thekkady (Kerala); 24 Feb. 2019; J.S. Grewal; ***Allotype.*** • 1♀; same data as holotype; S.K. Sharma. ***Paratype.*** • 2♂♂; same data as holotype • 3♂♂; Ramgrah (Bihar); 22 Mar. 1958; S.K. Sharma • 2♀♀; Ranchi (Bihar); 22 Mar. 1985; V.K. Kohli • 1♂; Ranikhet (U.P.); 8 Oct. 1985; S.K. Sharma; Depository: all INPC.

Distribution. India.

Remarks. Although not a Middle Eastern species, this is similar to *C. mantisphalliga* so relevant to this paper. From the detailed drawings of the male genitalia included in the original description (Kapoor et al. 1987), the taxon is transferred from *Eudorylas* to the *Claraeola.*

DNA barcoding

Pipunculidae is a taxonomically challenging family as are most parasitoid taxa. Many are small, most characters are related to male genitalia and many are subtle or difficult to interpret, sexes are difficult to associate, and females are character-poor. For this reason, incorporating both morphological and DNA-sequence data, such as COI DNA barcodes, is critical for species recognition. Based on morphology and DNA barcoding, the present paper introduces four new species of *Claraeola* and associated males and females of two of the new species, *C. bousynterga* sp. nov. and *C. khuzestanensis* sp. nov. DNA sequence data are provided for six Middle Eastern pipunculid species.

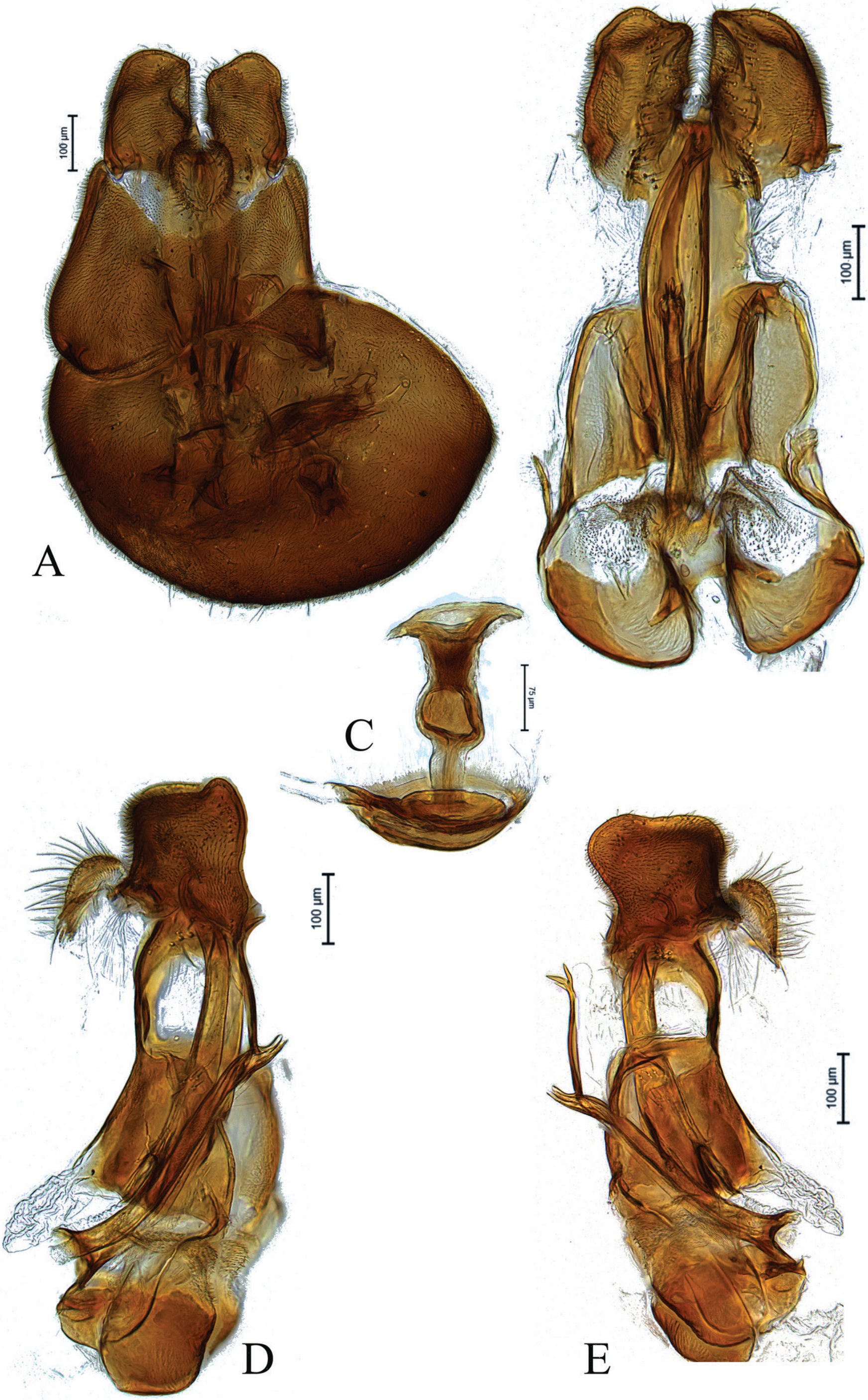

Figure 7. Male genitalia of *Claraeola parnianae* Motamedinia & Kehlmaier **A** in dorsal view **B** in ventral view **C** ejaculatory apodeme **D, E** in lateral view.

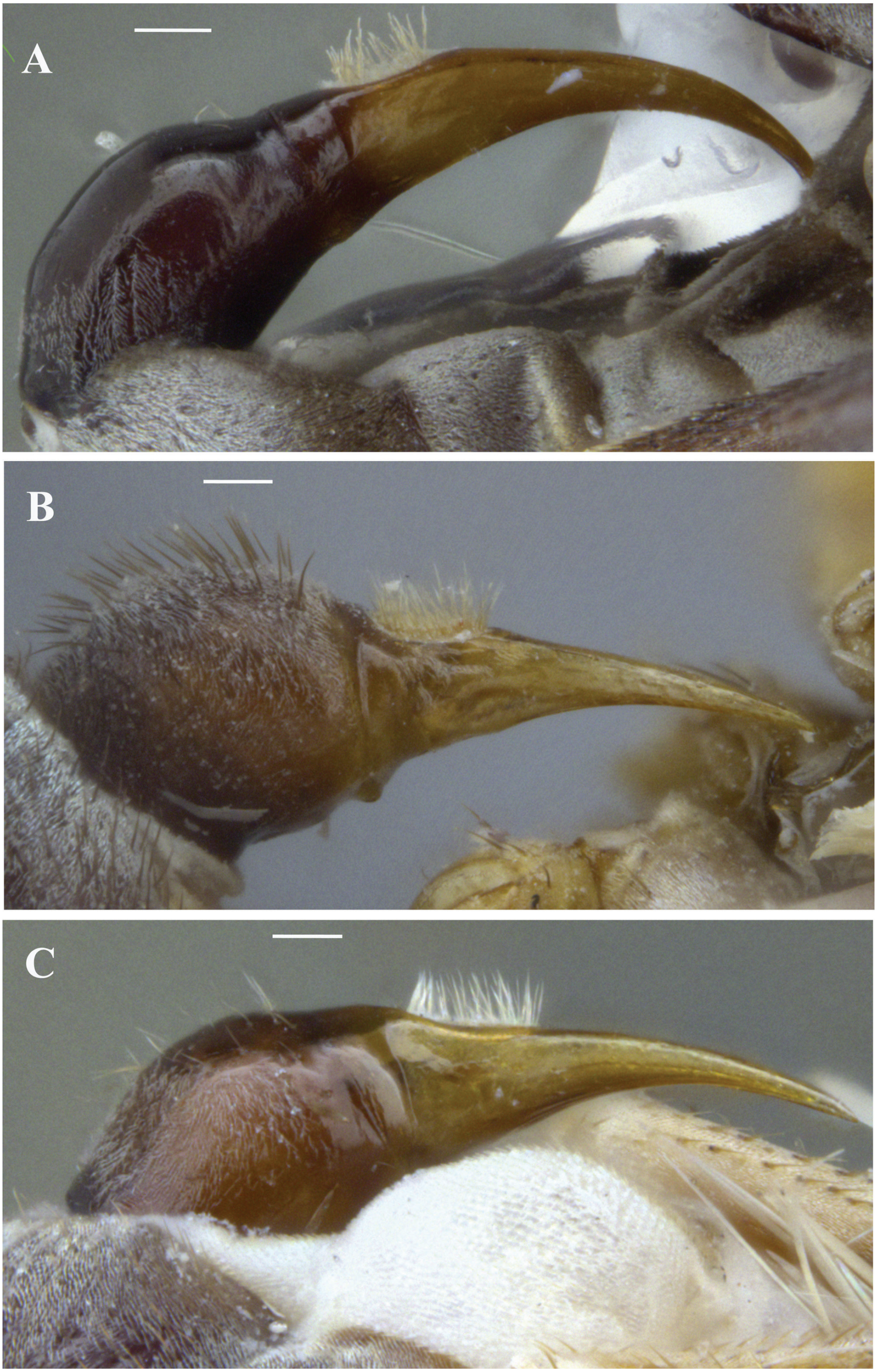

Figure 8. Ovipositor in lateral view **A** *Claraeola bousynterga* Motamedinia & Skevington, sp. nov. **B** *Claraeola khuzestanensis* Motamedinia & Skevington, sp. nov. **C** *Claraeola parnianae* Motamedinia & Kehlmaier. Scale bar: 0.1 mm (**A–C**).

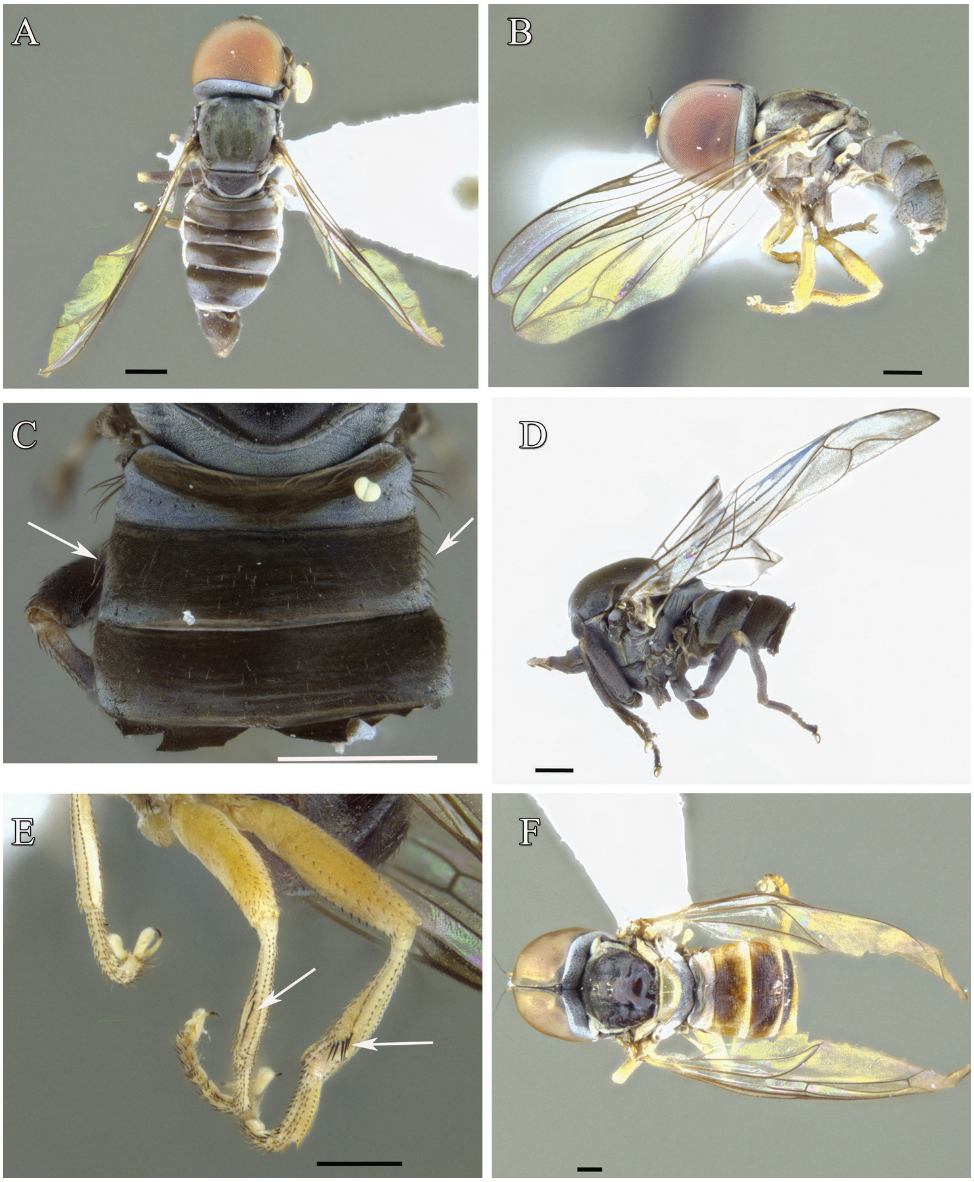

Figure 9. Male of *Claraeola* species **A** paratype of *Claraeola bousynterga* Motamedinia & Skevington, sp. nov. in dorsal view **B** holotype of *Claraeola mantisphalliga* Motamedinia & Skevington, sp. nov. in lateral view **C–D** *Claraeola halterata* (Meigen) **C** abdominal tergites in dorsal view **D** habitus in lateral view **E–F** paratype of *Claraeola khuzestanensis* Motamedinia & Skevington, sp. nov. **E** legs in lateral view **F** habitus in dorsal view. Scale bar: 0.5 mm (**A–F**).

Interspecific genetic distances within the Middle Eastern *Claraeola* range from 8.7% (*C. khorshidae* to *C. heidiae*) to 20.6% (*C. halterata* to *C. conjuncta* and *C. heidiae*), while intraspecific genetic distances range from 0% (in *C. khuzestanensis* and *C. parnianae*) to 1.2% (*C. heidiae*). Based on uncorrected pairwise genetic

Figure 10. *Claraeola* species distribution in the Middle East.

distances (p-distance), *C. heidiae* sp. nov., *C. bousynterga* sp. nov., and *C. conjuncta*, are close to *C. khorshidae* (LT626248), differing by 8.75%, 12.5% and 12.5% respectively. *Claraeola parnianae* is most similar to *C. khuzestanensis* sp. nov. differing by 9.38% (Table 2).

Table 2. Uncorrected pairwise distances among *Claraeola* species in the Middle East (intraspecific distances are highlighted in bold).

		1	2	3	4	5	6	7	8	9	10	11	12	13
1	*C. heidiae*-CD6823*(C)													
2	*C. heidiae*-CD9078*(C)	**0.012**												
3	*C. conjuncta*-JSS50784*(C)	0.118	0.125											
4	*C. halterata*-JSS51645*(ABC)	0.206	0.206	0.162										
5	*C. bousynterga*-JSS51829	0.168	0.168	0.150	0.168									
6	*C. parnianae*-JSS51910	0.162	0.162	0.137	0.112	0.137								
7	*C. parnianae*-JSS51911	0.162	0.162	0.137	0.112	0.137	**0.000**							
8	*C. bousynterga*-JSS51920*(C)	0.162	0.162	0.143	0.162	**0.006**	0.137	0.137						
9	*C. bousynterga*- JSS52173	0.168	0.168	0.150	0.168	**0.000**	0.137	0.137	**0.006**					
10	*C. khuzestanensis*-JSS52188	0.137	0.137	0.143	0.143	0.137	0.093	0.093	0.131	0.137				
11	*C. khuzestanensis*-JSS52208	0.143	0.143	0.150	0.150	0.143	0.100	0.100	0.137	0.143	**0.006**			
12	*C. khuzestanensis*-JSS52299*(C)	0.137	0.137	0.143	0.143	0.137	0.093	0.093	0.131	0.137	**0.000**	**0.006**		
13	*C. khuzestanensis*-JSS52300	0.137	0.137	0.143	0.143	0.137	0.093	0.093	0.131	0.137	**0.000**	**0.006**	**0.000**	
14	*C. khorshidae*-LT626248	0.087	0.087	0.125	0.168	0.131	0.118	0.118	0.125	0.131	0.093	0.100	0.093	0.093

* Specimen sequence data was obtained using the COI mini-barcode protocol. A, B, & C denote the COI mini-barcode regions sequenced.

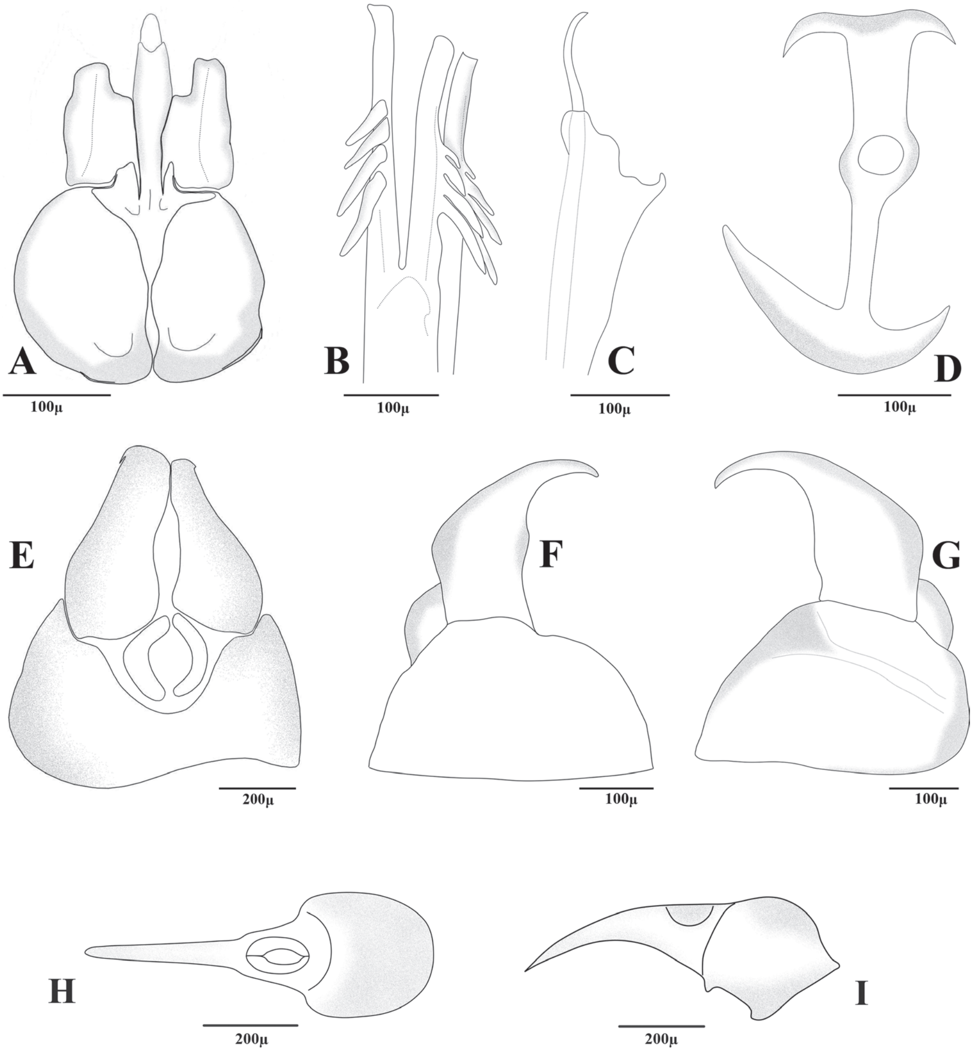

Figure 11. Terminalia of male (**A–G**) and female (**H–I**) of *Claraeola khorshidae* Motamedinia & Kehlmaier **A** phallic guide, gonopods and hypandrium in ventral view **B** distiphallus with ejaculatory ducts in lateral view **C** phallic guide in lateral view **D** ejaculatory apodeme **E** surstyli in dorsal view **F** left surstylus in lateral view **G** right surstylus in lateral view in ventral view **H** ovipositor in dorsal view **I** ovipositor in lateral view (plate reproduced with permission from copyright holder).

Acknowledgements

We would like to express our grateful thanks to C. Kehlmaier, A. Freidberg, and N. Dorchin for the loan of Israeli specimens to the CNC. Special thanks to E. Rakhshani from Zabol University for his ongoing collaboration and support (Grant NO. UOZ-GR-9517-2, University of Zabol, Iran). We are indebted to E. Gilasian, M. Parchami-Araghi, F. Hamzavi, H. A. Derafshan, and K. Ghahari for collecting and providing the specimens from Iran. Work was supported by grants 2349 and 3199 to Jeffrey H. Skevington from Agriculture & Agri-Food Canada. Permission to reproduce Fig. 11 was granted by Zootaxa.

References

Aczél ML (1940) Vorarbeiten zu einer Monographie der Dorylaiden (Dipt.). Dorylaiden-Studien V. Zoologischer Anzeiger 132: 149–169.

Földvári M (2013) Taxonomic revision of the Afrotropical species of the tribe Eudorylini (Diptera, Pipunculidae). Zootaxa 3656, 1–121. https://doi.org/10.11646/zootaxa.3656.1.1

Folmer O, Black M, Hoeh W, Lutz R, Vrijenhoek R (1994) DNA primers for amplification of mitochondrial cytochrome c oxidase subunit I from diverse metazoan invertebrates. Molecular Marine Biology and Biotechnology 3: 294–299.

Gibson JF, Kelso S, Jackson MD, Kits JH, Miranda GFG, Skevington J (2011) Diptera-Specific Polymerase Chain Reaction Amplification Primers of Use in Molecular Phylogenetic Research. Annals of the Entomological Society of America 104: 976–997. https://doi.org/10.1603/AN10153

Hardy DE (1964) Family Pipunculidae Zetterstedt. The big-headed or big-eyed flies. In: Zimmerman EC (Ed.) Insects of Hawaii. University of Hawaii Press, Honolulu, 302–379.

Jervis MA (1992) A taxonomic revision of the pipunculid fly genus *Chalarus* Walker, with particular reference to the European fauna. Zoological Journal of the Linnean Society 105: 243–352. https://doi.org/10.1111/j.1096-3642.1992.tb01232.x

Kapoor VC, Grewal JS, Sharma SK (1987) Indian Pipunculids (Diptera: Pipunculidae). A Comprehensive Monograph. Atlantic Publishers & Distributors, New Delhi, 201 pp.

Kehlmaier C (2005a) Taxonomic revision of European Eudorylini (Insecta, Diptera, Pipunculidae). Verhandlungen des Naturwissenschaftlichen Vereins in Hamburg, Neue Folge 41: 45–353.

Kehlmaier C (2005b) Taxonomic studies on Palaearctic and Oriental Eudorylini (Diptera: Pipunculidae), with the description of three new species. Zootaxa 1030: 1–48. https://doi.org/10.11646/zootaxa.1030.1.1

Kehlmaier C, Dierick M, Skevington JH (2014) Micro-CT studies of amber inclusions reveal internal genitalic features of big-headed flies, enabling a systematic placement of *Metanephrocerus* Aczél, 1948 (Insecta: Diptera: Pipunculidae). Arthropod Systematics and Phylogeny 72: 23–36.

Kehlmaier C, Gibbs D, Withers P (2019) New records of big-headed flies (Diptera: Pipunculidae) from the Mediterranean Basin. Bonn zoological Bulletin 68(1): 31–60.

Koenig DP, Young CW (2007) First observation of parasitic relations between big-headed flies, *Nephrocerus* Zetterstedt (Diptera: Pipunculidae) and crane flies, *Tipula* Linnaeus (Diptera: Tupulidae: Tipulinae), with larval and puparial descriptions for the genus *Nephrocerus*. Proceedings of the Entomological Society of Washington 109: 52–65.

Kozánek M, Kwon YJ (1991) Classification of the Family Pipunculidae from Korea (Diptera) Part I. On the genus *Moriparia* gen.nov. from North Korea. Insecta Koreana 8: 76–84.

Kozánek M, Suh SJ, Kwon YJ (2003) Taxonomy of the genus *Moriparia* Kozanek et Kwon (Diptera: Pipunculidae) from Korea. Korean Journal of Entomology 33: 99–103. https://doi.org/10.1111/j.1748-5967.2003.tb00057.x

Kumar S, Stecher G, Tamura K (2016) MEGA7: Molecular Evolutionary Genetics Analysis version 7.0 for bigger datasets. Molecular Biology and Evolution 33(7): 1870–1874. https://doi.org/10.1093/molbev/msw054

Littlefield R (2018) Zerene Stacker. http://zerenesystems.com/cms/stacker

Maddison WP, Maddison DR (2018) Mesquite: a modular system for evolutionary analysis. Version 3.51. http://www.mesquiteproject.org

Motamedinia B, Mokhtari A, Rakhshani E, Gilasian E (2017a) Review of Eudorylini (Diptera, Pipunculidae, Pipunculinae) from Iran with four new species records. Journal of Insect Biodiversity and Systematics 03(4): 335–346.

Motamedinia B, Kehlmaier C, Mokhtari A, Rakhshani E, Gilasian E (2017b) Discovery of the genus *Claraeola* Aczél in Iran with the description of two new species (Diptera: Pipunculidae). Zootaxa 4227: 563–572. https://doi.org/10.11646/zootaxa.4227.4.6

Rafael JA, De Meyer M (1992) Generic classification of the family Pipunculidae (Diptera): a cladistic analysis. Journal of Natural History 26: 637–658. https://doi.org/10.1080/00222939200770391

Rafael JA, Skevington JH (2010) Pipunculidae (Big-headed Flies). In: Brown BV, Borkent A, Cumming JM, Wood DM, Woodley NE, Zumbado MA (Eds) Manual of Central American Diptera. INBio, San Jose, 793–803.

Shorthouse (2010) SimpleMappr, an online tool to produce publication-quality point maps. http://www.simplemappr.net [accessed 20 April 2012.2012]

Skevington JH (2002) Phylogenetic revision of Australian members of the *Allomethus* genus group (Diptera: Pipunculidae). Insect Systematics and Evolution 33: 133–161. https://doi.org/10.1163/187631202X00109

Skevington JH (2019) Catalogue of the big-headed flies (Diptera, Pipunculidae) of the World. [Unpublished database]

Skevington JH, Marshall SA (1997) First record of a big-headed fly, *Eudorylas alternatus* (Cresson) (Diptera: Pipunculidae), reared from the subfamily Cicadellinae (Homoptera: Cicadellidae), with an overview of pipunculid-host associations in the Nearctic Region. The Canadian Entomologist 129: 387–398. https://doi.org/10.4039/Ent129387-3

Skevington JH, Yeates DK (2001) Phylogenetic classification of Eudorylini (Diptera: Pipunculidae). Systematic Entomology 26: 421–452. https://doi.org/10.1046/j.0307-6970.2001.00160.x

Wada S (1991) Morphologische Indizien für das unmittelbare Schwestergruppenverhältnis der Schizophora mit den Syrphoidea (‘Aschiza’) in der phylogenetischen Systematik der Cyclorrhapha (Diptera: Brachycera). Journal of Natural History 25: 1531–1570. [Morphological evidence for the direct sister group relationship between the Schizophora and the Syrphoidea (Aschiza) in the phylogenetic systematics of the Cyclorrhapha (Diptera: Brachycera)] https://doi.org/10.1080/00222939100770971

Weintraub PG, Beanland L (2006) Insect Vectors of Phytoplasmas. Annual Review of Entomology 51: 91–111. https://doi.org/10.1146/annurev.ento.51.110104.151039

ZooKeys 873: 113–131 (2019)
doi: 10.3897/zookeys.873.33901
http://zookeys.pensoft.net

RESEARCH ARTICLE

A peer-reviewed open-access journal
ZooKeys
Launched to accelerate biodiversity research

Seagrass *Halodule wrightii* as a new habitat for the amphioxus *Branchiostoma californiense* (Cephalochordata, Branchiostomidae) in the southern Gulf of California, Mexico

Lucía Campos-Dávila[1], Claudia J. Pérez-Estrada[1,2], Ricardo Rodríguez-Estrella[1], Enrique Morales-Bojórquez[1], Fernando G. Brun-Murillo[2], Eduardo F. Balart[1]

1 *Centro de Investigaciones Biológicas del Noroeste, S.C., Av. Instituto Politécnico Nacional 195, Col. Playa Palo de Santa Rita Sur, La Paz Baja California Sur, México* **2** *Universidad de Cádiz, Departamento de Biología, Estructura y Dinámica de Ecosistemas Acuáticos, Puerto Real, Cádiz, Spain*

Corresponding author: *Claudia J. Pérez-Estrada* (claudiap@cibnor.mx)

Academic editor: *Kyle Piller* | Received 16 February 2019 | Accepted 17 June 2019 | Published 29 August 2019

http://zoobank.org/7C081F97-6437-406B-B071-184FDE3479F0

Citation: Campos-Dávila L, Pérez-Estrada CJ, Rodríguez-Estrella R, Morales-Bojórquez E, Brun-Murillo FG, Balart EF (2019) Seagrass *Halodule wrightii* as a new habitat for the amphioxus *Branchiostoma californiense* (Cephalochordata, Branchiostomidae) in the southern Gulf of California, Mexico. ZooKeys 873: 113–131. https://doi.org/10.3897/zookeys.873.33901

Abstract

The first record of the amphioxus *Branchiostoma californiense* on seagrass patches of *Halodule wrightii* in the Gulf of California is reported. Sixty individuals (19 males, 18 females, and 23 undifferentiated) were collected in May 2017 at Bahía Balandra, Gulf of California, from subtidal seagrass patches at a depth of 0.5 m at low tide. The length and weight ranged from 15.88–28.44 mm and from 0.01–0.11 g for females and 11.7–27.9 mm and 0.01–0.09 g for males, respectively. The minimum size of sexually mature individuals was 11.70 mm for males and 15.88 mm for females; 62% of the specimens were sexually mature. Analysis of the total length-weight relationship suggested an allometric growth pattern among females, males and undifferentiated individuals, whereas an analysis of the entire sample suggested an isometric growth pattern. Typical and additional morphological characters were used to identify the amphioxi. High morphological variability between individuals was found, suggesting the presence of several morphotypes. *Branchiostoma californiense* had been previously reported as exclusively associated with bare sandy areas, but our study shows that this species can also be found in seagrass patches, using them as breeding and feeding grounds. Thus, seagrass patches are evidenced as suitable habitats for amphioxus.

Keywords

Allometric growth pattern, amphioxi, isometric growth pattern, morphological variability, new habitat, sex size structure

Introduction

Amphioxi are Cephalochordata often used as a model for studying the phylogeny and evolution of vertebrates (Stokes and Holland 1998, Bertrand and Escriva 2011, Vergara et al. 2012). Thus, research on this group has mainly focused on morphology, genetics (Holland 2010), embryology (Desdevises et al. 2011), and evolution (Putnam et al. 2008). Amphioxi are marine organisms inhabiting shallow waters near the coast, such as estuaries, coastal lagoons, open coasts, and even river deltas, in temperate and tropical waters (Laudien et al. 2007, Meerhoff et al. 2016). They are benthic, obligate filter feeders that play a key role in the transfer of microbial and phytoplanktonic production to higher trophic levels, including fishes (Ruppert et al. 2000, Vargas and Dean 2010). *Branchiostoma californiense* Andrews, 1893, is the only species reported for the eastern Pacific coast in Central and North America (Vargas 1987, Poss and Boschung 1996, Vargas and Dean 2010). In Mexico, it is distributed from the northwestern coast of the Baja California Peninsula to the coast of Oaxaca, including the Gulf of California; some records from Central America have also been reported (Poss and Boschung 1996, Vargas and Dean 2010, Del Moral-Flores et al. 2016). Two recent studies describe the occurrence and taxonomy of *B. californiense* in Mexico based on preserved specimens. Del Moral-Flores et al. (2016) examined the taxonomic composition and distribution of cephalochordates (Cephalochordata: Amphioxiformes) in Mexico based on specimens from collections of various institutions. Galván-Villa et al. (2017) reported new records of *B. californiense* for the central Mexican Pacific and included a taxonomic description of the species based on five specimens. In this study, we aim to highlight seagrass as a novel and likely suitable habitat for *B. californiense* during breeding in the southern part of the Gulf of California, as well as to add to the knowledge of its taxonomy and biology.

Study area

Bahía Balandra (24°18'54.8"N, 110°19'39.3"W) is a natural protected area located in Bahía de La Paz, Mexico, in the southern part of the Gulf of California (Fig. 1). Bahía Balandra is a coastal lagoon covering an area of 2512.5 ha where coastal vegetation is dominated by three mangrove species (*Rhizophora mangle*, *Laguncularia racemosa* and *Avicennia germinans*). Rocky reefs (Félix-Pico 2009) and patches of the seagrass *Halodule wrightii* also occur in the bay. The beach is gently sloping, shallow, and usually waveless; the tidal range is 1.0–1.5 m with a semidiurnal pattern. The climate is arid, and rainfall is limited to sporadic winter storms or summer hurricanes. Sediment in the bay consists of fine to coarse sand of mixed siliciclastic-calcareous composition (López 2013).

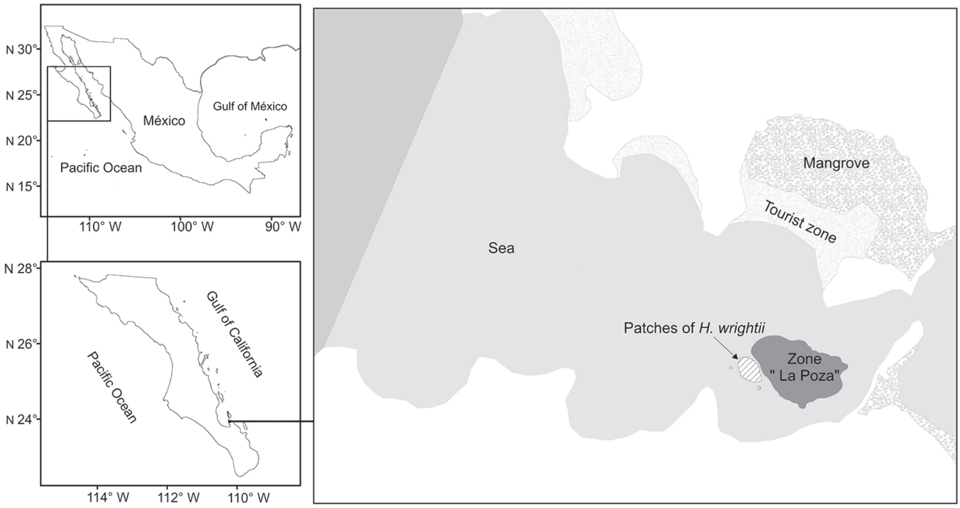

Figure 1. Amphioxus study area, Bahía Balandra southern Baja California Peninsula.

Materials and methods

Habitat

In 2017, a few individuals of the amphioxus *B. californiense* were observed during the course of surveys to monitor the metabolism of seagrass communities. In May 2017, 60 amphioxus specimens were collected in the area called La Poza in Bahía Balandra from a monospecific seagrass patch measuring approximately 24 m^2. Amphioxus density (individuals/m^2) was estimated by burying a 4.5 L bucket in the sand and dragging it horizontally in the seagrass patch ten times; a total area of 0.75 m^2 (0.50 m x 0.15 m x 10 m) was thus sampled. The specimens were placed in plastic bottles containing a bed of sand and seawater for transportation to the laboratory. Additional samplings were carried out to search for amphioxi in other areas of Bahía Balandra: i) in four seagrass patches near the sampled patch, ii) in bare sand areas 10 m away from the sampled patch and iii) in zones farther away (50–450 m) from the sampled patch. Environmental parameters were also recorded within the *H. wrightii* canopy. Water temperature (°C) was recorded during 24 hours using a HOBO data logger (UA-002–64). pH and salinity were measured at the beginning and end of the sampling with a multi-parameter YSI sonde. Chlorophyll concentration in water and sediment was determined using the technique described by Strickland and Parsons (1972). The measurement results are presented as the mean (± standard deviation).

Laboratory analysis

Amphioxi were kept alive in aquaria. Thus, morphological and meristic taxonomical characters were observed and recorded in live individuals, which allowed more accurate observations than individuals preserved in formaldehyde or alcohol. To record morphometric measurements, individuals were placed in a 300 mL beaker containing seawater with 12 drops (approx. 600 µL) of clove oil added as a sedative. The individuals were then transferred to a Petri dish (5–7 cm in diameter) with seawater and observed under a Nikon SMZ25 stereomicroscope. Photographs of each individual were taken and later processed with NIS-Elements imaging software for the analysis of morphometric traits.

Amphioxi were identified based on typical morphological characters, following Poss and Boschung (1996): 1) length; 2) total, preatriopore, atriopore-to-anus and postanal number of myotomes; 3) number of dorsal and preanal fin chambers; and 4) number of gonads. Based on the wide size range and the high variability of morphological characters observed in the collected specimens, we hypothesized that these might represent more than one morphotype. To explore this possibility, we examined additional characters, including 5) preatriopore, atriopore–anal distance, 6) postanal region length, 7) length of super- and sub-caudal fins, 8) body depth, 9) height of the caudal fin, 10) length and height of the rostral fin, 11) height and width of the tallest dorsal fin chamber, 12) the tallest preanal fin chamber, and 13) angle between the dorsal and super-caudal fin and between the preanal and sub-caudal fin. All counts and measurements were taken on the left side of the specimens, following Tchang and Koo (1936) and Zhang et al. (2006). Wet body weight (FW) was recorded to the nearest 0.001 g with an electronic scale (Ohaus Explorer, Florham Park, NJ, USA). Prior to weighing the specimens, excess water was removed with paper towels.

Sex determination

The criteria proposed by Henmi and Yamaguchi (2003) were used to sex mature individuals. Immature and unmatured specimens were classified as undifferentiated.

Statistics

The mean, standard deviation and coefficient of variation of each morphological trait were calculated separately by sex. Differences between sexes in each morphometric variable were tested with Student´s t-test ($\alpha = 0.05$) (STATISTICA v 8.0). To examine the relationship between total length (TL) and weight (W) of the specimens, the power equation $TW = \mathrm{a}TL^{\beta}$ was fitted to the data. In this equation, a is the average condition factor and β is the coefficient of allometry; a β value equal to 3 indicates an isometric growth pattern, whereas a value significantly different from 3 denotes allometric growth. Thus, the equation parameters and their 95% confidence intervals (CI) were estimated (Aguirre-Villaseñor et al. 2006, Esmaeili and Ebrahimi 2006), and the estimated β was subjected to Student’s t-test (Zar 1999) to determine whether growth was isometric or allometric. As allometric changes are related to the chronology of important life-history events and therefore reflect an ontogenetic response to functional demands, allometric analyses were conducted separately for females, males, both sexes, undifferentiated individuals, and for the entire sample.

To examine the size structure of the individuals, TL (mm) data were grouped in 2-mm class intervals separately for males and females; for undifferentiated individuals, a 1-mm class interval was used. To determine the expected number of TL groups, a multinomial probability density distribution was constructed as described by Haddon (2001). The 95% confidence interval for each group was calculated using *Student's t* distribution. To test whether the sex ratio deviated significantly from 1:1, a chi-square test was carried out ($\alpha < 0.05$) (Sokal and Rohlf 1995).

Results

Habitat

Branchiostoma californiense individuals (Fig. 2) were found within and at the margins of patches of *H. wrightii*. Amphioxus abundance decreased with the distance from seagrass patches: 10 m away from a sampled patch, only a few individuals were found; 50 m or farther away from a sampled patch, no amphioxi were found in bare sediments. The average density of amphioxi in seagrass patches was 80 ind. m^{-2}, for an estimated total abundance of 1920 individuals for the entire seagrass patch sampled. Temperature average in 24 hours was 23.1 ± 0.11 °C, with minimum and maximum values of 20.80 and 26.90 °C, respectively; During the survey, the average water surface temperature was 22.90 ± 0.11 °C, with minimum and maximum values of 22.04 and 24.44 °C, respectively; pH was 8.44 ± 0.39; salinity was 36.89 ± 0.31 ups; and chlorophyll *a* concentration was 0.22 ± 0.04 mg m^{-3} in seawater and 1.93 ± 0.44 mg/g in sediments.

Amphioxus characteristics

We collected 18 male and 19 female specimens, for a 0.94:1 male-female ratio, plus 23 sexually undifferentiated individuals. The TL ranged between 15.88 and 28.44 mm (19.76 ± 3.33 SD mm) in females, 11.7–27.9 mm (19.15 ± 3.78 SD mm) in males and 12.8–20.05 (14.97 ± 2.04 mm) in undifferentiated individuals, with no significant difference between males and females (t-test = 0.52; df = 35; $p = 0.60$). The total fresh weight (TW) ranged between 0.0143 and 0.1118 g (0.04 ± 0.03 g) in females and 0.014–0.08 g (0.04 ± 0.03 g) in males, with no significant difference between their means (t-test = 0.20; df = 35; $p = 0.84$). The TW of undifferentiated individuals ranged between 0.004 and 0.05 g (0.02 ± 0.01 g).

Analysis of the size structure of *B. californiense* revealed the following: 1) two size groups were identified in females, the first group with an average TL of 19.15 mm (CI = 18.50–19.81 mm, s = 2.51), and the second with an average TL of 26.11 mm (CI = 24.91–27.32 mm, s = 1.39); 2) a single size group was identified in males with an

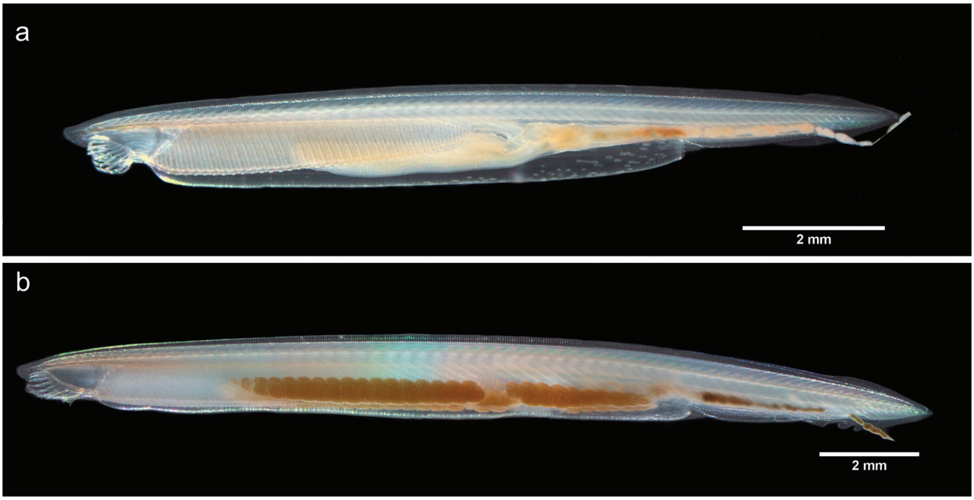

Figure 2. Amphioxus *Branchiostoma californiense*: **a** immature organism **b** mature organism (female).

Table 1. Total length-weight (TL-W) relationships for individuals of *Branchiostoma californiense* in Bahía Balandra, southern Baja California Peninsula.

Individual	N	r^2	a	CI	β	CI	Student's t-test	P value
Females	19	0.66	2.23E-6	7.49E-8–6.66E-5	3.28	2.14–4.42	44.51	< 0.007
Males	18	0.64	1.58E-6	3.79E-8–6.63E-5	3.39	2.12–4.66	56.88	< 0.005
Undifferentiated	23	0.51	1.84E-6	3.64E-8–9.30E-5	3.43	1.98–4.88	182.34	< 0.001
Whole Population	60	0.67	5.22E-6	1.09E-8–2.48E-5	3.01	2.46–3.55	4.06	< 0.07

N = number of data, CI = confidence interval, Student's t-test was estimated with $df = 1$.

average value of 19.97 mm (CI = 18.87–21.91 mm, s = 3.81); 3) a single size group was also identified in sexually undifferentiated individuals, with an average TL of 14.63 mm (CI = 14.40–15.0 mm, s = 0.65); and 4) three size groups were identified in the overall population, with the following average TL: 14.66 mm (CI = 14.45–14.87 mm, s = 0.81), 18.73 mm (CI = 18.42–19.03 mm, s= 1.18), and 23.99 mm (CI = 23.85–24.15 mm, s = 0.59) (Fig. 3).The relationship between total length and weight (TL-W) in females ($N = 19$), males ($N = 18$), and sexually undifferentiated specimens ($N = 23$) of *B. californiense* revealed an allometric growth pattern. The slopes were statistically analyzed between both sexes and no significant differences were found (t-test, $P < 0.05$), between males ($\beta = 3.39$, SE = 0.60) and females ($\beta = 3.28$, SE = 0.54); consequently, the TL-W relationship can be expressed jointly (a = 1.78E-06, IC = 1.69E-07-1.88E-05; $\beta = 3.35$, IC = 2.56-4.15); and the TL-W relationship was equally allometric; whereas a similar analysis over the entire sample ($N = 60$) showed an isometric growth pattern (Table 1, Fig. 4).

Thirty-seven individuals showed sexual dimorphism. Females had well-developed, beige-colored gonads, with oocytes visible under the stereoscope (Fig. 5). In males, gonads

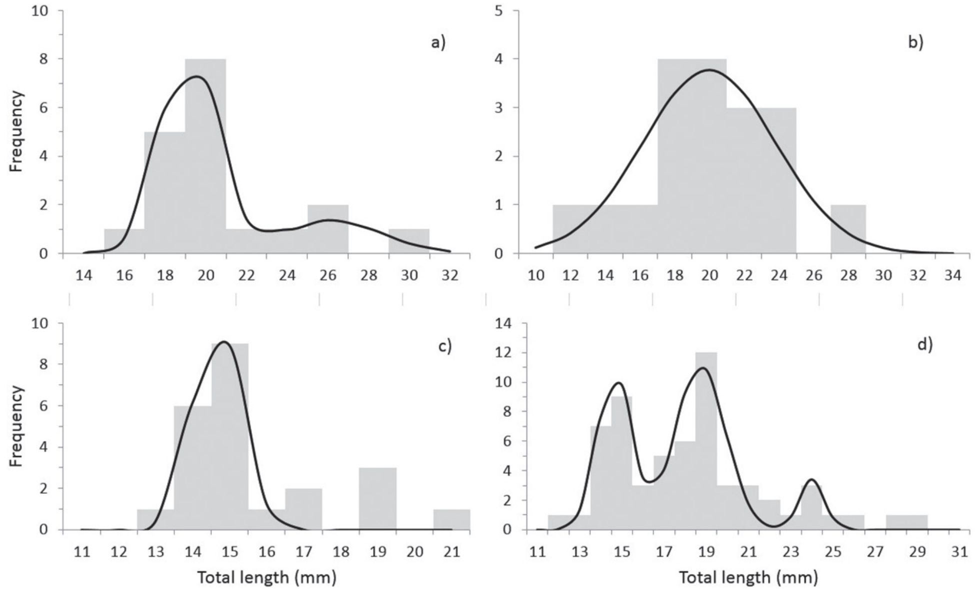

Figure 3. Length frequency intervals. Structure of size: **a** females **b** males **c** undifferentiated **d** all population, specimens of *Branchisotoma californiense* in Bahía Balandra, southern Baja California Peninsula.

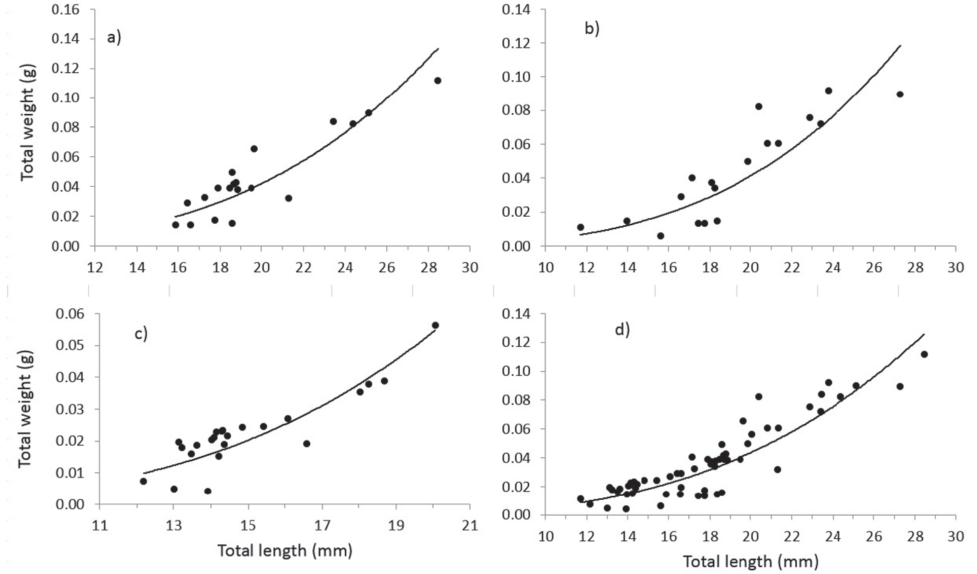

Figure 4. Length-weight relationship for: **a** females **b** males **c** undifferentiated and **d** all population specimens of *Branchisotoma californiense* in Bahía Balandra, southern Baja California Peninsula.

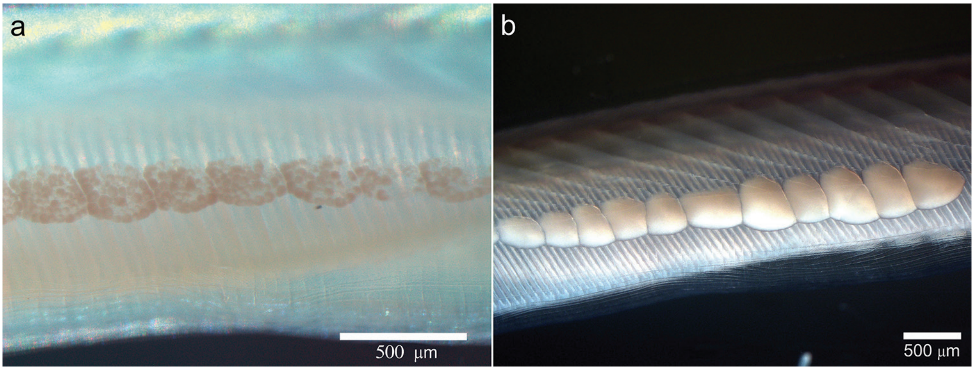

Figure 5. Sexual differentiation in amphioxus *B. californiense*, mature individuals: **a** female, with signs of some gonads having spawned (right side of the picture) **b** male with well-developed gonads (right side of the picture) and some gonads in the process of development (left side of the picture).

were whitish with no visible granules inside (Fig. 5). Individuals were bilaterally symmetrical, with well-developed gonads on both sides, although gonads were often more numerous on the right than on the left side, a trait usually associated with the maturation stage of the gonads. Spawning individuals had fewer gonads. The minimum size at sexual maturity was 11.70 mm in males and 15.88 mm in females; the largest gonad-bearing individuals measured 28.44 mm in females and 27.29 mm in males. Asynchronous gonadal maturation was observed in some individuals that bore maturing, mature and spawning gonads.

Taxonomical characters

The myotome formula of *B. californiense* was preatriopore 44.42 (40–49) + atriopore-anal 14.57 (13–19) + postanal 8.53 (6–10) = total 67.52 (59–76). Dorsal fin of moderate height. Dorsal fin chambers 389 (345–442). Preanal fin chambers 52.98 (36–74). Body length to body depth ratio: 11.83 (8.35–18.64) (Table 2). Maximum number of gonads 37 in females, 35 in males (Tables 2, 3).

Morphological characters

Branchiostoma californiense has an elongated body. The notochord extends beyond the oral hood and forms a well-developed rostral process. Buccal region with numerous fine cirri (up to 24), most of them longer than the tip of the rostrum (Fig. 6). Cirri with (75% of the individuals) or without (25%) serrations (Fig. 6). Rostral fin thickened, with a round end, although some variations (i.e., less thickened and larger rostral fins) were observed. Velar tentacle of the wheel organ with variable shape, some projections with varying length and shape (Fig. 6). Caudal fin with long, shallow expansions of

Table 2. Comparative data of the more relevant morphometric characteristics considered for traditional taxonomy of amphioxus for *Branchiostoma californiense*, including previous reports and those specimens caught in Bahía Balandra, southern Baja California Peninsula, Mexico. Values are given in mean (range). In bold the main differences of this study with respect to the other studies.

	Andrews (1893)	**Kirkaldy (1895)**	**Hubbs (1922)**	**Poss and Boschung (1996)**	**Del Moral-Flores et al. (2016)**	**Galván-Villa et al. (2017)**	**This Study**
TL (mm)	57–70	74 max.	37.5–83.5	No data	83.5	24.1–40.1	**11.70–28.44**
Total Myotomes	68 (64–69)	71 (69–73)	68–74	70.1(64–78)	67 (64–71)	69 (66–72)	67 (**59**–76)
Preatriopore myotomes	44 (42–45)	44–45	43–48	44.3 (42–47)	40 (40–45)	43 (39–46)	44 (40–**49**)
Myotomes between atriopore and anus	16 (13–16)	16–19	16–19	16.7 (13–19)	18 (14–19)	17 (16–19)	**14** (13–19)
Postanal myotomes	9 (8–9)	8–9	9.1 (7–11)	9 (8–9)	9 (8–9)	9 (9–10)	8 (**6**–10)
Dorsal fin chambers	No data	No data	337 (312–374)	355 (317–419)	355 (317–419)	364 (343–395)	**388 (345–442)**
Preanal fin chambers	No data	No data	50	44 (35–19)	44 (35–59)	58 (56–61)	53 (36–**74**)
Gonad pouches	No data	31	33 (273–6)	36 max.	36 max.	26 (18–31)	28 (**16–37**)
N	7	10	22	57	No data	5	60

Table 3. Meristic and non-meristic data of 37–60 individuals of *Branchiostoma californiense* found on seagrass *H. wrightii* at southern Baja California Peninsula.

Characteristics	***N***	**Minimum – Maximum**	**Mean**	**SD**	**SE**	**CV**
Number of myotomes anterior to atriopore	60	40–49	44.42	2.35	0.3	0.05
Number of myotomes between atriopore and anus	60	13–19	14.57	1.35	0.17	0.09
Number of myotomes posterior to anus	60	6–10	8.53	0.89	0.12	0.10
Total number of myotomes	60	59–76	67.52	3.29	0.41	0.05
Number of dorsal fin chambers	60	345–442	389	22.38	2.89	0.06
Number of preanal fin chambers	60	36–74	52.98	8.64	1.12	0.16
Number of gonads on the left side	37	16–37	28.27	4.5	1.84	15.74
Number of gonads on the right side	37	7–35	28.5	4.9	0.73	17.06
Length of body	60	11.70–28.44	17.74	3.73	0.48	0.21
Length of preatriopore region	60	8.54–20.89	12.92	2.71	0.35	0.21
Length of atriopore-anal-region	60	2.03–5.58	3.41	0.83	0.11	0.24
Length of postanal region	60	0.94–2.32	1.41	0.3	0.04	0.21
Lenght of super-caudal fin	60	1.31–3.46	2.01	0.46	0.06	0.23
Length of sub-caudal fin	60	1.46–4.18	2.43	0.5	0.06	0.21
Depth of body	60	0.75–2.22	1.52	0.3	0.04	0.20
Lenght of rostral fin	60	0.18–0.52	0.36	0.08	0.01	0.23
Height of rostral fin	60	0.11–0.44	0.24	0.08	0.01	0.33
Height of caudal fin	60	0.69–1.57	0.99	0.21	0.03	0.21
Length to depth of body	60	8.35–18.64	11.83	1.85	0.23	15.67
Heigth to width of tallest dorsal fin chamber	60	0.50–6.33	3.17	1.09	0.14	34.44
Height to width of tallest preanal fin chamber	60	1.0–4.5	2.39	0.72	0.09	30.02
Angle between dorsal and super-caudal fins	60	150.37–180.52	168.97	37.74	0.79	0.04
Angle between preanal and sub-caudal fins	60	111.19–184.31	167.68	9.09	1.17	0.05

dorsal and ventral fins. Anus well posterior to the center of the ventral lobe of the caudal fin (Fig. 7). Body color fully translucent. No significant differences between males and females in the morphometric variables examined were found (see Suppl. material 1).

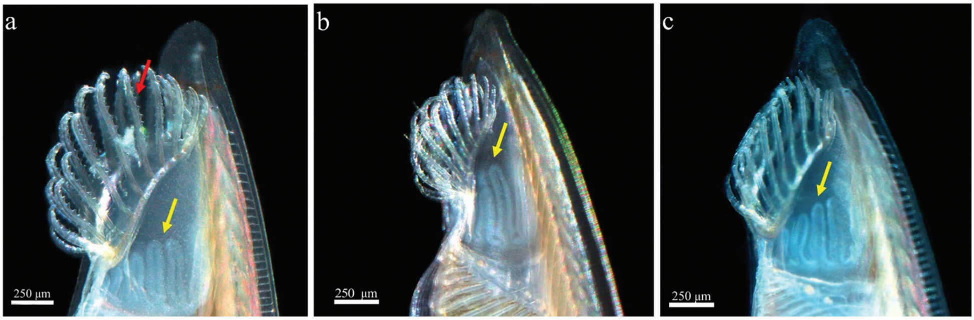

Figure 6. Morphology oral region. Serrations of the cirri (red arrow) (**a**). Velar tentacle (yellow arrow) of the wheel organ having a singular variation in the shape, some projections were different in length and shape (**b, c**).

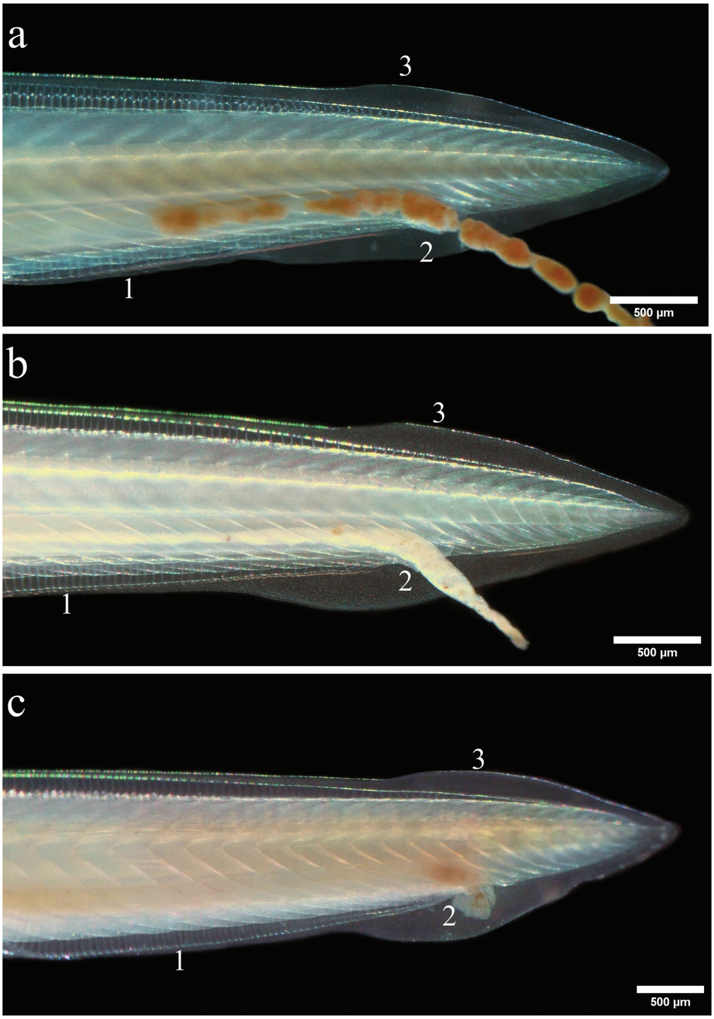

Figure 7. Morphology caudal region (**a–c**). Posterior part of *B. californiense* showing differences in caudal fin and preanal fin chambers: (**1**) preanal fin chambers, (**2**) anus, (**3**) lobe dorsal fin variability.

Discussion

Since 1932, *B. californiense* has been reported from 68 localities in the Baja California Peninsula, 31 of those in the Gulf of California and 37 along the Pacific coast (Poss and Boschung 1996, GBIF 2018), but no study had previously recorded the occurrence of amphioxus in a seagrass habitat. In addition, our study is one of the very few providing biological and ecological information, and it documents the most recent record of this species in the Gulf of California. Habitats more commonly reported for amphioxus are shallow subtidal sand flats in tropical, subtropical and temperate waters. Amphioxi usually prefer coarse sand with fairly fast water flow, although they can also be found in silty sediments (Berrill 1987, Nishikawa et al. 1997, Chen 2007). Most species have benthic habits, and the adults live burrowed in the sand, gravel, or shell deposits (Vargas and Dean 2010, Desdevises et al. 2011). *Branchiostoma californiense* is most commonly found in sandy flat bottoms (Vargas and Dean 2010, Galván-Villa et al. 2017). In contrast, all the specimens in this study were collected in patches of the seagrass *Halodule wrightii*; this reveals the wider habitat range and tolerance to seagrass habitat conditions of the amphioxus *B. californiense*. Remarkably, no individuals were found in bare areas.

Variables recorded during our sampling outline the environmental conditions in the seagrass patches where the population of *B. californiense* lives in Bahía Balandra. The temperature during the sampling period corresponds to the transition period (May-June) between the cold (December–April) and warm (July-November) seasons in the Gulf of California (Martínez-López et al. 2001). The concentration of chlorophyll *a* in water was low, as was already reported for the same dates (Martínez-López et al. 2001), but the concentration in sediment inside the patch was high. These values denote the productivity level prevailing at the time of sampling in this habitat occupied by amphioxus.

It is known that seagrass meadows are one of the most productive marine habitats (Larkum et al. 2006), and they are thought to play a key role in maintaining populations of commercially exploited marine fishes and invertebrates by providing crucial ecosystem services, including: (1) permanent habitat allowing completion of the life cycle, (2) nursery areas for the development of juvenile stages, (3) feeding grounds for various life-history stages and (4) refuge from predators (Jackson et al. 2001). In addition, the seagrass canopy structure attenuates hydrodynamic forces, and its belowground structures stabilize the sea floor, creating milder growing conditions (Brun et al. 2009). As active filter feeders, amphioxi living in the seagrass canopy benefit from the local reduction in the flow regime (i.e., higher sediment stability) and the lower disturbance that allow them to obtain food by filtering suspended particles from the surrounding waters. Additionally, amphioxi likely find refuge and suitable habitat inside and at the edge of seagrass patches, as has been observed in other filter-feeder organisms (Irlandi and Peterson 1991, Irlandi 1996, Brun et al. 2009, González-Ortiz et al. 2014, Jiménez-Ramos et al. 2018).

There is high variability in the size structure of *B. californiense* populations across its distribution range. The largest sizes (83.5 mm) have been recorded in northern latitudes (Monterey Bay, California) (Hubbs 1922), whereas the smallest sizes (5 mm) were reported by Vargas and Dean (2010) in southern latitudes (Costa Rica). Galván-Villa et al. (2017) reported sizes ranging from 24.1 to 40.1 mm at a depth of 5–8 m in the central Mexican Pacific. Our specimens are the smallest (11.70 to 28.44 mm) reported for the Gulf of California and the Mexican Pacific; they may represent recent recruits, as Vargas and Dean (2010) found for Costa Rica. The smallest sexually mature specimen in our sample was an 11.70 mm (TL) male. Thus, it can be assumed that juveniles are likely smaller than 11 mm. The lifespan for *B. californiense* is unknown, but according to growth models of *B. belcheri* (Chen et al. 2008), the body size range of one year and, two and three-years-old individuals was 5–28 mm, 28–38 mm and 38–45 mm length, respectively. Therefore, it is likely that *B. californiense* individuals in our study area (11.70–28.44 length) probably belong to a one-year-old group compared, for example, to the report of Hubbs (1922) (37.5–83.5 length), which individuals belong to the two- or three-years-old group. However, it is also possible that body size differences can be related to latitudinal variation following the Bergman´s rule, bigger individuals in higher latitudes (Lomolino et al. 2006). Thus, northern individuals (36°N; Hubbs 1922) were larger in comparison to the lower latitude at our study site in the Gulf of California (24°N).

This study documents, for the first time, the TL-W relationship in a natural population of *B. californiense*. This information is useful for understanding the relationship and expected trends of length and weight under natural conditions and helps to elucidate whether the species exhibits an allometric or isometric growth pattern. A positive allometric growth pattern ($\beta > 3$) means that the organism grows in weight proportionately faster than it does in length (NOAA 2006); this growth pattern was observed in the females, males and undifferentiated individuals in our sample. An isometric growth pattern ($\beta = 3$) means that any increment in length is associated with a proportional increment in weight (NOAA 2006); this growth pattern was observed when we analyzed the entire sample of *B. californiense*. The change from allometric (males, females and undifferentiated, or both sexes jointed) to isometric (all population specimens) may be associated to the different TL intervals among groups; the organisms undifferentiated had a range of TL (12–20 mm) 50% smaller than for males and females (12–28 mm and 16–29 mm, respectively). When the different groups were independently analyzed the variability in TL-W data influenced an apparent allometric condition. However, the analysis based on all population specimens allowed the estimate of an isometric growth pattern, which was influenced by a TL interval wider. Several factors, such as age, body shape, amount of body fat, sex, maturity stage, season, and abiotic variables (e.g., temperature, salinity and available nutrient), influence the value of β in the total length-total weight relationship, causing seasonal and between-habitat variations (Froese 2006, Froese et al. 2014, He et al. 2008).

Analysis of the size structure of the *B. californiense* sample revealed different groups, which might correspond to different cohorts being present in the population, as has been suggested for fish populations (Chang et al. 2012, Le Bris et al. 2015). In this study, three distinct length groups were identified, suggesting the presence of three distinct cohorts (two cohorts for females and one for males). A single size group was identified in the undifferentiated specimens, with an average length (14.63 ± 2.04 SD mm) smaller than that of females (19.76 ± 3.32 SD mm) or males (19.15 ± 3.77 SD mm). These smaller individuals might constitute the new recruits in the population; this hypothesis could have been verified had field data on age and reproduction been also obtained during the sampling. The fact that 62% of the specimens in our sample were sexually mature adults and that the size structure shows the presence of different cohorts in the population indicates that part of the cycle life of *B. californiense* takes place in this habitat. Thus, based on our results, we propose that the patches of *H. wrightii* in Bahía Balandra provide breeding grounds for *B. californiense*.

Diagnosis

Data obtained in this study on the meristic and morphometric characters of amphioxus significantly contribute to the knowledge of this species and will support future studies on other populations in the Gulf of California and Pacific coasts. Our data on the meristic characters of *B. californiense* show some differences from previous reports. All the characters necessary to determine the genus and species (Gill 1895, Hubbs 1922, Galván-Villa et al. 2017) could be observed in all our specimens. However, we recorded a wider range of total and postanal myotomes. These differences may stem from methodological issues rather than being due to actual differences in the organisms, as other authors reported meristic and morphometric data as recorded in preserved individuals (Poss and Boschung 1996, Galván-Villa et al. 2017). Preservation makes observation, counting, and measurement more difficult as the specimens turn whitish and opaque upon preservation, and tissues shrink because of fixation.

Poss and Boschung (1996) observed high morphometric variation between specimens of *B. californiense* without a well-defined geographical pattern. In our study, we also found high variation between individuals in morphometric characters, especially in the rostral and caudal fins (angles), body depth and preanal fin chambers; such variations suggest the presence of different morphotypes. For example, those characters have been considered diagnostic for distinguishing between the two species *B. japonicum* Willey, 1897 and *B. belcheri* Gray, 1847 (Zhang et al. 2006). On the other hand, Galván-Villa et al. (2017) observed an increasing north-south trend in the number of dorsal and preanal fin chambers of specimens collected in Mexico. However, our observations were performed on live organisms, and we found the largest numbers of dorsal (345–442) and preanal (36–74) fin chambers recorded so far, whereas Galván-Villa et al. (2017) reported smaller numbers of both dorsal and preanal fin chambers in an area much farther south.

Amphioxus is usually a bisexual or gonochoristic organism; the mature gonad is whitish in males and yellow in females (Zhang et al. 2001), as confirmed in our study. We also found a higher variation in the number of gonads than previously reported, thus widening the range previously reported to 16–37. A range of 18–31 gonads was reported by Galván-Villa et al. (2017) and a range of 27–36 gonads by Hubbs (1922). This difference may be related to either the maturation stage or the manner in which observations were made. In our study, we observed asynchronous gonadal development in some specimens, which showed gonadal remnants (still bearing a few reproductive cells, indicating that the organism had already spawned), mature and maturing gonads. In our study, we took all the gonadal development stages into account when counting the number of gonads.

The velar tentacles of the wheel organ showed some variations in the length and shape of the projections. Because the velar tentacles are retractable structures, such variations could well be due to the specimens showing different degrees of relaxation in response to the clove oil used to sedate them. By contrast, when observations are made on fixed organisms the velar tentacles will always be contracted. The filtering system of amphioxus consists of a mouth surrounded by a circular velum with velar tentacles (oral cirri), the branchial basket (pharynx) and the atrium chamber (Orton 1913, Weel 1937, Chen 2007). We found fewer oral cirri (up to 24) than the number reported by Galván-Villa et al. (2017) (up to 40). Hubbs (1922) described the oral hood and cirri becoming smaller with age, but we did not observe such trends in our study. Finally, 25% of the specimens in our sample did not show serrations in the cirri, and some showed damage to the caudal fin. Chen (2007) indicated that an increased content of suspended solids can cause physical damage to filter-feeding structures, such as the absence of serrations in the cirri of amphioxus, which coincides with our observations.

Conclusions

The occurrence of the amphioxus *B. californiense* in the Gulf of California was first reported 86 years ago. Our study is the first to provide information on its biology, particularly the population's size structure. Our results show that *B. californiense* is not strictly associated with bare sandy areas, as had been previously reported for the Gulf of California, but that seagrass beds are also an important habitat offering distinct structural characteristics for amphioxus. Further efforts of sampling both in time and space are needed to study the relationship between *B. californiense* and seagrasses to elucidate its ecological relevance and the role of *B. californiense* as active filter feeders in this ecosystem.

Acknowledgments

We thank the support of R.M. Ochoa Díaz, D. Méndez Jordán, M. Cota Castro, J. Cobos Anaya, A. Alvarez Casillas, J.J. Ramírez Rosas, M.D. Rondero Astorga and S.A. Juan Antúnez, from CIBNOR and S. López López from CICIMAR. J.A. Díaz-Sánchez, from the Instituto Nacional de Estadística y Geografía (INEGI), for providing the detailed maps used in this study. We appreciate the comments by V.H. Cruz Escalona and the reviewers which greatly improved the manuscript. The second author received a scholarship from the international affairs office of the University of Cadiz (UCA/R27REC/2017), this manuscript was writing during a sabbatical stay at the

University of Cadiz, Spain too. This study was funded by the following grants: Proy-PC027-CIBNOR, PEP-CIBNOR, Proy-179322-253738 CONACYT, Excellence of the Junta de Andalucía PRODESCA (P12-RNM3020), and Spanish National Plan of I+D+I PAVAROTTI (CTM2017-85365-R). Note. The first and second authors equally contributed to the research and drafting of the manuscript. Permit No. F00-CONANP/AFPBALANDRA/236/2016.

References

Aguirre-Villaseñor H, Morales-Bojórquez E, Morán-Angulo RE, Madrid-Vera J, Valdez-Pineda MC (2006) Indicadores biológicos de la pesquería de sierra (*Scomberomorus sierra*) al sur del Golfo de California, México. Ciencias Marinas 32: 471–484. https://doi.org/10.7773/cm.v32i3.1130

Andrews EA (1893) An undescribed acraniate: *Asymmetron lucayanum*. Stud. Biology Laboratory Johns Hopkins University 5: 213–247. https://doi.org/10.5962/bhl.title.29798

Berrill NJ (1987) Early chordate evolution. Part 1. Amphioxus, the riddle of the sands. International Journal of Invertebrate Reproduction and Development 11: 1–14. https://doi.org/10.1080/01688170.1987.10510263

Bertrand S, Escriva H (2011) Evolutionary crossroads in developmental biology: amphioxus. Development 138: 4819–4830. https://doi.org/10.1242/dev.066720

Brun FG, Zetten E, Cacabelos E, Bouma TJ (2009) Role of two contrasting ecosystem engineers (*Zostera noltii* and *Cymodocea nodosa*) on the food intake rate of *Cerastoderma edule*. Helgoland Marine Research 63(1):19–25. https://doi.org/10.1007/s10152-008-0134-7

Chang CW, Lin CH, Chen YS, Chen MH, Chang SK (2012) Age validation, growth estimation and cohort dynamics of the bony flying fish *Hirundichthys oxycephalus* off eastern Taiwan. Aquatic Biology 15: 251–260. https://doi.org/10.3354/ab00425

Chen Y (2007) The ecology and biology of amphioxus in Hong Kong. PhD thesis, City University of Hong Kong. http://lbms03.cityu.edu.hk/theses/c_ftt/phd-bch-b22178892f.pdf

Chen Y, Shin PK, Cheung SG (2008) Growth, secondary production and gonad development of two co-existing amphioxus species (*Branchiostoma belcheri* and *B. malayanum*) in subtropical Hong Kong. Journal of Experimental Marine Biology and Ecology 357(1): 64–74. https://doi.org/10.1016/j.jembe.2007.12.028

Del Moral-Flores LF, Guadarrama-Martínez MA, Flores-Coto C (2016) Composición taxonómica y distribución de los cefalocordados (Cephalochordata: Amphioxiformes) en México. Latin American Journal of Aquatic Research 44: 497–503. https://www.redalyc.org/pdf/1750/175046920008.pdf

Desdevises Y, Maillet V, Fuentes M, Escriva H (2011) A snapshot of the population structure of *Branchiostoma lanceolatum* in the Racou Beach, France, during its spawning season. PLoS ONE 6: e18520. https://doi.org/10.1371/journal.pone.0018520

Esmaeili HR, Ebrahimi M (2006) Length-weight relationships of some freshwater fishes of Iran. Journal of Applied Ichthyology 22: 328–329. https://doi.org/10.1111/j.1439-0426.2006.00653.x

Félix-Pico E (2009) Una evaluación de indicadores de integridad ecológica de manglares en la Península de Baja California. Sección: Estructura del manglar, cangrejos asociados y características del suelo de los dos esteros sitios: esteros Balandra y Enfermería en la Bahía de La Paz, Baja California Sur, México. Informe Final CICIMAR-IPN. La Paz, 15 de diciembre de 2009. https://cibnor.repositorioinstitucional.mx/jspui/bitstream/1001/892/1/Cap7_Libro_LOS%20MANGLARES%20DE%20LA%20PENINSULA%20DE%20BAJA%20CALIFORNIA.pdf

Froese R (2006) Cube law, condition factor, and weight-length relationships: history, meta-analysis and recommendations. Journal of Applied Ichthyology 22: 241–253. https://doi.org/10.1111/j.1439-0426.2006.00805.x

Froese R, Thorson JT, Reyes Jr RB (2014) A Bayesian approach for estimating length-weight relationships in fishes. Journal of Applied Ichthyology 30: 78–85. https://doi.org/10.1111/jai.12299

Galván-Villa CM, Ríos-Lara E, Ayón-Parente M (2017) New records of the Californian lancelet *Branchiostoma californiense* (Cephalochordata: Branchiostomidae) from the Pacific coast of Mexico. Revista Mexicana de Biodiversidad 88: 995–998. https://doi.org/10.1016/j.rmb.2017.10.032

GBIF (2018) GBIF Occurrence Download. https://doi.org/10.15468/dl.unpmoq

Gill T (1895) The genera of Branchiostomidae. The American Naturalist 29: 457–459. https://doi.org/10.1086/276154

González-Ortiz V, Egea LG, Jimeńez-Ramos R, Moreno-Mariń F, Pérez-Lloréns JL, Bouma TJ, Brun FG (2014) Interactions between seagrass complexity, hydrodynamic flow and biomixing alter food availability for associated filter-feeding organisms. PLoS ONE 9: e104949. https://doi.org/10.1371/journal.pone.0104949

Haddon M (2001) Modelling and quantitative methods in fisheries. Chapman and Hall, Boca Raton, Florida, 465 pp.

He JX, Bence JR, Johnson JE, Clapp DF, Ebener MP (2008) Modeling variation in mass–length relations and condition indices of lake trout and chinook salmon in Lake Huron: a hierarchical Bayesian approach. Transactions of the American Fisheries Society 137: 801–817. https://doi.org/10.1577/T07-012.1

Henmi Y, Yamaguchi T (2003) Biology of the Amphioxus, *Branchiostoma belcheri* in the Ariake Sea, Japan I. Population Structure and Growth. Zoological Science 20(7): 897–906. https://doi.org/10.1577/T07-012.1

Holland PW (2010) From genomes to morphology: a view from amphioxus. Acta Zoologica 91:81–86. https://doi.org/10.1111/j.1463-6395.2009.00427.x

Hubbs CL (1922) A list of the lancelets of the world with diagnosis of five new species of *Branchiostoma*. Occasional Papers of the Museum of Zoology, University of Michigan 105: 2–15. https://deepblue.lib.umich.edu/bitstream/handle/2027.42/56544/OP105.pdf?sequence=1&isAllowed=y

Irlandi EA (1996) The effects of seagrass patch size and energy regime on growth of a suspension-feeding bivalve. Journal of Marine Research 54: 161–185. https://doi.org/10.1357/0022240963213439

Irlandi EA, Peterson CH (1991) Modification of animal habitat by large plants: mechanisms by which seagrasses influence clam growth. Oecologia 87: 307–318. https://doi.org/10.1007/BF00634584

Jackson EL, Rowden AA, Attrill MJ, Bossey SJ, Jones MB (2001) The importance of seagrass beds as a habitat for fishery species. Oceanography and Marine Biology 39: 269–304.

Jiménez-Ramos R, Egea LG, Vergara JJ, Bouma TJ, Brun FG (2018) The role of flow velocity combined with habitat complexity as a top-down regulator in seagrass meadows. Oikos 128(1): 64–76. https://doi.org/10.1111/oik.05452

Kirkaldy JW (1895) A revision of the genera and species of the Branchiostomidae. Quarterly Journal of Microscopical Science 37: 303–323.

Larkum AWD, Orth RJ, Duarte CM (2006) Seagrasses: Biology, Ecology, and Conservation. Springer, Dordrecht, 691 pp.

Le Bris A, Pershing AJ, Hernandez CM, Mills KE, Sherwood GD (2015) Modelling the effects of variation in reproductive traits on fish population resilience. ICES Journal of Marine Science 72: 2590–2599. https://doi.org/10.1093/icesjms/fsv154

Laudien J, Rojo M, Oliva M, Arntz W, Thatje S (2007) Sublittoral soft bottom communities and diversity of Mejillones Bay in northern Chile (Humboldt Current upwelling system). Helgoland Marine Research 61: 103–116. https://doi.org/10.1007/s10152-007-0057-8

Lomolino MV, Sax DF, Riddle BR, Brown JH (2006) The island rule and a research agenda for studying ecogeographical patterns. Journal of Biogeography 33(9): 1503–1510. https://doi.org/10.1111/j.1365-2699.2006.01593.x

López LSG (2013) Caracterización física y evaluación del impacto antropogénico en los principales humedales de manglar en la Bahía de la Paz, Baja California Sur. Tesis de Licenciatura. Universidad Autónoma de Baja California Sur. http://biblio.uabcs.mx/tesis/te3107.pdf

Martínez-López A, Cervantes-Duarte R, Reyes–Salinas A, Valdez-Holguín JE (2001) Cambio estacional de clorofila a en la Bahía de La Paz, B.C.S., México. Hidrobiológica 11: 45–52. http://www.scielo.org.mx/pdf/hbio/v11n1/v11n1a4.pdf

Meerhoff E, Veliz D, Vega-Retter C, Yannicelli B (2016) The amphioxus *Epigonichthys maldivensis* (Forster Cooper, 1903) (Cephalochordata Branchiostomatidae) larvae in the plankton from Rapa Nui (Chile) and ecological implications. Biodiversity Journal 7: 7–10. https://www.researchgate.net/publication/316522753

Nishikawa T, Shirai H, Chen Y, Dai CF, Nohara M, Soong K (1997) First find of *Epigonichthys maldivensis* (Cooper) and rediscovery of *E. lucayanus* (Andrews) from Nanwan Bay, Southern Taiwan (Cephalochordata). Benthos Research 52: 103–109. https://doi.org/10.5179/benthos1996.52.2_103

NOAA (2006) NOAA fisheries glossary, rev. edition. NOAA Tech. Memo. NMFS-F/SPO-69. Silver Springs, MD: U.S. Department of Commerce. National Oceanic and Atmospheric Administration, 61 pp. https://www.st.nmfs.noaa.gov/st4/documents/FishGlossary.pdf

Orton JH (1913) The ciliary mechanisms on the gill and the mode of feeding in Amphioxus, ascidians and *Solenomya togata*. Journal of the Marine Biological Association of the United Kingdom 10: 19–49. https://doi.org/10.1017/S0025315400006706

Poss SG, Boschung HT (1996) Lancelets (Cephalochordata: Branchiostomatidae): how many species are valid? Israel Journal of Zoology 42: S-13/S-66. https://www.tandfonline.com/doi/abs/10.1080/00212210.1996.10688872

Putnam NH, Thomas B, David E, Ferrier DEK, Furlong FR, Hellsten U, Kawashima T, Rechavi RM, Shoguchi E, Terry A, Yu JS, Gutierrez BE, Dubchak I, Fernandez JG, Jeremy J, Gibson-Brown JJ, Grigoriev VI, Horton AC, Jong JP, Jurka J, Kapitonov VV, Kohara Y, Kuroki Y, Lindquist E, Lucas S, Osoegawa K, Pennachio LM, Salmov AA, Satou Y, Sauka-Spengler T, Schmutz J, Shin-I J, Toyoda A, Bronner-Fraser M, Fujiyama A, Holland LZ, Holland HWP, Sath N, Rokhsar D (2008) The amphioxus genome and the evolution of the chordate karyotype. Nature 453: 1064–1072. https://doi.org/10.1038/nature06967

Ruppert EE, Nash TR, Smith AJ (2000) The size range of suspended particles trapped and ingested by the filter-feeding lancelet *Branchiostoma floridae* (Cephalochordata: Acrania). Journal of the Marine Biological Association of the United Kingdom 80: 329–332. https://doi.org/10.1017/S0025315499001903

Sokal R, Rohlf J (1995) Biometry: the principles and practice of statistics in San Francisco: biological research. Blume Editions. Freeman W.H. and Company. San Francisco, California, 887 pp.

Stokes MD, Holland ND (1998) The lancelet. American Scientist 86: 552–560. https://doi.org/10.1511/1998.43.799

Strickland JDH, Parsons TR (1972) A practical handbook of seawater analysis, No. 167 (2nd edn). Fisheries Research Board of Canada, Ottawa, Ontario, 310 pp. https://epic.awi.de/id/eprint/39262/1/Strickland-Parsons_1972.pdf

Tchang S, Koo KC (1936) Description of a new variety of *Branchiostoma belcheri* Gray from Kiaochow Bay, Shantung, China. Contributions from the Institute of Zoology, National Academy of Peiping 3: 77–114.

Vargas JA (1987) The benthic community of an intertidal mud flat in the Gulf of Nicoya, Costa Rica: Description of the community. Revista de Biología Tropical 35: 229–316. https://revistas.ucr.ac.cr/index.php/rbt/article/view/24092/24218

Vargas JA, Dean HK (2010) On *Branchiostoma californiense* (Cephalochordata) from the Gulf of Nicoya estuary, Costa Rica. Revista de Biología Tropical 58: 1143–1148. https://doi.org/10.15517/rbt.v58i4.5399

Vergara M, Oliva ME, Riascos JM (2012). Population dynamics of the amphioxus *Branchiostoma elongatum* from northern Chile. Journal of the Marine Biological Association of the United Kingdom 92: 591–599. https://doi.org/10.1017/S0025315411000804

Weel PB van (1937) Die Ernahrungs biologie von *Amphioxus lanceolatus*. Pubblicazioni della Stazione Zoologica di Napoli 16: 221–272.

Zar JH (1999) Biostatistical analysis (Fourth Edition). Prentice-Hall, Englewood Cliffs, NJ 929 pp.

Zhang S, Li G, Zhu J, Su F (2001) Sex reversal of the female amphioxus *Branchiostoma belcheri tsingtauense* reared in the laboratory. Journal of the Marine Biological Association of the United Kingdom 81(1): 181–182. https://doi.org/10.1017/S0025315401003599

Zhang QJ, Zhong J, Fang SH, Wang YQ (2006) *Branchiostoma japonicum* and *B. belcheri* are distinct lancelets (Cephalochordata) in Xiamen waters in China. Zoological Science 23(6): 573–579. https://doi.org/10.2108/zsj.23.573

Supplementary material 1

Comparative morphometric variables of *Branchiostoma californiense*

Authors: Lucía Campos-Dávila, Claudia J. Pérez-Estrada, Ricardo Rodríguez-Estrella, Enrique Morales-Bojórquez, Fernando G. Brun-Murillo, Eduardo F. Balart

Data type: measurement

Explanation note: Differences between sex for each morphometric variable (t-Test).

Link: https://doi.org/10.3897/zookeys.873.33901.suppl1

ZooKeys 873: 133–153 (2019)
doi: 10.3897/zookeys.873.34630
http://zookeys.pensoft.net

RESEARCH ARTICLE

A peer-reviewed open-access journal
ZooKeys
Launched to accelerate biodiversity research

Description of two deep-water copepods of the genus *Leptotachidia* Becker from the northwestern Pacific (Harpacticoida, Pseudotachidiidae)

Jong Guk Kim[1], Ok Hwan Yu[1], Jimin Lee[1]

[1] *Marine Ecosystem Research Center, Korea Institute of Ocean Science & Technology, Busan 49111, Korea*

Corresponding author: *Jimin Lee* (leejm@kiost.ac.kr)

Academic editor: *Kai Horst George* | Received 18 March 2019 | Accepted 2 August 2019 | Published 29 August 2019

http://zoobank.org/8759E162-EDF3-4120-81A0-C2C62DD5E057

Citation: Kim JG, Yu OH, Lee J (2019) Description of two deep-water copepods of the genus *Leptotachidia* Becker from the northwestern Pacific (Harpacticoida, Pseudotachidiidae). ZooKeys 873: 133–153. https://doi.org/10.3897/zookeys.873.34630

Abstract

The monospecific genus *Leptotachidia* Becker, 1974 (Pseudotachidiidae Lang, 1936) was previously known only from the deep Atlantic. Female specimens of two unknown species of this genus were collected from abyssal sediments during an expedition to the northwestern Pacific on board research vessel *ISABU* (Korea Institute of Ocean Science and Technology) in November 2017. In this paper we describe the females of two new species, *L. senaria* **sp. nov.** and *L. apousia* **sp. nov.** The new species were attributed to the genus *Leptotachidia* by the combination of the five-segmented female antennule, presence of the Brodskaya organ on the distal antennulary segment, and the second exopodal segments of second to fourth legs without inner setae. An outstanding character of both Pacific species is the reduced armature of thoracic legs in contrast to the type species, *L. iberica* Becker, 1974. In addition, the setal armature of *L. senaria* **sp. nov.** and *L. apousia* **sp. nov.** is unique within the genus in that the female leg 5 of *L. senaria* **sp. nov.** has six elements instead of five; and the antennary exopod of *L. apousia* **sp. nov.** bears a single seta on the proximal segment instead of two. This is the first record of *Leptotachidia* from the Pacific. A key to all three species of *Leptotachidia* is provided.

Keywords

abyssal harpacticoids, biodiversity, Brodskaya organ, Danielsseniinae, deep-sea, *Paradanielssenia* group

Introduction

Despite their abundance and high biomass in deep-sea meiobenthic assemblages, little is known on the diversity of abyssal harpacticoids and more than 95% of them remain undescribed (Seifried 2004). Most taxonomic studies on abyssal harpacticoids have been performed in the Atlantic (Seifried 2004) and a limited number of papers are available on the deep-sea harpacticoid fauna from the Pacific (e.g. Itô 1982, 1983; Humes and Voight 1997; Huys and Conroy-Dalton 1997; Lee and Yoo 1998; Conroy-Dalton and Huys 1999, 2000; Lee and Huys 1999, 2000; López-González et al. 2000; Gollner et al. 2008; Back et al. 2010; Cho et al. 2016; Gómez and Díaz 2017; Vakati et al. 2017; Gómez 2018a-c; George and Schwabe 2019).

In the northwestern Pacific, 29 harpacticoid copepods belonging to the families Aegisthidae Giesbrecht, 1893, Ectinosomatidae Sars, 1903, Tegastidae Sars, 1904, Pseudotachidiidae Lang, 1936, Normanellidae Lang, 1944, Argestidae Por, 1986, and Parameiropsidae Corgosinho & Martínez Arbizu, 2010 have been reported from bathyal benthic and hyperbenthic habitats, such as trenches, cold seeps, and hydrothermal vents (Itô 1982, 1983; Lee and Yoo 1998; Lee and Huys 1999, 2000; Back et al. 2010; George and Schwabe 2019). Although the species of Pseudotachidiidae are important members in the deep-sea assemblage (Willen and Schulz 2007; Willen 2008, 2009; Kitahashi et al. 2012; George et al. 2014), three members of the genus *Pseudotachidius* Scott T., 1898 have been recorded only from the deep sea off Mindanao in the Philippines (Itô 1983).

Specimens of the family Pseudotachidiidae were collected from the deep sea in the northwestern Pacific during an oceanographic cruise on board RV *ISABU* of the Korea Institute of Ocean Science and Technology (KIOST). This paper deals with the second and third member of the genus *Leptotachidia* Becker, 1974. We provide the full description and detailed illustrations of the two new species. Additionally, a key to species of the genus is given. This is the first record of *Leptotachidia* from the Pacific.

Materials and methods

A KIOST cruise of the research vessel RV *ISABU* in November 2017 explored the deep-sea benthic fauna of the northwestern Pacific. As a result of this survey, two new species, *Leptotachidia senaria* sp. nov. and *L. apousia* sp. nov., were found from one sampling location (Fig. 1). Samples of abyssal sediments were taken using a multiple corer equipped with eight acrylic cores of 10 cm inner diameter. The upper layer (>5 cm) of each core was separately preserved in a 10 % formalin solution for quantitative or qualitative analyses. In the laboratory, meiofauna was removed from the sediments using the Ludox HS-40 method (Burgess 2001). Harpacticoids were sorted under a dissecting microscope (Leica M165 C, Germany). For taxonomic examination, the reverse slide method of Humes and Gooding (1964) was adopted. Animals were prepared in lactic acid on the reverse slide. All drawings of type specimens were made with

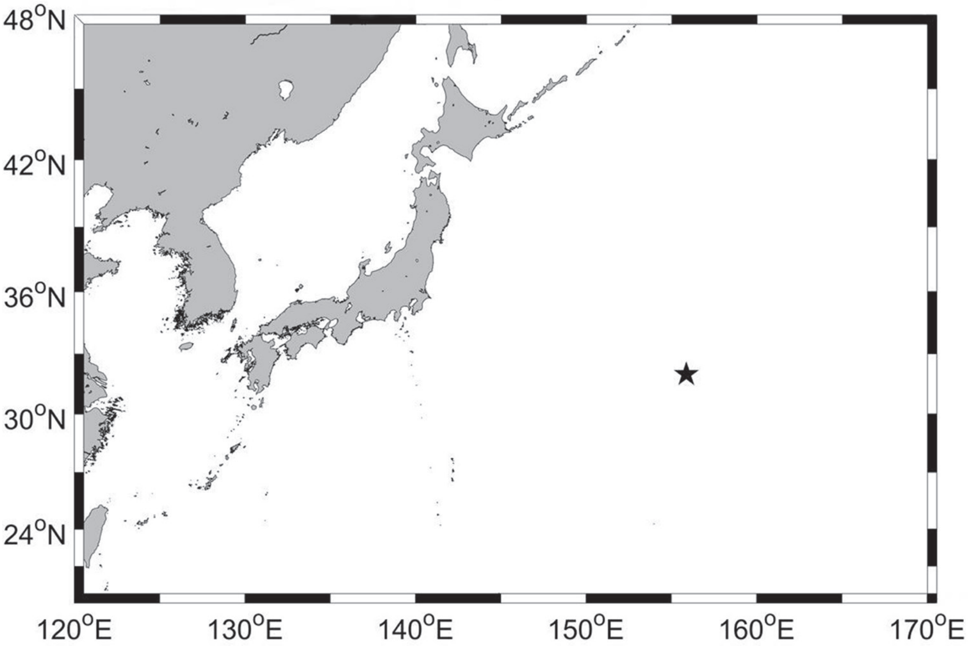

Figure 1. Map showing the sampling station.

the aid of a drawing tube under a differential interference contrast (DIC) microscope (Leica DM2500, Germany). The habitus of the material presented here was first depicted, and their appendages and urosome were drawn after dissection with tungsten needles. After examination, appendage and urosome were mounted in lactophenol on an H-S slide each (Shirayama et al. 1993). Type material was deposited in the Marine Biodiversity Institute of Korea (MABIK). We followed the descriptive terminology of Huys and Boxshall (1991). Scale bars in Figures 2–7 are given in μm.

Abbreviations used in text and figures are as follows:

ae	aesthetasc;
P1–P6	first to sixth thoracic legs;
Exp (enp)-1 (-2,-3)	proximal (middle, distal) segment of exopod (endopod).

Systematics

Family Pseudotachidiidae Lang, 1936
Subfamily Danielsseniinae Huys & Gee in Huys et al., 1996

Genus *Leptotachidia* Becker, 1974

Type species. *Leptotachidia iberica* Becker, 1974

***Leptotachidia senaria* sp. nov.**

http://zoobank.org/076F631E-0D2C-4F7B-B8C7-29F56BFD8C79
Figs 2–4

Type locality. Abyssal basin of the Northwest Pacific Ocean (31°58'42.9"N, 155°53'42.7"E), 5482 m depth (Fig. 1).

Material examined. Holotype: adult female dissected and mounted on 11 slides (cat. no. MABIK CR00246484) collected from the type locality on 1 November 2017.

Etymology. The specific epithet is derived from the Latin *senaria* meaning 'consisting of six' and refers to the female fifth leg with six elements in both rami, which is a unique characteristic within the genus *Leptotachidia*. It is in the nominative singular. Gender feminine.

Description of female. Total body length about 710 μm measured from anterior tip of rostrum to posterior margin of caudal rami in lateral view; greatest width about 106 μm measured at the middle of cephalothorax. Habitus (Fig. 2A, B) elongate, cylindrical, with weak constriction between prosome and urosome; urosome slightly narrower than prosome. Prosome (Fig. 2A, B) composed of cephalothorax and three free pedigerous somites. Cephalothorax bell-shaped, slightly longer than wide in dorsal view, as long as 21% of total body length; surface ornamented with several small and large pores, and short and long sensilla; hyaline frill smooth; arthrodial membrane of first pedigerous somite visible posteriorly. Metasome gradually narrowing posteriorly; second pedigerous somite with two, third and fourth pedigerous somites with a single mid-dorsal pore, all free pedigerous somites with paired large pores and sensilla dorsally and laterally, with two lateral rows of minute spinules; pleural areas of second and third pedigerous somites distinctly produced posteriorly, weak in fourth one; hyaline frills of second and third pedigerous somites well developed and weakly serrate, smooth in fourth one. Dorsal surface ridges on third and fourth pedigerous somites partly modified with internal chitinous ribs (Fig. 2A).

Urosome (Fig. 2A–C) gradually narrowing posteriorly, with large pores and paired sensilla dorsally and laterally; first urosomite with deeply incised and continuous hyaline frill, of genital double-somite interrupted ventrally by continuous row of strong spinules, of second abdominal somite interrupted ventrally by two short rows of strong spinules. Arthrodial membranes of all urosomites visible posteriorly. Original division between genital somite and third urosomite indicated by ventral and lateral subcuticular ridges, but dorsal aspect fused. Genital field with a transverse genital slit (Fig. 2G) covered by single plate with P6 represented by two vestigial setae and one row of minute spinules on both sides; copulatory pore located in a depression posterior to genital slit; seminal receptacles paired, placed inside genital aperture and connected with copulatory pore; one row of spinules and one large pore on ventrolateral surface; two pairs of large ventral pores on first abdominal somite. Second abdominal and penultimate somites with particular polygonal ribs along anteroventral surface (Fig.2C). Penultimate somite with pseudoperculum, the latter with long spinules; posterior margin

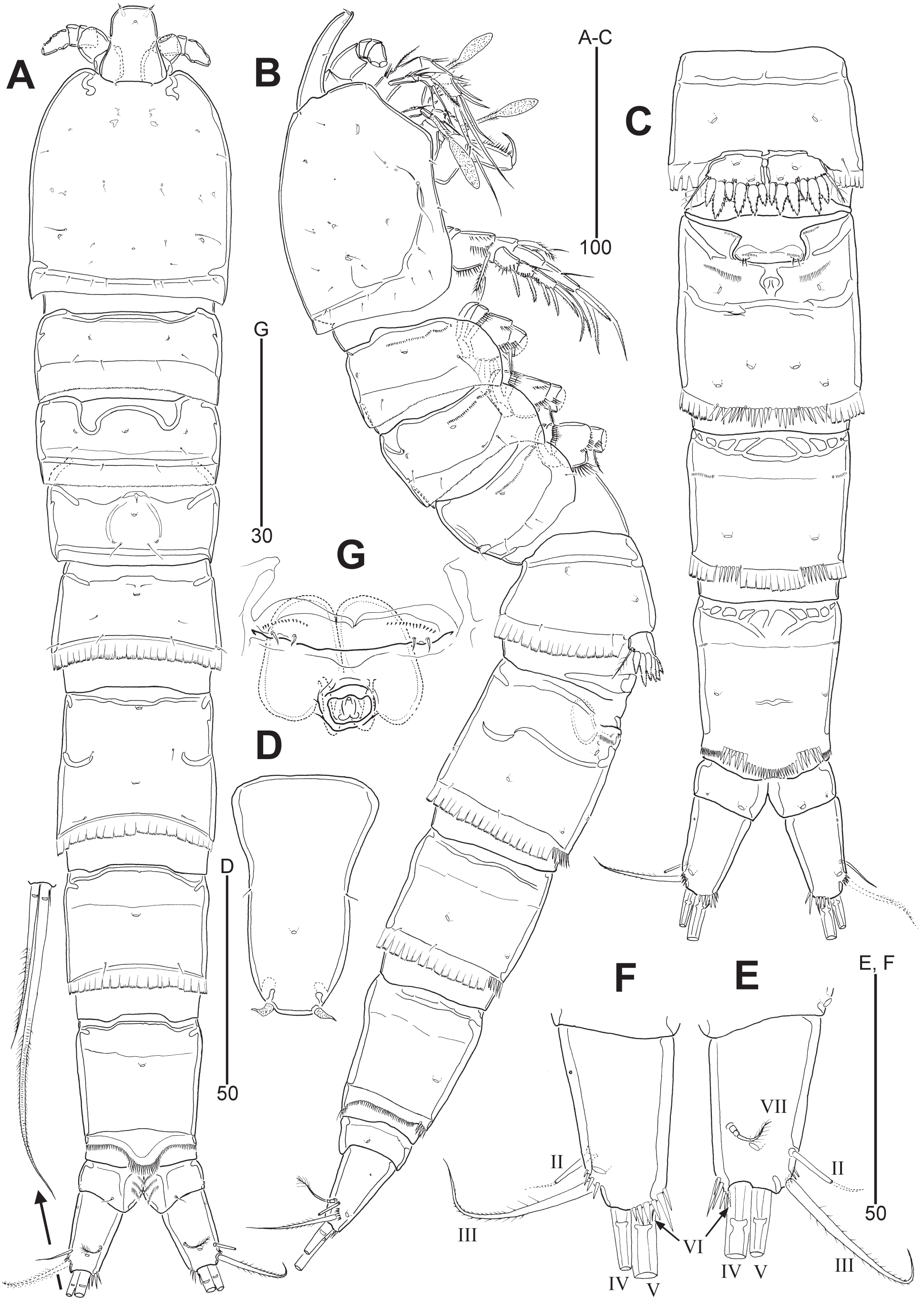

Figure 2. *Leptotachidia senaria* sp. nov., female **A** habitus, dorsal **B** habitus, lateral **C** urosome, ventral **D** rostrum, dorsal **E** caudal ramus, dorsal **F** caudal ramus, ventral **G** genital field, ventral.

finely dentate dorsally and laterally, coarsely dentate ventrally, with two rows of stout spinules ventrolaterally. Anal somite short, with one pair of sensilla dorsally, one lateral pore, and one small and one large pores ventrally; dorsal surface depressed medially forming anal opening, with three rows of setules on inner margin.

Caudal rami (Fig. 2A–C, E, F) divergent, slightly tapering towards posterior end, about 1.7 times as long as greatest basal width, with one dorsal and one ventrolateral large pore; rows of spinules present near base of setae III and V, and on inner distal corner; a small pore located at proximal forth of ventrolateral surface; with six caudal setae: seta I absent; seta II bare, small, at distal forth dorsolaterally; seta III pinnate, about three times as long as seta II, and inserted in lateral margin subdistally; principal setae IV and V well developed, distally pinnate and rat tail-like, seta V about twice as long as seta IV; seta VI minute, inserted at inner distal corner; seta VII tri-articulate at base, arising from distal third of inner-dorsal surface, with fine hairs distally.

Rostrum (Fig. 2D) large, bell-shaped, with one median pore, one pair of medial sensilla, and one pair of subdistal sensilla modified into aesthetascs-like structures.

Antennule (Fig. 3A) short, five-segmented; segment I with one long distal pinnate seta and two rows of stout outer spinules; segment II largest, about 1.2 times as long as wide, with one plumose and eight pinnate setae; segment III with eight pinnate setae; segment IV smallest, with three long bare and three pinnate setae, and one aesthetasc fused basally to adjacent one long bare seta; segment V with one pinnate, six spinulose and seven bare setae, one aesthetasc fused basally to adjacent two spinulose setae, and one densely opaque bulbous appendage (Brodskaya organ). Segment V with apical acrothek. Armature formula as follows: 1-[1], 2-[9], 3-[8], 4-[5 + (ae + 1)], 5-[12 + Brodskaya organ + acrothek].

Antenna (Fig. 3B). Coxa distinct, unornamented. Allobasis with one long pinnate seta and one group of long spinules on abexopodal margin. Exopod three-segmented; proximal segment elongate, 4.5 times as long as wide, with one bipinnate and one minute bare setae; middle segment small, with one spinulose seta; distal segment with two spinulose setae and one seta with distal part uniserrate. Free endopod with two rows of stout spinules laterally; lateral armature comprising one bare, one geniculate and two bipinnate setae; distal armature composed of two bipinnate and four geniculate setae, one of which bears spinules medially; distal margin with one row of stout spinules and one subdistal surface frill.

Mandible (Fig. 3C). Coxa with one medial protuberance ventrally and one row of setules near base of palp; gnathobase with one large uni-cuspidate and four multi-cuspidate teeth, and one unipinnate ventral seta. Palp uniramus, two-segmented; basis elongate, with three rows of spinules and one plumose seta; endopod small, one-segmented, with one small unipinnate seta and a claviform aesthetasc with peduncle partially bipinnate distally, and one rudimentary seta (indicated by arrowhead in Fig. 3C) on lateral margin.

Maxillule (Fig. 4A). Praecoxa with two rows of outer spinules; arthrite with nine distal elements and two surface setae anteriorly. Coxal endite with one anterior row of spinules, one lateral row of setules, and one bare, one plumose and three unispinulose

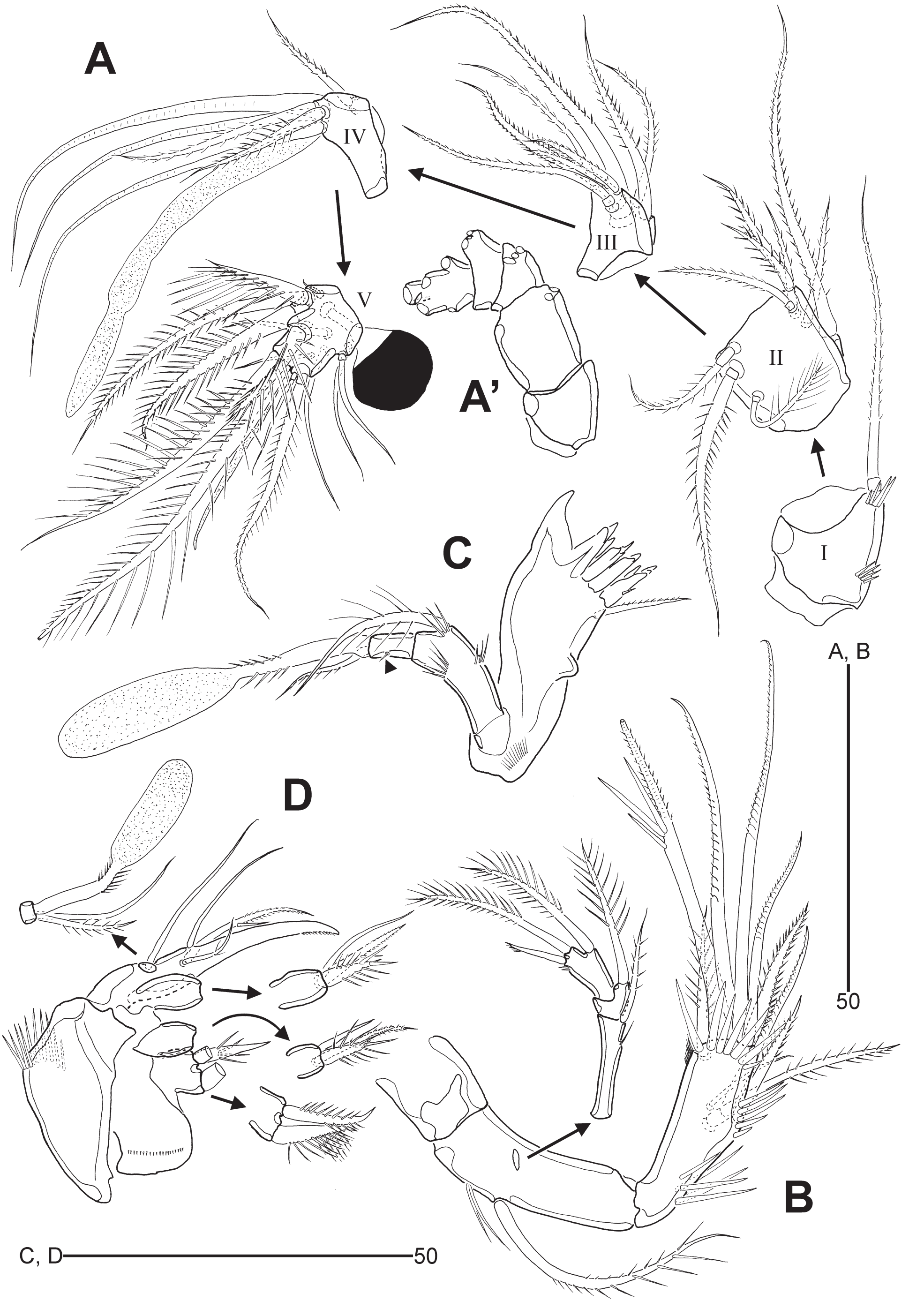

Figure 3. *Leptotachidia senaria* sp. nov., female **A** antennule **B** antenna **C** mandible (arrowhead indicates a rudimental lateral seta) **D** maxilla.

distal setae. Basis with two endites; distal endite largest, with one bare, one plumose and one pinnate setae, and a claviform aesthetasc with peduncle partially bipinnate distally, and one row of anterior spinules; subdistal endite with one long and one small bipinnate setae. Exopod broad, one-segmented, with three spinulose apical setae and one row of inner setules. Endopod one-segmented, with three bipinnate setae and one row of outer spinules.

Maxilla (Fig. 3D). Syncoxa with one transverse row of stout outer spinules and one row of minute surface spinules; with three endites: proximal endite bilobate, with one stout spinulose seta on proximal lobe, and one bipinnate and one spinulose setae on distal lobe; medial and distal endites with one bare, one bipinnate and one spinulose setae each. Allobasis with one long bare seta near base of endopod, drawn into a weakly pinnate claw bearing one bare seta, one pinnate element with an accessory spinule, and one weakly plumose seta. Endopod small, one-segmented, with one bare and one bipinnate setae, and a claviform aesthetasc with peduncle partially bipinnate.

Maxilliped (Fig. 4B). Praecoxa small, unornamented. Coxa elongate, with two pinnate geniculate setae subdistally, with two inner rows of stout spinules and one row of minute spinules proximally. Basis elongate, ovoid, with one row of stout inner spinules and one subdistal setulose seta. Endopod one-segmented, represented by a dentate claw bearing one vestigial accessory seta.

P1 (Fig. 4C). Praecoxa small, with one row of minute spinules distally. Intercoxal sclerite wide, slightly arched and unornamented. Coxa large, medially with three rows of minute spinules and one row of long spinules anteriorly; distally with one row of minute spinules and one row of stout spinules anteriorly; with two rows of spinules near outer distal corner; with one row of posterior spinules. Basis with one row of inner setules; with one row of stout spinules on distal pedestal of endopod; with one large pore near outer seta anteriorly; outer seta long, spinulose and arising from peduncle with three minute spinules; inner spine stout, spinulose and arising from peduncle bearing one row of spinules. Exopod three-segmented, reaching middle of enp-2; each segment with strong outer and distal spinules; exp-1 with one bipinnate outer spine; exp-2 with one bipinnate outer spine and one plumose inner seta; exp-3 with three bipinnate outer spines, and two rat tail-like setae with outer spinules and inner setules. Endopod longer than exopod, two-segmented; each segment with outer and distal spinules; enp-1 broad, with one plumose inner seta, with one large anterior pore, one row of posterior spinules, and one row of inner distal setules; enp-2 elongate, about 2.7 times as long as wide, with one pinnate distal outer spine, and two setae with pinnate outer and setulose inner margins.

P2–P4 (Fig. 4D–F). Praecoxa small, as wide as coxa, with one row of stout distal spinules. Intercoxal sclerite developed, concave distally, with two distal pointed projections. Coxa broad, with three rows of minute medial spinules, one row of longer spinules and one large pore anteriorly; one row of stout outer distal spinules; with one row of outer spinules and one row of distal spinules posteriorly; with one row of stout (P2) or minute (P3–P4) inner distal spinules anteriorly. Basis with one large anterior pore, one row of distal spinules on pedestal of endopod, and one row of spinules near base of outer seta; the latter unipinnate (P2) or uniplumose (P3–P4); outer setae of P3–P4

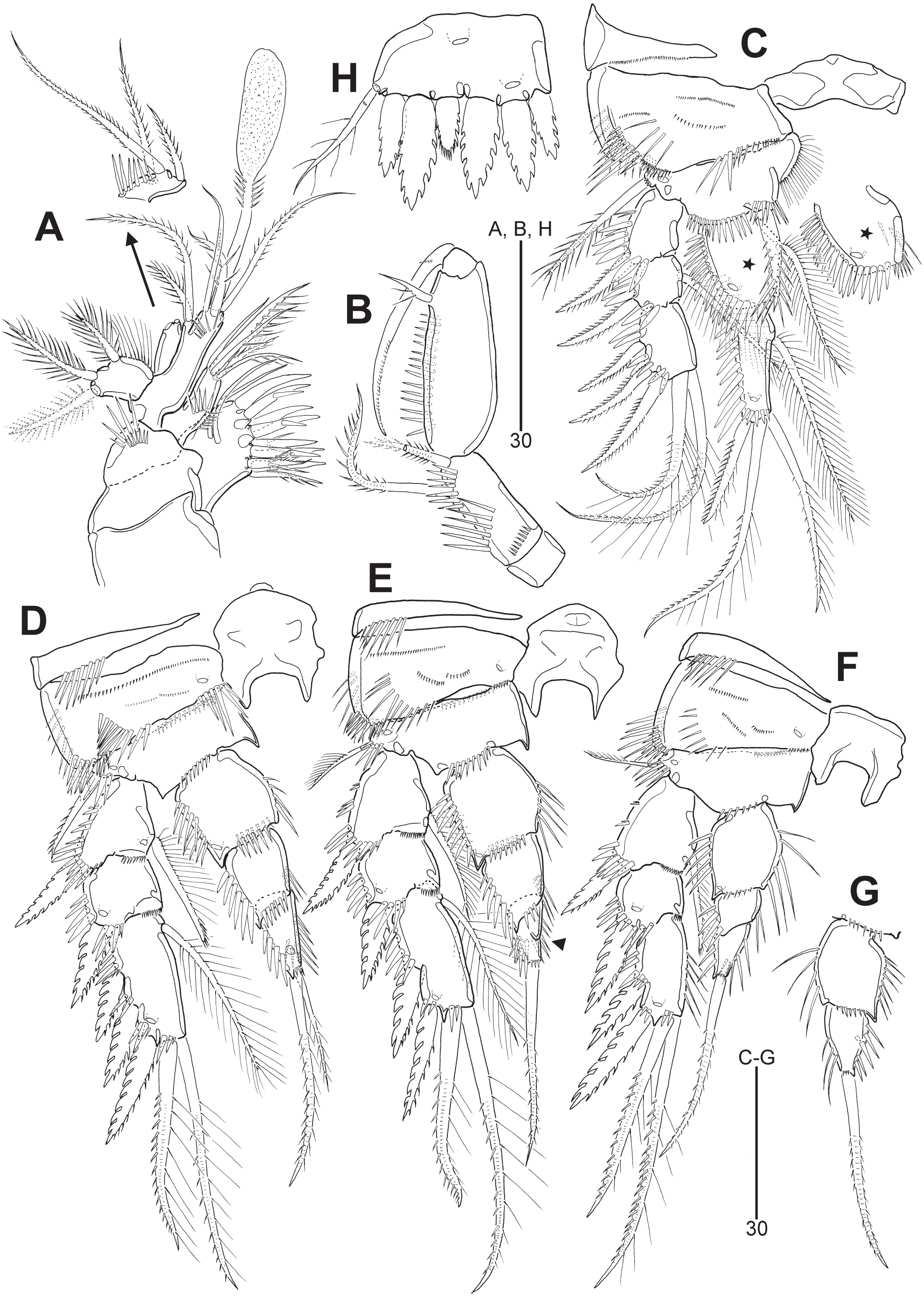

Figure 4. *Leptotachidia senaria* sp. nov., female **A** maxillule **B** maxilliped **C** P1, anterior **D** P2, anterior **E** P3, anterior (arrowhead showing the modified and dented inner margin) **F** P4, anterior **G** abnormality of P4 endopod, anterior **H** P5, anterior.

with internal fracture plane; inner distal corner produced. Exopod slightly longer than endopod, three-segmented; each segment with outer and distal spinules; exp-1 and exp-2 with inner distal frills; P4 exp-3 with one row of inner setules; anterior pores on all exopodal segments of P2, and exp-2 and exp-3 of P3–P4; exp-1 with one serrate outer spine and one uniplumose inner seta; exp-2 with one serrate outer spine; exp-3 with two (P3–P4) or three (P2) serrate outer spines, two rat tail-like distal setae with outer marine spinulose, and inner margin setulose, and with one plumose inner proximal seta (P2–P3), or without inner armature (P4). Endopod tapering distally, three-segmented; each segmented with outer, inner and distal spinules; with distal posterior spinules in P2–P3 enp-1; with anterior pores on P2–P3 enp-1 and P2 enp-3; all endopodal segments without inner element; P2 enp-3 with one pinnate, rat tail-like and one plumose setae; P3–P4 enp-3 with one pinnate, rat tail-like seta; inner margin of P3 enp-3 modified and dented (indicated by arrowhead in Fig. 4E). P1–P4 armature formulae:

	Exopod	Endopod
P1	0.1.023	1.121
P2	1.0.123	0.0.020
P3	1.0.122	0.0.010
P4	1.0.022	0.0.010

P5 (Figs 2C, 4H). Small sclerite present between both members. Exopod and baseoendopod fused, forming a single plate, with five coarsely serrate and one finely serrate distal spines; with two large anterior pores; outer seta plumose, arising from small peduncle and with internal fracture plane.

Male. Unknown.

Variability. Left P4 of the female holotype normal, right endopod of P4 with two segments (Fig. 4G).

Leptotachidia apousia **sp. nov.**

http://zoobank.org/D254F962-9EB5-4A3B-98F5-6E04BA0F295A
Figs 5–7

Type locality. Abyssal basin of the Northwest Pacific Ocean (31°58'42.9"N, 155°53'42.7"E), 5482 m depth (Fig. 1).

Material examined. Holotype (adult female) dissected and mounted on 11 slides (cat. no. MABIK CR00246485) collected from the type locality on 1 November 2017.

Etymology. The species name is derived from the Greek απουσία, *apousia*, meaning absence, lacking, and alludes to the absence of an inner seta in P3 enp-3. It is in the nominative singular. Gender feminine.

Description of female. Total body length about 608 μm, greatest width about 99 μm measured at the middle of cephalothorax. Habitus (Fig. 5A, B) slightly damaged (thoracic legs detached), as in *L. senaria* sp. nov., but slightly narrower; ornamentation of somites slightly different from *L. senaria* sp. nov. in number and position of both sensilla and pores.

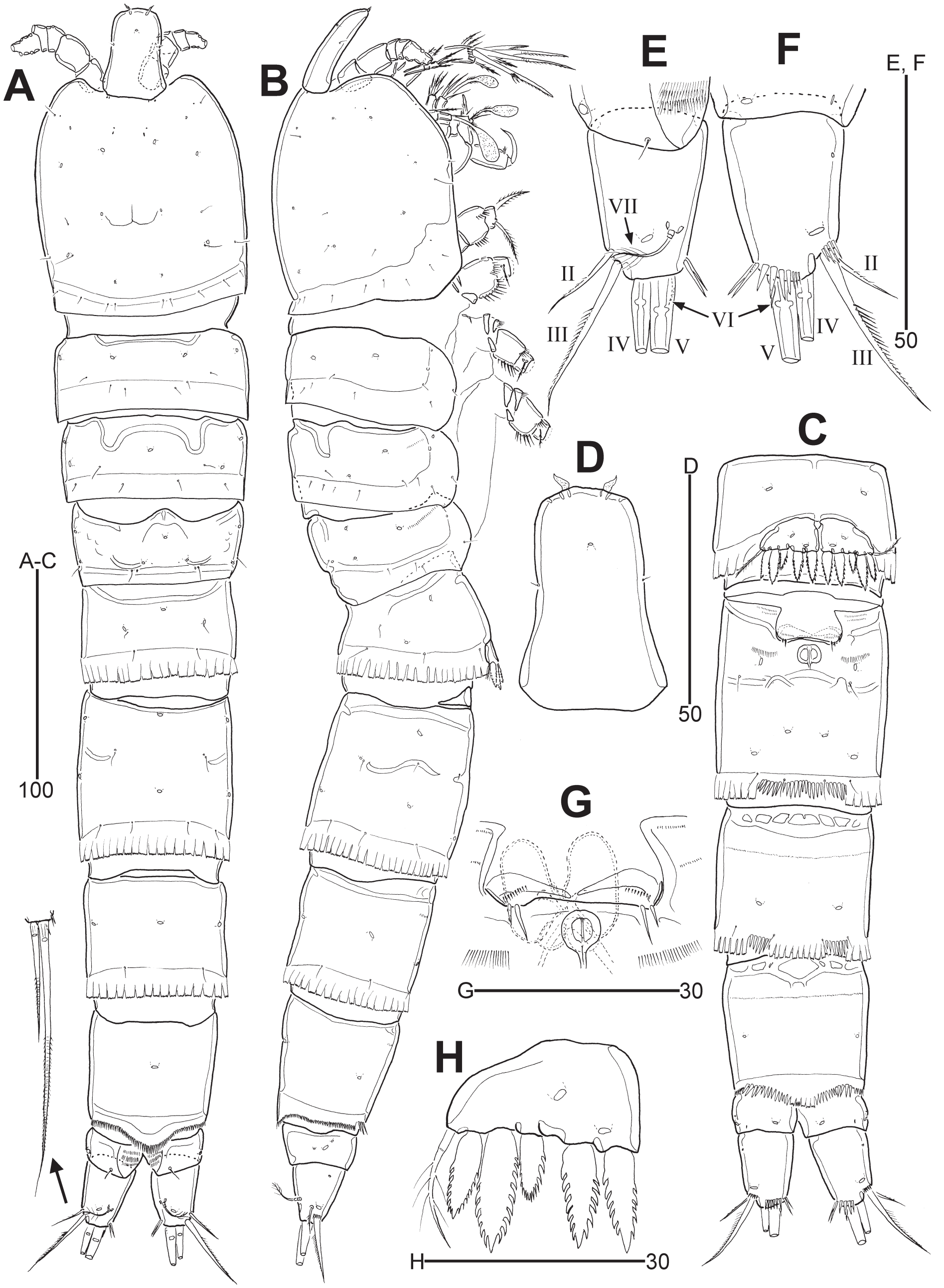

Figure 5. *Leptotachidia apousia* sp. nov., female **A** habitus, dorsal **B** habitus, lateral **C** urosome, ventral **D** rostrum, dorsal **E** caudal ramus, dorsal **F** caudal ramus, ventral **G** genital field, ventral **H** P5, anterior.

Cephalothorax (Fig. 5A, B) about 1.2 times as long as wide in dorsal view, as long as 18 % of total body length. Pleural areas of free pedigerous somites more weakly developed than in *L. senaria* sp. nov. Hyaline frills of second to fourth pedigerous somites smooth.

Urosome (Fig. 5A–C) about 1.1 times as long as prosome. With deeply incised hyaline frills as in *L. senaria* sp. nov. except for penultimate somite with weakly incised hyaline frill ventromedially. Genital double-somite divided by lateral and ventral ridges, but fused dorsally and ventrolaterally. Genital slit (Fig. 5G) covered by single plate with two minute setae, inner about twice as long as outer, and one row of minute spinules on both sides; copulatory pore posterior to genital slit; seminal receptacles smaller than in *L. senaria* sp. nov. Pseudoperculum (Fig. 5A) on penultimate somite slightly wider than in *L. senaria* sp. nov. Anal somite small, with one pair of sensilla, one large and two small lateral pores, and one large and one small ventral pores; anal opening fringed with three pairs of setular rows.

Caudal rami (Fig. 5A–C, E, F) slightly shorter than in *L. senaria* sp. nov., about 1.4 times as long as greatest width, with one large pore anteriorly and posteriorly; ventral spinule rows present near base of seta III and seta V, and closed to inner distal corner; armature as in *L. senaria* sp. nov. except for seta V about 2.8 times as long as seta IV.

Rostrum (Fig. 5D) as in *L. senaria* sp. nov. except for a pair of aesthetasc-like sensilla on distal margin closer to each other than in *L. senaria* sp. nov.

Antennule (Fig. 6A) as in *L. senaria* sp. nov. except for arrangement of elements on segments II, IV and V; segment II 1.1 times as long as wide, with one plumose, one bare and seven pinnate setae; segment IV with two pinnate and four weakly pinnate setae, and one aesthetasc fused to adjacent long weakly pinnate seta; segment V with one weakly bipinnate, two plumose, five spinulose and six bare setae; with distal acrothek composed of one aesthetasc and adjacent two spinulose setae, and one densely opaque bulbous appendage (Brodskaya organ). Armature formula as follows: 1-[1], 2-[9], 3-[8], 4-[5 + (ae + 1)], 5-[12 + Brodskaya organ + acrothek].

Antenna (Fig. 6B) as in *L. senaria* sp. nov. except for exp-1 with only one plumose seta.

Mandible (Fig. 6C) as in *L. senaria* sp. nov. except for absence of a rudimentary seta on lateral margin.

Maxillule (Fig. 6D), maxilla (Fig. 6E), and maxilliped (Fig. 6F) as in *L. senaria* sp. nov.

General shape of P1–P4 (Fig. 7A–D) as in *L. senaria* sp. nov. except for setal armatures of P3 exp-3 and P2–P4 enp-3; P3 exp-3 (Fig. 7C) with three outer spines; P2 enp-3 (Fig. 7B) with one small bipinnate outer spine, one long apical seta with outer spinules and inner setules, and one small plumose apical seta; P3–P4 enp-3 (Fig. 7C–D) with one small pinnate outer spine and one long bipinnate apical seta; inner margin of P3 enp-3 modified and dented as in *L. senaria* sp. nov. (indicated by arrowhead in Fig. 7C).

P1–P4 armature formulae:

	Exopod	**Endopod**
P1	0.1.023	1.121
P2	1.0.123	0.0.111
P3	1.0.123	0.0.011
P4	1.0.022	0.0.011

General structure of P5 (Fig. 5H) as in *L. senaria* sp. nov. except for setal armature; distal margin with one finely serrate and four coarsely serrate spines.

Male. Unknown.

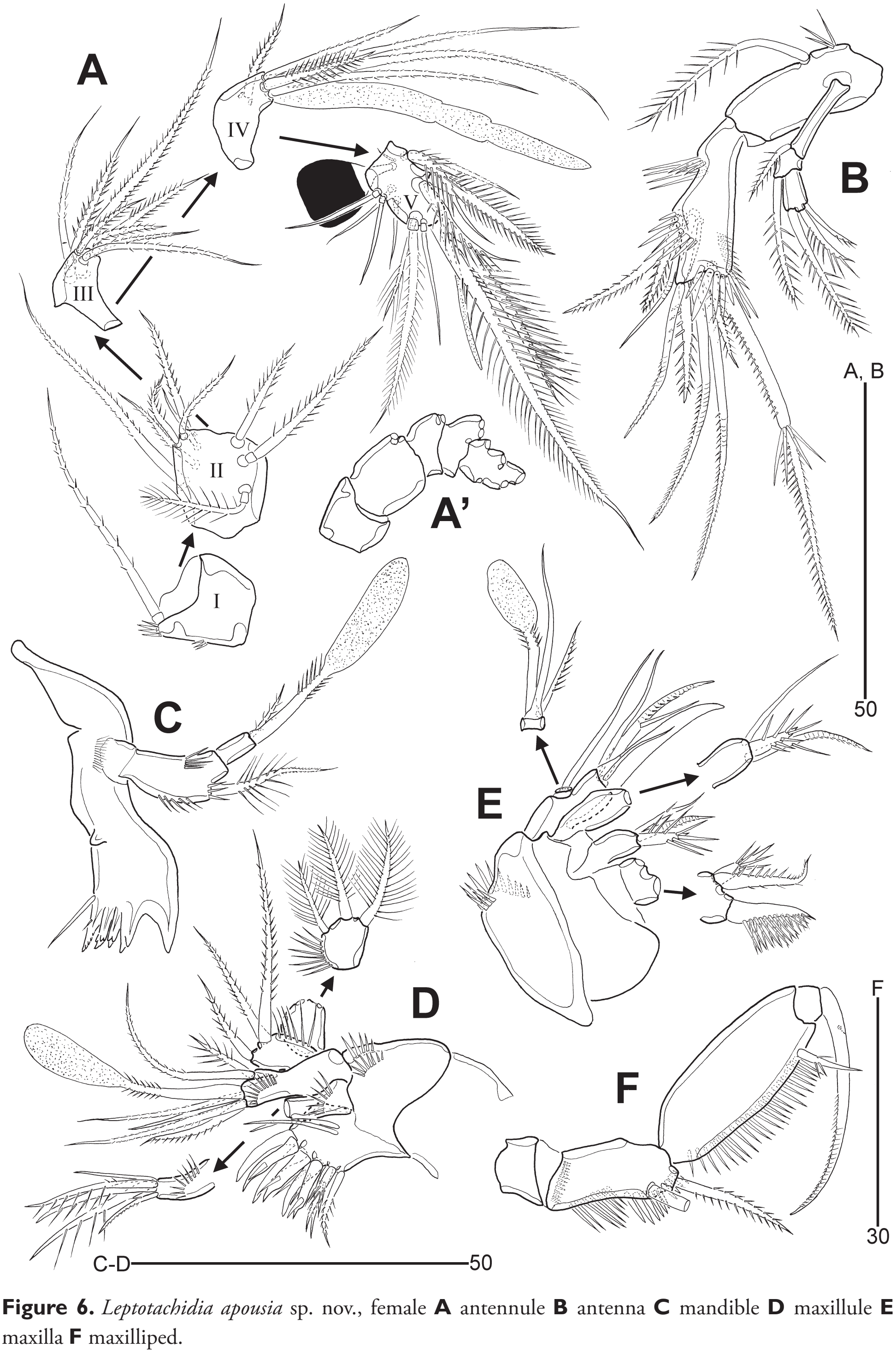

Figure 6. *Leptotachidia apousia* sp. nov., female **A** antennule **B** antenna **C** mandible **D** maxillule **E** maxilla **F** maxilliped.

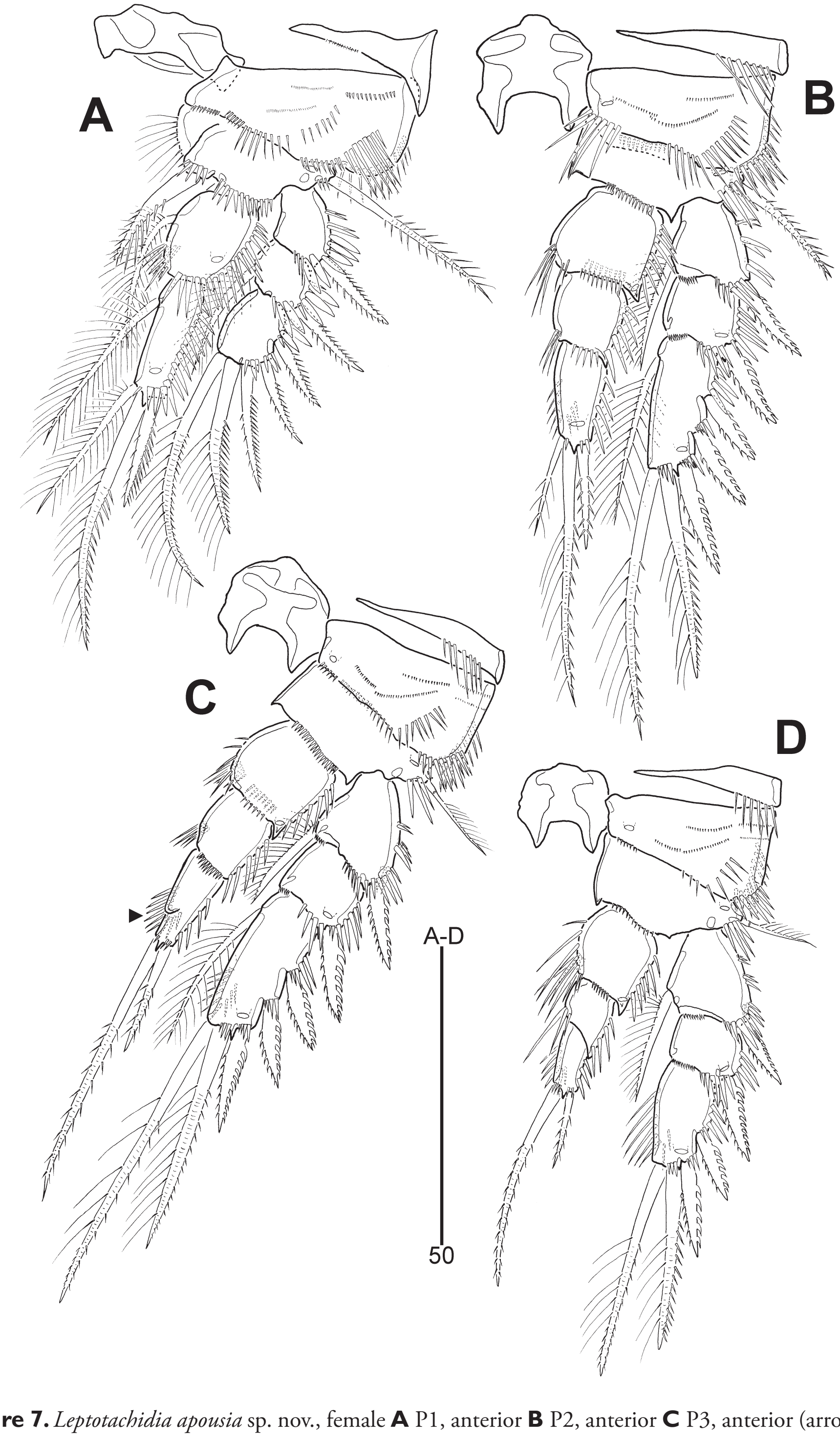

Figure 7. *Leptotachidia apousia* sp. nov., female **A** P1, anterior **B** P2, anterior **C** P3, anterior (arrowhead showing the modified and dented inner margin) **D** P4, anterior.

Discussion

The series of papers by Gee and Huys (1990, 1991, 1994) and Huys and Gee (1992, 1993, 1996a, b) contributed to defining the phylogenetic relationships among the danielsseniin genera and to establishing several new genera of the family Paranannopidae Por, 1986 (= Danielsseniinae Huys and Gee in Huys et al. 1996; *cf.* Huys 2009). The presence of aesthetascs on the mouthparts, which character is unique within other harpacticoid families and its position is homologous, is a significant synapomorphy for a core of genera, *Jonesiella* Brady, 1880, *Paradanielssenia* Soyer, 1970, *Leptotachidia* Becker, 1974, *Micropsammis* Gee & Huys, 1991, *Telopsammis* Gee & Huys, 1991, *Peltisenia* Huys & Gee, 1996, *Sentiropsis* Huys & Gee, 1996, and *Nyxis* Willen, 2009 (Gee and Huys 1991; Willen 2005, 2008, 2009; Willen and Schulz 2007; Kim et al. 2011).

The danielsseniin *Paradanielssenia* group composed of *Paradanielssenia*, *Leptotachidia*, *Micropsammis* and *Telopsammis* shares the aesthetascs on the mouthparts modified into claviform stuructures (Gee and Huys 1991; Willen 2008, 2009). Willen (2008, 2009) suggested that the genera of the *Paradanielssenia* group are more derived than the other congeners given four autapomorphies: (1) the loss of the mandibular exopod; (2) reduced setation of the mandibular basis (less than three setae); (3) the presence of a rigid apophysis on the male P2 enp-3 instead of an outer seta, except for *Leptotachidia*; and (4) the comparatively shorter innermost seta on the female P5 baseoendopod.

Three genera, *Leptotachidia*, *Micropsammis* and *Telopsammis*, seem to be more derived than *Paradanielssenia* and share the following synapomorphies: (1) presence of deeply incised hyaline frills on urosomites; (2) presence of an elongate mandibular basis with one seta; (3) presence of rat tail-like terminal setae on both rami of P1; (4) armature complement of P2–P4 reduced, for example the presence of only two outer spines on P4 exp-3, the absence of inner setae on P2 endopod, P3 enp-1 and enp-3, and P4 enp-3; and (5) fusion of both rami of P5 in both sexes (Gee and Huys 1991; Mielke 1997; Willen 2008). The presence of three basal setae in mandible is a primitive character and indicates that *Paradanielssenia* is situated in a basal position within this lineage.

The genus *Leptotachidia* is closely related to *Telopsammis* (Gee and Huys 1991; Huys 2009), although there is a marked difference in the sexual dimorphism of the male P2 endopod between these two genera (the outer element of distal segment is developed into an apophysis in the male of the latter genus except the absence of this modification in *T. pelobionta* Kornev & Chertoprud, 2008) (Mielke 1975, 1997; Gee and Huys 1991; Kornev and Chertoprud 2008). The sister group relationship between *Leptotachidia* and *Telopsammis* is demonstrated by five synapomorphies identified by Gee and Huys (1991) and Huys (2009) including the presence of two rat tail-like apical setae on P1 enp-2, the absence of an inner seta on P3 enp-2 and P4 exp-3, the completely fused female P5 without a distinguishable division between the exopod and baseoendopodal lobe, and the presence of two setae on the male P6. The presence of only two setae on the male P6 is an advanced state compared with the presence of three setae in more primitive congeners bearing aesthetascs on the mouthparts (*Paradanielssenia*, *Peltisenia*, *Sentiropsis*, *Jonesiella* as well as *Micropsammis*). Additionally, the genera

Leptotachidia and *Telopsammis* both possess the following features: (1) both members of female P5 are completely separated, with a small sclerite between them; and (2) the penultimate somite has no deeply incised frills. *Leptotachidia* can be considered the most advanced genus because of the following features: (1) presence of the Brodskaya organ on the terminal antennular segment; the Brodskaya organ is a densely opaque bulbous appendage that is a sensory organ for a bathyal existence; (2) female antennule five-segmented instead of six; (3) loss of sexual dimorphism in the male P2; and (4) the absence of an inner seta on P2–P4 exp-2 (Gee and Huys 1991).

Becker (1974) erected the genus *Leptotachidia* for *L. iberica* Becker, 1974, which was found at 3800 m depth off the Atlantic coast of Portugal. Upon careful re-examination of the type material, Gee and Huys (1991) identified some discrepancies between the original description and type specimens, and provided an amended diagnosis of the genus (Gee and Huys 1991: 1136). The two new species from the northwestern Pacific were placed into *Leptotachidia* based on Gee and Huys (1991) and on the autapomorphies of the genus mentioned above, except for rostrum and genital double-somite (see below). However, we were unable to confirm the male condition due to the lack of male specimens although the sexual dimorphic character could provide a significant evidence for the phylogenetic relationships among the danielsseniin genera (e.g. Gee and Huys 1990, 1991, 1994; Huys and Gee 1992, 1993, 1996a, b).

The most important character to discriminate both new Pacific species from the type species *L. iberica* is the setal armature of the thoracic legs (Table 1): (1) *L. senaria* sp. nov. possesses two elements on P2 enp-3 instead of three as in *L. iberica*, (2) P3–P4 enp-3 possesses a single apical element instead of three and two, respectively, as in *L. iberica*, (3) P3 exp-3 possesses two outer spines instead of three as in *L. iberica*, and (4) the female P5 possesses six elements instead of five as in *L. iberica*. In contrast, the reduced elements in P3 enp-3 of *L. apousia* sp. nov. possesses two setae only. In addition, the armature of the antennary exopod of *L. apousia* sp. nov. is unique by having a single seta on the proximal segment, whereas both *L. iberica* and *L. senaria* sp. nov. have two elements on the corresponding segment.

The two new species described here can be separated from *L. iberica* by (1) the presence of two pairs of sensilla on the rostrum, of which the distal ones modified into aesthetasc in the new species, but with one pair of normal sensilla on the rostrum of *L. iberica*, (2) peduncle of the claviform aesthetasc of the mouthparts with spinules in the new species, but naked in *L. iberica*, (3) accessory seta on the maxillipedal claw rudimentary in the new species, but clearly visible and well developed in *L. iberica*, and (4) both halves of genital double-somite separated by surface ridges laterally and ventrally, but completely fused in *L. iberica*. However, the two new species are clearly distinguishable from each other by the setal armature of the antennary exopod and thoracic legs, the structure and shape of the genital double-somite (ventral and lateral surface ridges are clearly separate in *L. apousia* sp. nov., but they are continued in *L. senaria* sp. nov.), the lateral armature of the mandibular endopod (with rudimentary seta in *L. senaria* sp. nov., but unarmed in *L. apousia* sp. nov.), and the length/width-ratio of the caudal ramus (about 1.7 times in *L. senaria* sp. nov. vs. 1.4 in *L. apousia* sp. nov.).

Table 1. Comparison of morphological characters among *Leptotachidia* species based on the female.

		L. iberica	***L. senaria* sp. nov.**	***L. apousia* sp. nov.**
No. of sensilla on Ro		1 pair	2 pairs	2 pairs
Sensilla form of distal margin on Ro		sensilla-like	ae-like	ae-like
No. of setae on A2 exp-1		2	2	1
Lateral seta on Md enp		delicate	rudimentary	absent
Claviform ae on Md, Mxl, and Mxa		naked	with spinules	with spinules
Seta on claw of Mxp enp		delicate	rudimentary	rudimentary
Setal armature	P2 enp-3	021	020	021
	P3 exp-3	123	122	123
	P3 enp-3	021	010	011
	P4 enp-3	011	010	011
	P5	5	6	5
Genital double-somite		fused completely	divided by ventral and lateral ridges	divided by ventral and lateral ridges (each separate)
CR L/W ratio		1.2	1.7	1.4
Reference		Becker 1974; Gee and Huys 1991	present study	present study

Abbreviation: A2, antenna; ae, aesthetasc; CR, caudal ramus; enp, endopod; L/W ratio, length to width ratio; Md, mandible; Mxa, maxilla; Mxl, maxillule; Mxp, maxilliped; Ro, rostrum

Members of the family Pseudotachidiidae are important component of harpacticoid assemblages in deep-sea habitats (Seifried 2004; Willen and Schulz 2007; Willen 2008, 2009; Kitahashi et al. 2012; George et al. 2014). Within the group of pseudotachidiids bearing aesthetascs on the mouthparts, only two species, *L. iberica* and *Nyxis rostrocularis* Willen, 2009, have been recorded from abyssal habitats (Becker 1974; Willen 2009). Many abyssal harpacticoids show extraordinary adaptations to deep-sea habitats (Seifried and Schminke 2003; Mercado-Salas et al. 2019), one of which is the Brodskaya organ which serves as a sensory structure on the antennule in both sexes, as in *L. iberica* and in the deep-sea *Cerviniopsis obtusirostris* Brotzkaja, 1963 (Aegisthidae) (Por 1969; Gee and Huys 1991). However, Gee and Huys (1991) suggested that the Brodskaya organ of *L. iberica* and *C. obtusirostris* is not homologous based on the morphological or phylogenetic discrepancies. Within *Cerviniopsis* Sars, 1903, only *C. obtusirostris* possesses this organ, suggesting that the presence of this structure in Pseudotachidiidae and Aegisthidae is probably a result of convergent evolution. The presence of the Brodskaya organ in the antennule is an important autapomorphy supporting the monophyly of *Leptotachidia* within the family, including two new *Leptotachidia* species from the Pacific deep sea. We also identified an additional sensory structure in both *L. senaria* sp. nov. and *L. apousia* sp. nov., that is, a pair of distal sensilla on the rostrum modified into aesthetascs (Figs 2C, 6C). Although Gee and Huys (1991) depicted the corresponding structures of *L. iberica* as nominal sensilla, we believe that this modification in both Pacific species is also a result of adaptation to the deep sea.

Despite the high abundance and species diversity of abyssal harpacticoids, few taxonomical studies are available (Seifried 2004). Our knowledge on the distribution of the genus *Leptotachidia* was limited to the deep sea of the Atlantic Ocean (Becker 1974; Gee and Huys 1991). The record of the two new species co-occurring in the same subsample presented herein expands the distribution range of the genus to the northwestern Pacific in abyssal sediments at 5482 m depth suggesting that *Leptotachidia* species display a wider geographical distribution than previously thought, and that the scant record of the genus is due to a lack of sampling and to the lack of taxonomical studies in abyssal habitats.

Key to species of the genus *Leptotachidia* Becker, 1974

1 P3 exp-3 with three outer spines; female P5 with five elements in all **2**
– P3 exp-3 with two outer spines; female P5 with six elements in all .... ***L. senaria* sp. nov.**
2 Proximal segment of the antennary exopod with two setae; P3 enp-3 with three elements.. ***L. iberica* Becker, 1974**
– Proximal segment of the antennary exopod with one seta; P3 enp-3 with two elements.. ***L. apousia* sp. nov.**

Acknowledgements

We thank the captain and crew members of the RV *ISABU* for help and support during the cruises. We are also grateful to two reviewers for their critical and helpful comments that greatly improved the manuscript. This research was supported by the research program of Korea Institute of Ocean Science & Technology with contract No.PE99772 and PE99724. This work was also conducted with the support offered through a grant from the National Research Foundation of Korea (NRF) funded by the Ministry of Education, Science and Technology (2018R1A6A3A01012703) to J. G. Kim.

References

Back J, Huys R, Lee W (2010) A new species of the genus *Tegastes* (Copepoda: Harpacticoida: Tegastidae) from hydrothermal vents in the Okinawa Trough. Zoological Science 27: 678–688. https://doi.org/10.2108/zsj.27.678

Becker KH (1974) Eidonomie und Taxonomie abyssaler Harpacticoidea (Crustacea, Copepoda). Teil I. Cerviniidae – Ameiridae. Meteor Forschungs-Ergebnisse 18D: 1–28.

Burgess R (2001) An improved protocol for separating meiofauna from sediments using colloidal silica sols. Marine Ecology Progress Series 214: 161–165. https://doi.org/10.3354/meps214161

Cho DH, Wi JH, Suh HL (2016) Two new species of the deep-sea genus *Parameiropsis* (Copepoda: Harpacticoida) from the eastern central Pacific. Zootaxa 4132: 521–539. https://doi.org/10.11646/zootaxa.4132.4.4

Conroy-Dalton S, Huys R (1999) New genus of Aegisthidae (Copepoda: Harpacticoida) from hydrothermal vents on the Galapagos Rift. Journal of Crustacean Biology 19: 408–431. https://doi.org/10.1163/193724099X00222

Conroy-Dalton S, Huys R (2000) Systematics and phylogeny of the Ancorabolidae (Copepoda: Harpacticoida). I. The *Ancorabolus*-lineage, with the description of three new genera. Cahiers de Biologie Marine 41: 343–397.

Gee JM, Huys R (1990) The rediscovery of *Danielssenia intermedia* Wells, 1965 (Copepoda, Harpacticoida): a missing link between the "danielssenid" genera and *Paranannopus* Lang, 1936 (Paranannopidae). Journal of Natural History 24: 1549–1571. https://doi.org/10.1080/00222939000770891

Gee JM, Huys R (1991) A review of Paranannopidae with claviform aesthetascs on oral appendages. Journal of Natural History 25: 1135–1169. https://doi.org/10.1080/00222939100770741

Gee JM, Huys R (1994) Paranannopidae (Copepoda: Harpacticoida) from sublittoral soft sediments in Spitsbergen. Journal of Natural History 28: 1007–1046. https://doi.org/10.1080/00222939400770541

George KH, Veit-Köhler G, Martínez Arbizu P, Seifried S, Rose A, Willen E, Bröhldick K, Corgosinho PH, Drewes J, Menzel L, Moura G, Schminke HK (2014) Community structure and species diversity of Harpacticoida (Crustacea: Copepoda) at two sites in the deep sea of the Angola Basin (Southeast Atlantic). Organisms Diversity & Evolution 14(1): 57–73. https://doi.org/10.1007/s13127-013-0154-2

George KH, Schwabe E (2019) A new species of Ectinosomatidae Sars (Copepoda, Harpacticoida) associated with *Pseudoikedella achaeta* (Zenkevitch, 1958) (Echiura, Bonelliida). Progress in Oceanography 173: 1–8. https://doi.org/10.1016/j.pocean.2019.02.003

Gollner S, Ivanenko VN, Martínez Arbizu P (2008) A new species of deep-sea Tegastidae (Crustacea: Copepoda: Harpacticoida) from 9°50'N on the East Pacific Rise, with remarks on its ecology. Zootaxa 1866: 323–336. https://doi.org/10.11646/zootaxa.1866.1.16

Gómez S (2018a) A new record and a new species of the genus *Rhizothrix* (Copepoda: Harpacticoida: Rhizothrichidae) from the deep sea of the Gulf of California. Proceedings of the Biological Society of Washington 131: 7–18. https://doi.org/10.2988/17-00021

Gómez S (2018b) New species of the genus *Mesocletodes* Sars, 1909 from the deep Gulf of California (Copepoda, Harpacticoida). ZooKeys 751: 75–112. https://doi.org/10.3897/zookeys.751.20387

Gómez S (2018c) Two new deep-sea species of Argestidae and Ameiridae (Copepoda: Harpacticoida) from the Eastern Mexican Pacific and Gulf of California, with proposal of a new genus of the family Argestidae. Journal of Natural History 52: 2613–2638. https://doi.org/10.1080/00222933.2018.1546915

Gómez S, Díaz K (2017) On some new species of Ancorabolidae Sars, 1909 from the Gulf of California: the genera *Ceratonotus* Sars, 1909, and *Dendropsyllus* Conroy-Dalton, 2003 (Crustacea, Copepoda, Harpacticoida). Zookeys 657: 43–65. https://doi.org/10.3897/zookeys.657.10725

Humes AG, Gooding RU (1964). A method for studying the external anatomy of copepods. Crustaceana 6(3): 238–240. https://doi.org/10.1163/156854064X00650

Humes AG, Voight JR (1997) *Cholidya polypi* (Copepoda: Harpacticoida: Tisbidae), a parasite of deep-sea octopuses in the North Atlantic and northeastern Pacific. Ophelia 46: 65–81. https://doi.org/10.1080/00785326.1997.10432478

Huys R (2009) Unresolved cases of type fixation, synonymy and homonymy in harpacticoid copepod nomenclature (Crustacea: Copepoda). Zootaxa 2183: 1–99. https://doi.org/10.11646/zootaxa.2183.1.1

Huys R, Boxshall GA (1991) Copepod Evolution. The Ray Society, London, 468 pp.

Huys R, Conroy-Dalton S (1997) Discovery of hydrothermal vent Tantulocarida on a new genus of Argestidae (Copepoda: Harpacticoida). Cahiers de Biologie Marine 38: 235–249.

Huys R, Gee JM (1990) A revision of Thompsonulidae Lang, 1944 (Copepoda: Harpacticoida). Zoological Journal of the Linnean Society 99: 1–49. https://doi.org/10.1111/j.1096-3642.1990.tb01221.x

Huys R, Gee JM (1992) A revision of *Danielssenia perezi* Monard, *D. paraperezi* Soyer, *D. eastwardae* Coull (Harpacticoida; Paranannopidae) and their transfer to a new genus. Zoological Journal of the Linnean Society 104: 31–56. https://doi.org/10.1111/j.1096-3642.1992.tb00913.x

Huys R, Gee JM (1993) A revision of *Danielssenia* Boeck and *Psammis* Sars with the establishment of two new genera *Archisenia* and *Bathypsammis* (Harpacticoida: Paranannopidae). Bulletin of the National History Museum (Zoology) 59: 45–81.

Huys R, Gee JM (1996a) *Prionos* gen. nov. from the meiofauna of a Malaysian mangrove forest and the status of *Psammis borealis* (Copepoda, Harpacticoida, Paranannopidae). Cahiers de Biologie Marine 37: 227–248.

Huys R, Gee JM (1996b) *Sentiropsis*, *Peltisenia* and *Afrosenia*: three new genera of Paranannopidae (Copepoda: Harpacticoida). Cahiers de Biologie Marine 37: 49–75.

Huys R, Gee JM, Moore CG, Hamond R (1996) Marine and Brackish Water Harpacticoid Copepods. Part 1. Field Studies Council, Shrewsbury, 352 pp.

Itô T (1982) Harpacticoid copepods from the Pacific abyssal off Mindinao. I. Cerviniidae. Journal of the Faculty of Science, Hokkaido University, Series VI, Zoology 23: 63–127.

Itô T (1983) Harpacticoid copepods from the Pacific abyssal off Mindinao. II. Cerviniidae (cont.), Thalestridae, and Ameiridae. Publications of the Seto Marine Biological Laboratory 28: 151–254. https://doi.org/10.5134/176059

Kitahashi T, Kawamura K, Veit-Köhler G, Danovaro R, Tietjen J, Kojima S, Shimanaga M (2012) Assemblages of Harpacticoida (Crustacea: Copepoda) from the Ryukyu and Kuril Trenches, north-west Pacific Ocean. Journal of the Marine Biological Association of the United Kingdom 92(2): 275–286. https://doi.org/10.1017/S0025315411001536

Kim K, Lee W, Huys R (2011) A new species of *Sentiropsis* (Copepoda: Harpacticoida: Pseudotachidiidae) from the upper sublittoral zone off Hyeopjae beach, Jeju Island, Korea, and a key to genera of the subfamily Danielsseniinae. Proceedings of the Biological Society of Washington 124(3): 179–197. https://doi.org/10.2988/11-08.1

Kornev PN, Chertoprud ES (2008) Harpacticoid Copepods of the White Sea: Morphology, Systematics, Ecology. KMK Scientific Press Ltd, Moscow, 379 pp.

Lang K (1936) Copepoda Harpacticoida. In: Bock S (Ed.) Further zoological Results of the Swedish Antarctic Expedition 1901–1903 under the Direction of Dr Otto Nordenskjöld. P.A Norstedt & Sponer, Stockholm, 3(3): 1–68.

Lee W, Huys R (1999) New Normanellidae (Copepoda: Harpacticoida) from western Pacific cold seeps including a review of the genus *Normanella*. Cahiers de Biologie Marine 40: 203–262.

Lee W, Huys R (2000) New Aegisthidae (Copepoda: Harpacticoida) from western Pacific cold seeps and hydrothermal vents. Zoological Journal of the Linnean Society 129: 1–71. https://doi.org/10.1006/zjls.1999.0197

Lee W, Yoo K-I (1998) A new species of *Neocervinia* (Copepoda: Harpacticoida: Cerviniidae) from the hyperbenthos of the Hatsushima cold-seep site in Sagami Bay, Japan. Hydrobiologia 377: 165–175. https://doi.org/10.1023/A:1003248419795

López-González PJ, Bresciani J, Huys R, González AF, Guerra A, Pascual S (2000) Description of *Genesis vulcanoctopusi* gen. et sp. nov. (Copepoda: Tisbidae) parasitic on a hydrothermal vent octopod and a reinterpretation of the life cycle of cholidyinid harpacticoids. Cahiers de Biologie Marine 41: 241–253.

Mercado-Salas NF, Khodami S, Martínez Arbizu P (2019) Convergent evolution of mouthparts morphology between Siphonostomatoida and a new genus of deep-sea Aegisthidae Giesbrecht, 1893 (Copepoda: Harpacticoida). Marine Biodiversity 49(4): 1635–1655. https://doi.org/10.1007/s12526-018-0932-3

Mielke W (1975) Systematik der Copepoda eines Sandstrandes der Nordseeinsel Sylt. Microfauna Meeresbodens 52: 1–134.

Mielke W (1997) Interstitial Fauna of Galapagos. XL. Copepoda, part 8. Microfauna Marina 11: 153–192.

Por FD (1969) Deep-sea Cerviniidae (Copepoda: Harpacticoida) from the western Indian Ocean, collected with R/V Anton Bruun in 1964. Smithsonian Contributions to Zoology 29: 1–60. https://doi.org/10.5479/si.00810282.29

Seifried S, Schminke HK (2003) Phylogenetic relationships at the base of Oligoarthra (Copepoda, Harpacticoida) with a new species as cornerstone. Organisms Diversity & Evolution 3: 13–37. https://doi.org/10.1078/1439-6092-00056

Seifried S (2004) The importance of a phylogenetic system for the study of Deep-Sea harpacticoid diversity. Zoological Studies 43(2): 435–445.

Shirayama Y, Kaku T, Higgins RP (1993) Double-sided microscopic observation of meiofauna using an HS-slide. Benthos Research 44: 41–44. https://doi.org/10.5179/benthos1990.1993.44_41

Vakati V, Thistle D, Lee W (2017) Two new species of the genus *Mesocletodes* (Copepoda, Harpacticoida, Argestidae) from the Pacific Ocean, San Diego Trough. Proceedings of the Biological Society of Washington 130(1): 34–51. https://doi.org/10.2988/16-00013

Willen E (2005) A new species of *Paranannopus* Lang, 1936 (Copepoda, Harpacticoida, Pseudotachidiidae) with atrophic mouthparts from the abyssalof the Angola Basin. Organisms, Diversity & Evolution 5: 19–27. https://doi.org/10.1016/j.ode.2004.10.002

Willen E (2008) Pseudotachidiidae (Copepoda: Harpacticoida) from the Angola Basin and the Antarctic deep sea, with the description of a new species of *Paradanielssenia* Soyer, 1970. Organisms, Diversity & Evolution 8: 249e1-249e16. https://doi.org/10.1016/j.ode.2007.06.004

Willen E (2009) *Nyxis rostrocularis*, a new genus and species of Paranannopinae Por, 1986 (Copepoda, Harpacticoida) from the Southern Atlantic deep sea. Zootaxa 2096: 299–312. https://doi.org/10.11646/zootaxa.2096.1.17

Willen E, Schulz M (2007) Rediscovery of *Bathypsammis* Huys & Gee, 1993 (Copepoda, Harpacticoida, Pseudotachidiidae) with description of a new species from the Antarctic deep sea. Zootaxa 1555: 53–68. https://doi.org/10.11646/zootaxa.1555.1.4